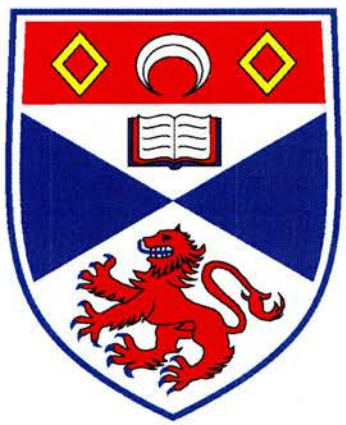

New Transdermally Delivered NO-Donor Drugs for Peripheral Vasodilation.

by

Russell James Pearson

A Thesis Presented for the Degree of

Doctor of Philosophy

in the

School of Chemistry

University of St Andrews

St Andrews **February 2002**

Declaration

I, Russell James Pearson, hereby certify that this thesis, which is approximately 62,000 words in length, has been written by me, that it is the record of work carried out by me and that it has not been submitted in any previous application for a higher degree.

Date 03-04-02 .....Signature of Candid

I was admitted as a research student in October 1998 and as a candidate for the degree of Ph.D. in September 1999; the higher study for which this is a record was carried out in the University of St. Andrews between 1998 and 2001.

Date 03-04-02 .....Signature of Candidate

I hereby certify that the candidate has fulfilled the conditions of the Resolution and Regulations appropriate for the degree of Ph.D. in the University of St. Andrews and that the candidate is qualified to submit this thesis in application for that degree.

Date 3-4-02 .....Signature of Supervisor.

Copyright

In submitting this thesis to the University of St. Andrews I understand that I am giving permission for it to be made available for use in accordance with the regulations of the University Library for the time being in force, subject to any copyright vested in the work not being affected thereby. I also understand that the title and abstract will be published, and that a copy of the work may be made and supplied to any *bona fide* library or research worker.

Date 03-04-02 .....Signature of Candidate.

Acknowledgements

On reflecting over the past three years, there are many people, who in one form or another have influenced the work presented here. Due to the numbers I will concentrate in detail on just a few. First and foremost I must thank my supervisor, Dr Tony Butler, for supplying such an interesting piece of work. This was completely born out of his enthusiasm for the NO story. Most importantly I wish to acknowledge Tony's trust and loose reign, which allowed me to take the project in the direction I wanted. This was made all the easier by Tony's philosophy that good science is only possible by bridging many different disciplines. Whilst this approach adds a great deal of lateral thinking into the work, it also relies heavily on strong collaborations, which we were lucky enough to enjoy.

The first of these collaborations came about from our mutual chemical interest and a shared lab space with Professor Field's group. I would particularly like to thank Rob Field himself, for his encouragement and advice throughout. The carbohydrate chemistry reported in this thesis would have been impossible without Rob's guidance and Ravi Kartha's practical and theoretical excellence. I am under no illusion that the skills I picked up by working along side Ravi were the most valuable, of any, that I acquired over the three years. Having Ravi's attitude and perfectionism in the lab was worth more, in terms of helping my synthetic progress, than our first class laboratory, and all of its contents, could ever offer.

With the compounds synthesised the work would have soon ran a ground without a biological testing facility. This is where our major collaboration with Ninewell's teaching hospital (Dundee), entered into the equation. In particular I would like to thank Professor Jill Belch, Dr Faisel Kahn, Dr David Newton and Mr Fraser Walker for providing me with the freedom to devise experiments and perform them, at will, with their Laser Doppler imager (LDI). Very few weeks went by when I did not visit the hospital, but over the whole duration I was made to feel like one of the team. However as a recruiter for Raynaud's patients, sitting for four-hour intervals in the waiting room of the clinic, and taxiing patients home to Anstruther in time for their appointment with the gasman, perhaps marks the point whereby I became a little too involved!

Of our other collaborations, which proved to be of equal benefit, I would like to say a huge thank you to Professor Alberta Gasco, Professor Roberta Fruttero and Dr Giulia Caron, of the University of Torino. The hospitality they showed during my stay, to determine Log P data, was nothing short of wonderful.

Closer to home I would like to thank Professor Lyn Williams group in Durham for allowing me to use their NO electrode and for providing some evening tours of their city. Back in St Andrews I would like to acknowledge Chris and Tim for the surface chemistry work, Catherine and Robin for successfully clearing the mountain of mass spec forms, and Alexandra (x-ray crystal structure), Melanya (NMR), Marjory (stores), Brian (UV repairs), Jim (computing) and Sylvia (atomic absorption) together with all of the other technical staff.

On a personal note I would like to mention Francesca, Jenny, Darren, Climber and Kannan for making lab 3.07 a happy and often interesting place to be. From that lab I have also found a great mate in Giles, "we are nearly there now youth!"

Since I am currently four months into my work with Dr Douglas Philp's group, I feel I should also acknowledge Doug and the workers of lab 4.05/6 (Elef, Julie, Mairead and Rosalyne) for putting up with me during this transition.

Finally I would like to thank Amy, not least for lending me her laptop over the past six months. This now feels like an extra body part after the many late nights/mornings spent in isolation. By some strange twist of fate, the lab actually supplied me with a big interest outside of chemistry. This was probably the last thing I anticipated from working long hours in the lab. So perhaps I should thank those de-*S*-acetylating reactions for not always quite working first time and consequently giving me the opportunity to work and dine late into the night with Amy. I would like to thank her in particular for her support, relentless encouragement and for generally putting up with me, and my work ethic, over the past year.

Confidence is something that can only grow from encouragement. Some of this was given to me when I met Bob Furchgott at the world NO meeting in Stockholm. Whilst kind words from a worthy Nobel Prize winner, of that year, is always welcome, nothing can compare to the constant support and wisdom that I have received over the last twenty-five years. For this reason I dedicate this thesis to my mother and father.

We are grateful to both the BBSRC and the BMA for funding this work.

CONTENTS

Chapter 3. Discussion & Results 89-131

~ Biology

In vivo performance of the NO donor compounds

Abbreviations

A_∞	absorbance (by UV) at infinity
Ac	acetyl
AC	adenylate cyclase
ACh	acetylcholine
AUC	area under curve
A-V shunts	arteriolar-venous shunts
AVAs	arteriovenous anastomeses
BF_3	boron trifluoride
Br	bromide
BUT	butyrionylated
cGMP	cyclic guanosine monophosphate
CGRP	calcitonin gene related peptide
CI	chemical ionisation
CLOGP	computational Log P values
CO	carbon monoxide
$CuSO_4$	copper sulphate
Cys	cysteine
DETA-NO	diethylenetriamine-NO complex
DNA	deoxyribonucleic acid
D-SNARB	*S*-nitroso-1-thio-2,3,4-tri-*O*-acetyl-α-D-arabinopyranose
D-SNAX	*S*-nitroso-1-thio-2,3,4-tri-*O*-acetyl-β-D-xylopyranose
EDHF	endothelium-derived hyperpolarising factor
EDTA	ethylenediaminetetraacetic acid
EI	electron impact
ENO	*O*-nitrosoethanol
eNOS	endothelial NO synthase
EtOH	ethanol
FAB	fast atom bombardment

Fe^{2+}	iron (ferrous ion)
Fe^{3+}	iron (ferric ion)
fmol	femto mole (10^{-15} mol)
GAGs	glycosaminoglycans
GLUT	glucose transporter
GRAS	generally recognised as safe
GSNO	*S*-nitrosoglutathione
GTN	glyceryl trinitrate
GTP	guanosine triphosphate
HBr	hydrogen bromide
HCl	hydrogen chloride
HET	hen's egg test
HEX	hexionylated
HMDS	hexamethyldisilane
HPLC	high performance liquid chromatography
H_2SO_4	sulphuric acid
5-HT	5-hydroxytryptamine
I	iodide
iNOS	inducible NO synthase
KSAc	potassium thioacetate
L-NAME	*N*-nitro-L-arginine methyl ester
L-NMMA	N^G-monomethyl-L-arginine
L-SNARB	*S*-nitroso-1-thio-2,3,4-tri-*O*-acetyl-α-D-arabinopyranose
L-SNAX	*S*-nitroso-1-thio-2,3,4-tri-*O*-acetyl-β-L-xylopyranose
LTP	long term potentiation
MALDI-TOF	mass spectroscopy (time of flight)
Me	methyl
mM	milli molar (10^{-3} M)
μM	micro molar (10^{-6} M)
MS	mass spectroscopy
NADP(H)	nicotinamide adenine dinucleotide phosphate
NaOMe	sodium methoxide
NEDD	*N*-(1-naphthyl)-ethylene-diamine dihydrochloride

nM	nano molar (10^{-9} M)
NMDA	*N*-methyl-D-aspartate
NMR	nuclear magnetic resonance
nNOS	neuronal NO synthase
NO	nitric oxide
N_2O	nitrous oxide
NOP	nitric oxide probe
NOS	nitric oxide synthase
OBz	benzolylated
oxy-Hb	oxygenated haemoglobin
PG	propylene glycol
PGI_2	prostacyclin
pmol	pico mole (10^{-12} mol)
ppm	parts per million
PROP	propionylated
PRP	primary Raynaud's phenomenon
PU	perfusion units
RBC	red blood cell
R_f	retention factor
RP	Raynaud's phenomenon
RSSR	disulphide
SAGA	*S*-nitroso-1-thio-2-acetamido-3,4,6-tri-*O*-acetyl-2-deoxy-β-D-glucopyranose
SAGAL	*S*-nitroso-1-thio-2-acetamido-3,4,6-tri-*O*-acetyl-2-deoxy-β-D-galactopyranose
sGC	soluble guanylate cyclase
SH	thiol
SNAC	*S*-nitrosothio-*N*-acetyl-L-cysteine
SNAG	*S*-nitroso-1-thio-2,3,4,6-tetra-*O*-acetyl-β-D-glucopyranose
6-SNAG	*S*-nitroso-6-thio-2,3,4,6-tetra-*O*-acetyl-β-D-glucopyranose
SNAGAL	*S*-nitroso-1-thio-2,3,4,6-tetra-*O*-acetyl-β-D-galactopyranose
SNA-GLY	*S*-nitroso-3-thio-1,2-di-*O*-acetyl propane

SNAL	*S*-nitroso-1-thio-2,2',3,3',4',6,6'-hepta-*O*-acetyl-4-*O*-(*β*-D-galactopyranosyl)-*β*-D-glucopyranose
SNAM	*S*-nitroso-1-thio-2,2',3,3',4',6,6'-Hepta-*O*-acetyl-4-O-(*α*-D-glucopyranosyl)-*β*-D-glucopyranose
SNAP	*S*-nitroso-N-acetylpenicillamine
SNO/RSNO	*S*-nitrosothiol
SNOB	*S*-nitroso-1-thio-2,3,4,6-tetra-*O*-benzoyl-*β*-D-glucopyranose
SNO-BUT	*S*-nitroso-1-thio-2,3,4,6-tetra-*O*-butyrionyl-*β*-D-glucopyranose
SNOC	*S*-nitrosocysteine
SNOG	*S*-nitroso-1-thio-*β*-D-glucopyranose
SNO-GLY	*S*-nitroso-3-thio-1,2-propanediol
SNO-HEX	*S*-nitroso-1-thio-2,3,4,6-tetra-*O*-hexionyl-*β*-D-glucopyranose
SNO-PROP	*S*-nitroso-1-thio-2,3,4,6-tetra-*O*-propionyl-*β*-D-glucopyranose
SNO-VAL	*S*-nitroso-1-thio-2,3,4,6-tetra-*O*-valerionyl-*β*-D-glucopyranose
SNP	sodium nitroprusside
SULPH	sulphanilamide
$t_{1/2}$	half-life
t_{∞}	infinity
THF	tetrahydrofuran
TLC	thin layer chromatography
TMS	trimethylsilane
TNF	tumour necrosis factor
TVD	traumatic vasospastic disease
UV	ultra-violet
VAL	valerionylated
VWF	vibrational white finger
XPS	X-ray photoelectron spectroscopy
ZnI_2	zinc iodide

Glossary of Medical Terms

Dermatomyositis / Polymyositis	*Two closely related conditions. Caused by inflammation of the skin and underlying skeletal muscle.*
Diabetes mellitus	*An endocrine disorder in which there is inadequate insulin levels.*
Connective tissue disorder	*Most common secondary form of Raynaud's. Results ultimately in digital ischaemia.*
Psoriasis	*Epidermal hyperplasia (increased cell number)*
Scleroderma	*Tight and thickened skin, usually of the limbs.*
Sjorgens syndrome	*Characterised by dry eyes and mouth. Salivary and lacrimal glands are enlarged. Occurs frequently in combination with rheumatoid arthritus.*
Systemic lupus erythematosis	*Commonly presents as a sun-sensitive rash over the face. The inflammation can result in scarring.*
Systemic sclerosis	*Also known as CREST (Calcinosis, Raynaud's, oEsophagitis, Sclerodactyly (pitted scars), Telangiectasia)*
Rheumatoid arthritis	*Results from occlusion of small vessels. Commonly present in the hands where joint changes are observed.*

Abstract

Using carbohydrate chemistry a whole family of novel *S*-nitrosothio-sugars were synthesised. All of these potential NO-donor compounds were chosen in an attempt to identify how subtle chemical differences can alter their vasodilatory action on the peripheral circulation and thus shed light on the biological mechanisms in place. Among the differences under scrutiny were, size, conformation, isomerism, lipophilicity and stability. In relation to this later property the decomposition of the *S*-nitrosothiols in aqueous solution, providing free NO *in vitro*, was extensively examined, so that relative stabilities between the various donors could be established. Transdermal delivery was the preferred route by which all of these compounds were then tested biologically. Such work was performed, on the forearm, of two volunteer groups. The first consisted of healthy volunteers, whilst the latter involved a heterogeneous group of Raynaud's patients. From the *in vivo* data supported by the pharmacokinetic findings, we were able to show by LDI (laser Doppler imager) that all of the NO-donors applied (20.58mM in ethanol : water (or KY jelly), 1:1) were able to enhance blood flow in the forearm of healthy subjects. However, from the vast array of test compounds, none showed greater benefit than that of our lead compound known as SNAG [5]. In addition, the dose response data from the Raynaud's group illustrated a clear difference in profile to that reproducibly observed in our control subjects. By way of trying to explain these differences, a wide range of smaller studies, are reported, where the effects of concentration, light, copper and transdermal enhancers were examined. Application to body regions other than the forearm, were also investigated. From such work many interesting findings were uncovered. In summary the results suggest that the NO-donors are not effective in the treatment of Raynaud's, but rather provide a better understanding of the condition itself.

Chapter 1 Introduction

1.1 Nitric Oxide (NO)

1.1.1 The story at a glance.

NO is one of the smallest molecules known to man. It is frequently confused with laughing gas (nitrous oxide, N_2O). Otherwise it was, until recently, best known as a pollutant in city air and in cigarette smoke. Now it is known to be an important molecule in many biological systems. It was named 'molecule of the year', by *Science*[1] in 1992. Two Nobel Prizes have been awarded for work involving NO. The first was awarded to Ostwald in 1908 for his synthesis of NO from ammonia and oxygen [Scheme 1]. Some ninety years later, the Nobel prize for physiology/medicine was split between Furchgott,[2] Ignarro[3] and Murad.[4,5] Their work, together with that of a British team led by Moncada,[6] showed endothelium derived relaxing factor to be nitric oxide. This discovery caused great surprise within the scientific community.

Scheme 1. *The Ostwald Process (Nobel Prize for Chemistry), 1908*

$$\mathbf{4NH_3 + 5O_2 \xrightarrow[900^{\circ}C]{Pt\ /\ Rh\ cat} 4NO + 6H_2O}$$

Without giving an over elaborate account and ultimately rehashing what is becoming routinely incorporated into biological textbooks, the decisive work in the discovery of NO will be very briefly described. This will be followed by a description of the NOS isoforms, primarily to illustrate, with examples, the scope of NO in human physiology and pathophysiology. Having presented examples of the vast array of NO based research, the remainder of this chapter will then deal with NO's role in the vasculature and how this can be augmented by NO-donor compounds.

1.1.2 The discovery of NO in the body.

The pioneering findings came out of Murad's work in 1979.[4] He provided the first clear evidence that, for the smooth muscle of blood vessels to relax, guanylate cyclase must be activated [Fig.1]. Concurrent with this process, he reported that GTP is converted into cGMP. Within the vascular laboratories, Furchgott further heightened the interest. He showed, the following year, how acetylcholine and bradykinin only function as smooth muscle relaxing agents in the presence of the endothelium.[2] Prior to this work it was assumed that such agents directly acted upon the smooth muscle. The need for the endothelium ignited a surge of research and centred on the chemical identification of a further messenger molecule. Only with this in place could the link between the endothelium and guanylate cyclase be appreciated. Eventually, an American group, led by Ignarro[3] and Moncada's British group[6] independently solved this, reporting nitric oxide as the key messenger.

Fig.1 *A schematic representation of the role of NO in the relaxation of an arterial blood vessel.*

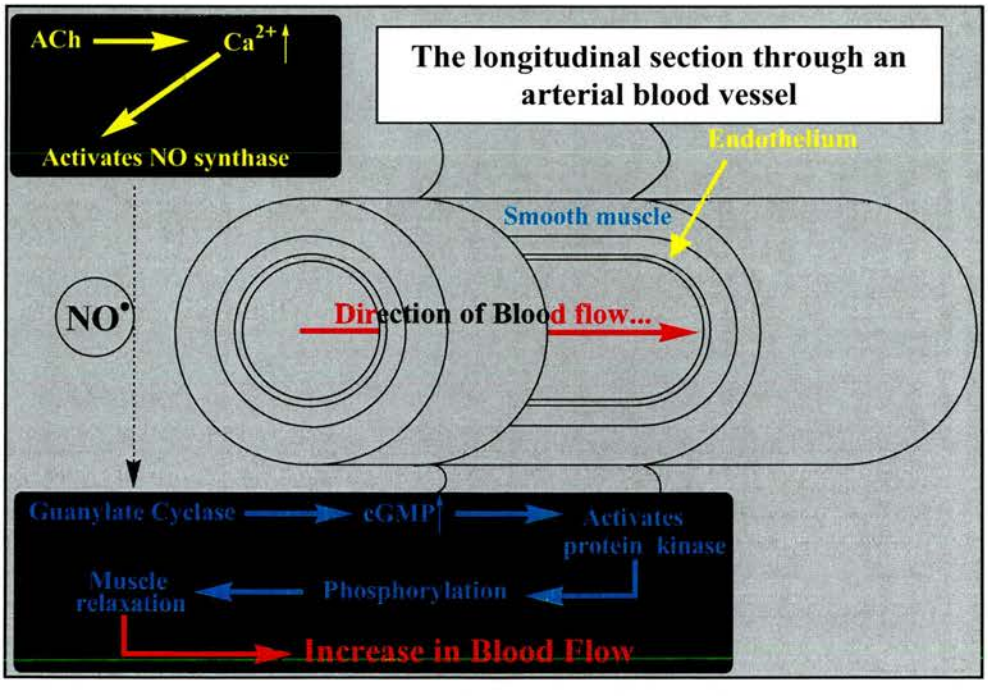

The yellow text highlights the biochemical process in the endothelial cell, while the blue text shows the process, which occurs in the smooth muscle upon activation by NO.

In hindsight, the importance of NO might have been uncovered much earlier since its

use in medicine was underway as far back as 1859. Sir Thomas Lauder Brunton described "a sudden throbbing of the arteries of the neck,"[7] when amyl nitrite [Fig. 2] was held to the nostrils. From 1867 this compound was administered for chest pain and angina, though its metabolism to NO *in vivo*, was clearly not understood at the time.[8] Around the same period, Murrel[9] showed the benefit of glyceryl trinitrate (GTN) for the same diseased state.

Similarly, the ability of glyceryl trinitrate (GTN) and sodium nitroprusside (SNP) to activate guanylate cyclase was ignored. Heidenhahn's description[10] (1891) of the endothelium as "an active secretory cell system" also appears to be a costly oversight. So too were comments by Cannon in 1939, who stated that "the dilation of the arterioles and capillaries in active muscle is one of the most remarkable emergency adjustments....What causes them to dilate is not yet understood....however the capillaries may be opened, the great importance of their being opened should not be overlooked."[11]

Fig.2 *Early NO treatment.*

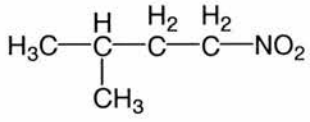

Iso-amyl nitrite

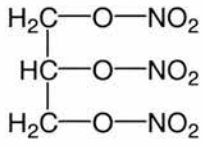

Glyceryl trinitrate (GTN)

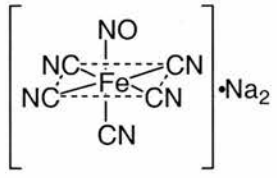

Sodium nitroprusside (SNP)

The biosynthetic pathway for nitric oxide was another significant breakthrough. This was shown by ^{15}N labelling at the terminal end of arginine, which was then given to endothelial cells in culture to produce an *S*-nitrosothiol. Arginine's role as a precursor was thus established.[12,13] This process was then linked to a NO producing enzyme, termed NO synthase (NOS). The work was able to move quickly since nitric

oxide activity in the immune system had been discovered soon after the vascular findings were fully in place. Much of the evidence involving NO with the immune system was centred on high levels of nitrite and nitrate in the urine from humans suffering from diarrhoea.[14,15] This was substantiated by elevated amounts recorded in activated macrophages cultured from a mouse model.[16] Three groups independently showed NO to be responsible for these observations.[17-19] The cytotoxic nature exhibited by macrophages in response to tumour cells could then be explained,[20] since superoxide (O_2^-) is the other common precursor from the body's cellular defence and reacts with NO to generate peroxynitrite[21] [Scheme 2]. Alternative mechanisms include NO's potential to nitrosate either active site thiols[22] or to form iron complexes. This latter process supports the idea of attack at the haem portion[23,24] of enzymes and cofactors important in cellular metabolism. Nitrosation of thiols important in protein structure may also contribute to NO's reported toxicity.[25]

Scheme 2[21]. *The production of peroxynitrite.*

$$NO + O_2^- \xrightarrow{\text{Rapid}} OONO^-$$

It was soon rationalised that NO production must be governed by more than one form of NOS. Clearly in the vasculature a continuous low level of NO is required, whilst the need from the immune system will be high concentrations, but only upon demand. The iso-enzymes must therefore fulfil the role of being constitutive and inducible, respectively. Even with such specificity in place, septic shock is capable of providing a worst case scenario. The levels of NO generated from the immune system alone are such that vascular relaxation ensues with a dangerous drop in blood pressure.[26]

As if nitric oxide was not receiving enough coverage, the selective activation at a glutamate receptor subtype by *N*-methyl-D-aspartate (NMDA), in the brain, showed the levels of cGMP to follow trends observed in the vascular smooth muscle[27-28] [Fig. 3]. Soon after such experiments NO synthase activity was reported.[29] This third enzyme was then purified[30] from a rat model, the following year. As with NOS from the endothelium, neuronal NOS is also a constitutive isoform. Further work showed that the peripheral[31] and *inter alia*[32] nervous systems are governed by NO synthase.

Fig. 3. *The production and role of NO at synapses.*

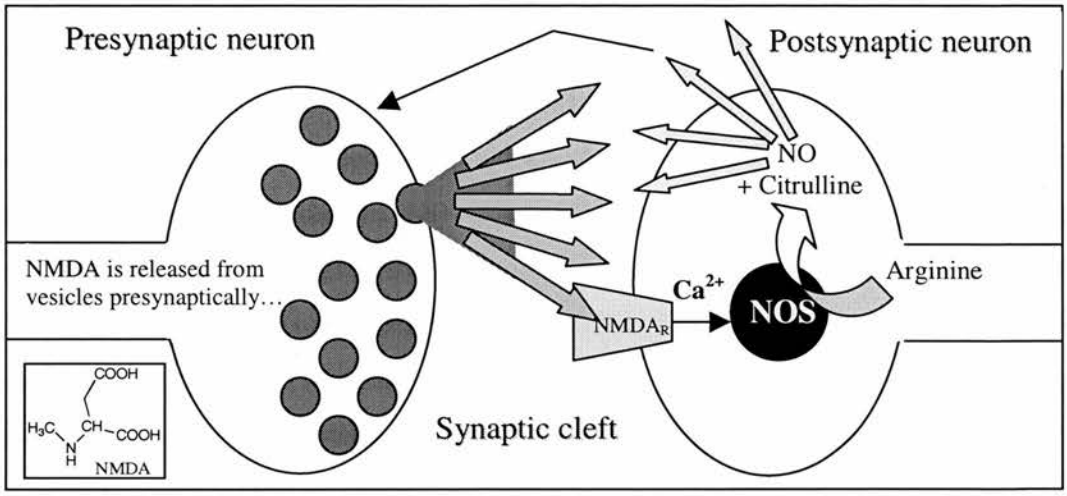

The activation of the NMDA receptors located post-synaptically results in NO release into the synapse and ultimately activation pre-synaptically. It is the repetitive transmission across this synapse, which is believed to trigger learning.[25,33]

1.1.3 NO synthase (NOS)

In general terms, the production of free NO along with citrulline, as outlined in scheme 3, requires two monoxygenations by NOS, consuming NADPH (1.5 mole eq.) and dioxygen (2 mole eq.) in the process [Scheme 3].[25] By the 1990s biologists were suddenly confronted with the knowledge that an enzyme available in at least three isoforms was responsible for producing an essential mediator for an extensive array of physiological processes.

Endothelial, neuronal and inducible NOS are known as eNOS, nNOS and iNOS, respectively. This nomenclature is based on the tissue/cell origin from which they were first identified. However this situation is confused somewhat by the isolation of all three isoforms in many different anatomical regions. For instance, eNOS appears to occupy many sites, including platelets, kidney cells and neurones from the hippocampus. The kidneys as well as the brain contain nNOS. In fact this isoform has many hosts, such as epithelial, pancreatic and skeletal muscle cells. As for iNOS, any nucleated cell can potentially house this enzyme provided the correct stimulus is applied.[25] Thus, as well as being biochemically similar, the three isoforms of NOS have a complex distribution within the body. It is therefore inaccurate to label them in a manner that suggests they occupy separate biological compartments. Whether

these isoforms associate predominantly in the cytosol or within membranes appears to be a contentious issue.

Scheme 3.[25] *The conversion performed by NO synthase.*

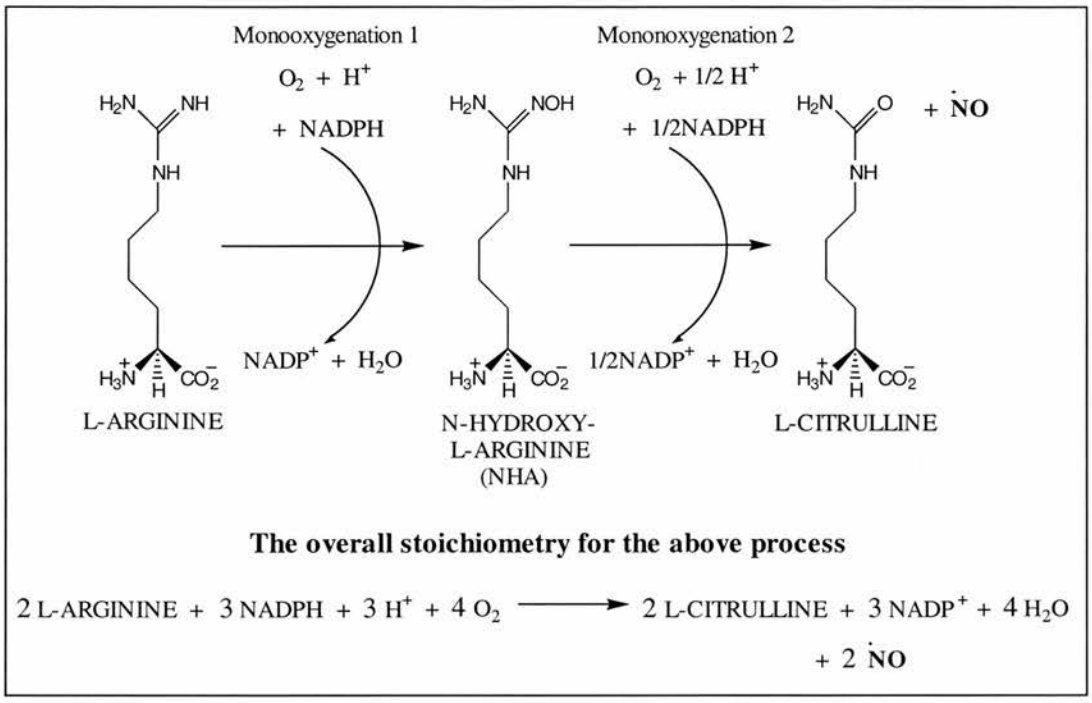

Despite the variation in size and primary structure, it is the regulatory controlling factors that prove to be the most decisive in at least separating the inducible and constitutive forms of NOS. The catalytic activity of the latter is completely dependent on intracellular Ca^{2+}, whilst iNOS regulation appears to be governed by transcriptional control and the availability of substrate and essential cofactors.[34] However, reports of iNOS acting in a constitutive manner[34] leaves the categorisation and definition of the individual isoforms of NOS in a state of disarray. At the same time it would be wrong to imply that differences do not exist, since in a particular tissue/cell type each NOS isoform plays a subtly different role. It is only when attempts to summarise the bigger picture are made that exceptions and contradictions surface.

Utilising the differences observed within the NOS family will quickly narrow the therapeutic field and uncover more reliable biological observations. One approach here would be to develop compounds, which selectively activate or inhibit particular NOS isoforms. Alternatively NO donors that either act locally or accumulate in a tissue selective manner could be applied. This project involves the latter in an

attempt to improve selectively forearm blood flow. However to aid in the appreciation of NO's global role within the body, three examples of selective NO donation, in very different anatomical regions, will first be described. Whilst remembering the equally viable route of NOS activation and inhibition, at least when endothelial function is not compromised, their remains the potential for a combined therapy with an NO donor.

1.1.4 Extreme examples of NO donors with local or selective activity.

1.1.4a NO donation in the airways and lungs

One of the newest therapeutic applications of NO, which appears to have great potential, is in the treatment of cardiopulmonary disease. Since the lungs house a plentiful supply of eNOS, iNOS and nNOS this is not particularly surprising.[35] Their central role appears to be in maintaining pulmonary vascular tone and preventing hypertension. However bronchial tone, permeability to sodium/water, ciliary motility, mucus secretion and protection to pollutants and pathogens, would all appear to be under the homeostatic control of this enzyme family.[35]

In the lungs of healthy subjects, an increase in NO production accompanies the administration of acetylcholine. In contrast, the vasculature that supplies the lungs of patients with primary pulmonary hypertension, may be incapable of generating sufficient NO.[36] The inhalation of an exogenous source would appear a logical therapy in such circumstances. Such a theory was substantiated by the reversal of pulmonary hypertension in animal models,[37] following inhalation of pure NO. The major advantage of this treatment, other than it being endothelium independent, is its ability to act locally with no systemic side effects. This may be due to the removal of unwanted NO as nitrosylhaemoglobin.[38]

A large multi-centred trial[39] showed ventilator free survival to be reduced following NO usage in acute lung disorders. This may be explained by the so-called "rebound"[35] in pulmonary artery pressure, leading to cardiovascular collapse, upon termination of NO gas therapy. Such observations were reconstructed in a porcine model induced with pulmonary hypertension.[35] These findings suggested the need for a sustained NO supply. Schutte and co-workers[40] showed in the rabbit lung how NO

donors such as sodium nitroprusside (SNP) could provide the therapeutic benefits of NO over a prolonged period. The more medically significant consequence of this was a way of combating the "rebound" response. This idea was fine tuned by Stamler and co-workers, who suggested "channelling NO into SNOs,"[35] since this would provide a slow release system, whilst eliminating the potential for lung toxicity.

In order to maintain local administration, the use of an aerosol was an attractive one. What was required was a volatile compound, stable in oxygen yet reactive enough in the presence of endogenous glutathione to cleave heterolytically and thus enable *S*-nitrosation. This criterion was matched to *O*-nitrosoethanol (ENO). Production of *S*-nitrosoglutathione by this route provides the potential to bolster NO stores within patients with endothelial dysfunction. Following inhalation of ENO in neonatal pigs, a high *S*-nitrosothiol content within the lungs was observed upon analysis [Fig.4]. Nucleophilic attack by glutathione upon free NO is a far less favourable reaction. This was illustrated by a low SNO yield from the same *in vivo* experiment after NO inhalation.[35]

Fig.4[35] *The ability of free NO and ENO to nitrosate endogenous thiols, of which glutathione is the most abundant, in the lungs of neonatal pigs.*

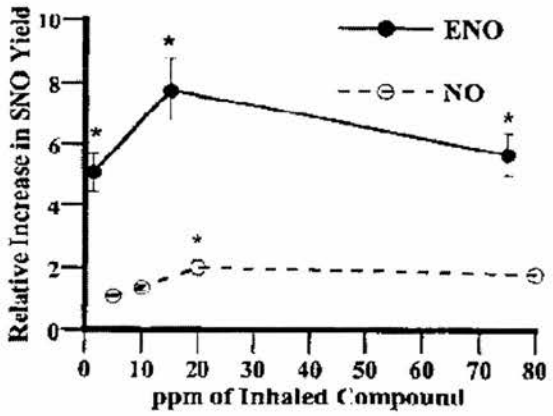

This data is expressed as a fold-increase over endogenous levels of SNO.

Pulmonary hypertension was induced in the pig model before inhalation of either NO or ENO for a two-hour period. However the "rebound" was only seen in the NO treated animals. No fall in pulmonary pressure was observed in the ENO treated animals for up to 20 minutes after drug termination. Such work, together with *in vitro* experiments where the airways of the lungs remain relaxed in the presence of

endogenous concentrations of GSNO provide encouraging signs in the treatment for asthma, cystic fibrosis and hypoxemic respiratory failure.[35]

1.1.4b NO donation as a cytotoxic agent

The potential of NO as a cytotoxic agent appears far less obscure than its role as a regulatory mediator in autoimmune disease.[41] For instance, NO has been shown to exhibit immune responses to bacteria, parasites and tumour cells.[42] This defensive action has encompassed attack at many levels from inhibition of cell growth to inducing genomic mutations. As already described NO can form peroxynitrite [Scheme 2] in the correct environment and thus act as a potent chemical oxidant at the level of DNA and protein.[42] While NO donors appear attractive agents for targeting cancer cells, the indiscriminate release of NO is problematic. What is really required is a tissue selective NO donor. On the basis of such logic NO donors containing monosaccharide moieties were synthesised.[42] It was hoped that the transmembrane GLUT proteins of DU-145 cancer cells, from the human prostate, would provide facilitated transport due to the recognition of the sugar component. This was achieved and consequently, *in vitro* work, showed enhanced cytotoxic effects.

1.1.4c NO donation in the understanding of behavioural learning

The mechanism by which neuronal NO is released postsynaptically has already been described [Fig.3]. Garthwaite[27] first showed the role of nNOS, in the brain in 1988. The idea of nitric oxide being a "brain gas"[43] produced scepticism. After all it is not a conventional neurotransmitter as outlined by Stahl,[43] "it is not an amine, amino acid, or peptide; it is not stored in synaptic vesicles or released by exocytosis; and it does not interact with specific receptor sites in neuronal membranes. However, NO is synthesised upon demand in the brain, diffuses to receptor sites within the enzyme guanylate cyclase and has neurotransmitter-like functions."

In the hippocampus, at the CA1-Schaffer collateral synapses, long term potentiation (LTP), which is thought to be responsible for learning, occurs when the post synaptic neurone CA-1 is in a state of depolarisation while neurotransmitter is being released pre-synaptically from the CA-3 nerve terminals.[33] This is also referred too as

increased synaptic strength. NO is considered as a diffusible retrograde signalling molecule in LTP. This is supported by the observed reduction in LTP by haemoglobin, due to the associated NO scavenging role.[44] Thus it can be assumed that NO is mopped up and prevented from travelling from its post-synaptic origin to the pre-synaptic neuron.

Since NO is diffusible, in the absence of elevated haemoglobin levels, it is capable of stimulating pre-synaptic terminals in the general region and not only in the cleft from which it was formed. A spreading of the effect is therefore possible[33,45,46]. However recreating LTP with exogenous NO and NO donors has been difficult. One team[44] was able to overcome this problem and study the effect of NO donation on LTP in the CA-1 terminal of rat hippocampal slices. A very novel way of delivering NO was devised using potassium pentachloronitrosyl ruthenate ($K_2Ru(NO)Cl_5$). Here NO exists in a ligated form, requiring flash photolysis to initiate its release. Obviously in such work exact quantities, delivered at precise time points, is essential. With such a model in place, the group were able to show that NO dictates the induction but not the maintenance of LTP.

The importance of NO and LTP in animal behavioural learning has been widely studied. One such study[47] using the Morris water maze showed how rats' training was hampered by prior administration of the NOS inhibitor, L-NAME. However, no such effect was seen upon co-administration of L-arginine. To rats already trained, NOS inhibition also had no effect. This strongly suggests the acquisition but not the retention of memory is governed by NOS activity. Thus the results of this study, which are supported,[48] show a beautiful overlap with the findings from the tissue study[44] of NO's role with LTP, as reported previously.

It is hoped that the three examples outlined, indicate the range of roles played by NO. New NO-related work is continually emerging. For instance, the importance of NO in bone maintenance, growth and disease is just one topic still in its infancy.[49,50] Across the living world NO is also strongly implicated. An example of this is NOS activity in plants,[51,52] where NO plays a key role in disease resistance.[53] As Murad himself confesses, it is difficult to "believe that a simple free radical could be a second messenger, autocoid, paracrine substance, neurotransmitter and hormone."[54] Perhaps NO's best description, thus far, is as a "mediator, murder and medicine,"[55]

though in the future years it will be preferentially labelled with this latter quality as its potential is fully unveiled.

1.1.5 The current ideas and debate with regard to NO in the vasculature.

In this thesis the emphasis is upon NO in the peripheral vascular system. Thus, in terms of the NO story, the primary interest here lies within the interplay between NO and the endothelial, smooth muscle and circulating red blood cells. To address adequately the current thinking in these areas this discussion will be split into two sections. The first will deal with NO circulating freely in blood and the latter will consider NO at the level of guanylate cyclase.

1.1.5a NO and the circulation of RBCs.

The effects of NO in the vascular system, have for a long time been considered to be very localised; indeed one study[56] has shown that NO diffuses identically in all directions from a single generator cell. Lancaster[57] proposed a scavenging role for haemoglobin in red blood cells (RBC), with respect to NO, and dismisses claims of long-range action. In fact it is known that 70% of any NO reaching the blood is immediately excreted via the kidneys in the form of nitrate. However the true situation is more complex than the model proposed by Lancaster.

The diffusion of NO from its endothelial origin can be best understood by taking a section through a blood vessel, allowing for a cylindrical source of NO and a RBC-free zone [Fig.5]. It would be expected that equal amounts of NO, produced in the endothelium, would travel into the lumen and out towards the smooth muscle. However, upon calculating the concentrations travelling into the RBC-free zone[58,59] (inward) and vascular smooth muscle (outward), it was discovered that this was dependent upon vessel radius.[60] When the radius size dropped below 1mm, more NO entered the RBC-free zone as opposed to smooth muscle. Despite a plentiful supply of NO, once at the inner boundary of the RBC-free zone, this would obviously all be mopped up immediately due to the NO to haemoglobin ratio being in the range of 1:1000 to 1:2500, in favour of the globular molecule.[61,62]

Fig.5 *A section through a blood vessel to illustrate the idea of spherical NO diffusion from endothelial cells.*

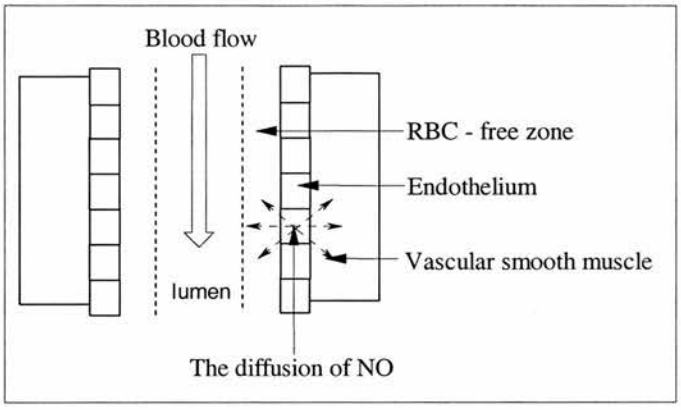

The RBC-free zone represents the blood that is in direct contact with the endothelium. Whilst the majority of the lumen contains a dynamic flow of RBCs this peripheral volume is largely made up of plasma and can be considered as a separate fluid model.
*Extracted from an article by A.R. Butler, I.L. Megson and P.G. Wright, Biochem. Biophys. Acta., 1998, **1425**, 168.*[60]

Whilst this scenario appears to clearly outline the role of haemoglobin and the levels of nitrate found in the urine, it does not explain how physiologically detected NO levels (10nM – 1μM)[57,61,63] are possible. With such a huge excess of haemoglobin and the reported[61,64] speed with which the NO/oxy-Hb reaction [Scheme 4] occurs (~3 x 10^7 $M^{-1}s^{-1}$), free NO would be inconceivable. The situation is therefore more complex. Stamler and co-workers[61] were the first to address this issue by suggesting that rather than scavenge and eliminate NO, haemoglobin actually conserves NO in its bioactive state. An *S*-nitrosylation reaction, similar to the example described earlier in the lungs,[35] was thus proposed in order to explain how NO levels are physiologically sustained in the face of the dominant oxy-Hb reaction.

Scheme 4 *Illustrating the dominant NO/oxy-Hb reaction (oxidation)*

$$\mathbf{Fe(II)O_2 + NO \rightarrow Fe(III) + NO_3^-}$$

(methemoglobin)

This work led Gross and Lane[65] to describe the situation as an abyss in our understanding of biochemistry. They also suggest the need for major revision of NO and haemoglobin reactivity under normal physiological conditions. In agreement with Stamler and co-workers,[61] they too were sceptical of the standard scavenging story of haemoglobin, since this would prevent NO ever reaching concentrations necessary to evoke vasorelaxation. It was also agreed that the rate of the NO/oxy-Hb reaction is so rapid that soluble guanylate cyclase would never become activated by NO, should there be no competitive reactions. There is of course the other classical reaction in which NO reacts with free Fe(II)-Hb [Scheme 5]. However since oxygen saturation is typically in the range of 70-99%,[65] this scenario struggles to explain how NO is retained.

Scheme 5 *The other classical reaction between NO and haemoglobin (addition)*

Fe (II) + NO → NO-Fe (II)

A third physiological reaction between NO and haemoglobin was proposed[65] in accordance with Stamler's findings[61] [Scheme 6]. This centred upon a cysteine residue located on the β-globin of haemoglobin, which has been evolutionarily conserved in all mammals and birds (βCys^{93} of human haemoglobin).[66-68] *S*-nitrosothio-haemoglobin (SNO-Hb) provides a protected delivery route for NO whilst having the potential to supply NO to low molecular weight thiols.[65] However the really intriguing suggestion from this model is one of molecular gymnastics in the presence of a changing oxygen environment. On the basis of haemoglobin allostery, it was proposed[65] that *S*-nitrosylation of haemoglobin could occur in highly oxygenated regions such as the lungs,[35] since haemoglobin is then found in its R structural form. Upon release of oxygen in deoxygenated and ischaemic tissue, haemoglobin reverts to its T structure, which could act as a trigger for NO release. Therefore in addition to supplying oxygen to hypoxic tissue, the concurrent release of NO would enable the dilatation of the capillaries in the surrounding vicinity. This would result in a greater blood flow to further enhance the delivery of nutrients to the deficient area.

Scheme 6 *S-nitrosylation: the third potential reaction.*

NO + Hb-βCys^{93} → SNO-Hb

On the basis of *S*-nitrosylation of Hb-βCys^{93}, the formation of NO-Fe (II)-Hb, can be assumed to result from transfer between thiol and iron haem. Such a transfer could again be explained on allosteric grounds. This has led haemoglobin to be described as a molecular switch by Gross and Lane.[65] However in reporting their proposal they are cautious and admit the mechanism leaves a question mark as to how NO is inactivated and perhaps more significantly, how plasma nitrate is formed.

Using a one hundred fold excess of KCN and $K_3Fe(CN)_6$, to selectively remove NO from haem alone, Gladwin and co-workers,[62] directly compared the levels of SNO-Hb and NO-Fe(II)-Hb, by a chemiluminescence technique. NO release was controlled by addition of I_3^-/O_3, which clearly illustrated the majority of NO to originate from NO-Fe(II)-Hb. As well as dismissing the *S*-nitrosation mechanism as merely as salvage pathway built into red blood cells for use only in severely stressed tissue, the group put the emphasis back onto the oxidation reaction as the primary pathway for NO to undertake. The data[62] to substantiate this latter claim were obtained by mapping nitrite, nitrate and red cell methemoglobin levels before, during and after NO inhalation. The correlation between nitrate and Fe(III) clearly identified the reaction outlined in scheme 4, to be the dominant one. While this revisits the problem of trying to explain how physiological levels of NO can be accounted for, it should be appreciated that NO scavenging and elimination is not quite as rapid as one may think. The half life for NO release from the haem of intact erythrocytes is twenty-one minutes.[69] During this time there is the potential for the redox activation of NO (NO^+), in the red blood cell, enabling not only reaction with Hb-βCys^{93}, present at concentrations of 10mM,[62] but also with glutathione, which is found to exist in the same cells at concentrations of 5mM.[62]

Extended work by Gladwin and fellow workers[70] suggests that nitrite may be the actual bioactive source of NO. There is evidence to support this, since it is relatively stable and circulates in plasma at concentrations of 500nM.[70] It can also be readily converted to NO by xanthine oxidase,[71,72] which is found in abundance within vascular endothelium.[73] Thus upon formation from free NO in the lungs it can be

transported and then reduced back into active NO once in the peripheral vascular beds.

Amidst all the contradictions and counter claims, it is clear that this area of the NO story is still volatile and incomplete. The various groups all make valid statements with experimental backing. What appears clear is the need to maintain physiological conditions during such investigative work. This is well exemplified by the chemiluminescence work by Gladwin,[62] since the requirement of ozone in the procedure must have implications as to the allosteric state of haemoglobin. The assay does not allow for comparison in high and low oxygen environments which markedly affect the ease with which NO is released from SNO-Hb. Inappropriate conditions such as these appear only to further confuse the discussion. In the words of Gross and Lane[65] the unforeseen complexities which have surfaced are more than a little surprising, when it is considered that essentially we are studying the interaction between the best understood protein and a simple small gaseous molecule.

1.1.5b Soluble guanylate cyclase

It is with surprise, that soluble guanylate cyclase (sGC) remains inadequately understood, despite its pivotal role in the NO story. In comparison with its potent endogenous activator (NO) it is regarded as being new on the biochemical scene. It was discovered in 1969[74-77] yet its three-dimensional structure, cellular distribution and expression are still unresolved. There is also little known about its changes in conformation, the number of isoforms in existence or a complete list of its endogenous activators.[78] Much of this uncertainty is attributed to difficulties in its isolation and purification, though this has been reported with bovine lung using an immunoaffinity chromatography method.[79] The NO story has accelerated sGC work yet in reality the protein has a lot of ground to make up in comparison to its highly documented sister enzyme, adenylate cyclase (AC).

In contrast to a low affinity for oxygen, NO is able to readily stimulate the haem binding domain on His 105 of sGC. This results in the formation of a penta-coordinate nitrosyl-haem complex. As illustrated [Fig. 6][78] even NO's carbon relative, carbon monoxide (CO), is unable to evoke anything like the same activity, at physiological concentrations.

Fig. 6 *Illustrating the ability of NO, but not CO, in forming a penta-coordinate nitrosyl-haem.*

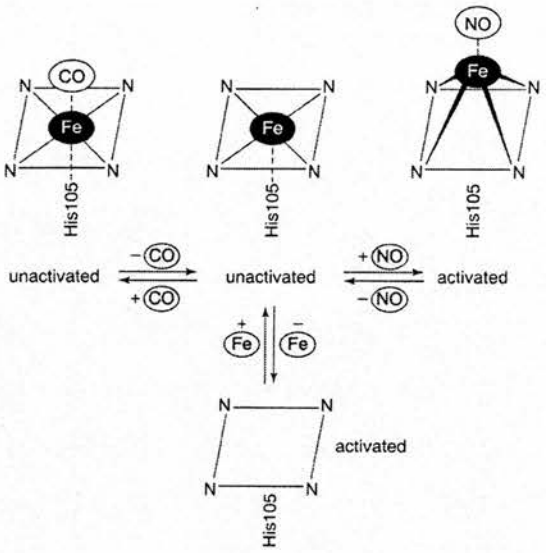

The formation of the penta-coordinate nitrosyl-haem, consequently triggers the activation of guanylate cyclase.
*This was extracted from a review by A.J. Hobbs, TiPS, 1997, **18**, 484.*[78]

With a better understanding of sGC, it should be possible to tailor NO donors, which are specific to the enzyme's needs. For now the two most useful observations are the reported presence of thiols[80] and copper.[81] The former is thought to maintain iron in the reduced state and thus ready to accept free NO.[78] Two cysteine residues have been identified[80] near the haem binding site. This has led to the suggestion[82] that *S*-nitrosothiol formation may occur prior to NO binding upon the active site. The idea is reinforced with the identification of Cu(I) ions, in the protein of sGC,[81] since they are known to decompose *S*-nitrosothiols with the release of NO.[83,84] Thus the enzyme may have in place all the necessary components in the correct vicinity to deal with NO or *S*-nitrosothiols from an endogenous or exogenous source.

Interestingly when a copper deficient diet was fed to animals, endothelium dependent relaxation was compromised.[85] This further supports a role for *S*-nitrosothiols at the active site of sGC. Therefore NO donors of this form would appear the logical choice (section 1.4.2) based on our current level of sGC understanding. Alternative NO donors and indeed sGC inhibitors may be synthesised once the enzyme's profile is fully appreciated. Advances in the area are certainly in progress. For example, earlier

this year a regulatory site, independent of NO, was reported[86] together with a potent stimulating agent capable of altering platelet and blood homeostasis.

Taking all of the NO knowledge described here, its role in Raynaud's Phenomenon will now be discussed. With an understanding of this peripheral vascular condition, the reasons for choosing NO donation as a potential therapy of benefit to Raynaud's sufferers will become apparent.

1.2 Targeting our understanding of NO to Raynaud's Phenomenon

1.2.1 Overview.

In this section the potential role of NO donation in the treatment of Raynaud's phenomenon (RP) will be described. Since many other peripheral disorders occur in combination with RP, such as scleroderma,[87] attempts to design a successful NO donor for RP may actually prove to be of greater benefit elsewhere. Due to the abundance of different peripheral vascular disorders there is the need to specialise our efforts. Raynaud's phenomenon is one of the most common disorders in this field with no satisfactory treatment. Thus our focus is on Raynaud's phenomenon whilst appreciating the scope for the work in related disorders such as systemic sclerosis, mixed connective tissue disease, dermatomyositis/polymyositis, systemic lupus erythematosis, rheumatoid arthritis and diabetes mellitus. In order to improve blood flow and elevate the symptoms seen in RP patients a clear understanding of the condition is required. The following aims to address such a need whilst remaining open minded with regard to alternative therapeutic pathways that do not relate to NO.

1.2.2 What is Raynaud's Phenomenon?

"...It was at the beginning of 1860 that one of the cases reported later (Observation IV) attracted strongly my attention. It had to do with the spontaneous gangrene of the four extremities appearing unexpectedly in a young woman of 27 years. During more than one month I saw a series of strange and remarkable phenomena unroll themselves before my eyes – and disconcerted the great experience

of many eminent physicians who saw this patient with me. In vain all the organs were minutely explored. In vain all the known or probable causes of gangrene were investigated. It was necessary to admit the presence of some influence up to that time unknown ..... All appear to me to show as a common character, the absence of any appreciable material obstacle to the course of the blood either arterial or venous ..... This affection, which constitutes scarcely a slight inconvenience and which often passes unperceived so that it does not require any treatment, is moreover very common. There is scarcely any physician who has not many times had occasion to observe it... ".[88,89]

- Maurice Raynaud, 1888, thesis extract.

Raynaud's phenomenon (RP) is a vascular disorder that has long been recognised. It is caused by insufficient blood flow to the extremities and is frequently triggered by low temperatures.[90] Interestingly; it is five times more prevalent in woman[91] and is characterised by cold, pale digits. Patients complain mainly of an unbearable pain usually in the fingers, during and after exposure to cold conditions. The original description of the disorder, as presented above, was by Maurice Raynaud in 1888. This stands, as rigidly today as it did over a century ago yet, its pathophysiological mechanism remains "a landmark to our ignorance."[92]

1.2.3 The observations during a Raynaud's attack.

In many studies, attention is drawn to the different skin colours that are observed in Raynaud's sufferers when exposed to cold. As reported by Hines and Christensen in 1945, a single pallor phase is most frequently observed.[91] Later, Gifford and Hines in 1957,[93] found the most common skin colour sequence to be, white to blue to red [Fig. 7]. A biphasic coloration appears to be another popular observation in both of the aforementioned studies.

Fig.7 *A schematic diagram of the triphasic colour changes seen in the hand.*

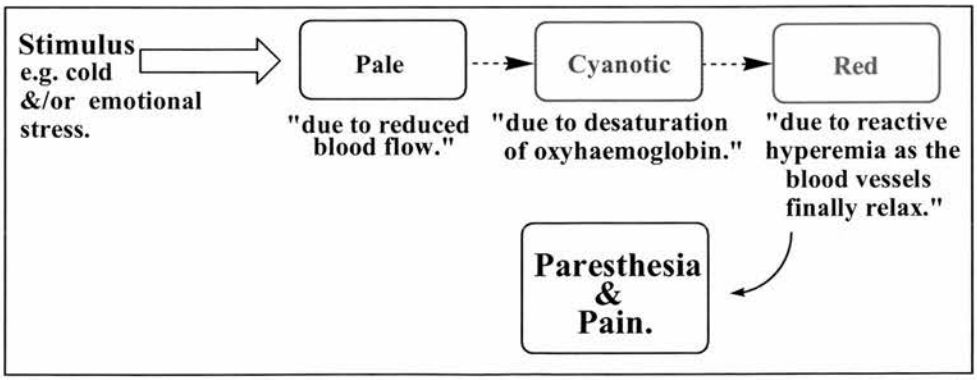

Based upon a description outlined by J. Loscalzo, M.A. Creager and V.J. Dzau, Vascular Medicine, Little, Brown and Company, Boston, 1992, 379-382 & 975-995.[94]

Despite the hands and less frequently the feet being the sites most prone to this disorder, further work by Gifford and Hines[93] on a larger group of sufferers, describe how anatomical areas such as the nose, ears, face, chest and lips show similar symptoms. Whilst approximately 55% of sufferers experienced the condition only upon the hands, it was also noticed that the thumbs were frequently unaffected. The explanation for this latter observation is suspected to be a consequence of direct arterial linkage from the radial artery, thus permitting a plentiful blood supply.

1.2.4 The nomenclature used to describe the variants of Raynaud's disorder.

Thirteen years after its christening, Raynaud's disease was renamed Raynaud's phenomenon. Unfortunately confusion in nomenclature did not end there. To date, this vasospasmic disorder has been referred to as a phenomenon, disease and as a syndrome. Medically the terms are quite distinct.[95] Raynaud's phenomenon is used as a blanket term for all forms of the digital vasospasmic disorder. Raynaud's disease, which is usually labelled primary Raynaud's disease, is a benign condition and is the most common form of vasospasm [Fig. 8a]. The more serious disorder, in which there is the potential for digital gangrene, is Raynaud's syndrome, or more correctly secondary Raynaud's syndrome [Fig. 8b]. This is distinguished from the former by occurring in combination with an associated vascular disorder, such as systemic sclerosis, systemic lupus erythematosis, Sjorgens syndrome or dermatomyositis.[89] At the extreme end of the scale is severe Raynaud's syndrome in which, in addition to vasospasm, there is also a permanent vascular obstructive element.[96] The situation is further confused by the description of both primary and secondary Raynaud's phenomenon. Primary Raynaud's phenomenon is in fact primary Raynaud's disease and secondary Raynaud's phenomenon is secondary Raynaud's syndrome. Thus primary refers to the disease and secondary relates to the syndrome. These two variations can be differentiated by thermography and by measuring finger blood flow with changing temperature [Fig. 8c & d]. Whilst primary Raynaud's patients show an increase and decrease in blood flow with a rise and drop in temperature, in a manner similar to normal subjects, secondary Raynaud's patients do not.[97]

Although the nomenclature outlined here is widely excepted within Europe, physicians in North America and Australasia insist on discussing the syndrome and the phenomenon in an interchangeable manner. Correlating global literature is consequently very difficult. This explains why there is an ever-increasing drive[95] for the European conventions [Fig.9] to become globally recognised. However, it is already the most popular choice and therefore the one that shall be adopted in this work.

Fig.8 *Illustrating the two forms of RP and how finger blood flow and thermography measurements help to distinguish between them.*

(a) Primary Raynaud's disease.

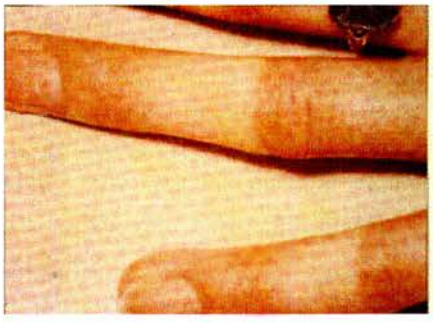

(b) Secondary Raynaud's syndrome.

(c) Thermography applied to secondary Raynaud's syndrome (top) & primary Raynaud's (bottom).

(d) Finger blood flow in control patients & in patients with primary and secondary RP.

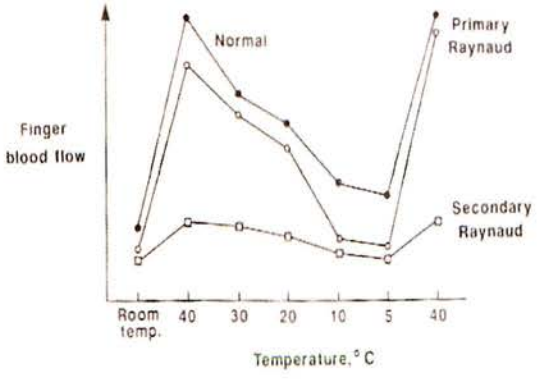

Figures 1(a), (b) & (c) are extracted from the "Colour Atlas of Peripheral vascular diseases,"[96] *Mosby-Wolfe, London, 1996, 4. Figure 1(d) was extracted from "Vascular Diseases in the limbs,"*[97] *Mosby, London, 1993, 153.*

Fig.9 *The European nomenclature that unambiguously labels the two major types of Raynaud's phenomenon (RP).*

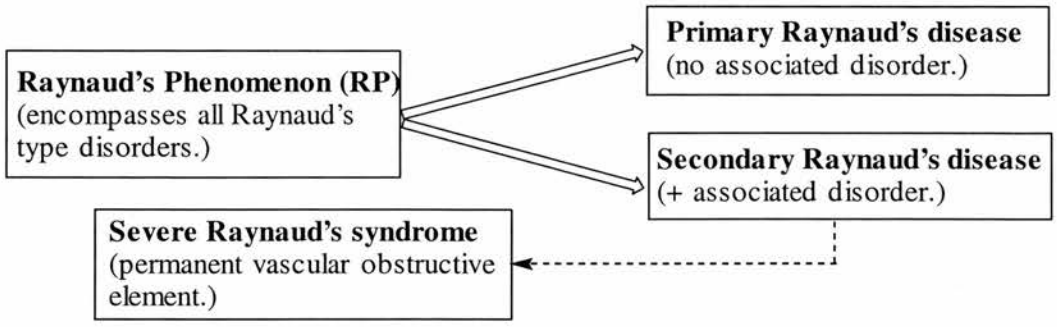

A representation of the nomenclature used by British and other European clinicians, which are supported by an editorial[95] that discusses the overlap and resulting confusion within the field.

1.2.5 Diagnosis of Raynaud's phenomenon.

With the disease having such subtle subdivisions, diagnosis in the earlier years may well have been hampered. It was perhaps with this in mind that Allen and Brown, in 1932,[97-99] devised a five-point criterion for determining the existence of primary Raynaud's phenomenon (PRP). Following the elimination of any possible secondary causes, PRP was defined by the medical profession using a globally accepted set of recommendations. A subject was labelled as a sufferer if symptoms remained in place over a two-year period and although exhibiting vasospasm on climatic or emotional stimulus, showed no evidence of gangrene or an associated vascular disorder.

It is interesting that, despite the existence of a diagnostic procedure, reported figures on the numbers affected by the condition vary from 4 to 30% of the population.[90,96,99-101] This may be as a consequence of varying diagnostic skills, though it is far more likely to be as a result of climatic differences. There is evidence to support this claim. For instance, when a group of forty-four sufferers were moved to a warmer climate, it was observed that more than fifty percent exhibited alleviated symptoms.[90] Indeed the five countries with the most reported cases of Raynaud's disease (Canada, Norway, Sweden, Finland and North America)[102] are all capable of experiencing cold, variable climates.

During hand blood flow work[103] in the late 1950's, patients reported that symptoms were always more severe in the left hand. Such findings are supported by Davies and

co-workers[104] who describe the skin temperature in the left hand as always being lower than that in the right. Whilst the two observations appear to be consistent, care is required since skin temperature cannot be used as a measure of relative blood flow. This was demonstrated by Cooper and fellow workers[105,106] who observed large rises in hand temperature when low flow rates were slightly elevated, yet only small increases in cutaneous temperature, when the flow was substantially improved. Thus in this work the need to measure blood flow is a clear requirement.

The range of methods now available for accurately measuring blood flow in the fingers is huge (section 1.3.3), though due to financial and time restraints, such methods are not suitable for routine diagnosis and are instead reserved for clinical trials. Due to this, measurement of digital systolic pressure, before and after local cooling of the hand, is the favoured methodology used in the clinic. On the basis of whether the pressure drops by a significant amount the patient can be diagnosed accordingly. A drop greater than 30mmHg is associated with the existence of the condition. Another diagnostic tool, devised by Maricq,[107,108] looks for nailfold capillaries using an ophthalmoscope. Such vessels are not observed in healthy individuals. However in subjects likely to experience the progression of Raynaud's the vessels are dilated and consequently are forced to adjust their position through 90°, resulting in their detection [Fig. 10]. Though this diagnostic work is considered elegant by current clinicians,[95] the same vessels have been observed in diabetic patients and following digital trauma.

Fig.10 *How nailfold microscopy utilises the two possible alignments of capillary blood vessels in the finger tip.*

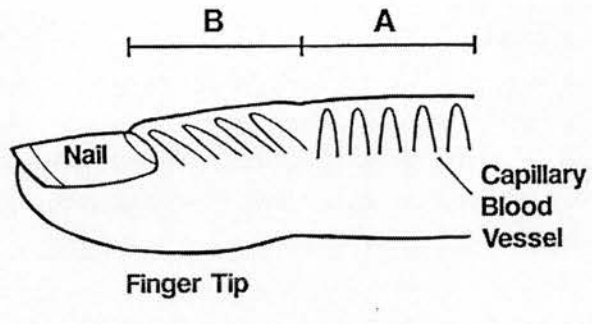

A - Vessels perpendicular, NOT visible.
B - Vessels becoming parallel. Visible if enlarged.

Extracted from thesis by C.S. Lau, University of Dundee, 1992, 60.[89]

1.2.6 The occupational form of Raynaud's phenomenon.

Occupational Raynaud's phenomenon is another form of the disorder. This is also known as occupational white finger disease. It is commonly exhibited in workers of vibrational tools with prime culprits being chain saws, industrial polishers and pneumatic drills.[96,109] This form is commonly named vibrational white finger (VWF). In other studies[110] this is referred to as TVD (traumatic vasospastic disease) or dead finger, due to the numb sensation experienced.

The work implicating an occupational origin spans over forty years and provides conclusive evidence to directly link the disorder to vibrational exposure. However, results from one study[104] comparing rivetters from a dockyard in Singapore with equivalent workers in England, suggest that whilst vibrational tools may "precipitate" Raynaud's phenomenon, the requirement of cold conditions is essential to "induce" such a disorder. In England 81% of rivetters showed signs of Raynaud's phenomenon. In comparison, no sufferers were identified from the thirty men tested in Singapore, a country with a uniform climate above 22°C. This suggests that a combination of vibration and intermittent cooling are the dual necessity on which Raynaud's phenomenon may develop. Such an idea was substantiated by a similar report[111] conducted in a sea fish processing plant. The study, performed in Poland, showed 90% of workers to have the disorder, yet reported no new cases when the plant eventually switched from manual to mechanical operation. Occupational Raynaud's phenomenon has also been attributed to workers exposed to vinyl chloride[112] and interestingly in ammunition workers during holiday periods.[89] This latter observation was first identified in girls who packaged explosives during the first world war.[113] Excessive NO exposure from nitroglycerine (glyceryl trinitrate) is thought to be responsible for their reported low blood pressure when at work. However, as a result of tolerance, the life threatening scenario for these individuals occurred during periods away from work due to a prolonged absence of NO exposure. Under such circumstances the workers were more prone to heart attacks due to elevated blood pressure. Such vasoconstriction, during times away from work, also explains the concurrent onset of Raynaud's attacks.

For occupations involving the use of vibratory tools, particularly in cold climates, it has been calculated that following a 2-7 year latent period, as many as 90% of

workers will be diagnosed with the condition.[89] In 1985 due to the scale of this disorder, the UK officially recognised Raynaud's phenomenon as a prescribed disease eligible for compensation.[114] Indeed Raynaud's phenomenon, despite little publicity, now has its own nation-wide association.[115] Sufferers are therefore able to acquire advice that has been medically approved. Amongst the information supplied, is the suggestion to avoid vasoconstricting drugs. This is in accordance with knowledge that certain drugs, such as β-blockers, are actually capable of inducing Raynaud's phenomenon.[89] Another preventative measure is to educate subjects who smoke with the evidence that this can further reduce cutaneous blood flow whilst enhancing vascular resistance.[110,116]

It has been shown that smoking a single cigarette, at ambient temperature, can reduce the fingertip temperature in a healthy individual by 2-3°C.[117] The effects of tobacco smoke can be better appreciated by comparing blood flow and vascular resistance in the foot before and after administration of adrenoceptor antagonists, reserpine and guanethidine[110] [Fig. 11]. The former affects noradrenaline synthesis whilst the latter inhibits noradrenaline release from the nerve terminals by preventing the vesicular uptake of noradrenaline.

Fig.11 *The effect of smoking on blood flow and vascular resistance in the foot.*

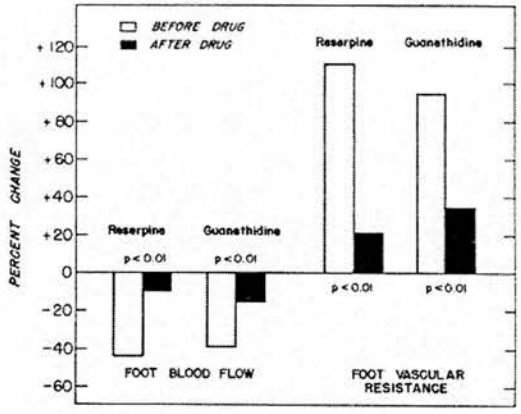

The beneficial effects of reserpine and guanethidine in dampening the increase in vascular resistance & drop in blood flow, following two regular cigarettes.
*Extracted from "Vasospasmic diseases: A Review," Prog. Cardiovas. Disease, 1975, **18**, 123.*[110]

Clearly cigarette smoke acts at the level of the sympathetic nervous system and ultimately results in vasoconstriction of the extremities. This heavily implies a

neuronal role, as at least one factor, in Raynaud's phenomenon. Such a theory will now be discussed in more detail.

1.2.7 Aetiological factors that may contribute to Raynaud's phenomenon and the subsequent treatments.

In addition to the effects of cigarettes, other studies have shown that migraine is related to Raynaud's syndrome.[118-120] This is no great surprise given the involvement of the 5-HT serotonergic two-phase pathway known for migraine. S_2-serotonergic receptors have been located in the human fingers.[121] These are activated by the sympathetic nervous system.

It has been recognised for some time that the hands and feet, the two body parts most commonly effected by vasospasm, contain only sympathetic nerve fibres,[110] with blood flow doubling when such nerves are blocked. The α_2 adrenoceptors, also activated by the sympathetic nervous system, have been strongly linked to Raynaud's phenomenon for many years.[122-125] Such receptors show a higher abundance in the platelets from Raynaud's patients[124] adding weight to their involvement. This explains the role of reserpine, introduced previously, as an agent capable of improving nutritional finger blood flow whilst reducing vascular resistance.[123] In the early seventies, this led Coffman and co-workers[123] to describe reserpine, which had shown benefit for fifteen years, as "a valuable addition to the physicians armamentarium in the treatment of Raynaud's disease and phenomenon." However this alkaloid from the *Rauwolfia* shrub is not used clinically today, due to its side effects such as postural hypotension and severe nasal congestion.[123] Yohimbine, which is another adrenoceptor antagonist, has also shown promise in treating Raynaud's, as it too is capable of producing the beneficial effects reported for reserpine.[125]

Neurogenic control of blood flow is not a new concept. In 1858, Claude Bernard described the action of the sympathetic nervous system as a vasoconstriction nerve.[89] Bevan (1979)[126] indicated that the microcirculation is largely under sympathetic neuronal control since such vessels are highly innervated with adrenergic nerves.

The hypothalamus appears to be one of the major neuronal control centres for digital circulation[127] since this is able to adjust the activity of the sympathetic nervous

system. The arteriovenous anastomeses (AVAs) known to be important in blood flow regulation are under the control of α_2 adrenoceptors. It has been calculated that these shunt vessels are able to transport fifty times more blood to the peripheral circulation than skin capillaries.[128] Thus the fact that such vessels are highly supplied with sympathetic nerve endings has to be significant.[128] The vasoconstrictor impulses produced in response to sympathetic activity have been shown to fluctuate in response to temperature and emotional stimuli. This correlates very well with the Raynaud's story.

As well as a neuronal control, there is also substantial evidence to implicate a chemical control of peripheral blood flow. Such chemicals come from two mayor stores, these being the endothelium and aggregating platelets. From the latter serotonin and thromboxane A_2 are produced, both of which are vasoconstrictors as is endothelin from endothelial cells. More importantly in terms of this work, the source of chemical vasodilators also centres upon the endothelial cells, which in addition to NO also supply prostacyclin (PGI_2).[89] This bicyclic prostaglandin is known to inhibit serotonin release and platelet aggregation. A study by Martin and co-workers,[129] substantiates these characteristics, as they showed how infusion of prostacyclin improved conditions in 88% of patients on the trial.

It should be appreciated at this stage that not only do platelets reduce blood flow by releasing vasoconstricting agents, but also as a result of aggregating, as this effectively impedes the transport through the blood vessels. In fact the two different scenarios actually happen simultaneously. In addition to platelet aggregation, resulting from the adherent surface generated by the action of thromboxane A_2, there is also platelet adhesion to the sub-endothelial layer taking place.[89]

Recent work[130] at the level of the endothelial cells suggests they may be responsible for the production of a third vasodilator. This has been termed EDHF, endothelium-derived hyperpolarising factor. In NO synthase knockout mice, *in vivo* and *in vitro* work has shown a vasodilation independent of NO or PGI_2. Whilst this would further intensify the interest upon the endothelium, supporting work, including the chemical identity of this species is required before it can be adequately compared with the currently recognised chemical mediators.

The significance of Raynaud's phenomenon being far more prevalent in females should not be overlooked. 80-90%[96,97] of sufferers are woman, commonly between 11 and 45 years of age.[97] This has sparked a number of studies trying to identify

Raynaud's patterns in menstrual and postmenopausal woman.[99] Enthusiasm in such work is heightened by one group[131] who report that cutaneous blood flow is greater in men, though go on to report how finger blood flow in women rises after the menopause. Alternatively, Ringqvist and co-workers[99] have shown how cGMP levels vary in females depending upon the season from which the measurements were taken. However, on the whole, despite the striking sex divide with regard to the numbers effected, the contribution of oestrogen and other female sex hormones remains poorly understood and is only discussed in very vague terms.[117]

Despite the clear level of chemical control within blood vessels, the majority of vasodilatory therapy on offer to Raynaud's patients appears to work on the neuronal pathway. For instance naftidofuryl[132,133] is a mild peripheral vasodilator with 5-HT antagonist properties,[133] while thymoxamine[117] enhances blood flow by blocking α_1 adrenoceptors.[133] Other vasoactive drugs do work at a chemical level, including the prostaglandins of which iloprost[89,134,135] appears to be the most effective. Strangely following injection the effects only remain in place for six weeks. The source of administration is another drawback although oral and transdermal forms are now available. Evening primrose oil and fish oil are also considered beneficial, as both are rich in vasodilatory prostaglandin precursors.[89,136,137]

As well as oily fish and fish supplements, it has been suggested that ginger and garlic do show benefit when dietary intake is enhanced.[138] Another recommended remedy for sufferers involves ginkgo biloba extracts, which have been shown by thermography to provide vasodilation.[139] In fact ginkgo biloba is one of the most widely used herbal products in the US as in addition to providing peripheral artery benefit, it is given in connection with Alzheimer's disease.[140] The ginkgo trees from which it is harvested are among the oldest living plant species and are notoriously hardy, which explains their existence in large cities.[140]

The leaves from such trees contain two useful substances, these being the flavanoids and the terpenes.[141] The latter inhibit platelet activating factor, which most probably accounts for their reported use in raising blood flow. However a German study[142] has shown that alkylphenols which are, for the most part, removed by an aqueous extraction process, have embryotoxic effects in the hen's egg test (HET). Thus although this treatment is widely advertised to Raynaud's sufferers,[138] it must be remembered that in effect one is dealing with a mixture of several active agents.[140]

Based on the toxicity data, it would appear important to obtain a highly pure batch before considering its vasodilatory potential.

Alternative therapies have evolved from first uncovering other abnormalities seen in Raynaud's patients. This explains the use of ketanserin, which is a serotonin antagonist. Its benefit was identified after higher serotonin plasma levels were reported in sufferers.[89] Conversely it was discovered that calcitonin gene related peptide (CGRP) is less frequent in the synapses of Raynaud's patients.[133,143] Since it is known to be a potent vasodilator, this has proven to be a useful treatment for RP.[95] However, by far and away the most prescribed drug in Raynaud's patients, to date, is nifedipine, which is now considered as the "gold standard"[89,144] for the condition. It is classed as a calcium channel antagonist and therefore operates by reducing intracellular calcium levels and disrupting the supply of calcium required for the actin-myosin interactions associated with muscle contraction. By operating at this late stage of the biochemical cascade it is able to inhibit abnormal activity at a neuronal and chemical level, thus it can be considered as a big safety net to abnormal activity at many levels.

To prevent tolerance to nifedipine it is usually administered via a controlled release preparation, which is also referred to as a retard prep. Its use in emergency situations, such as, severe spasmic attacks, is also documented.[133] In such instances the capsule form is crushed and then taken in a sublingual fashion. Long term usage of nifedipine can result in ankle swelling,[145] which is regarded as the biggest side effect of the drug. The more common side effects include dizziness, headache and flushing. Such effects are seen in one-third of patients taking the conventional dose.[117] However, its other major drawback is its forbidden use during pregnancy, presumably due to fears surrounding the change in fetoplacental blood flow and pressure.

Substitutes for nifedipine, which manipulate the same mechanism, are also being studied. Of these, diltiazem would appear attractive as this boasts fewer adverse effects. However, its beneficial properties are also dampened.[133] As well as peripheral vasodilators, these calcium channel blockers also function as antiplatelet and anti-white cell agents. Abnormal white cell behaviour is another characteristic of Raynaud's disorder.[133] The importance of the immune/inflammatory system in such patients is still not fully understood and explains why all drug targeting work is at the level of the sympathetic nervous system and the blood vessels themselves. However

it is known that the cytotoxic mediators, TNF and lymphotoxin, are capable of inhibiting endothelial growth.[133]

It is abnormalities at the level of the endothelium that form the basis behind the work here. Whilst a neuronal role for vasospasm is not being ruled out as a contributing factor, it has been suggested that perhaps it operates more as an aggrevation[123] to the condition than a direct stimulus. For instance, sympathectomy is not effective in abolishing Raynaud's in the upper limbs.[89] Similarly, drugs designed to target an overactive sympathetic nervous system only partially alleviate the situation at best, and even then such benefit is only of a temporary nature.[129]

In contrast, it is clear that an intact functioning endothelium is an essential requirement in avoiding RP, since it supplies many chemicals important in the maintenance of blood flow.[133] This view is supported by work on occupational Raynaud's phenomenon that highlights how arterial wall shear stress results in endothelial damage.[110] Since the occupational form shows the same symptoms as other forms of RP, this endothelial damage or dysfunction can be seen as a likely defect in all patients. Such a theory is supported and indeed taken a stage further by Freedman and co-workers.[87] They have findings consistent with the hypothesis that the NO pathway is involved in vasospastic attack. By supplying NO locally, it is hoped that improvements in the microcirculatory flow of the digits will be possible. This aim is made all the more tempting since, at present, there is no drug available that specifically dilates only the blood vessels of the fingers.[110]

The lack of a finger selective vasodilator may be argued by the description of a topically applied nitric-oxide-generating system by Benjamin and co-workers.[146] This involves mixing sodium nitrite and ascorbic acid in KY jelly upon the forearm and fingertips. However huge concentrations, of up to 15% (weight/volume) are reported and the release of NO is in no way controlled. The method is also very messy and painful when applied to broken skin. Thus, although this system has been improved[147] with a semipermeable membrane that is said to allow the passage of only NO, a more elegant system is required. Of course one system used extensively, particularly in the treatment of angina, is glyceryl trinitrate in topical form. However its effects on cutaneous blood flow are transient and subjects complain that the only noticeable long term effect is a throbbing head when administered at doses necessary for a beneficial RP responses.[146] On the basis of such reports, the challenge for a

satisfactory NO donor able to enhance blood flow in the digits alone, appears to be unresolved and therefore the goal of this work.

1.3 Transdermal drug delivery

1.3.1 Anatomy and physiology of the skin.

As the largest organ in the body, contributing to 16% of total body weight, skin has the role of being the body's main protective barrier. Despite this, drugs have been applied topically since Egyptian times.[148] Scopolamine, nitroglycerin, clonidine and estradiol are just four medications which take advantage of this "attractive" and "non-invasive method,"[148] which eliminates the potential of pain and infection associated with some administrative techniques.[149]

In studying the properties of skin there is a clear need for background on its anatomy.[150] For such an understanding it should first be appreciated that skin is based upon three major layers, these being the hypodermis, dermis and the most externally lying epidermis [Fig. 12]. Within such layers a fibrous protein known as keratin is found. This protein is responsible for the skin's protective function to toxic substances, whilst melanin found exclusively in the epidermis is a pigment that provides additional protection against UV light. The interface between the highly protected epidermis and the dermis is characterised by a series of ridges and grooves. This gives a fingerprint region known as the dermal papillae.

The epidermis, which is noticeably thinner than the underlying dermis, is defined as a keratinised epithelium with a stratified morphology. Keratinocytes make up the bulk of the cells in this region. Such cells undergo a process known as keratinisation which gives rise to the production of dead skin layers. Dendritic cells, which are commonly referred to as octopus-like cells, are found in the deepest layers of the epidermis. They are present as either melanocytes or Langerhan cells. Both cell types provide a form of protection to skin. The melanocytes are responsible for the production of the pigment melanin, whilst the Langerhan cells are antigen-presenting

cells derived from bone marrow. A third cell type found in the epidermis, either scattered as solitary cells or as aggregates, are merkel cells. Their role as touch receptors explains why they are often referred to as tactile corpuscles.

Fig.12 *The structure of the skin.*

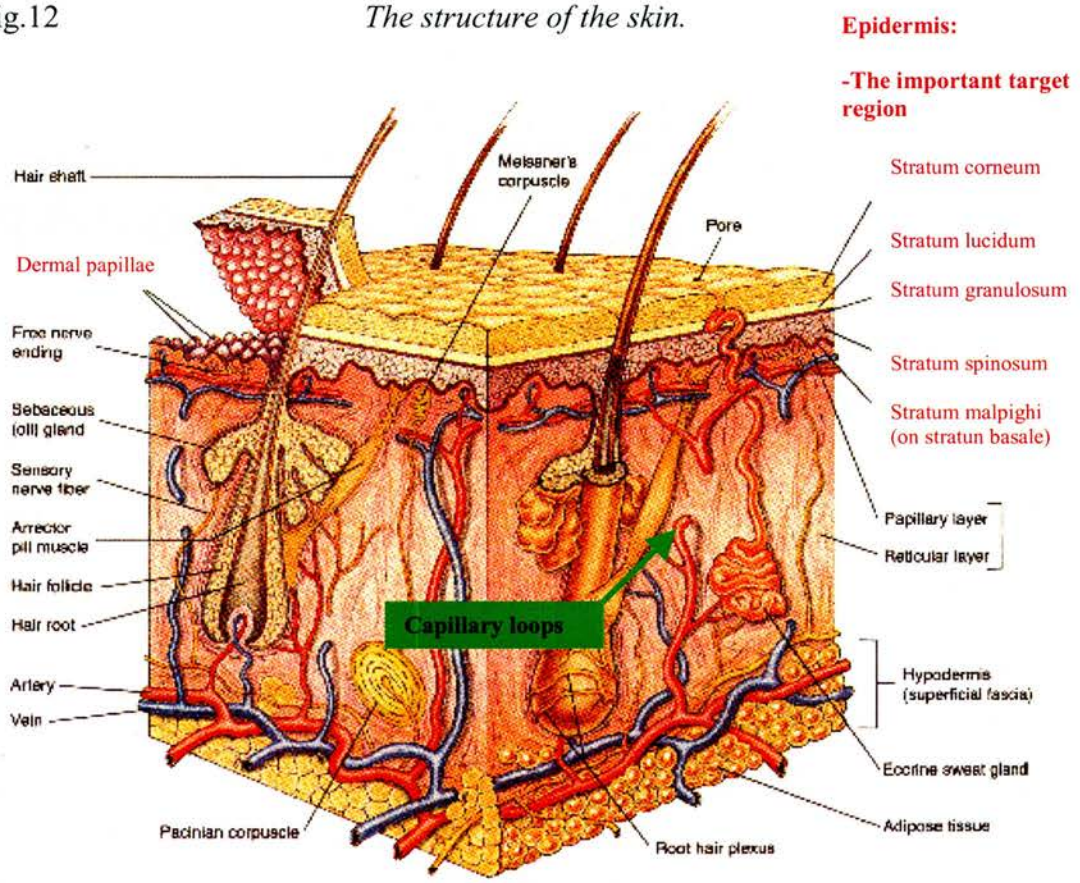

Extracted from 'Human Anatomy and Physiology' textbook, by E.N. Marieb, 1995, 3rd Edition, The Benjamin / Cummings Publishing Company, Inc., California, 136.[151]

Histological views of the epidermis show five very distinct layers. The deepest of these, the stratum malpighi, consists of a single cell layer resting on the stratum basale. Above this is found a prickle cell layer referred to as the stratum spinosum. The next region is a granular layer called the stratum granulosum. This sits beneath the stratum lucidum, which is constructed from a clear cell layer. Most superficial of all is the stratum corneum, totalling 10-20μm in thickness;[148] this horny layer is made up of cells full of keratin, thus fully keratinised and consequently dead. To obtain such a dead skin layer, the keratinocytes must first pass through the dermis, replacing all metabolically active cytoplasm with keratin, as they are continually displaced higher due to mitotic cell division below. Such a process, which takes

between 15 and 30 days depending on the body region, is the basis of keratinisation and ultimately responsible for the 10-12 cell layers making up the protective outer coating of human skin.

Pirot et al,[152] summarised the situation by stating that the excellent diffusional resistance of the stratum corneum makes the transdermal delivery of drugs at best difficult and frequently impossible. It has also been described as the major barrier to the percutaneous absorption of most topically contacting chemicals.[148] Extensive research in the field of topical administration, using electrical current[148] and low frequency ultrasound[149] suggests that the larger molecular weight compounds, and not just those with the correct presence of hydrophobic and hydrophilic groups, will branch into transdermal delivery systems. Alternatively, cis-oleic acid has been found to fluidize the intracellular lipid domains of the stratum corneum.[148] Another avenue of research is in the production of rate-controlled drug administration.[153] Based on such work, the passive diffusion progress made by radio-labelled drug candidates across the stratum corneum can be monitored by repeated adhesive tape stripping, together with scintillation counting.[152]

In this work the diffusion of NO-donors has been monitored by observing the related blood flow increases using a laser-Doppler imager (LDI) [section 1.3.3]. The lipophilic character of the stratum corneum is the factor most significant in any rationale for designing a suitable drug for transdermal delivery. The other major requirement is an understanding of NO's role, if any, within the skin. As far as we are aware this is a largely unexplored model, though as presented in the following section, the potential for NO in cutaneous tissue has not escaped the attention of all dermatologists.

1.3.2 NO in the skin.

The identification of nNOS in mouse epidermis and outer root sheath cells in 1994 was a significant finding.[154] Further to this, in healthy human skin, eNOS was found in the cytoplasm of basal keratinocytes[155] and also in the blood vessels of the deep dermis and papillary.[156] The third isoform of NOS, that of iNOS, has also been isolated from host cells including the keratinocytes[157] along with Langerhans cells.[158] The role of NO in the skin is the next obvious question. Weller[159] admits that much

remains to be discovered, but provides evidence of its involvement in sunburn, wound healing and psoriasis.

Taking these three medical situations in order, there is undoubted evidence[159] that NO can prevent UVA induced apoptosis for up to 6 hours after irradiation. UVA can penetrate down into the dermis, but Weller has shown how apoptosis of keratinocytes can be suppressed by exogenous NO in the form of the diethylenetriamine-NO complex (DETA-NO) [Fig. 13]. The visual characteristic of sunburn is a result of keratinocyte apoptosis which, coincides with high levels of epidermal iNOS. During this erythema period, NO has actually been detected as it diffuses from the skin's surface.[159,160] This suggests that the levels of NO are important in governing the fate of the keratinocyte after UVA exposure. This was confirmed by applying a NOS antagonist.[159]

Fig.13 *Illustrating how UVA induced apoptosis of HaCaT keratinocytes is suppressed in the presence of exogenous NO for up to 6 hours.*

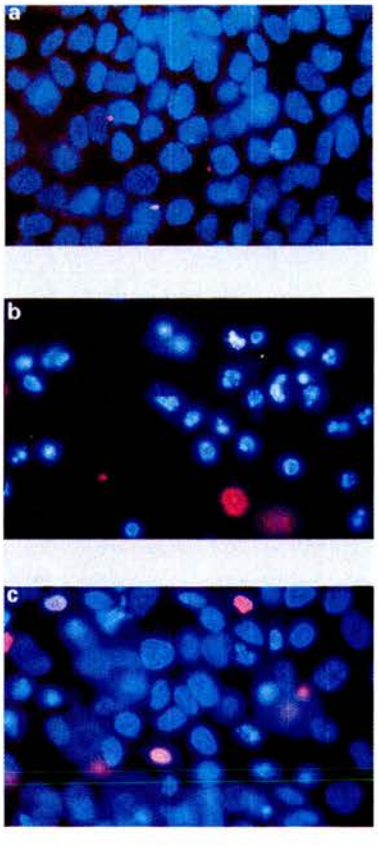

(a) Coincubation of 0.5mM DETA-NO and keratinocytes with no UVA irradiation (CONTROL)

(b) UVA irradiation in the absence of exogeneous NO. (using 0.5mM DETA without NO)

(c) UVA irradiation in the presence of exogeneous NO (using 0.5mM DETA-NO)

The fluorescence photographs were obtained by microscopy after cell staining with Hoechst 33342 and propidium iodide. Blue = normal healthy nuclei, white = apoptotic body, and red = necrotic cell. This was extracted from a review by R. Weller, Clinical and Experimental Dermatology, 1999, ***24****, 388.*[159]

In a rat model,[161] a NOS inhibitor was again called upon, this time in order to illustrate the involvement of NO in epidermal wound healing. Using *N*-nitro-L-arginine methyl ester (L-NAME) the healing of UVA-induced necrosis was stunted. This same effect was observed with iNOS knockout mice. After observing a prolonged healing time, the normal rate was re-established by transfecting the iNOS gene.[162]

Whereas the latter example shows how a deficiency in NO can be adverse, patients with psoriasis illustrate how the reverse scenario can be equally damaging. Typically NO concentrations are 100-1000 fold greater than in healthy subjects.[163] This is due to overactivity of iNOS, which has led to treatments targetted at iNOS suppression. One upshot of such elevated levels of NO may be the low number of reported bacterial infections in this subject group.[164,165] This is supported by bactericidal work which shows NO's potent role in fighting infection.[166]

The production of NO in many different cell types situated on the body's outermost core is good in evolutionary terms, given NO's antibacterial activity. Yet the body goes one stage further by also generating a continuous low level of NO by a NOS-independent mechanism on the skin surface.[167] Using bacterial nitrate reductase in the skin flora, sweat nitrate can be reduced to nitrite. This can be further reduced to free NO due to the slight acidity of skin. In healthy subjects, NO levels are obviously higher in skin regions of lowest pH and on skin surfaces prone to sweating, such as the hands (120 fmol/cm^2 per minute). While NO acts as an extra defence mechanism here, its production is clearly under the control of bacterial nitrate reductase. This is highlighted by patients on antibiotics to treat acne, where NO levels are typically reduced to 30 fmol/cm^2 per minute, due to the loss of the reduction pathway.[165]

For the benefit of this work there was simply a need to know if NO can exist in the skin. Clearly the answer is yes. It appears that NO is not scavenged, metabolised or excreted by the skin and there is free passage across the various layers. This is reassuring, since if the proposed NO donors fail to operate at the active site of guanylate cyclase, their decomposition in the local vicinity may be adequate in supplying sufficient NO. Weller[165] describes how NO biosynthesised from normal human skin is important in maintaining the resting dermal microvascular tone, thus supporting the notion of NO travelling through tissue before acting upon guanylate cyclase. NO derived from skin, is not necessarily produced by endothelial cells

adjacent to the vascular smooth muscle, as is thought to be the case in the deeper vascular beds. Instead the NO may have originated from the keratinocytes or even from the skin's surface.

The requirement for NO in the homeostasis of cutaneous blood flow has been emphasised by Goldsmith and colleagues.[168] They showed, by LDI, that administration of the constitutive NOS inhibitor, L-NAME, by transdermal injection, led to a drop in blood flow. Using our new NO donors we will endeavour to show the opposite effect on the microcirculation. As in the work by Goldsmith the laser Doppler imaging technique will monitor all blood flow responses.

1.3.3 Using the laser Doppler imager (LDI) to measure superficial blood flow.

Over the years many methods have been adopted for measurement of finger blood flow. The idea of correlating temperature changes, from thermography and calorimetry, into meaningful blood flow readings, has already been discredited in earlier discussion (section 1.2.5). In contrast, techniques such as venous occlusion plethysmography present data on blood volume as opposed to flux.[89] Based upon a slightly different line of thought, radio isotopic clearance work has been applied, though the reported[89] high costs have restricted its use as a standard protocol. More importantly, the experimental error here is high, due to the variable depth with which the administrator can potentially inject the tracer substance.

The ideal situation is to obtain a blood flow measurement by direct means. This can be achieved using the ultrasonic Doppler instrument. Unfortunately this detects blood flow down to a tissue depth of 2.5cm, where the AVAs (section 1.2.7) and other larger vessels are housed. Thus the obtained reading is not a true reflection of the blood supply to the microvasculature. Although this particular piece of equipment is inappropriate for this work, the theory involving the Doppler effect, described first by Austrian astromer physicist Johann Christian Doppler, has been incorporated into the laser Doppler imager (LDI).

In 1990, Oberg[169] described the use of this apparatus as a new method for the continuous and non-invasive measurement of tissue blood flow, utilising the Doppler shift of laser light as the information carrier. It is widely accepted that the vast

majority of the signal obtained will be as a result of the travelling red blood cells, which can be detected using a helium-neon laser, capable of penetrating the skin only to a depth of between 0.6 and 1.5mm [Fig. 14]. Such equipment, to measure capillary fingertip flow, appears to have replaced the techniques described previously. That said, the LDI has its own drawbacks. For instance epidermal thickness, skin pigmentation and blood haemoglobin content, may all distort the output signal.[89] However, all of these limitations are based upon subject variability, which will exist in one form or other in all systems. On the positive side, the instrument is easy to use and requires minimum patient preparation, making the technique the one of choice in this field. Its ability to respond within 0.2 seconds to fluctuations in blood flow, is obviously another advantage, as this allows a clear interpretation of the acquired data, as drugs are applied, removed or altered in dosage.

Fig.14 *The basic set-up of a laser Doppler flowmeter.*

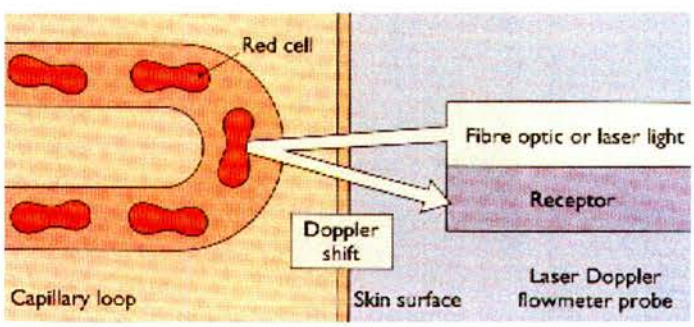

The monochromatic light from the optical fibre of the laser, upon skin penetration, will be absorbed and scattered. Any back scattered light will result from interactions with both static and mobile entities. Light returning from mobile collisions will be of a slightly different frequency and will be largely as a result of RBC interactions. Thus following detection, this frequency difference will be transformed into an electrical signal equivalent to a red blood cell flux.

Extracted from the "Colour Atlas of Peripheral vascular diseases," Mosby-Wolfe, London, 2nd ed., 1996, 26.[96]

1.4 Designing a transdermal NO donor drug.

1.4.1 What is required?

In addressing this question, it is first necessary to look at the existing NO donor compounds. The obvious example is GTN (section 1.1.2). This is a widely known venoselective drug that requires metabolism to produce free NO. However it is also acknowledged that tolerance to GTN ensues with continuous administration. This is attributed to a reduction in biological activity rather than a deficiency in the metabolic pathway.[170] Despite this, the requirement for biological intervention in order to obtain the active form of the drug is clearly imposing an additional level of dependence that would be best avoided. Certain other avenues should also be treated with caution, particularly if there is the potential for faults at many levels. For instance, the β-1 selective blocker, celiprolol[171] is thought to utilise endogenous NO. This clearly restricts the drug's potency by introducing dependence at the level of the endothelium, since it requires this inner lining of the blood vessel to be both fully intact and functional, for an optimum response. Thus, by using NO-donor drugs we bypass this difficulty.

The ideal situation, from a design specification, is for a NO-donor compound with a long shelf life yet with the ability to decompose, at albeit a slow rate, once at or near the *N*-terminal region of guanylate cyclase. At concentrations which give the desired biological response, the parent compound and its metabolites should show no toxic responses or any skin irritation. In addition the compound should be easily incorporated into a cream or gel. From such a formulation the drug should be able to penetrate the skin without assistance from ultrasound,[149] electrophoresis[148] or any other technique that would narrow its potential therapeutic use. Upon uptake, the compound should not be rapidly excreted but should instead preferentially sit in the target tissue. One of the old NO donors to fit this latter criterion, is Roussin's Black salt [Fig. 15]. This selectively accumulates in the vascular beds and releases NO over a prolonged period.[172]

Fig. 15 *The structure of Roussin's Black salt; one of the original NO donors.*

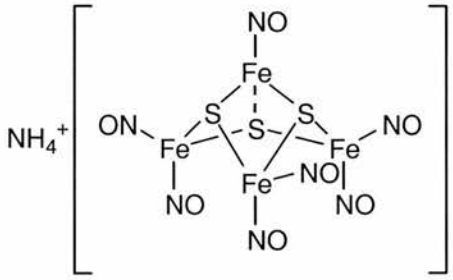

Roussin's Black Salt

1.4.2 The use of *S*-nitrosothiols.

The target compounds in this work all contain the *S*-nitrosothiol functionality. While their presence and activity continues to be utilised in many situations, their actual role is highly debatable. Gladwin and co-workers[70] suggest they have a limited involvement in the maintenance of basal vascular tone, even during NO synthase inhibition. In sharp contrast, Gross and Lane[65] propose that SNO levels may be diminished in vascular diseased tissue and predict that *S*-nitrosothiols may give a direct route for NO delivery to the vessel wall more effectively than NO itself. Reports[173-4] of prolonged *S*-nitrosothiol activity, with no tolerance, in human saphenous vein and rat femoral artery, add support to this view. The third possibility rests between these two extreme ideas. This proposes that *S*-nitrosothiols act as intermediates for endogenous NO and nitrates. Thus their role is one of storage and transportation.[22] This suggestion is well supported as the half life of NO can be substantially enhanced by its binding to either glutathione, serum albumin or other thiol groups of tissue protein.[175]

From work in *E. coli*, Stamler and co-workers[176] have data to support the idea of *S*-nitrosothiols having evolutionarily conserved metabolic pathways. Whilst such findings may eventually spread to the animal and plant kingdoms, we shall attempt to utilise *S*-nitrosothiol's more convention degradation pathways. In concentrating on the thermal,[177-8] photochemical[178-9] and copper catalysed[83-84] decomposition of these compounds, we will hopefully eliminate the extra constraints, previously described, in relation to metabolic requirements [see Scheme 7].

On the basis of these factors, it may be possible to design a more elaborate NO donor. Such an idea may require the incorporation of some form of chemical handle

by which the rate of NO release could be controlled. This additional feature would make the compound significantly more versatile and appealing.

Scheme 7. *The thermal, photochemical and copper catalysed decomposition of S-nitrosothiols, to give the corresponding disulphide and free NO.*

2 RSNO → RS-SR + 2NO

Thermal,
Photochemical,
Copper catalysed.

The action of copper is perhaps the most intriguing of the three decomposition factors, since levels in the micromolar range are significant enough to elicit a faster release of NO. Thus *in vivo* copper levels from dietary in-take may allow for these same rate enhancements. From blood, bone and muscle such levels are reported[180] to be in the region of 0.1g / 75kg (body weight), though most of this is protein-bound making *in vitro* correlations with the *in vivo* scenario even more difficult.

The relevance of copper in the decomposition of the S-NO bond is widely known and accepted. However, upon closer inspection, the situation is more confusing than it appears. The discovery of copper catalysis[83] was quickly followed by the appreciation of Cu(I) as the important ion.[84] As illustrated in scheme 8 this requires the initial presence of free thiol for the necessary oxidation state change. However, as well as acting as a reducing agent, free thiol can also complex with adventitious Cu(II), thus effectively arresting the release of NO.[181] While this introduces an extra determining factor into the equation, the picture is further distorted by the knowledge that certain resulting disulphides are themselves involved in copper complexation.[182] This is exemplified by the disulphide produced from glutathione, as its glutamate residues provide perfect sites for sequestering Cu(II).

From an understanding of these copper catalysed decompositions, it would appear that the main chemical body to which S-NO is tethered, is fundamental to the rate of NO release. Such a conclusion is not merely based on the chemical potential of the free thiol or the corresponding disulphide, but is also related to the chemical environment around the SNO group. Williams[180] states that the most reactive *S*-nitrosothiols are those, which can coordinate bidentally with Cu(I). As illustrated

below in Fig. 16, such coordination can be achieved with *S*-nitrosocysteine (SNOC) and in so doing so the S-NO bond is sufficiently weakened for the release of NO. When the carbon chain is extended by one carbon atom to give homocysteine, the SNO group is shown to be indefinitely stable in comparison to its slightly smaller sister compound. The dramatic difference in reactivity is attributed to the formation of the highly unfavourable seven membered ring complex [Fig. 16].

Scheme 8. *The decomposition of an S-nitrosothiol in the presence of adventitious levels of Cu(II).*

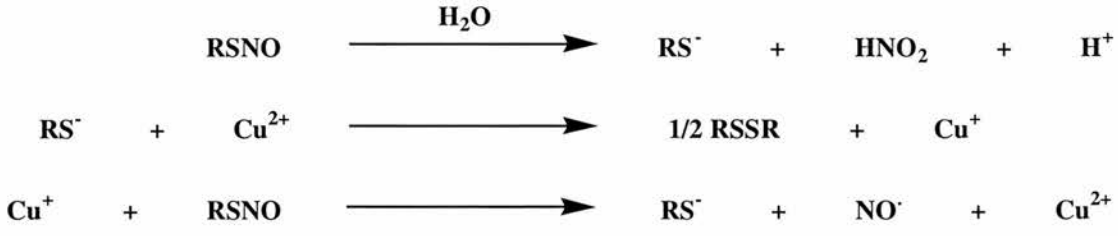

Fig. 16 *Illustrating the bidentate potential of cysteine and homocysteine with Cu(I).*

Cu(I) complexed to *S*-nitrosothio-cysteine

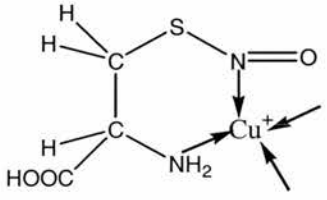

Rate of reaction with Cu(I) is,

k_a 24 500 $(dm^3\ mol^{-1}\ s^{-1})$[180]

Cu(I) complexed to *S*-nitrosothio-homocysteine

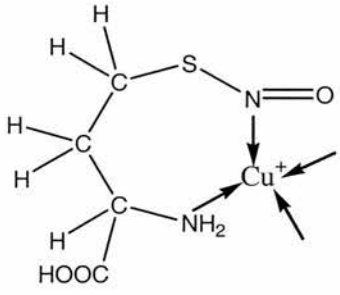

Rate of reaction with Cu(I) is,

k_a *ca.* 0 $(dm^3\ mol^{-1}\ s^{-1})$[180]

In keeping with the suggested model by Williams and co-workers,[180] *the bidentate complex is shown with direct interaction between Cu(I) and the nitrogen of the SNO group, rather than with the sulphur atom.*

Control upon reactivity is therefore possible by altering the ring size. Alternatively substantial rate changes have been encountered[180] by incorporation of an acetyl /ester group on the electron donating substituent [Fig. 17] which forms the 'non-SNO' half of the bidentate complex. Consequently the chemical handle, described earlier, may indeed exist, allowing the potential manipulation of NO release.

Fig. 17 *An alternative electron donating substituent from which a bidentate complexation can be formed.*

Cu(I) complexed to another electron donating substituent.

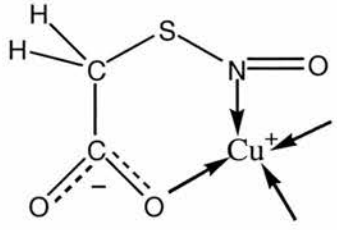

Alkylation of this electron donating carboxylate group will dramatically reduce the ease of complexation to this site and consequently result in a slower rate of NO degradation. A similar effect is seen upon N-acetylation of an electron donating amine group.

Further to this line of thought, it has been suggested that the lower complexation rate of *S*-nitroso-*N*-acetylpenicillamine, SNAP (k_a 20 dm^3 mol^{-1} s^{-1}),[180] compared with *S*-nitrosocysteine (k_a 24 500 dm^3 mol^{-1} s^{-1}),[180] can be explained by steric factors. It is believed[183] that the two methyl groups positioned adjacent to the SNO group of SNAP are sufficient to interfere with the formation of a bidentate complex. Thus we have electronic, steric and ring constraining factors with which to fine-tune the stability of the S-NO bond. However, whilst accepting the steric effect it should be treated with some scepticism since the true comparison, in this instance, is that between *S*-nitroso-*N*-acetylpenicillamine (k_a 20 dm^3 mol^{-1} s^{-1})[180] and *S*-nitrosopenicillamine (k_a 67 000 dm^3 mol^{-1} s^{-1}).[180] These compounds allow us to selectively look at the effect of *N*-acetylation, as in both cases the two adjacent methyl groups are present. The massive difference in the rate of copper complexation strongly suggests that while the steric factor may have a contribution, the electronegativity of the substituent in the gamma position to the SNO functionality is by far the over-riding feature that ultimately governs the liberation of NO.

1.4.3 Carbohydrate based *S*-nitrosothiols.

All of the compounds synthesised and tested in this work are carbohydrates. There are several reasons for this choice. Firstly, it is well documented that the chiral pool is one of the most frequently used sources within the pharmaceutical industry. As described by Petsko,[184] nearly all 'wonder drugs' in use today are derived from natural products due to their proven record. In terms of transdermal agents, compounds such as polypeptides[185] are inappropriate due to being unable passively to permeate the various skin layers. While passive diffusion may well exist for carbohydrates (section 1.4.4) there is unequivocal evidence of sugar transporters in biological membranes. For instance, epithelial cells[186] lining the intestines have shown facilitated glucose transport with such transport increasing in the presence of elevated carbohydrate levels.[187] D-Glucose and D-galactose have also shown uptake through brain tissue by utilising the mammalian sugar transporter, known as GLUT3.[188] The facilitated transport of monosaccharides in mammalian cells by the GLUT transmembrane protein family, as described earlier (section 1.1.4b), adds weight to their potential in dermal applications. Cell surface carbohydrates have also been clearly defined from organotypical cultures of skin.[189] From a toxicological stance, carbohydrates are very user-friendly compounds, as the degradation of free thiols or resulting disulphides will be well within the body's metabolic capabilities. This is supported by the finding that all of the enzymes required in the glycolytic pathway and the resulting tricarboxylic acid cycle, have been identified within skin.[190] Indeed the metabolism of glucose has been confirmed by radiolabelling.[191] Such evidence should increase the chances of ethical permission for this work to be carried out on healthy subjects and Raynaud's patients as strict regulations are in place (section 3.1). Disturbingly, work by Tesfamariam and co-workers,[192] described how elevated glucose levels can evoke endothelial dysfunction similar to that seen in diabetics. Obviously in this work such a finding is highly unfavourable. However, Hansen and co-workers[193] have more recently discredited this suggestion.

1.4.4 Rationale behind the list of target compounds.

The rationale behind the chosen target compounds, shown on the following page [Fig. 18], will now be introduced, with the favoured sugars, positioning of the SNO group and choice of ring substituents being central to the discussion. One of the first observations from the list of target molecules is the use of acronyms, these are all derived on the basis of their sugar template, as explained in table 1.

Fig. 18 *Illustrating the Synthetic Aims*

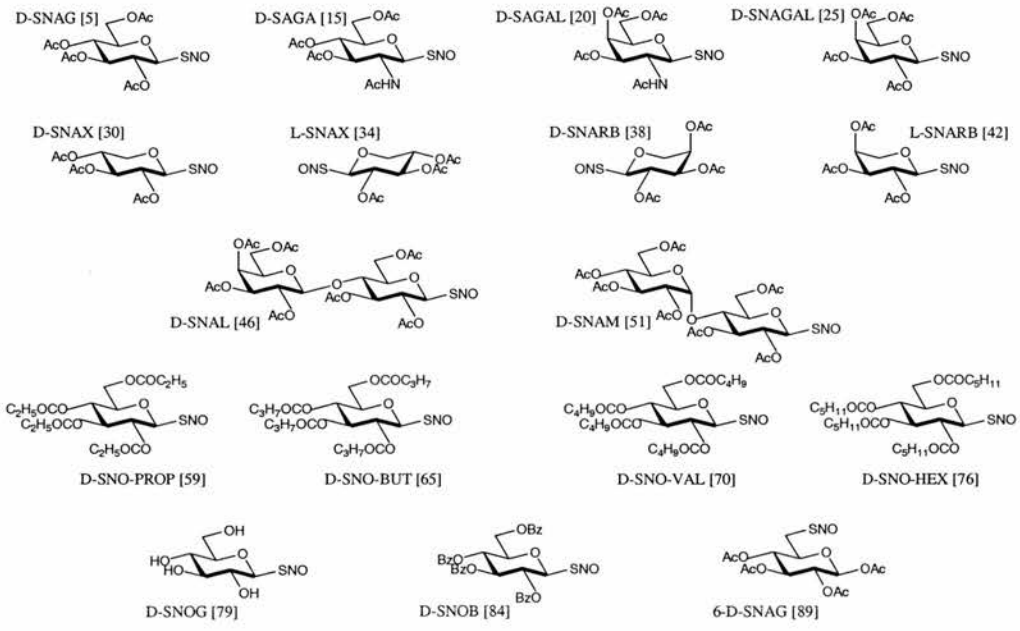

Table 1 *The acronym, full chemical name and the necessary starting material for each of the target compounds.*

Acronym	*Full chemical name*	*Starting material*
D-SNAG	*S*-Nitroso-1-thio-2,3,4,6-tetra-*O*-acetyl-*β*-D-glucopyranose	D-glucose
D-SAGA	*S*-Nitroso-1-thio-2-acetamido-3,4,6-tri-*O*-acetyl-2-deoxy-*β*-D-glucopyranose	D-glucosamine
D-SAGAL	*S*-Nitroso-1-thio-2-acetamido-3,4,6-tri-*O*-acetyl-2-deoxy-*β*-D-galactopyranose	D-galactosamine
D-SNAGAL	*S*-Nitroso-1-thio-2,3,4,6-tetra-*O*-acetyl-*β*-D-galactopyranose	D-galactose
D-SNAX	*S*-Nitroso-1-thio-2,3,4-tri-*O*-acetyl-*β*-D-xylopyranose	D-xylose
L-SNAX	*S*-Nitroso-1-thio-2,3,4-tri-*O*-acetyl-*β*-L-xylopyranose	L-xylose
D-SNARB	*S*-Nitroso-1-thio-2,3,4-tri-*O*-acetyl-*α*-D-arabinopyranose	D-arabinose
L-SNARB	*S*-Nitroso-1-thio-2,3,4-tri-*O*-acetyl-*α*-L-arabinopyranose	L-arabinose
D-SNAL	*S*-Nitroso-1-thio-2,2',3,3',4',6,6'-hepta-*O*-acetyl-4-*O*-(*β*-D-galactopyranosyl)-*β*-D-glucopyranose	D-lactose
D-SNAM	*S*-Nitroso-1-thio-2,2',3,3',4',6,6'-Hepta-*O*-acetyl-4-O-(*α*-D-glucopyranosyl)-*β*-D-glucopyranose	D-maltose
D-SNO-PROP	*S*-Nitroso-1-thio-2,3,4,6-tetra-*O*-propionyl-*β*-D-glucopyranose	D-glucose

D-SNO-BUT	*S*-Nitroso-1-thio-2,3,4,6-tetra-*O*-butyrionyl-*β*-D-glucopyranose	D-glucose
D-SNO-VAL	*S*-Nitroso-1-thio-2,3,4,6-tetra-*O*-valerionyl-*β*-D-glucopyranose	D-glucose
D-SNO-HEX	*S*-Nitroso-1-thio-2,3,4,6-tetra-*O*-hexionyl-*β*-D-glucopyranose	D-glucose
D-SNOG	*S*-Nitroso-1-thio-*β*-D-glucopyranose	D-glucose
D-SNOB	*S*-Nitroso-1-thio-2,3,4,6-tetra-*O*-benzoyl-*β*-D-glucopyranose	D-glucose
6-SNAG	*S*-Nitroso-6-thio-2,3,4,6-tetra-*O*-acetyl-*β*-D-glucopyranose	D-glucose

In order of appearance [Fig. 18], the first structure is that of SNAG, *S*-nitroso-1-thio-2,3,4,6-tetra-*O*-acetyl-*β*-D-glucopyranose. This was the lead compound[194-6] when this project began. In a clinical trial during 1997/8, inconsistencies in its stability and biological response in healthy subjects suggested it should be re-investigated before contemplating other derivatives.

SNAG itself was chosen for several reasons. Most obvious of all, was the fact that it is sugar based, which at the time set it a part from the commonly available amino acids (e.g. *S*-nitrosocysteine, SNOC), penicillamines (e.g. *S*-nitroso-*N*-acetyl-penicillamine, SNAP) and peptides (e.g. *S*-nitrosoglutathione, GSNO). The potential benefits of incorporating a carbohydrate structure into a target molecule have already been postulated (section 1.4.3). However, due to the many free hydroxyl sites there is also the potential to add many different substituents, whilst keeping the SNO group at the reactive anomeric position. This property shows how the drug's lipophilicity could be varied in accordance with the skin's known lipophilic character. Using this logic, SNOG, SNOB and the propionylated, butyrionylated, valerionylated and hexanionylated derivatives of SNAG were synthesised. Such an investigation is solely concerned with enhancing the uptake of the NO donor. Thus Log P work accompanies the biological data to allow for adequate comment on the effect of the drug's lipophilicity.

On a similar theme, the galactose derivative was chosen based on solubility grounds. It is widely known to carbohydrate chemists that the equatorial to axial change in configuration at the C-4 position [Fig. 18] substantially alters the solubility of the molecule. In fact this subtle structural difference brought about solubility differences so great that even the synthetic strategy required adjustment (section 6.6).

On the basis of the copper complexing work by Williams,[180] the sugar molecule should show adequate stability in aqueous solutions, if the 2-position of the ring is *O* or *N*-acetylated [see Fig. 19]. For completeness, the galactosamine derivative was

also included, so that the dual idea of solubility and *O*/*N*-copper complexation could be examined.

Fig. 19 *Considering the potential for copper complexation in SNAG and SAGA.*

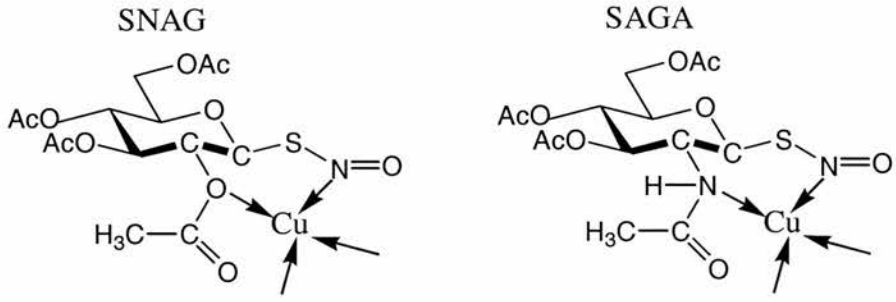

Although the sugar backbone lends itself to copper complexation by housing a site able to form a six membered intermediate, the likelihood in the acetylated derivatives is dramatically reduced, according to Williams.[180]

Upon closer focus of the skin's anatomy, the selection of the four previously mentioned sugars can be explained in a biological sense. From work[197] exclusively investigating glucose concentrations in the epidermis, it was found that levels in the extracellular space were lower than expected. It has therefore been proposed that the epithelial cells may also accommodate glucose. For such a scenario, it was further suggested that glucose could freely diffuse into such cells and therefore take full advantage of an extra host site. Alternatively, using membrane structural probes specific for sugar residues, a different group[198] have reported that glucose, galactose, glucosamine and galactosamine are all present on the surface of these epithelial cells. Later work,[199] with pig skin, has found a range of glycosaminoglycans (GAGs) in the epidermis. From studying the composition of these GAGs, three of the previously mentioned sugars were again confirmed. In addition D-xylose was also identified. As Fig. 18 shows, both D- and L-SNAX (see also Table 1) have been selected for synthesis and testing. The rationale here, in addition to the reported presence of the D-form in skin, is that in studying both isomeric forms, a difference between the two in a biological sense, would support the idea that these molecules act at the level of the active site of an enzyme. Based on this same rationale, D- and L-SNARB were

also included in the target list. Their inclusion is also related to their axial C-4 and the resulting solubility change that this entails.

Moving onto the disaccharides, the study of lactose and maltose is simply to see if the increase in size of the NO donor is significant to the biological response. Finally, the last requirement is for 6-SNAG. This will enable, by comparison, investigation into the importance of having the thiol at the anomeric position. For instance, the stability of this compound will be of prime interest, since the potential for copper complexation involving the ring oxygen, would in theory allow the formation of the six membered complex, as shown [Fig. 20].

Fig. 20 *The possibility of copper complexation at the 6-position of the sugar.*

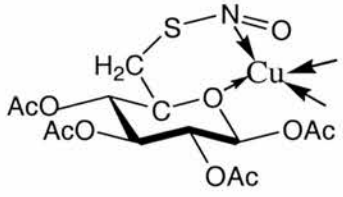

This idea, again based on work by Williams,[180] heavily relies on the potential of the ring oxygen to act as an electron donating substituent.

On the basis of the SNO decomposition data and the biological literature on the skin, it is clear that SNO-tethered carbohydrates are of value.

1.5 References

1 D.E. Koshland, *Science*, 1992, **258**, 1861.

2 R.F. Furchgott and J.V. Zawadzi, *Nature*, 1980, **288**, 373.

3 L.J. Ignarro, G.M. Buga, K.S. Wood, R.E. Byrns and G. Chaudhuri, *Proc. Natl. Acad. Sci. USA*, 1988, **84**, 9265.

4 F. Murad, W.P. Arnold, C.K. Mittal and J.M. Braughler, *Adv. Cyclic Nucleotide Res.*, 1979, **11**, 175.

5 C.R. Molina, J.W. Andresen, R.M. Rapoport, S. Waldman and F. Murad, *J. Cardiovasc. Pharmacol.*, 1987, **10**, 371.

6 R.M.J. Palmer, A.G. Ferrige and S. Moncada, *Nature*, 1987, **327**, 524.

7 F. Guthrie, *J. Chem. Soc.*, 1859, **11**, 245.

8 T.L. Brunton, *Lancet*, 1867, **2**, 97.

9 W. Murrell, *Lancet*, 1879, **1**, 80.

10 A. Ringquist, Thesis, Goteborg University, Sweden, 1998.

11 W.B. Cannon, *The Wisdom of the Body*, W.W. Norton and Company, Inc., New York, 1939.

12 R.M.J. Palmer, D.S. Ashton and S. Moncada, *Nature*, 1988, **333**, 664.

13 H.H.H.W. Schmidt, H. Nau, W. Wittfoht, J. Gerlach, K.E. Prescher, M.M. Klein, F. Niroomand and E. Bohme, *Eur. J. Pharmacol.*, 1988, **154**, 213.

14 E. Hegesh and J. Shiloah, *Clin. Chim. Acta*, 1982, **125**, 107.

15 D.A. Wagner, V.R. Young and S.R. Tannenbaum, *Proc. Natl. Acad. Sci. USA*, 1983, **80**, 4518.

16 D.J. Stuehr and M.A. Marletta, *Cancer Res.*, 1987, **47**, 5590.

17 M.A. Marletta, P.S. Yoon, R. Iyengar, C.D. Leaf and J.S. Wishnok, *Biochemistry*, 1988, **27**, 8706.

18 J.B. Hibbs, R.R. Taintor, Z. Vavrin and E.M. Rachlin, *Biochem. Biophys. Res. Commun.*, 1988, **157**, 87.

19 D.J. Stuehr, S.S. Gross, I. Sakuma, R. Levi and C.F. Nathan, *J. Exp. Med.*, 1989, **169**, 1011.

20 R. Farias-Eisner, M.P. Sherman, E. Aeberhard and G. Chaudhuri, *Pharmacol*, 1994, **91**, 9407.

21 J.S. Beckman, T.W. Beckman, J. Chen, P.A. Marshall and B.A. Freeman, *Proc. Natl. Acad. Sci. USA*, 1990, **87**, 1620.

22 J.S. Stamler, D.I. Simon, J.A. Osborne, M.E. Mullins, O. Jaraki, T. Michel, D.J. Singer and J. Loscalzo, *Proc. Natl. Acad. Sci. USA*, 1992, **89**, 444.

23 A. Mulsch, P.I. Mordvintcev, A.F. Vanin and R. Busse, *Biochem. Biophys. Res. Commun.*, 1993, **196**, 1303.

24 A.F. Vanin, P.I. Mordvintcev, S. Hauschildt and A. Mulsch, *Biochim. Biophys. Acta*, 1993, **1177**, 37.

25 D.R. Adams, M. Brochwicz-Lewinski and A.R. Butler, *Prog. Chem. Org. Nat. Prod.*, SpringWien, New York, 1999, **76**, 13.

26 M.P. Glauser, G. Zanetti, J-D. Baumgartner and J. Cohen, *Lancet*, 1991, **338**, 732.

27 J. Gartwaite, S.L. Charles and R. Chess-Williams, *Nature*, 1988, **336**, 385.

28 E. Southam and J. Garthwaite, *Neurosci. Lett.*, 1991, **130**, 107.

29 R.G. Knowles, M. Palacios, R.M.J. Palmer and S. Moncada, *Proc. Natl. Acad. Sci. USA*, 1989, **86**, 5159.

30 D.S. Bredt and S.H. Snyder, *Proc. Natl. Acad. Sci. USA*, 1990, **87**, 682.

31 J. Martin and J.S. Gillespie, *Novel Peripheral Transmitter*, C. Bell, Ed., Pergamon Press, New York, 1990, 65.

32 D.S. Bredt, P.M. Hwang and S.H. Snyder, *Nature*, 1990, **347**, 768.

33 E.M. Schuman and D.V. Madison, *Ann. Rev. Neurosci*, 1994, **17**, 153.

34 C. Natham and Q.W. Xie, *J. Biol. Chem.*, 1994, **269**, 13725.

35 M.P. Moya, A.J. Gow, T.J. McMahon, E.J. Toone, I.M. Cheifetz, R.N. Goldberg and J.S. Stamler, *Proc. Natl. Acad. Sci. USA*, 2001, **98**, 5792.

36 D.J. Stewart, *Arzemittelforschung*, 1994, **44**, 451.

37 H. Ogura, W.G. Cioffi, P.J. Offner, B.S. Jordan, A.A. Johnson and B.A. Pruitt, *Surgery*, 1994, **116**, 313.

38 C.G. Frostell, H. Blomqvist, G. Hedenstierna, J. Lundberg and W.M. Zapol, *Anaesthesiology*, 1993, **78**, 427.

39 S. Lundin, H. Mang, M. Smithies, O. Stenqvist and C. Frostell, *Intensive Care Med.*, 1999, **25**, 911.

40 H. Schutte, F. Grimminger, J. Otterbein, R. Spriestersbach, K. Mayer, D. Walmrath and W. Seeger, *J. Pharmacol. Exper. Ther.*, 1997, **282**, 985.

41 H. Kolb and V. Kolb-Bachofen, *ViewPoint – Immunology Today*, 1998, **19**, 557.

42 Y. Hou, J. Wang, P.R. Andreana, G. Cantauria, S. Tarasia, L. Sharp, P.G. Braunschweiger and P.G. Wang, *Bioorg. Med. Chem. Lett.*, 1999, **9**, 2255.

43 S.M. Stahl, *J. Clin. Psych.*, 1998, **59**, 6.

44 K.P.S.J. Murphy and T.V.P. Bliss, *J. Physiol.*, 1999, **515**, 453.

45 T. Bonhoeffer, V. Staiger and A. Aertsen, *Proc. Natl. Acad. Sci. USA*, 1989, **86**, 8113.

46 A. Kossel, T. Bonhoeffer and J. Bolz, *NeuroReport*, 1990, **1**, 115.

47 P.F. Chapman, C.M. Atkins, M.T. Allen, J.E. Haley and J.E. Steinmetz, *NeuroReport*, 1992, **3**, 567.

48 G.A. Bohme, C. Bon, M. Lemaire, M. Reibaud, O. Piot, J.M. Stutzmann, A. Doble, J.C. Blanchard, *Proc. Natl. Acad. Sci. USA*, 1993, **90**, 9191.

49 S.H. Ralston, L.P. Ho, M.H. Helfrich, P.S. Grabowski, P.W. Johnston and N. Benjamin, *J. Bone Miner. Res.*, 1995, **10**, 1040.

50 N. McCartney-Francis, J.B. Allen, D.E. Mizel, J.E. Albina, Q.W. Xie, C.F. Nathan and S.M. Wahl, *J. Exp. Med.*, 1993, **178**, 749.

51 M. Cueto, O. Hernandez-Perera, R. Martin, M.L. Bentura, J. Rodrigo, S. Lamas, M.P. Golvano, *FEBS Lett.*, 1996, **398**, 159.

52 H. Ninnemann and J. Maier, *Photochem. Photobiol.*, 1996, **64**, 393.

53 M. Delledonne, Y. Xia, R.A. Dixon and C. Lamb, *Nature*, 1998, **394**, 585.

54 F. Murad, *Recent Prog. Hormone Res.*, 1998, **53**, 43.

55 R. Young, presented as part of the Industrial chemistry lecture module, University of St Andrews, 2000.

56 T. Malinski and Z. Taha, *Nature*, 1992, **358**, 676.

57 J.R. Lancaster, *Proc. Natl. Acad, Sci. USA*, 1994, **91**, 8137.

58 G. Bugliarello and J. Savilla, *Biorheology*, 1970, **7**, 85.

59 G.R. Cokelet, *Biomechanics*, ed. Y.C. Fung, Prentice-Hall, New Jersey, 1972, 63.

60 A.R. Butler, I.L. Megson and P.G. Wright, *Biochem. Biophys. Acta.*, 1998, **1425**, 168.

61 A.J. Gow, B.P. Luchsinger, J.R. Pawloski, D.J. Singel and J.S. Stamler, *Proc. Natl. Acad. Sci. USA*, 1999, **96**, 9027.

62 M.T. Gladwin, F.P. Ognibene, L.K. Pannell, J.S. Nichols, M.E. Pease-Fye, J.H. Shelhamer and A.N. Schechter, *Proc. Natl. Acad. Sci. USA*, 2000, **97**, 9943.

63 P. Vallance, S. Patton, K. Bhagat, R. MacAllister, M. Radomski, S. Moncada and T. Malinski, *Lancet*, 1995, **346**, 153.

64 R.F. Eich, T. Li, D.D. Lemon, D.H. Doherty, S.R. Curry, J.F. Aitken, A.J.X.J.K. Mathews, R.D. Smith, G.N. Phillips and J.S. Olson, *Biochemistry*, 1996, **35**, 6976.

65 S.S. Gross and P. Lane, *Proc. Natl. Acad. Sci. USA*, 1999, **96**, 9967.

66 L. Jia, C. Bonaventura, J. Bonaventura and J.S. Stamler, *Nature*, 1996, **380**, 221.

67 A.J. Gow and J.S. Stamler, *Nature*, 1998, **391**, 169.

68 J.S. Stamler, L. Jia, J.P. Eu, T.J. McMahon, I.J. Demchenko, J. Bonaventura, K. Gernert, C.A. Piantadosi, *Science*, 1997, **276**, 2034.

69 T.H. Huang, *J. Biol. Chem.*, 1979, **254**, 11467.

70 M.T. Gladwin, J.H. Shelhamer, A.N. Schechter, M.E. Pease-Fye, M.A. Waclawiw, J.A. Panza, F.P. Ognibene and R.O. Cannon, *Proc. Natl. Acad. Sci. USA*, 2000, **97**, 11482.

71 Z. Zhang, D.P. Naughton, D.R. Blake, N. Benjamin, C.R. Stevens, P.G. Winyard, M.C. Symons and R. Harrison, *Biochem. Soc. Trans*, 1997, **25**, 524S.

72 T.M. Millar, C.R. Stevens and D.R. Blake, *Biochem. Soc. Trans.*, 1997, **25**, 528S

73 M. Houston, A. Esterez, P. Chumley, M. Aslan, S. Marklund, D.A. Parks and B.A. Freeman, *J. Biol. Chem.*, 1999, **274**, 4985.

74 J.G. Hardman and E.W. Sutherland, *J. Biol. Chem.*, 1969, **244**, 6363.

75 E. Ishikawa, S. Ishikawa, J.W. Davis and E.W. Sutherland, *J. Biol. Chem.*, 1969, **244**, 6371.

76 G. Schultz, E. Bohme and K. Munske, *Life Sci.*, 1969, **8**, 1323.

77 A.A. White and G.D. Aurbach, *Biochim. Biophys. Acta.*, 1969, **191**, 686.

78 A.J. Hobbs, *TiPS Rev.*, 1997, **18**, 484.

79 P. Humbert, F. Niroomand, G. Fischer, B. Mayer, D. Koesling, K.D. Hinsch, H. Gausepohl, R. Frank, G. Schultz and E. Bohme, *Eur. J. Biochem.*, 1990, **190**, 273.

80 A. Friebe, B. Wedel, C. Harteneck, J. Foerster, G. Schultz and D. Koesling, *Biochemistry,* 1997, **36**, 1194.

81 A. Schrammel, D. Koesling, A.C. Gorren, M. Chevion, K. Schmidt and B. Mayer, *Biochem. Pharmacol.*, 1996, **52**, 1041.

82 L.J. Ignarro, H. Lippton, J.C. Edwards, W.H. Baricos, A.L. Hyman, P.J. Kadowitz and C.A. Gruetter, *J. Pharmacol. Exp. Ther.*, 1981, **218**, 739.

83 J. McAninly, D.L.H. Williams, S.C. Askew, A.R. Butler and C. Russell, *Chem. Comm.*, 1993, **23**, 1758.

84 A.P. Dicks, H.R. Swift, D.L.H. Williams, A.R. Butler, H.H. Al-Sa'doni and B.G. Cox, *J. Chem. Soc. Perkin Trans 2*, 1996, 481.

85 R. Zakhary, S.P. Gaine, J.L. Dinerman, M. Ruat, N.A. Flavahan and S.H. Snyder, *Proc. Natl. Acad. Sci. USA*, 1996, **93**, 795.

86 J.P. Stasch, E.M. Becker, C. Alonso-Alija, H. Apeler, K. Dembowsky, A. Feurer, H. Schroder, W. Schroeder, E. Stahl, W. Steinke, A. Straub, M. Schramm, *Nature*, 2001, **410**, 212.

87 R.R. Freedman, R. Girgis and M.D. Mayes, *Lancet*, 1999, **354**, 739.

88 M. Raynaud, Ph. D. Thesis, 1888, translated by T. Barlow, New Sydenham Society, London.

89 C.S. Lau, MD. Thesis, University of Dundee, 1992.

90 J.D. Coffman, *Raynaud's Phenomenon*, Oxford University Press, New York and Oxford, 1989, 25.

91 E.A. Hines and N.A. Christensen, *J. Am. Med. Assoc.*, 1945, **129**, 1.

92 W.H. Merrit, *Clin. Plast. Surg.*, 1997, **24**, 133.

93 R.W. Gifford Jr. and E.A. Hines Jr., *Circulation*, 1957, **16**, 1012.

94 J. Loscalzo, M.A. Creager and V.J. Dzau, *Vascular Medicine*, Little, Brown and Company, Boston, 1992, 379 and 975.

95 J.J.F. Belch and F. Khan, *J. Rheumatology*, 1998, **25**, 2295.

96 J.J.F. Belch, P.T. McCollum, P.A. Stonebridge and W.F. Walker, *Colour Atlas of Peripheral Vascular Diseases*, Mosby-Wolfe, London, 2nd Ed., 1996, 4 & 26.

97 D.L. Clement and J.T. Shepherd, *Vascular Diseases in the Limbs*, Mosby, London, 1993, 153.

98 E.V. Allen and G.E. Brown, *Am. J. Med. Sci.*, 1932, **183**, 187.

99 A. Ringqvist, Ph. D. Thesis, Goteborg University, Sweden, 1998.

100 R. Marcolongo, F. Cora, F. Laveder, M. Carallo, A. Busato and A.M. Rigloi, *Minerva. Med.*, 1997, **88**, 307.

101 G.J. Landry, J.M. Edwards and J.M. Porter, *Adv. Surg.*, 1996, **30**, 333.

102 W.F. Ashe, W.T. Cook and J.W. Old, *Arch. Enviro. Health*, 1962, **5**, 333.

103 J.H. Peacock, *Clin. Sci.*, 1957, **17**, 575.

104 T.A. Lloyd-Davies, E.M. Glaser and C.P. Collins, *Lancet*, 1957, **1**, 1014.

105 K.E. Cooper, K.W. Cross, A.D.M. Greenfield, D. McK. Hamilton and H. Scarborough, *Clin. Sci.*, 1949, **8**, 217.

106 J.H. Peacock, *Circ. Res.*, 1959, **7**, 821.

107 H.R. Maricq, *Systemic Sclerosis: Scleroderma*, 1988, John Wiley and sons Ltd, New York, 151.

108 C.G. Kallenberg, *Rheumatic Disease Clinics in North America*, 1990, **16**, 11.

109 M. Vayssairat, B. Patri, J.-F. Mathieu, M. Lienard, J. Dubrisay and E. Housset, *Euro. Heart J.*, 1987, **8**, 417.

110 J.D. Coffman and W.T. Davies, *Prog. Cardiovas. Dis.*, 1975, **18**, 123.

111 Z. Mackiewicz and A. Piskorz, *J. Cardiovas. Surg.*, 1977, **18**, 151.

112 H.R. Maricq, M.N, Johnson, C.L. Whetstone and E.C. LeRoy, *J. Am. Med. Assoc.*, 1976, **236**, 1368.

113 A.R. Butler, *Chem. Br.*, 1990, **24**, 419.

114 W.Taylor, *Br. Med. J.*, 1985, **291**, 921.

115 The Raynauds Association – 112 Crewe road, Alsager, Cheshire ST7 2JA, UK.

116 J.D. Coffman, *Am. Heart J.*, 1967, **74**, 229.

117 E.D. Cooke and A.N. Nicolaides, *Br. Med. J.*, 1990, **300**, 553.

118 P. Strang, B. Sternfeld and S. Sidney, *Headache*, 1996, **36**, 69.

119 I. Zahavi, A. Chagnac, R. Hering, S. Davidovich and A. Kuritzky, *Arch. Intern. Med.*, 1984, **144**, 742.

120 J.C. de Trafford, K. Lafferty and C.E. Potter, *Euro. J. Vasc. Surgery*, 1988, **2**, 167.

121 J.D. Coffman and R.A. Cohen, *Am. J. Physiol. (Heart Circ. Physiol. 23)*, 1988, **254**, H889.

122 V.J. Parks, A.G. Sandison, S.L. Skinner and R.F. Whelan, *Clin. Sci.*, 1961, **20**, 289.

123 J.D. Coffman and A.S. Cohen, *N. Engl. J. Med.*, 1971, **285**, 259.

124 E.J. Keenam and J.M. Porter, *Surgery*, 1983, **94**, 204.

125 J.D. Coffman and R.A. Cohen, *Eur. J. Clin. Inv.*, 1988, **18**, 309.

126 J.A. Bevan, *Cir. Res.*, 1979, **45**, 161.

127 E. Simon, *Physiol. Rev.*, 1986, **66**, 235.

128 G.S. Molyneux, *Proc. Royal Soc. Queensland*, 1977, **88**, 1.

129 P.M. Dowd, M.F.R. Martin, E.D. Looke, S.A. Bowcock, R. Jones, P.A. Dieppe and J.D.T. Kirby, *Br. J. Dermat.*, 1982, **106**, 81.

130 R.P. Brandes, F.-H. Schmitz-Winnental, M. Feletou, A. Godecke, P.L. Huang, P.M. Vanhoutte, I. Fleming and R. Busse, *Proc. Natl. Acad. Sci. USA*, 2000, **97**, 9747.

131 J.P. Cooke, M.A. Creager, P.J. Osmundson and J.T. Shepherd, *Circulation*, 1990, **82**, 1607.

132 K.H. Nilsen, *Br. Med. J.*, 1979, **1**, 20.

133 J.J.F. Belch and M. Ho, *Drugs*, 1996, **52**, 682.

134 M. Rademaker, R.H. Thomas, G. Provost, J.A. Beacham, E.D. Cooke and J.D. Kirby, *Postgrad. Med. J.*, 1987, **63**, 617.

135 D.A. Yardumian, D.A. Isenberg, M. Rustin, G. Belcher, M.L. Snaith, P.M. Dowd and S.J. Machin, *Br. J. Rheumatology*, 1988, **27**, 220.

136 J.J.F. Belch, B. Shaw, A. O'Dowd, A. Saniabadi, P. Leiberman, R.D. Sturrock and C.D. Forbes, *Thrombosis and Haemostasis*, 1985, **54**, 490.

137 R.A. DiGiacomo, J.M. Kremer and D.M. Shah, *Am. J. Med.*, 1989, **86**, 158.

138 S. Brewer, *The Daily Telegraph*, February 16th 2000, 21.

139 M. Gautherie, P. Barjat, E, Grosshans, Y. Quenneville, *Therapie*, 1972, **27**, 881.

140 J. Philips, *Harvard Heart Lett.*, 2000, Online.

141 A. Z'Brun, *Schweiz Rundsch Med. Prax.*, 1995, **3**, 1.

142 G. Baron-Rupport and N.P. Luepke, *Phytomedicine*, 2001, **8**, 133.

143 C.B. Bunker, G. Terenghi, D.R. Springall, J.M. Polak and P.M. Dowd, *Lancet*, 1990, **336**, 1530.

144 D.G. Waller, V.F. Challenor, D.A. Francis and O.S. Roath, *Br. J. Clinic. Pharmacol.*, 1986, **22**, 449.

145 M. Rademaker, E.D. Cooke, N.E. Almond, J.A. Beacham, R.E. Smith, T.G. Mant and J.D. Kirby, *Br. Med. J.*, 1989, **298**, 561.

146 A.T. Tucker, R.M. Pearson, E.D. Cooke and N. Benjamin, *Lancet*, 1999, **354**, 1670.

147 J.B.J. Hardwick, A.T. Tucker, M. Wilks, A. Johnston and N. Benjamin, *Clin. Sci.*, 2001, **100**, 395.

148 C. Harvsch, P. Scemmes and J. Taylor, *Comp. Med. Chem.*, 1990, **5**, 645.

149 S. Mitragotri, D. Blankschtein and R. Langer, *Science*, 1995, **269**, 850.

150 Based on a series of lecture notes from a 1st year lecture course designed for medical students, The University of St Andrews, 1999.

151 E.N. Marieb, *Human Anatomy and Physiology*, The Benjamin / Cummings Publishing Company, Inc., California, 1995, 3rd ed., 136.

152 F. Pirot, Y.N. Kalia, A.L. Stichcomb, G. Keating, A. Bunge and R.H. Guy, *Proc. Natl. Acad. Sci.*, 1997, **94**, 1562.

153 N.H. Parikh, A. Babar and F.M. Plakogiannis, *Pharm. Acta. Helv.*, 1985, **60**, 34.

154 E. Dippel, B. Mayer, G. Schonfelder, B.M. Czarnetzki and R. Paus, *J. Invest. Dermatol.*, 1994, **103**, 112.

155 M. Sakai, Y. Shimizu and I. Nagazu, *Arch. Dermatol. Res.*, 1996, **288**, 625.

156 H.A. Bull, J. Hothersall, N. Chowdhury, J. Cohen and P.M. Dowd, *J. Invest. Dermatol.*, 1996, **106**, 655.

157 A. Sirsjo, M. Karlsson, A. Gidlof, O. Rollman and H. Torma, *Br. J. Dermatol.*, 1996, **134**, 643.

158 A.A. Qureshi, J. Hosoi, S. Xu, A. Takashima, R.D. Granstein and E.A. Lerner, *J. Invest. Dermatol.*, 1996, **107**, 815.

159 R. Weller, *Clin. Exp. Dermatol.*, 1999, **24**, 388.

160 R. Weller, presented in part at the 3rd Scottish NO meeting, University of St Andrews, UK, November 2000.

161 J. Benrath, M. Zimmermann and F. Gillardon, *Neurosci. Lett.*, 1995, **200**, 17.

162 K. Yamasaki, H.D.J. Edington, C. McClosky, E. Tzeng, A. Lizonova, I. Kovesdi, D.L. Steed and T.R. Billiar, *J. Clin. Invest.*, 1998, **101**, 967.

163 R. Weller, A. Ormerod and N. Benjamin, *Br. J. Dermatol.*, 1996, **134**, 569.

164 T. Henseler and E. Christophers, *J. Am. Acad. Dermatol.*, 1995, **32**, 982.

165 R. Weller, *Br. J. Dermatol.*, 1997, **137**, 665.

166 R. Weller, R. Hobson, A.D. Ormerod, *Br. J. Dermatol.*, 1996, **135** (Suppl. 47), 21.

167 R. Weller, S. Pattullo, L. Smith et al., *J. Invest. Dermatol.*, 1996, **107**, 327.

168 P.C. Goldsmith, T.A. Leslie, N.A. Hayes et al., *J. Invest. Dermatol.*, 1996, **106**, 113.

169 P. Oberg, *Crit. Rev. Biomed. Eng.*, 1990, **18**, 125.

170 T. Munzel, H. Sayegh and D.G. Harrison, *Circulation* (Suppl. I), 1994, **90**, I-321.

171 K. Noda, M. Oka, F. Ma, S. Kitazawa, Y. Ukai and N. Toda, *Eur. J. Pharmacol.*, 2001, **415**, 209.

172 F.W. Flitney, I.L. Megson, D.E. Flitney and A.R. Butler, *Brit. J. Pharamacol.*, 1992, **107**, 842.

173 I.L. Megson, N. Sogo, C. Campanella, F.A. Mazzai, A.R. Butler and D.J. Webb, *Br. J. Pharmacol.* (Suppl. S), 1998, **124**, 16P.

174 I.L. Megson, M.J. Roseberry, M.R. Miller, F.A. Mazzei, A.R. Butler and D.J. Webb, *Br. J. Pharmacol.* (Suppl. S), **126**, 78P.

175 J. Kloek, I. van Ark, G. Folkerts, N. Bloksma, F.P. Nijkamp and F. De Clerk, unpublished findings, 2000, Janssen Research Foundation, Belgium.

176 A. Hauladen, A.J. Gow and J.S. Stamler, *Proc. Natl. Acad. Sci. USA*, 1998, **95**, 14100.

177 H. Rheinboldt and F. Mott, *J. Prakt. Chem.*, 1932, **133**, 328.

178 D.J. Sexton, A. Muruganandam, D.J. McKenny and B. Mutus, *Photochem. Photobiol.*, 1994, **59**, 463.

179 J. Barrett, L.J. Fitzgibbons, J. Glauser, R.H. Still and P.N.W. Young, *Nature*, 1966, **211**, 848.

180 D.L.H. Williams, *J. Chem. Soc. Chem. Comm.*, 1996, 1085.

181 A.P. Dicks, P.H. Beloso and D.L.H. Williams, *J. Chem. Soc. Perkin Trans 2*, 1997, 1429.

182 D.R. Noble and D.L.H. Williams, *Nitric Oxide*, 2000, **4**, 392.

183 A.R. Butler and D.L.H. Williams, unpublished observations, the University of St Andrews and Durham University, UK.

184 G.A. Petsko, *Nature*, (Suppl.), 1996, **384**, 7.

185 P. Evers, *Pharmaceut. Tech. Eur.*, 1997, **9**, 22.

186 B. Thorens, *Ann. Rev. Physiol.*, 1993, **55**, 591.

187 D.H. Solberg and J.M. Diamond, *Am. J. Physiol. Gastrointest. Liver. Physiol.*, 1987, **252**, G574.

188 M.J. Seatter, S. Kane, L.M. Porter, M.I. Arbuckle, D.R. Melvin and G.W. Gould, *Biochemistry*, 1997, **36**, 6401.

189 B. Gron, A. Andersson and E. Dabelsteen, *APMIS*, 1999, **107**, 779.

190 T.A. Johnson and R. Fusaro, *Adv. Metab. Disord.*, 1972, **6**, 1.

191 R.K. Freinkel, *J. Invest. Dermatol.*, 1960, **34**, 37.

192 B. Tesfamariam, M.L. Brown, D. Deykin, R.A. Cohen, *J. Clin. Invest.*, 1990, **85**, 929.

193 K. Hansen and O.A. Nedergaard, unpublished work, 2000, Odense University, Denmark.

194 I.R. Grieg, Ph.D. Thesis, University of St Andrews, UK, 1997.

195 A.R. Butler, R.A. Field, I.R. Greig, F.W. Flitney, S.K. Bisland, F. Khan, and J.J.F. Belch, *Nitric Oxide Biol. Chem.*, 1997, **1**, 211.

196 F. Khan, I.R. Grieg, D.J. Newton, A.R. Butler and J.J.F. Belch, *Lancet*, 1997, **350**, 410.

197 A. Kahlenberg and N. Kalent, *Can. J. Biochem.*, 1966, **44**, 801.

198 P.J. Holt, J.H. Anglin and R.E. Norquist, *Br. J. Dermatol.*, 1979, **100**, 237.

199 I.A. King, A. Tabiowo and R.H. Williams, *Biochem. J.*, 1980, **190**, 65.

Chapter 2 Discussion & Results.

Chemistry

Organic synthesis of existing & novel S-nitrosothiols

2.1 A novel synthetic route for *S*-Nitroso-1-thio-2,3,4,6-tetra-*O*-acetyl-β-D-glucopyranose, (SNAG) [5].

The complete synthetic route for SNAG [5] from the cheap and readily available glucose molecule at first glance appears very straightforward. As illustrated in the scheme below, the first four steps are all essentially routine. However, the yields obtained were far lower than those reported in previous work[1] (see red pathway of scheme 9). With this news, together with the demand for gram scale quantities, in order to combat the renowned problems associated with the nitrosation step, it soon became clear that an alternative pathway was required (see blue pathway; scheme 9).

Scheme 9 *Illustrating the old (red) & new (blue) synthetic route to SNAG.*

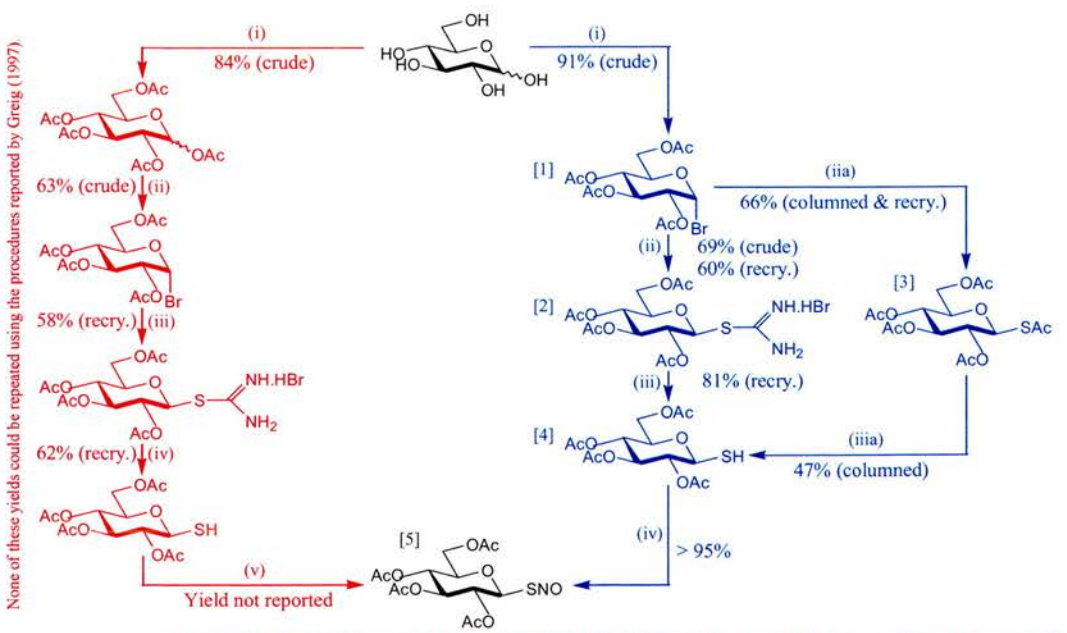

Reagents and conditions: (i) 1.8eq. $NaOAc/Ac_2O$, heat, 1.5hr., (ii) 30%HBr/AcOH (1ml/g), DCM, ice bath, 2hr., (iii) 1eq. Thiourea, dry acetone, reflux, 20min., (iv) 1eq. $K_2S_2O_5$, Reflux, 15min., (v) $NaNO_2$ + cHCl, $MeOH/H_2O$ (in situ). (i) 45% HBr/AcOH (1ml/g) + Ac_2O, then 45%HBr/AcOH (5ml/g), 17hr., (ii) 1.5eq. Thiourea, dry 2-propanol, reflux, 15min., (iia) 4eq. KSAc, dry acetone, 24hr., (iii) 2eq. $K_2S_2O_5$, reflux, $N_{2(g)}$, 5min., (iiia) 2eq. benzylamine, dry THF, $N_{2(g)}$, 1hr. (iv) $NaNO_2$ + cHCl (fuming method).

Only with a more efficient strategy in place could our collaboration with Ninewells hospital properly function, as obviously in human trials there is a need to guarantee a plentiful supply of the test compound. The demand for high yields can be further appreciated when it is considered that all compounds are applied transdermally, which is by far the most exhaustive and wasteful route of administration.

The first and highly significant alteration to the pathway was in substituting the acetylation and bromination reactions with a one-pot procedure described by Kartha and Jennings.[2] This simple, clean reaction exhibits an excellent yield, which is partly due to the added benefit of no competing side reactions. The first addition of 45% HBr/acetic acid (1ml/g of sugar) is responsible for the acetylation. On a small scale the literature predicts this reaction to require 5 hours in the case of glucose. However, since this is an exothermic reaction, when performed on a 20g scale there was sufficient heat to catalyse the process and thus reduce the time period to just ten minutes (section 6.2.1). The second portion of HBr/acetic acid (5ml/g of sugar) is responsible for the bromination step, which is usually very high yielding and results exclusively in the production of the α-bromide, due to the anomeric effect. The product is also very easy to crystallise in diethyl ether after either co-evaporating with toluene or an aqueous wash, in order to remove excess acid. Experience suggests best results when both stages are incorporated into the work-up.

Conversion of the acetobromosugar into the thiouronium salt by nucleophilic substitution remains the most troublesome step of the synthesis. This is due to the reaction relying on the salt precipitating out of solution (section 6.2.2). Extensive work and many publications on this matter by Cerny, Stanek and co-workers,[3-5] shows high yields are possible for this conversion, in a wide range of sugars, though massive quantities of starting material were always common practice. Whilst we, likewise, demanded large-scale synthesis, these procedures were impractical and beyond our requirement. On the smaller scale of several grammes, refluxing in 2-propanol as opposed to acetone, as described by Bonner and Kahn,[6] proved to be a highly favourable alternative, with turbid solutions routinely obtained.

The hydrolysis step (section 6.2.4) using potassium metabisulphite[5] also required revision. After many failed attempts following a reflux period of 15 minutes, it was observed early in the reflux that a white solid formed in the reaction vessel. After further heating this re-dissolved to again give a clear solution. It was proposed that this insoluble material may have been the desired thiol and that further heating drives

the conversion to the disulphide, with a different solubility. Limiting the reaction time to just 5 minutes together with continuous nitrogen flushing, to discourage thiol oxidation, gave the precursor to SNAG in very respectable yield. An alternative protocol using potassium carbonate at room temperature has also been reported.[7] The drawback of this methodology rests in the reaction time. If allowed to stir for periods longer than 30 minutes acetyl group hydrolysis can occur. For this reason alone, the reflux protocol is the one of choice (scheme 10).

Scheme 10. *Postulating the mechanism by which potassium metabisulphite hydrolyses the thiouronium species to give urea and the desired thiol.*

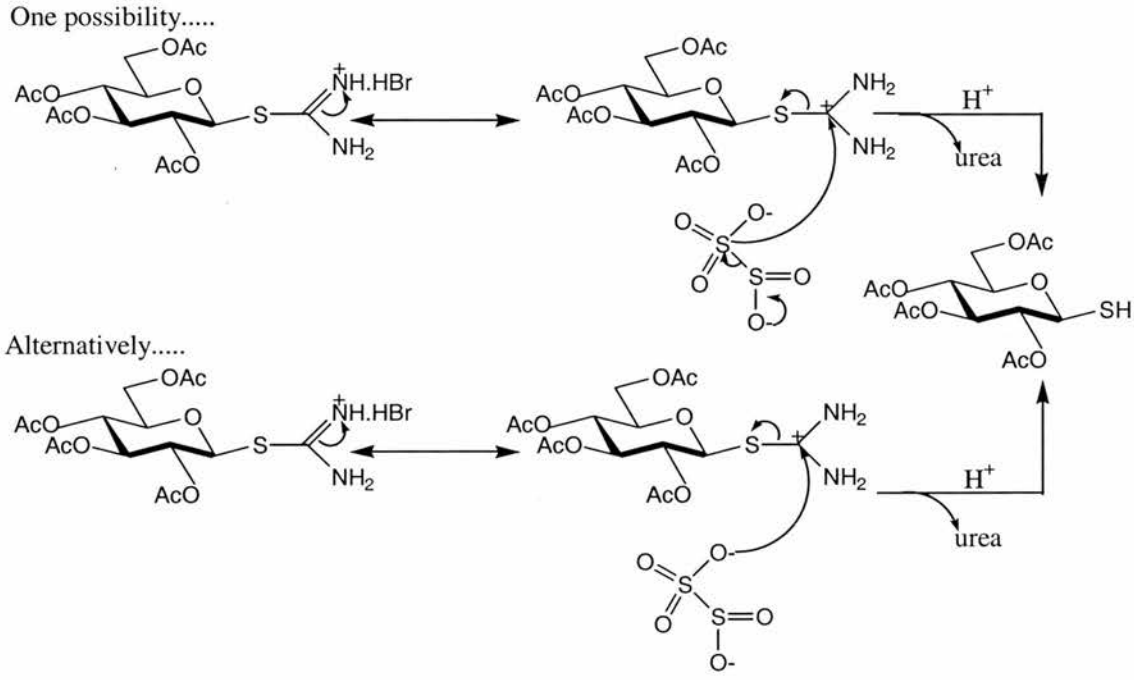

Purification of the thiol in any of the alcoholic solvents was very simple, allowing multiple crystallisations of the compound with very little loss in yield. Variations in the melting point of compound [4], suggesting that it may be dimorphic, as reported by Horton,[7] were proved incorrect by powder diffraction. Clear NMR spectra, in which the highly diagnostic S*H* doublet (*J* 9.89Hz) at δ_H 2.30ppm was clearly observed gave confidence that the changes to the protocol provided the right product. Other conclusive data such as the known H-1 and C-1 differences for the thiol (δ_H 4.54ppm, triplet, *J* 9.89Hz; δ_C 78.9ppm) and the disulphide (δ_H 4.64ppm, doublet, *J* 9.61Hz; δ_C 87.4ppm) left no doubt as to what was formed. However, optimism was dampened somewhat by difficulties in routinely acquiring accurate elemental

analysis and high resolution mass spectroscopy. In the case of the latter, electron impact (EI), chemical ionisation (CI) and fast atom bombardment (FAB) were all unrewarding. So too was the softer technique of electrospray. All analysis suggested the loss of the group at the anomeric position. These characterisation problems were not exclusive to compound [4]. Consequently the very soft technique of MALDI-TOF (time of flight) mass spectroscopy was called upon. High resolution MS (+/- 10ppm), using this relatively new analytical tool, was possible for all of the compounds synthesised.

Further guarantee that the thiol was indeed the sole product, was supplied by the characteristic infrared S-H stretch at 2550-2600cm^{-1}. Qualitative analysis was also provided by the nitroprusside test[8] though the quantitative data available by applying Ellman's test[9,10] soon led to this being the favoured approach for determining product purity. This quick and reliable colorimetric test to identify thiol content with a high degree of accuracy was employed throughout the course of this work. Using Ellman's reagent, otherwise known as 5,5'-dithiobis(2-nitrobenzoic acid) and cysteine hydrochloride as the reference signal, the purity was determined by UV-Vis spectroscopy. The intensely coloured yellow solution formed upon generation of the thio-bis(2-nitrobenzoic acid) dianion, by the reaction shown in scheme 11, occurs instantaneously upon the addition of free thiol. Such a process is monitored at a wavelength of 412nm. Thus the purity of the thiol prior to nitrosation was confirmed in a satisfactory manner. Using Ellman's reagent no significant degradation of compound [4] was observed when the crystalline material was repeatedly analysed after prolonged periods of storage at -20°C. Indeed we believe the compound to be indefinitely stable, despite reports to the contrary.[1]

Scheme 11. *Determination of thiol concentration in the presence of Ellman's reagent.*

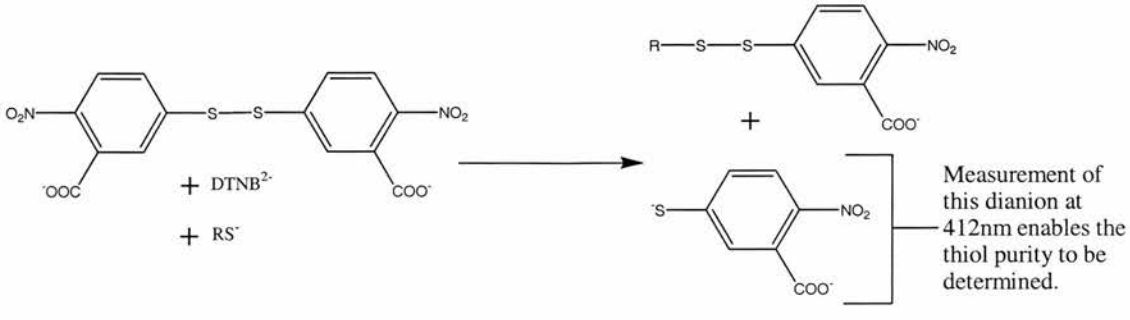

Whilst encountering problems with the protocol for the thiouronium salt, an alternative route to the anomeric thiol was on going. From the offset it was always anticipated that a second route would be necessary, since from the list of target compounds [Fig. 18], we could envisage that many would not form solids due to the sugar component, the attached substituents, or as a result of both of these factors. Using a procedure described and modified by Kartha and co-workers,[11] the bromide of compound [1] was displaced with a thioacetate group (section 6.2.3) using an excess of KSAc in dry acetone. The rationale for using acetone as opposed to dichloromethane is that the reaction progresses faster due to the solvent being homogeneous for both reactants. Purification of compound [3] by recrystallisation was only possible from methanol after washing the crude material through a charcoal bed and performing one round of column chromatography. This was the only drawback to this pathway that was otherwise a very robust and reliable reaction, which required little supervision, with complete conversion from the halide to the thio-ester. This was routinely observed at room temperature, despite reports by others,[12] suggesting the need to reflux the system.

The de-*S*-acetylation step was achieved using benzylamine in dry THF. This was a modification of an earlier method described by Bennett and co-workers.[13] In contrast to the previous step, this was a highly sensitive reaction, requiring very dry solvent, a complete nitrogen atmosphere, at least four equivalents of reagent and close monitoring of the reaction's progression by TLC. This latter point was of particular significance, since as will be shown later (section 2.3), should the reaction be left stirring for a longer period than necessary, disulphide formation will ensue. The reaction therefore requires careful preparation to ensure that a swift work-up and purification process is in place, once the reaction is complete. It was, in fact, common practice to halt the reaction prior to total completion. This was necessary with the arrival of a new TLC spot, of lower R_f value than either the starting material or thiol product. This was found, as expected, to correspond to the disulphide. Identification of this spot as the disulphide was also possible by careful TLC plate charring, since the 5% ethanolic solution of H_2SO_4 only gives deep red charring for thiols whilst partially pink spots are observed for other sulphur containing compounds, such as the *S*-acetyls and the disulphides.

Halting the reaction at this point and sacrificing the last traces of starting material, proved to be the best compromise. Despite the lower yield, thiol synthesis via the *S*-

acetyl certainly remains a viable secondary route for cases in which crystallisation is not possible. Further work in this area by Kiefel and co-workers[14] on anomeric thiol moieties has more recently been published, showing the current interest in these compounds.

Requests for 2,2',3,3'4,4'6,6'-octa-*O*-acetyl-di-*β,β'*-D-glucopyranosyl disulphide [6] as a biological control (section 3.5) was a far less troublesome synthesis. Indeed many grams were formed from the failed nitrosation steps, as will be discussed. Interestingly, NO, in addition to its clear capability of oxidising thiols to disulphides via *S*-nitrosothiol intermediates,[15] has also been reported by Itoh and co-workers,[16] as a promotor for the disproportionation of disulphides. However with a single thiol and a symmetric disulphide, the requirement in this work, was met by the simple addition of hydrogen peroxide.

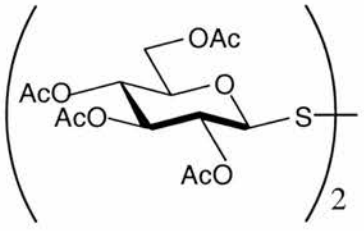

[6]

With ample starting material for the nitrosation step, it was possible to explore the reaction at some length. Previous reports[1,17,18] had favoured the *in situ* nitrosation method. This involves the addition of sodium nitrite to an ice-cold acidified aqueous solution containing the desired thiol. Isolation of the *S*-nitrosothiol relies on the precipitation of the compound out of the reaction mixture upon the addition of a suitable organic solvent such as methanol[1] or acetone.[18] However despite this method working consistently for *S*-nitrosoglutathione, GSNO [7], it has proved, from our experience, to be a highly unreliable method in the synthesis of common S-nitrosothiols such as *S*-nitrosothio-*N*-acetyl-DL-penicillamine, SNAP [8], *S*-nitrosothio-L-cysteine, SNOC [9] and *S*-nitrosothio-*N*-acetyl-L-cysteine, SNAC [10]. One of the frequent problems was the production of a sticky gum as opposed to crystalline material. Obviously this in turn makes handling and purity tests far more difficult. This same problem perhaps explains why Loscalzo and co-workers[19] made SNAC [10] by the *in situ* method, an hour before testing the compound in human platelet studies, without ever actually isolating the material as a solid. There are of course many potential problems with such methodology as even when using

equimolar equivalents of both reactants one can never be sure that all is used up in the reaction. The inability to isolate the material as a solid is more understandable, since in a similar way to its sister compound SNOC [9], decomposition is rapid once out of solution.

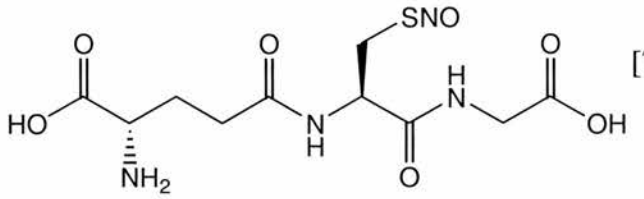

[7] GSNO

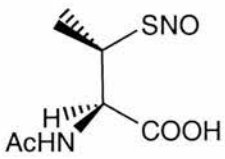

[8] SNAP

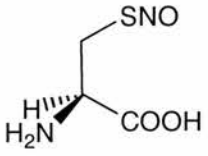

[9] SNOC

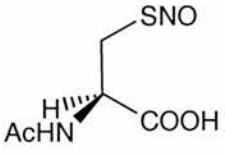

[10] SNAC

With these problems in mind attention moved to the nitrous fuming method. Generation of the nitrosating species NO^+, from N_2O_3 and N_2O_4 in an adjacent flask by the dropwise addition of concentrated hydrochloric acid onto ground sodium nitrite immediately eliminates problems of purification. The resulting brown fumes, characteristically this colour due to degradation of the tri and tetra-oxide species to NO_2, are then flushed, via a calcium chloride drying tube, through a minimum quantity of a volatile solvent containing the desired thiol. Following removal of this solvent under vacuum the target compound should be obtained in a swift and simple manner. Such a procedure worked effectively for SNAP, SNOC and SNAC, using tetrahydrofuran, water and methanol, respectively, in order to carry out the reactions. In the case of SNOC, the sample had to be left overnight on the freeze drier to remove all water content. The following day a deep orange precipitate had formed. This was stable enough to be weighed, though initial decomposition which was observed with the production of brown pungent fumes, led to complete loss of the precipitate within seconds, suggesting that the degradation is self catalysed.

Using this same protocol GSNO was also synthesised. When compared by UV at the characteristic wavelength for *S*-nitrososthiols of 345nm, they appeared identical.

On the basis of this work and after many failed attempts and oily formations of SNAG [5] by the *in situ* method, the fuming method was applied to 1-thio-2,3,4,6-

tetra-*O*-acetyl-β-D-glucopyranose. On each occasion an orange solution was formed when the thiol, dissolved in ethanol, was flushed with the nitrous fumes. However upon rotary evaporation, a white solid identified as the disulphide was formed each time. After trying various techniques, such as reducing the vacuum and heat source whilst still attempting to remove the solvent, the procedure was abandoned. Alternative attempts, in which water was added to try and precipitate SNAG out of solution also proved unsuccessful, as even filtering under suction was too harsh upon the SNO group. The problem was the requirement for reduced pressure. On the basis of what was observed in the case of SNOC upon degradation, it could be imagined how applying a vacuum would only aggravate the situation further.

Attempts at blowing off the solvent with an inert gas such as nitrogen, was considered. However this proved to be equally unsuccessful. With all of these findings in mind and based on the scheme below, flushing away the solvent with pure $NO^{\cdot}$, produced by the addition of ascorbic acid to sodium nitrite, looked like an attractive option. It was thought that saturating the system may help drive the equilibrium in the opposite direction. At the same time the solvent should be blown away. However, whilst this latter event did occur, this rather expensive approach still resulted in the production of the disulphide. This suggests that SNAG is simply not stable as a solid and that its existence in solution is based on the need for solvation.

Scheme 12 *The degradation of S-nitrosothiols*

By saturating the system outlined in scheme 12, it was hoped that the equilibrium could be driven in the opposite direction. At the same time, based on the same scheme, the detrimental effect of applying a vacuum can be fully appreciated.

Reconsidering Loscalzo's work and the benefit of not actually isolating the *S*-nitrosothiol, the fuming method was repeated using a known concentration of thiol in ethanol. This solvent was chosen not only the grounds that it allows the reaction to progress smoothly, but also due to the knowledge that it is the one of choice in the biological testing. Consequently, after the generation of an orange solution this

material was analysed by UV spectroscopy. This gave a signal as expected, in the region of 345nm. However rather than a nice clean single peak, a spiked spectrum was observed. Williams[20] was able to explain this confusing result by describing the potential for nitrosation at both a thiol and hydroxyl group. As illustrated in the following scheme, both nitrosations are reversible reactions. The formation of the *S*-nitroso compound is the faster of the two forward processes due to sulphur being more nucleophilic than oxygen, whilst due to sulphur being more basic that oxygen the reverse reaction is faster for the *O*-nitrosated species.

Scheme 13. *S- & O-Nitrosation and the potential for the reverse reaction.*

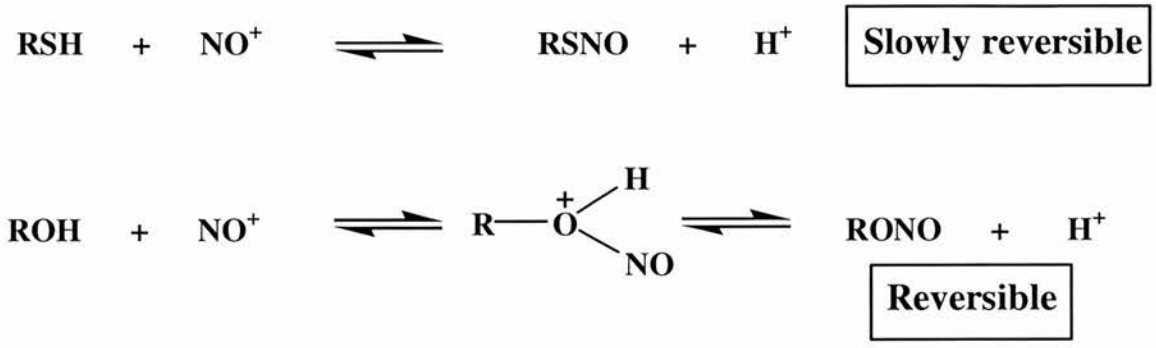

Extracted from D.L.H. William's book on "Nitrosation", Cambridge University Press, Cambridge, 1988, 173.[20]

The nitrosation of ethanol, as discussed earlier by Stamler (section 1.1.4a), was confirmed by passing the nitrous fumes through an ethanolic solution in the presence and the absence of thiol. Both samples gave orange solutions. These were exposed to a further period of flushing, this time with oxygen free nitrogen, before analysis by UV. Whilst the thiol sample, which was still orange in colour, showed a clean SNO peak [Fig. 21], the thiol deficient sample, observed as a clear, colourless solution, showed very little signal. This process was repeated with the nitrogen-flushing period being more closely examined. As shown by overlaying the spectra in Fig. 21, this suggests that nitrogen flushing for 4 minutes removes any trace of nitrosated ethanol from the system. Thus the ability to nitrosate ethanol, in a reversible manner, may actually prove to be an advantage in this reaction, since withholding a saturated NO supply for a prolonged period, should ensure complete thiol conversion, though on the basis of previous discussion, the thiol should preferentially nitrosate first in

any case. Indeed NMR analysis, when nitrosating in deuterated methanol, confirmed that this step completely reacts with all starting material in a very efficient manner. This was possible to monitor by observing the loss of the SH peak. While degradation prevented a clean interpretation of the target compound, any impurity, as in the thiol-generating step, was clearly seen to be that of the disulphide.

From studying the reactions for the thiol and alcohol species further (scheme 13), the generation of nitrous acid, formed by reaction of the thiol proton with any nitric oxide, posed yet another problem. However as outlined in section 6.2.5, filtering the product, under gravity, through dry potassium carbonate, circumvented any possible interference by this side reaction.

Fig. 21 *The removal of nitroso-ethanol by nitrogen flushing.*

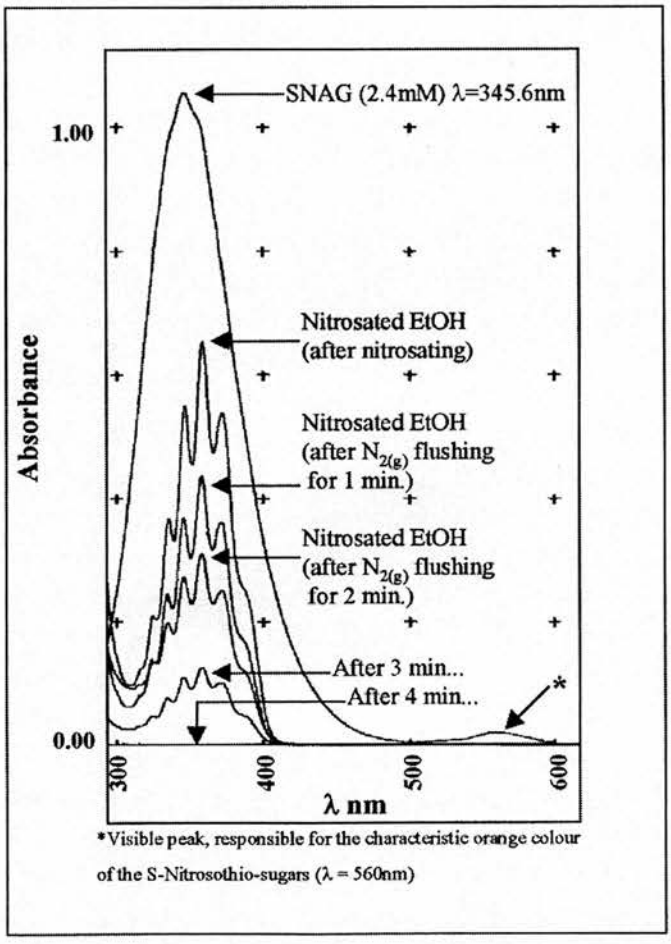

Illustrating the characteristic spectra for SNAG (2.4mM) and ethanol's ability to reversibly nitrosate. Flushing with $N_{2(g)}$ over a 4 minute period is shown to completely eliminate the presence of NO.

Further UV analysis on SNAG and all of the other *S*-nitrosothiols, was performed in partnership with the Griess test,[17,21-22] by measuring the absorbance at 550nm following the production of an azo dye [Scheme 14]. Using this technique, SNAG was identified in yields greater than 95%. Such a yield is comparable to other nitrosation techniques.[23] Therefore the Tayside committee for medical ethics approved the transdermal application of these ethanolic solutions of *S*-nitrosothiols. Such approval was based on the grounds that these NO donating solutions were valid alternatives to the isolated semi-solid products, previously used, which were agreed to be of substandard quality and thus more likely to contain impurities. From the biologist's point of view these solutions were also welcomed, since the handling of the material prior to administration to the subject was simplified to such an extent that addition of one-equivalent of water, was the only necessary requirement.

Scheme 14 *The Griess test. Quantitative, colorimetric analysis for S-nitrosothiols.*

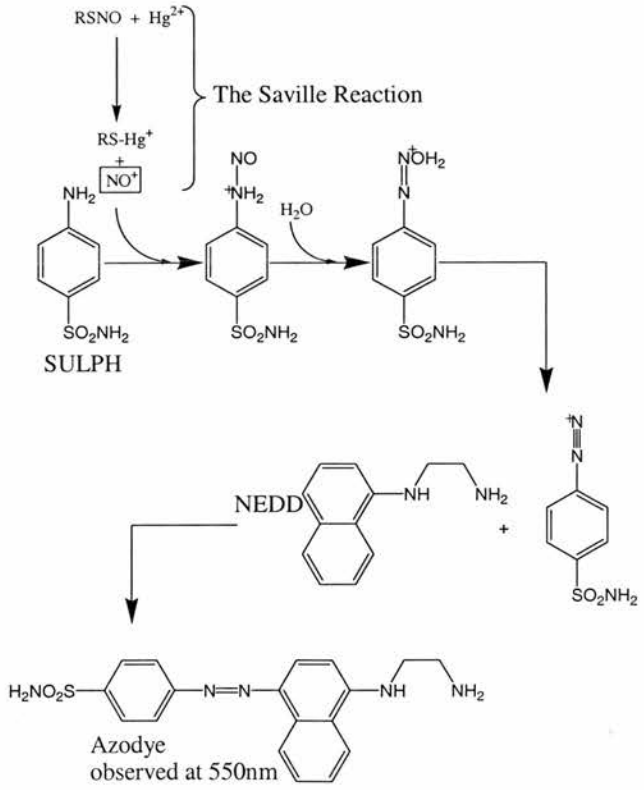

*The importance of mercury as opposed to copper in the decomposition of the RSNO, as shown, is due to the requirement for NO^+ rather than NO· [SULPH = Sulphanilamide, whilst NEDD = N-(1-naphthyl)-ethylene-diamine dihydrochloride]. This scheme was reconstructed from a similar representation in a paper by J.A. Cook and co-workers, Analyt. Biochem., 1996, **238**, 150.*

2.2 Synthesis of an extensive range of *S*-nitroso-1-thio-sugars.

2.2.1 Synthesis of *S*-Nitroso-1-thio-2-acetamido-3,4,6-tri-*O*-acetyl-2-deoxy-β-D-glucopyranose, SAGA [15].

Initially starting from glucosamine hydrochloride, an acetylation[24] was attempted using pyridine and acetic anhydride, both in the presence and absence of NaOMe. Due to a combination of slow conversion, together with the fact that *N*-acetyl-glucosamine is a cheap starting material, this study was abandoned. Instead an acetylation/halogenation reaction, incorporated into a one-pot method was, as in the case of acetobromoglucose, adopted here. As a result of the reported[25] instability of acetobromo-D-glucosamine, the chloro derivative was used instead, since this is a known crystalline compound. The procedure used in the production of 2-acetamido-3,4,6-tri-*O*-acetyl-2-deoxy-α-D-glucopyranosyl chloride was described very precisely by Horton.[26] A modification to this protocol, reported by Smith,[27] was also incorporated into the procedure. This involved prior flushing of the reagent with HCl to compensate for the loss of any HCl produced *in situ*; this also catalyses the reaction, thus the reaction time was improved and a reasonable yield of 72% was obtained (Scheme 15). However, despite the ease with which this material crystallises from diethyl ether, acceptable purity could only be obtained by performing column chromatography (section 6.4.1).

Scheme 15 *The catalytic effect of HCl in the acetylation/chlorination of N-acetyl glucosamine.*

Scheme 15 (cont.)

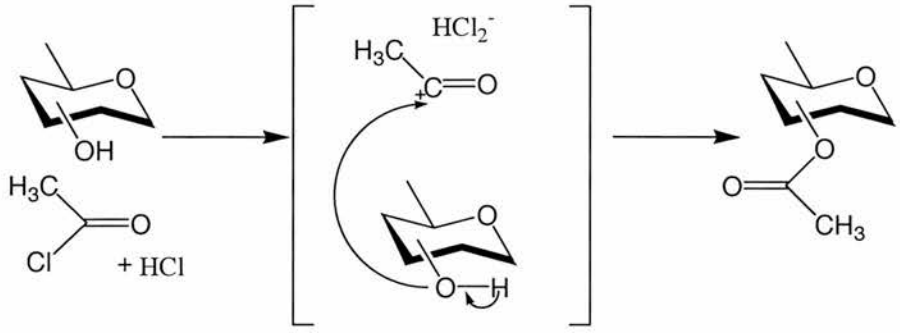

In a parallel fashion, the thiouronium salt (section 6.4.2) [12] and the thioacetate (section 6.4.3) [13] methods were performed, so that a direct comparison for glucosamine with glucose could be observed. From the synthetic attempts, the thioacetate product [12] was obtained in a crude yield of 85%, after stirring for 3 hours, though after chromatography and recrystallisation this dropped to 35%. The thiourea reaction, by contrast, gave compound [12] in a yield of 70% in just 15 minutes. With a better yield and a quicker reaction time and purification process, the salt procedure (section 6.4.2) quickly became the one of choice.

Compound [14] was synthesised by an identical route to that used for compound [5], though for the recrystallisation ethanol was the solvent of choice. Following a nitrosation by our fuming method, SAGA [15] was obtained, in an overall yield of 24%.

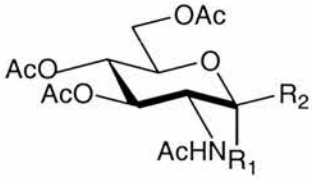

[11] R_1 = Cl, R_2 = H
[12] R_1 = H, R_2 = $SC(NH_2)NH.HCl$
[13] R_1 = H, R_2 = SAc
[14] R_1 = H, R_2 = SH
[15] R_1 = H, R_2 = SNO

2.2.2 Synthesis of *S*-Nitroso-1-thio-2-acetamido-3,4,6-tri-*O*-acetyl-2-deoxy-β-D-galactopyranose, SAGAL [20].

In a similar manner, *S*-nitroso-1-thio-2-acetamido-3,4,6-tri-*O*-acetyl-2-deoxy-β-D-galactopyranose, SAGAL [19] was synthesised. The only difference in this protocol was the extra initial step due to the *N*-acetyl form of the starting material being over two hundred fold more expensive to buy than the closely related *N*-acetyl-

glucosamine compound. This is exemplified by reported methods[28] in which D-galactosamine is synthesised from D-glucosamine.

Taking the D-galactosamine hydrochloride salt and acetylating with anhydride in the presence of pyridine,[29,30] gave the fully acetylated sugar in 72% yield. Thus to obtain the acetochlorosugar a simple chlorination with HCl gas at low temperature (section 6.5.2), as described by Fox and Goodman,[31] was sufficient to give compound [17]. Due to the much smaller scale of this reaction the thioacetate pathway was taken, due to this not relying on crystallisation, as already discussed. With the biological tests for SAGA and SNAG on going at the time, the de-*S*-acetylation was only performed as a test reaction. Had SAGA shown dramatic biological differences to SNAG, suggesting the amino sugars are a more favourable class of compounds, this would have prompted further work in the synthesis of SAGAL. However from the data obtained and the difficulties in scaling up, this was not considered worthwhile, though the synthesis itself was clearly viable (see section 6.5.3 & 6.5.4).

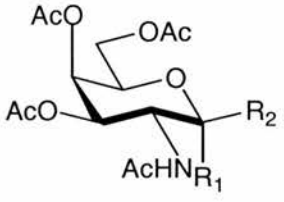

[16] R_1 = H/OAc, R_2 = H/OAc
[17] R_1 = Cl, R_2 = H
[18] R_1 = H, R_2 = SAc
[19] R_1 = H, R_2 = SH
[20] R_1 = H, R_2 = SNO

2.2.3 Synthesis of *S*-Nitroso-1-thio-2,3,4,6-tetra-*O*-acetyl-β-D-galactopyranose, SNAGAL [25].

The galactose derivative was synthesised via the thiouronuim salt method despite worries regarding its solubility in comparison to glucose. In fact the purification for the first three steps were all possible by recrystallisation. The first of these steps was the full acetylation of the sugar. This was the only sugar, with the exception of galactosamine, where the acetohalo-compound was preferentially synthesised in two steps as opposed to one-pot. Whilst we also present experimental data for this one-pot method, in a yield of 27%, the separate acetylation and bromination gave an overall yield of 77% for the two steps. This highlights the need in the one pot procedure to be completely certain that all of the sugar is fully acetylated before adding the second portion of HBr/acetic acid. Whilst this was monitored by TLC, the

very strong acidic environment of the reaction causes hydrolysis upon the TLC plates making analysis difficult in some instances. This was certainly the case here. However, what we lost from the low yield in the one pot procedure was more than made up for by the introduction of iodine chemistry. Such chemistry was chosen in the penta-acetylation of galactose in preference to the rather traditional pyridine method[29,30] used in the synthesis of compound [16] (section 6.5.1).

As described by Kartha,[32] iodine acts as an effective Lewis acid promotor in the per-*O*-acetylation of unprotected sugars, as shown in scheme 16. Consequently, this cheap, easy to handle reagent gave the desired compound in high yield and in an exceptionally clean form (section 6.6.1). The faster this reaction occurs the greater the proportion of α-product. Thus when this reaction was performed on a large scale, the exothermic nature of the process drove the reaction to completion in just 30 minutes yielding 93% of the product [21] in the α-form and just 7% as the β-anomer.

Scheme 16. *Kartha's proposed iodine-promoted acetylation reaction*

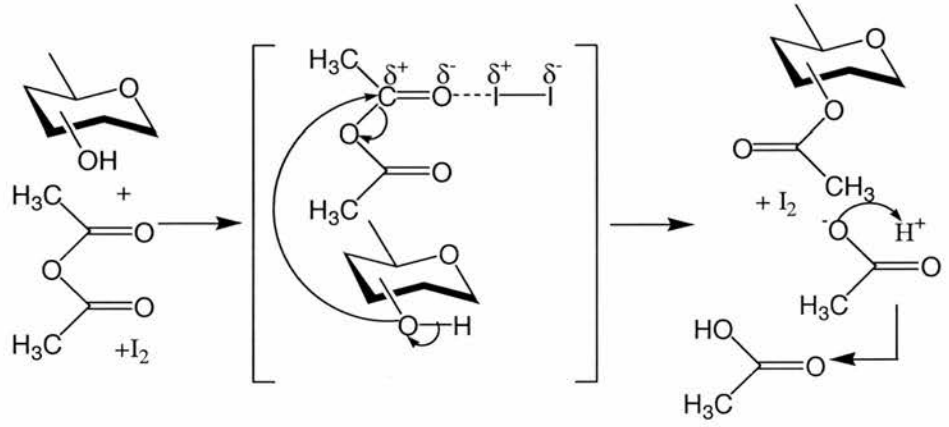

*As illustrated by K.P.R. Kartha & R.A. Field in Tetrahedron, 1997, **53**, 11753.*

Performing the bromination step (section 6.6.2a) with reassurance that the starting material was fully acetylated, allowed the swift progression to obtain SNAGAL [25], in an overall yield of 13.5%. This low productivity was primarily attributed to the hydrolysis step (section 6.6.4) and the requirement thereafter for purification by column chromatography.

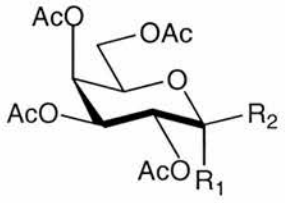

[21] R_1 = H/OAc, R_2 = H/OAc
[22] R_1 = Br, R_2 = H
[23] R_1 = H, R_2 = $SC(NH_2)NH.HBr$
[24] R_1 = H, R_2 = SH
[25] R_1 = H, R_2 = SNO

Full characterisation for the disulphide of octa-acetylated galactose [26] can also be found in the experimental chapter (section 6.6.6) due to much of the pioneering work on the nitrosation step involving attempts to synthesis compound [25] as a solid. At the time this appeared a significant challenge, not least because of its reported differences in solubility with respect to SNAG [5].

2.2.4 Synthesis of D and L-SNAX [30], [34] and D and L-SNARB [38], [42].

The D- and L- forms of tri-acetyl-thio xylose and arabinose were synthesised by the preferred route outlined in scheme 9 (section 6.7-6.10). Thus all were prepared by a one-pot acetylation/bromination followed by conversion to the thiouronium salt. In this step crystallisation was possible for each compound allowing the hydrolysis methods, reported by Cerny, Stanek and co-workers,[3,5] to be performed in quick succession. In the case of the xylose compounds potassium metabisulphite was used, whilst for the arabinose compounds sodium sulphite was reported as the reagent of choice. This would still fit in with our proposed mechanistic scheme for this step (scheme 10) and, upon reacting with the relevant salt, gave the desired thiols just as efficiently. The only other appreciable difference between the two sets of sugars was at the thiol-generating step where only the 1-thio-2,3,4-tri-*O*-acetyl-xylopyranose compounds, [29] and [33], gave crystalline materials. As a result column chromatography was an added necessity for purification of both arabinose derivatives [37] and [41], illustrating once again the effect of the axial C-4. Apart from these minor points, the synthesis of all four target compounds, [30], [34], [38] & [42], was achieved, after nitrosation by the fuming method, with overall yields ranging between 6–9%.

One further observation which, was not seen in any of the other sugar compounds, was the decomposition of the acetobromo-derivatives when stored at -20° for

prolonged periods. This can only suggest that the C-6 functionality is of some importance in maintaining the stability of the crystals. Perhaps this could imply that the crystal packing arrangement relies on intermolecular bonding between the C-6 of one molecule and the anomeric position of another (related work can be seen in section 4.1.1). Such a finding could be of great importance in this work. However in relation to the anomeric thiols, such instability was not observed.

D-xylose

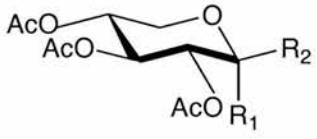

[27] R_1 = Br, R_2 = H
[28] R_1 = H, R_2 = SC(NH2)NH.HBr
[29] R_1 = H, R_2 = SH
[30] R_1 = H, R_2 = SNO

L-xylose

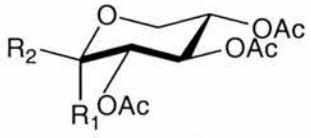

[31] R_1 = Br, R_2 = H
[32] R_1 = H, R_2 = SC(NH_2)NH.HBr
[33] R_1 = H, R_2 = SH
[34] R_1 = H, R_2 = SNO

D-arabinose

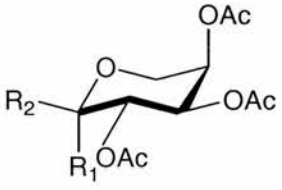

[35] R_1 = Br, R_2 = H
[36] R_1 = H, R_2 = SC(NH_2)NH.HBr
[37] R_1 = H, R_2 = SH
[38] R_1 = H, R_2 = SNO

L-arabinose

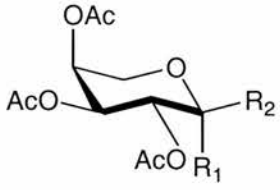

[39] R_1 = Br, R_2 = H
[40] R_1 = H, R_2 = SC(NH_2)NH.HBr
[41] R_1 = H, R_2 = SH
[42] R_1 = H, R_2 = SNO

2.2.5 Synthesising fully acetylated S-nitroso-1-thio-disaccharides, SNAL [46] & SNAM [51].

Starting from D-lactose and D-maltose, the two target compounds, [46] and [51],

were obtained in highly satisfactory overall yields of 52% and 47% respectively, as described in chapter 6 (sections 6.11 & 6.12). Such yields were possible with the initial production of crystalline material from the one pot acetylation/bromination reactions in excellent yields of 93% and 94% for [43] and [47] (section 6.11.1 and 6.12.1). This provided ample material for conversion into the thioacetates [44] and [49]. Using four equivalents of KSAc and purification by column chromatography in each case, yields of 94% and higher, were recorded (section 6.11.2 and 6.12.3).

In the case of maltose, attempts were also made to synthesis the thiouronium salt equivalent [48]. This proved to be difficult due to a lack of precipitation. Changing the solvent to 2-propanol had no effect on isolation of pure material so extraction of the salt into water remained the only alternative option. Upon freeze drying, as expected, one was left with a mixture of compounds, including the desired product, urea, starting material and unreacted thiourea. Clearly in this instance opting for the thioacetate procedure was essential due to the inability to form a crystalline material, despite Cerny, Stanek and Sindlerova[5] reporting otherwise. However the use of large-scale reactions, as already discussed, may have aided in initial crystal formation in their work, for instance, a massive 34g of acetobromomaltose was used in their thiourea reaction.

For both the lactose and maltose derivatives, two equivalents of benzylamine were used, giving reaction times in the range of 4 to 6 hours. The maltose derivative was purified by simple crystallisation whilst for lactose, perhaps as a consequence of its axial C-4, column chromatography was required. This solubility difference was again highlighted upon nitrosation, as the routinely used thiol concentration (41.2mM) for this step, had to be drastically reduced for the SNAM [51] (3.4mM), whilst for SNAL [46] the standard protocol remained unchanged. Such a huge difference in solubility meant direct biological comparison of these two disaccharides (as shown in section 3.7) was impossible.

D-SNAL

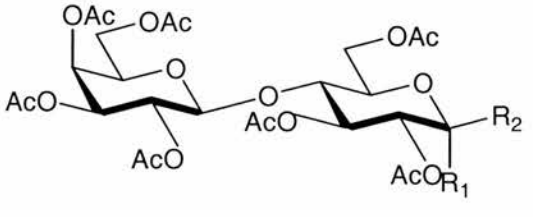

[43] R_1 = Br, R_2 = H
[44] R_1 = H, R_2 = SAc
[45] R_1 = H, R_2 = SH
[46] R_1 = H, R_2 = SNO

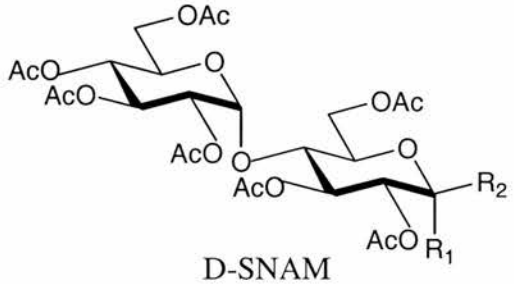

D-SNAM

[47] R_1 = Br, R_2 = H
[48] R_1 = H, R_2 = $SC(NH_2)NH.HBr$
[49] R_1 = H, R_2 = SAc
[50] R_1 = H, R_2 = SH
[51] R_1 = H, R_2 = SNO

2.3 Synthesis of a lipophilic family of compounds based on SNAG.

Remaining with disarming sugar ring substituents, preparation of the propionylated derivative of SNAG was attempted [section 6.13]. Like in all the other synthetic work this initially required full acylation with the generation of the halide at the anomeric centre. To obtain this, the first method used was a one-pot propionylation/bromination using HBr in propionic acid together with propionic anhydride. However, as in the related reaction to form acetobromogalactose [22] (section 2.2.3 & 6.6.2(b)), this was not the characteristically clean reaction, which was seen in the case of most other sugars. The problem was further amplified since, in contrast to the galactose compound [22], the desired product could not be isolated by crystallisation methods due to the enhanced lipophilic character. This is of little surprise, as even the penta-propionylated compound, reported in the literature,[33] would not give a crystalline material. Interestingly, when the same one-pot procedure was carried out using HBr in acetic acid, together with propionic anhydride, a mixture of acetylated and propionylated side arms was observed (section 6.13.4b). In hindsight this may have been expected, as this simply illustrates the ability for nucleophilic attack at the acid and the anhydride. However due to a complicated NMR spectrum, the ratio and hence the preferred site of attack could not be determined.

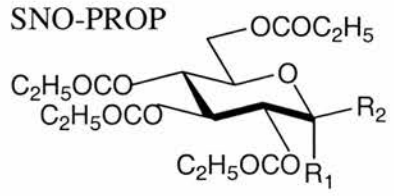

[52] R_1 = H/$OCOC_2H_5$, R_2 = H/$OCOC_2H_5$
[53] R_1 = Cl, R_2 = H
[54] R_1 = H, R_2 = SMe
[55] R_1 = Br, R_2 = H
[56] R_1 = I, R_2 = H
[57] R_1 = H, R_2 = SAc
[58] R_1 = H, R_2 = SH
[59] R_1 = H, R_2 = SNO

Eventually the decision was taken to perform a separate acylation and halogenation step as already discussed for galactose. Using the promoting properties of iodine (scheme 16) the propionylated compound [52] was obtained in quantitative yield (section 6.13.1). Due to an unfavourable bromination step with HBr in propionic acid, formation of the chloro derivative was attempted using gaseous HCl, as described in the synthesis of compound [17] (section 6.5.2). It was also hoped that the greater ability of the chloro compounds to crystallise out of solution would enable easier purification, should it have been required. However much to our surprise, despite various attempts, all efforts resulted in the fully propionylated sugar being retrieved. As described in section 6.13.2, changing the solvent from diethyl ether, as used by Fox and Goodman,[31] to dichloromethane, as used in section 6.5.2, made no effect on reactivity. Since the addition of an extra carbon appeared unlikely to change drastically the deactivating nature of the ring substituents, the lack of reactivity was instead attributed to steric hindrance.

With no success for either bromide or chloride insertion at C-1, more attention was again channelled towards iodine chemistry. Using work again by Kartha and Field,[34] the thio-glycoside of propionylated glucose was synthesised [54] using a methyl disulphide-hexamethyldisilane system (section 6.13.3). As reported by the previously mentioned authors, such a system provides a cheap alternative to using (methylthio)-trimethylsilane as the reagent. For such a system to function there is a clear need for a suitable Lewis acid catalyst (outlined in scheme 17). In contrast to other work[35] that has reported the use of BF_3, ZnI_2 and TMS triflate as suitable catalysts, Kartha and Field once more highlight the potential role of iodine, which in addition to being an economical and clean alternative, also lacks the moisture sensitivity of the compounds listed above.

Scheme 17. *The methyl disulphide-hexamethyldisilane system, catalysed by iodine.*

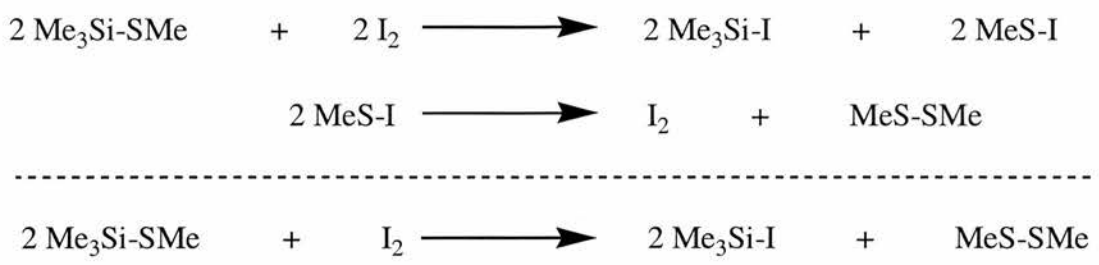

When the reaction time for this iodine promoted methyl disulphide-hexamethyldisilane system was compared to the more expensive and commonly used (methylthio)-trimethylsilane procedure, no difference in efficiency was encountered.[34]

This supports the theory that the same mechanism is in operation following the generation of the reacting species, Me_3Si-I and MeS-I, which in turn shows that the promoting effect of iodine, when present in adequate amounts (1 equivalent), is not the rate determining step in the production of the thio-glycoside [54] (see scheme 18).

Scheme 18. *The proposed mechanism for the generation of the thio-glycoside.*

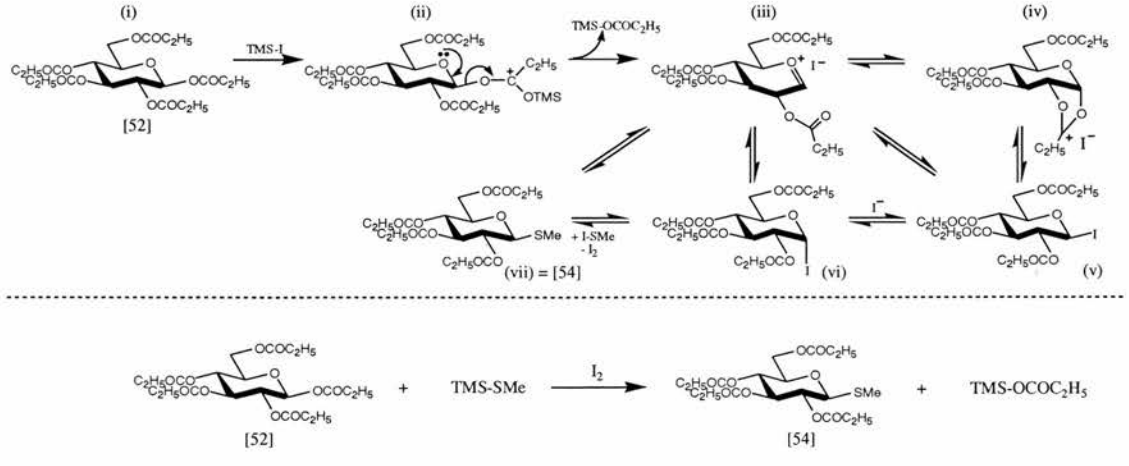

The above scheme illustrates how the β-thio-glycoside (vii) is generated from the oxocarbenium

ion (iii) and the α-glycosyl iodide (v & vi). The importance of the cyclic carbonium ion (iv) is also shown.

The β-propionylated sugar (i) is shown as the starting material simply because it was the major product of the acylation (90% of the product from section 6.13.1). The same scheme could also be shown for the α-propionylated derivative (10% of the product from section 6.13.1).

*This representation is a modification of the one by K.P.R. Kartha and R.A. Field, J. Carbohydr. Chem., 1998, **17**, 693.*

Using further work by Kartha and Field[36] the glycosyl halide was produced by the reaction of compound [54] with iodine monobromide (I-Br). This was chosen ahead of typical reagents, including I-I, due to the greater potency of I-Br as an iodonium ion source. Despite the attempted synthesis not being a completely clean conversion, the glycosyl bromide [55] obtained was exclusively the α-anomer as reported in the original work (section 6.13.4a).

On the basis of the thioglycoside step, using iodine to generate the methyl disulphide-hexamethyldisilane system, a study was performed using iodine in only catalytic amounts.[34] This showed the reaction to be suppressed together with the detection of the glycosyl iodide intermediate over many days. Based on the stability of the glycosyl iodide being low, yet clearly greater than anticipated, these findings triggered an additional study in which methyl disulphide was absent from the reaction vessel.[37] Olah and co-workers,[38] due to the need for the *in situ* generation of TMSI, were the first to report the use of the hexamethyldisilane-iodine system (HMDS-I_2). Such a need stemmed from the knowledge that TMSI is unstable when reacted directly, thus hampering its use in the de-alkylation of esters and ethers. With no by-products and no limits on solvent choice the system is clearly an attractive one. Therefore Kartha and Field[37] applied the simplified system to a range of fully acetylated sugars producing, as anticipated, the glycosyl iodide. When we repeated the same procedure with fully propionylated glucose, using one equivalent of each reactant, the α-glycosyl iodide [56] was obtained in near quantitative yield (section 6.13.5). This material was of such high purity that no further purification was needed, which in view of the lipophilicity and handling problems of these compounds, was highly desirable.

Scheme 19. *The in situ generation of TMSI and its reaction with propionylated glucose.*

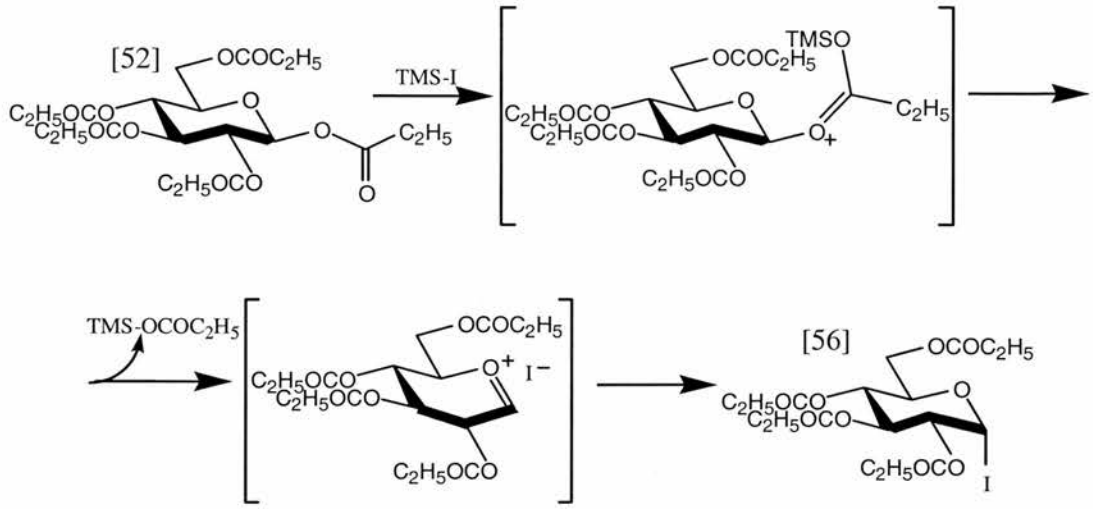

*A modification from work by K.P.R. Kartha and R.A. Field, Carbohydr. Lett., 1998, **3**, 179.*[37]

Since this reaction was clean, presenting a one step synthesis to the anomeric halide, it immediately became the one of choice in the synthesis of the whole range of lipophilic targets. The only drawback and thus point on which extra attention was needed, was with regard to the rapid decomposition of glycosyl iodides. This is significantly faster than that of either the chlorides or bromides, thus efficiency during the work-up, immediate storage at -20°C and quick conversion to the thioacetate were all high requirements at this stage.

Obviously the thioacetate route, as alluded to previously, was the only available pathway for this set of compounds for reasons again based on lipophilic grounds (section 6.13.6). Consequently, for the propionylated, butyrionylated, valerionylated and hexionylated glycosyl iodides, reaction in dry acetone with four equivalents of potassium thioacetate was the standard option. Similarly in the de-*S*-acetylation step, all of the reactions gave the desired thiols when using 2 equivalents of benzylamine in a nitrogen flushed, moisture free environment.

SNO-BUT

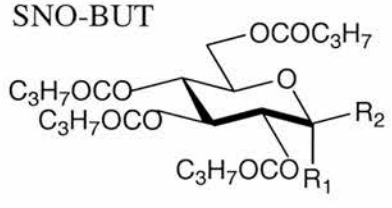

[61] R_1 = H/$OCOC_3H_7$, R_2 = H/$OCOC_3H_7$
[62] R_1 = I, R_2 = H
[63] R_1 = H, R_2 = SAc
[64] R_1 = H, R_2 = SH
[65] R_1 = H, R_2 = SNO

SNO-VAL

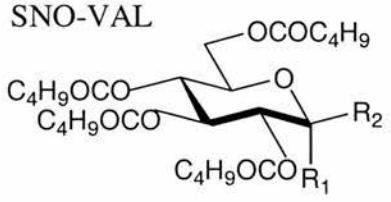

[66] R_1 = H/$OCOC_4H_9$, R_2 = H/$OCOC_4H_9$
[67] R_1 = I, R_2 = H
[68] R_1 = H, R_2 = SAc
[69] R_1 = H, R_2 = SH
[70] R_1 = H, R_2 = SNO

SNO-HEX

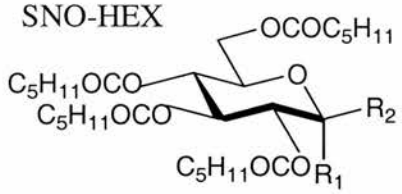

[71] R_1 = H/$OCOC_5H_{11}$, R_2 = H/$OCOC_5H_{11}$
[72] R_1 = I, R_2 = H
[73] R_1 = H, R_2 = SAc
[74] R_1 = H, R_2 = $SCOC_5H_{11}$
[75] R_1 = H, R_2 = SH
[76] R_1 = H, R_2 = SNO

Having obtained the four precursors to the desired targets using column chromatography after both of the aforementioned steps, the nitrous fuming method was employed to give the requested *S*-nitrosothiols (sections 6.13-6.16). This subsequently allowed the effects of increasing lipophilicity to be studied in both a biological and *in vitro* model.

The synthesis of these lipophilic compounds was mastered in a relatively short time span when considering the difficulties faced in the handling of these viscous oils. Overall yields were as high as 57% in some cases, which is obviously very satisfactory. However, one instance where a clear problem existed was in the de-*S*-acetylation step when the reaction was left stirring over many hours. For instance, in the case of both the propionylated and hexionylated compounds complete conversion to the corresponding disulphides was observed (section 6.13.9 & 6.16.6). Compounds [60] and [77] respectively, were confirmed as the decomposition products by a downfield shift in the carbon NMR spectrum for *C*-1. Instead of the characteristic thiol signal at δ_C ~79ppm, a shift relating to the presence of disulphide, in the region of δ_C ~87ppm was identified. Since the production of disulphide clearly signified the successful removal of the acetyl group, reducing the reaction time was quickly suggested and the problem solved.

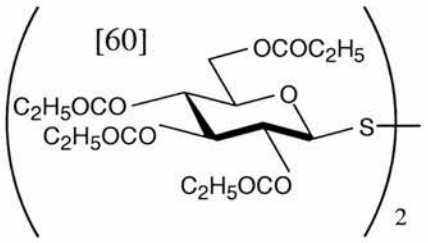

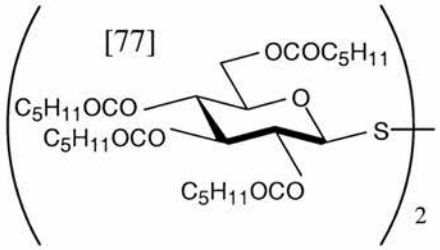

Further complications in the hexionylated series resulted due to the unsuccessful removal of excess hexanoic anhydride from the initial step (section 6.16.1). As a result, during the *S*-acetylation step, a minor portion of *S*-hexionylated material was also identified (section 6.16.3). Using a long, thin, slow eluting silica column, the two compounds and any remaining hexanoic anhydride were separately isolated. Interestingly, when the benzylamine reaction was performed on the *S*-hexionylated sugar, TLC analysis, illustrated the same desired thiol product was formed (section 6.16.4b). This reinforces the idea that this reaction, if performed under the correct conditions and for the required length of time is a reliable route to the free thiol.

In light of the problems seen for the hexionylated compound, a nucleophilic catalysis process was incorporated into the initial acylation step using pyridine in the presence of trace amounts of water. As illustrated in scheme 20, the rationale here was to generate the related acid from the anhydride, thereby enabling the removal of the excess reagent by a simple aqueous work-up process. This proved to be an effective addition to the protocol, except in the case of the most lipophilic derivative, as described (section 6.16).

Scheme 20. *The nucleophilic catalysis performed to remove excess anhydride.*

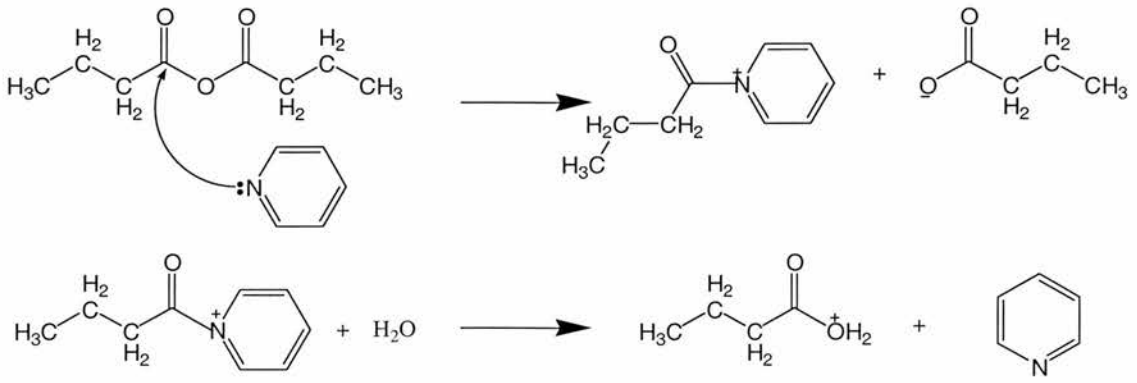

Having synthesised a systematic range of lipophilic compounds, the other extreme was addressed by the generation of the unprotected, hydrophilic SNOG molecule [79].

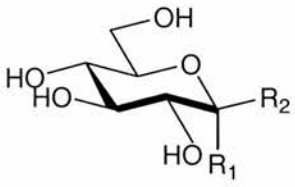

[78] R_1 = H, R_2 = SH
[79] R_1 = H, R_2 = SNO

The 1-thio-β-D-glucopyranose sodium salt is commercially available. We therefore simply nitrosated the free thiol form of this compound as described in section 6.17. Alternatively we could have obtained the free thiol by the de-*O*/*S*-acetylation of 2,3,4,6-tetra-*O*-acetyl-1-*S*-acetyl-1-thio-*β*-D-glucopyranose [3], using sodium methoxide, as described by Laine and co-workers.[39]

For completeness, the *S*-nitroso-1-thio-2,3,4,6-tetra-*O*-benzoylated glucopyranose compound referred to as SNOB [84] was targeted. With such substituents attached, one is still dealing with a lipophilic disarmed sugar, which in fact generates an anomeric position that is even less reactive than that of the straight chain ester laden glucose compounds [5], [59], [65], [70] and [76]. The novelty of incorporating aromatic groups was the main thrust behind its inclusion together with the knowledge that *in vivo*, such groups hydrolyse to simply give benzoic acid which is a well known endogenous by-product, in any case, thus not presenting any appreciable toxicology risks.

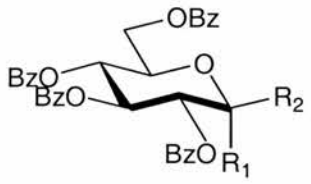

[80] R_1 = H/OBz, R_2 = H/OBz
[81] R_1 = I, R_2 = H
[82] R_1 = H, R_2 = SAc
[83] R_1 = H, R_2 = SH
[84] R_1 = H, R_2 = SNO

The synthesis of compound [84] was essentially the same as that just described for the lipophilic series (section 6.18). The only significant difference was in the initial step, which involved the use of benzoyl chloride in pyridine as opposed to anhydride promoted by iodine. This procedure was performed at low temperature. Literature reports suggest that under such conditions the α-product predominates,[29,40,41] though

we found a 9:1 ratio in favour of the β-anomer.

Steps 2,3,4 and 5 were all routine using the procedures already outlined in this section. Indeed for this particular compound the synthesis was even more straight-forward as crystalline materials were obtained in two of the steps (compounds [80] and [82]) and all the compounds enroute to the product, including the iodide, were more stable than any of the related ester compounds (sections 6.2, 6.13, 6.14, 6.15 and 6.16). Despite good general stability in obtaining the target, when this was diluted in the standard way for UV analysis, the white solid of the corresponding disulphide [85] precipitated out of solution (section 6.18.6). This clearly emphasises the high lipophilic character of this compound.

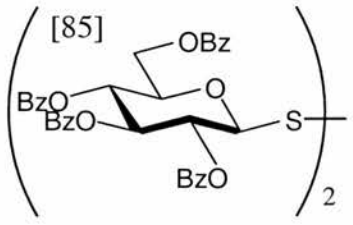

2.4 Synthesis of *S*-Nitroso-6-thio-2,3,4,6-tetra-*O*-acetyl-β-D-glucopyranose, (6-SNAG) [89].

In order to tether the NO source to the 6-position of the sugar, selective protection at this site was the initial necessity in this synthetic pathway. Since the primary hydroxyl is an exclusive characteristic of *C*-6, the use of tosyl chloride known to preferentially attack at such primary centres provided the required specificity. To prevent further tosylation at sites other than the 6-position, only one equivalent of tosyl chloride was used prior to the addition of acetic anhydride. Using this protocol described by two separate groups,[42,43] compound [86] was obtained in 24% yield prior to recrystallisation. This low yield was also observed when the reaction was repeated on twice the scale (section 6.19.1), despite reports of a 40% yield in the literature. Tosyl protection was chosen based on the knowledge that it yields a stable crystalline product, yet is also a good leaving group. This latter property was

exemplified by direct conversion to the *S*-acetyl without the need to first form the halide. In choosing the thioacetate pathway (section 6.19.2) the demand for the crystalline form of the thiouronium salt was also avoided and so instead compound [87] was obtained in a highly pure form in just two steps. As reported by Whistler and Seib[44], the production of compound [87] was only possible with the introduction of a reflux period to drive the reaction to completion. This is in sharp contrast to all similar reactions performed at the anomeric position, which gave complete conversion at room temperature.

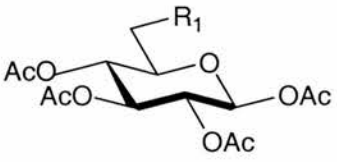

[86] R_1 = OTs
[87] R_1 = SAc
[88] R_1 = SH
[89] R_1 = SNO

To our surprise, de-*S*-acetylation using benzylamine, to give compound [88], proved to be unsuitable in this instance. Having repeated this step (section 6.19.3a) using varying proportions of the primary amine, without any success, the decision was eventually taken to modify the conditions. Addition of the same nucleophile in the presence of silver triflate was considered as a suitable adjustment to the synthesis, on the basis of work by Ley and co-workers.[45-48] As outlined in section 6.19.3b, this pathway showed promise with the generation of a white crystalline material believed to be that of the thio-silver salt. However, many problems were encountered in isolation and purification of this material. Having employed similar purification tactics to those described[48] (section 6.19.3b), the free thiol was not identified, despite numerous attempts.

Alternative strategies for generating the free thiol include work by Defaye and Guillot,[49] using 2-aminoethanethiol as the transfer reagent. However it was postulated that this would only increase confusion upon isolation due to the potential for disulphide formation that was not simply restricted to that between two sugar thiols. In other words, a non-symmetrical disulphide made up of half sugar thiol and half transfer reagent, could in theory be produced. Thus, this avenue was not pursued. Similarly, work by Yelm[50] was not considered as a viable alternative method, despite the reported de-*S*-acetylating properties of pyrrolidine. This suggestion was dismissed on the grounds that the free thiol was only produced in situ ready for a further reaction, rather than being adequately isolated, purified and

characterised. On the basis of the results in the laboratory and from literature reports, attempts to synthesise compound [88] were eventually abandoned.

2.5 Synthesis of free/acetylated *S*-Nitroso-3-thio-glycerol, [90] and [93].

Since glycerol is a central building block to sugar formation, the production and testing of *S*-nitroso-3-thio-1,2-propanediol [90] and *S*-nitroso-3-thio-1,2-di-*O*-acetyl propane [93] was seen as a necessary part of this research. Whilst the former simply required a nitrosation step from the commercially available thiol (section 6.20) the latter required an initial acetylation and selective de-*S*-acetylation (section 6.20.2). Clearly the obvious choice of reagent to give the free thiol [92] was again benzylamine, though as in the case of compound [87], no reactivity was observed.

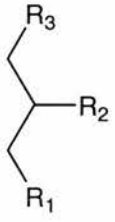

[90] R_1 = OH, R_2 = OH, R_3 = SNO
[91] R_1 = OAc, R_2 = OAc, R_3 = SAc
[92] R_1 = OAc, R_2 = OAc, R_3 = SH
[93] R_1 = OAc, R_2 = OAc, R_3 = SNO

For reasons identical to those described for compound [88] (section 2.4), 1,2-di-*O*-acetyl-3-thio-propane [92] was not successfully synthesised. These observations would suggest that the use of benzylamine requires the thioacetate to occupy the highly reactive anomeric position in order to successfully allow the de-*S*-acetylation to proceed.

Whilst we were disappointed not to have synthesised the complete range of target compounds listed in section 1.4.4, we took heart from the fact that compounds [25], [30], [46] and [51] had previously been reported as being too unstable to characterise and test biologically.[1,51] Our ability to obtain these compounds in a pure form and show their vasodilatory action along with a whole host of other carbohydrate based *S*-nitrosothiols illustrates the progression made. The full impact of this chemical development on the biological testing will be discussed in the following chapter

where we present the collated *in vivo* data.

2.6 References

1 I.R. Greig, Ph. D. Thesis, University of St Andrews, UK, 1997.

2 K.P.R. Kartha and H.J. Jennings, *J. Carbohydr. Chem.*, 1990, **9**, 777.

3 M. Cerny, J. Vrkoc and J. Stanek, *Coll. Czech. Chem. Commun.*, 1957, **24**, 64.

4 M. Cerny, J. Stanek and J. Pacak, *Monatsh.*, 1963, **94**, 290.

5 J. Stanek, M. Sindlerova and M. Cerny, *Coll. Czech. Chem. Commun.*, 1965, **30**, 297.

6 W.A. Bonner and J.E. Kahn, *J. Am. Chem. Soc.*, 1951, **73**, 2241.

7 D. Horton, *Methods in Carbohydrate Chemistry*, 1963, Academic Press, Inc., London and California, ed. R.L. Whistler and M.L. Wolfrom, **2**, 433.

8 A.R. Butler, A.M. Calsy-Harrison, C. Glidewell and P.E. Sorensen, *Polyhedron*, 1988, **7**, 1197.

9 G.L. Ellman, *Arch. Biochem. Biophys.*, 1959, **82**, 70.

10 P.W. Riddles, R.L. Blakeley and B. Zerner, *Anal. Biochem.*, 1979, **94**, 75.

11 K.P.R. Kartha, P. Cura, M. Aloui, S.K. Readman, T.J. Rutherford and R.A. Field, *Tet. Asymm.*, 2000, **11**, 581.

12 T.C. Zheng, M. Burkart and D.E. Richardson, *Tet. Lett.*, 1999, **40**, 603.

13 S. Bennett, M. von Itzstein and M.J. Kiefel, *Carbohydr. Res.*, 1994, **259**, 293.

14 M.J. Kiefel, R.J. Thomson, M. Radovanovic and M. von Itzstein, *J. Carbohydr. Chem.*, 1999, **18**, 937.

15 A.S. Demir, A.C. Igdir and A.S. Mahasneh, *Tetrahedron*, 1999, **55**, 12399.

16 T. Itoh, N. Tsutsumi and A. Ohsawa, *Bioorg. Med. Chem. Lett.*, 1999, **9**, 2161.

17 B. Saville, *Analyst*, 1958, **83**, 670.

18 T.W. Hart, *Tet. Lett.*, 1985, **26**, 2013.

19 M.E. Mendelsohn, S. O'Neill, D. George and J. Loscalzo, *J. Biol. Chem.*, 1990, **265**, 19028.

20 D.L.H. Williams, *Nitrosation*, Cambridge University Press, Cambridge, 1988, 173.

21 L.C. Green, D.A. Wagner, J. Glogowski, P.L. Skipper, J.S. Wishnok, S.R. Tannenbaum, *Analyt. Biochem.*, 1982, **126**, 131.

22 J.A. Cooke, S.Y. Kim, D. Teague, M.C. Krishna, R. Pacelli, J.B. Mitchell, Y. Vodovotz, R.W. Nims, D. Christodoulou, A.M. Miles, M.B. Grisham and D.A. Wink, *Analyst. Biochem.*, 1996, **238**, 150.

23 M. Cavero, A. Hobbs, D. Madge, W.B. Motherwell, D. Selwood and P. Potier, *Bioorg. Med. Chem. Lett.*, 2000, **10**, 641.

24 P. Brajeswar, R.J. Bernacki and W. Korytnyk, *Carbohydr. Res.*, 1980, **80**, 99.

25 B.R. Baker, J.P. Joseph, R.E. Schaub and J.H. Williams, *J. Org. Chem.*, 1954, **19**, 1786.

26 D. Horton, *Methods in Carbohydrate Chemistry*, Academic Press, New York and London, 1972, **6**, 282.

27 S.L. Smith, Ph. D. Thesis, University of St Andrews, UK, 1997.

28 P.A. Gent, R. Gigg and R. Conant, *J. Chem. Soc. Perkin Trans. 1*, 1972, 277.

29 R. Behrend and P. Roth, *Ann.*, 1904, **331**, 359.

30 M.A. Probert, J. Zhang and D.R. Bundle, *Carbohydr. Res.*, 1996, **296**, 149.

31 J.J. Fox and I. Goodman, *J. Am. Chem. Soc.*, 1951, **73**, 3256.

32 K.P.R. Kartha and R.A. Field, *Tetrahedron*, 1997, **53**, 11753.

33 I.A. Wolff, *J. Am. Chem. Soc.*, 1945, **67**, 1623.

34 K.P.R. Kartha and R.A. Field, *J. Carbohydr. Chem.*, 1998, **17**, 693.

35 V. Pozsgay and H.J. Jennings, *Tet. Lett.*, 1987, **28**, 1375.

36 K.P.R. Kartha and R.A. Field, *Tet. Lett.*, 1997, **38**, 8233.

37 K.P.R. Kartha and R.A. Field, *Carbohydr. Lett.*, 1998, **3**, 179.

38 G.A. Olah and S.C. Narang, *Tetrahedron*, 1982, **38**, 2225.

39 V. Laine, A. Coste-Sarguet, A. Gadelle, J. Defaye, B. Perly and F. Djedaini-Pilard, *J. Chem. Soc. Perkin Trans. 2*, 1995, 1479.

40 H.G. Fletcher, *Methods in Carbohydrate Chemistry*, 1963, Academic Press, Inc., London and California, ed. R.L. Whistler and M.L. Wolfrom, **2**, 234.

41 H.G. Fletcher and C.S. Hudson, *J. Am. Chem. Soc.*, 1947, **69**, 1145.

42 E. von Hardegger and R.M. Montavon, *Helvetica Chemica Acta*, 1946, **29**, 1199.

43 J. Stanek and L. Tajmr, *Collect. Czech. Chem. Commun.*, 1959, **24**, 1013.

44 R.L. Whistler and P.A. Seib, *Carbohydr. Res.*, 1966, **2**, 93.

45 K.M.J. Brands and L.M. Di Michele, *Tet. Lett.*, 1998, **39**, 1677.

46 P.M. Booth, C.M.J. Fox and S.V. Ley, *Tet. Lett.*, 1983, **24**, 5143.

47 S.V. Ley and P.R. Woodward, *Tet. Lett.*, 1987, **28**, 3019.

48 P.M. Booth, C.M.J. Fox and S.V. Ley, *J. Chem. Soc. Perkin Trans. 1*, 1987, 121.

49 J. Defaye and J.-M. Guillot, *Carbohydr. Res.*, 1994, **253**, 185.

50 K.E. Yelm, *Tet. Lett.*, 1999, **40**, 1101.

51 A.R. Butler, R.A. Field, I.R. Greig, F.W. Flitney, S.K. Bisland, F. Kahn and J.J.F. Belch, *Nitric Oxide: Biol. Chem.*, 1997, **1**, 211.

Chapter 3 Discussion & Results. Biology

In vivo performance of the NO donor compounds

3.1 Ethical consent

In all of the work described in this chapter, human volunteers were used. Of these the healthy subjects were categorised as such if no clinical history of Raynaud's phenomenon or any associated vascular disorder was evident. In contrast, a heterogeneous group of primary and secondary Raynaud's patients was recruited from clinics at Ninewells Hospital, upon the recommendation of general practitioners.

All individuals had the purpose and expected duration of the study explained to them in both a verbal and written sense prior to signing a consent form. This described how the subjects were free to withdraw from the study at any stage and without explanation. Such a procedure is in accordance with the requirements outlined by Tayside committee on medical ethics. This committee granted approval for this work based on the knowledge that the test compounds give naturally occurring byproducts[1] and originate from a whole host of harmless biological sources. Cow's milk, malted barley, cherry gum, bran, grape sugar and lobster shells are just some of the commonly encountered natural products from which the test compounds were developed. This illustrates the low risk associated with this work. Such safety is further reinforced when one considers that all of the compounds are delivered transdermally rather than via oral or intravenous routes. Topical application of this kind obviously lends itself to the use of the laser Doppler imager, which as already described (section 1.3.3) provides quantitative biological data in a non-invasive manner.[2] These safety issues were fully explained to prospective subjects. This was reflected in the willingness and ease of recruitment.

3.2 Targeting the nutritional blood vessels.

Using the MoorLDI scanning laser-Doppler imager (courtesy of Vascular Medicine Department of Ninewells Hospital in conjunction with The University of Dundee) an ethanol : water (1:1) solution containing 0.75% (20.58mM) *S*-nitroso-1-thio-2,3,4,6-tetra-*O*-acetyl-β-D-glucopyranose (SNAG) [5], was tested on the forearm of healthy subjects. This body region is often the one of choice in peripheral blood flow work due to the high abundance of nutritional blood vessels innervating such tissue [Fig. 22]. These vessels are our primary target for improving blood flow to ensure a continuous supply of essential nutrients, oxygen and energy, as well as flushing away unwanted metabolites, whilst limiting heat loss from the body. Such a process is highly favourable and of great importance in reversing the more severe symptoms associated with Raynaud's phenomenon.

Fig. 22 *The vascular anatomy of the skin upon the forearm.*

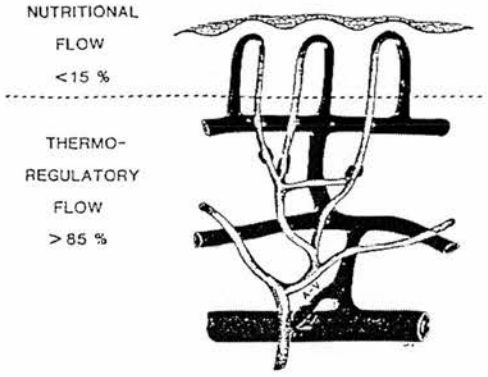

The nutritional blood vessels, illustrated above, are the most superficially lying. They comprise of 15% of the associated vascular network. The remaining 85% of the cutaneous blood supply is made up of the thermoregulatory blood vessels, which are situated in the deeper layers of the dermis. All such vessels are supplied with oxygenated blood from the arteriolar-venous (A-V) shunts.
Extracted from P. Oberg, Crit. Rev. Biomed. Eng., 1990, ***18****, 125.*[2]

3.3 The most recent publications in this area.

From within our own research group, all of the preliminary work reported to date has centred around the vasodilatory action of SNAG.[3-5] Whilst the forearm and dorsum of the fingers have shown encouraging results, the finger pulps have been less responsive to such treatment. This can be explained by the finger pulps housing a greater proportion of thermoregulatory vessels. Using N^G-monomethyl-L-arginine (L-NMMA), a nonselective NOS inhibitor, in regions under strict thermoregulatory control has shown that NO is not an important regulator of blood flow.[6] Due to the high temperature sensitivity of this finger region, blood flow enhancement due to relaxation of nutritional vessels is essentially masked by reflex sympathetic vasoconstriction. However, maintaining the limited nutritional vessels in a relaxed form is still essential in the prevention of gangrene as NO does play a significant role in the basal dilator tone.[6] Thus NO donation may be beneficial in Raynaud's though, to date, the responsiveness of *S*-nitrosothiols has only been seen in sites such as the forearm [Fig. 23] which show a high abundance of nutritional vessels [Fig. 22], as described previously [section 3.2].

Fig. 23 *Forearm blood flow responses to SNAG when administered to a healthy male volunteer*

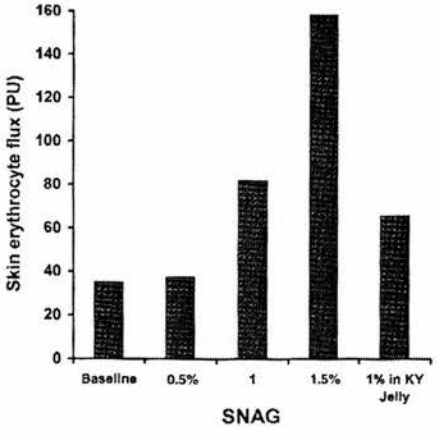

Early data from administrating SNAG to the forearm. The dose effect and delivery medium will be the main focus of our initial biological work since these appear to be significant variables.
*This graphical representation was extracted from Nitric Oxide: Biol. Chem., 1997, **1**, 211.*[3]

As already described (section 1.2.7), the use of transdermally delivered NO for this clinical application is not exclusive to our laboratory, since it has also been investigated, in a parallel manner, by a group led by Benjamin.[7,8] Their rather classical NO-generating system, is difficult to use and rather inefficient. The incorporation of a semipermeable membrane on the skin, to allow only NO passage has the additional effect of producing local skin warming as it provides an extra outermost protective layer. As a result, experimental measurements reported by the LDI are difficult to interpret. However using this technique, it is somewhat surprising that Benjamin reports[8] a higher blood flux in the absence of this membrane. While the direct application of ascorbic acid and sodium nitrite could explain a greater NO supply, and hence a greater flux, the enhanced response is far more likely to be as a result of the high concentrations of acid and nitrite upon the skin producing an inflammatory response. The membrane could also be considered to impede penetration by the laser. We are therefore confident that our approach provides somewhat more reliable data and a less questionable protocol provided by studying the effects of NO alone. The smaller concentrations and high purity of applied samples is undoubtedly attractive. Since there is no requirement for a nitric oxide generating step once introduced to the skin, a true measure of increases in blood flow is possible, as no additional layers other than the test solution itself, are applied to the skin's surface.

3.4 Preparation of forearm.

Having prepared the test site for transdermal administration by stripping dead skin and excess hair with surgical tape and alcoholic wipes, perspex rings of 2cm diameter, used as drug wells, were attached to the forearm by double sided adhesive rings of identical diameter. Unlike in many other transdermal studies where iontophoresis[9] is routinely incorporated (section 1.3.1), no current was applied across the skin tissue. Instead, after running an initial dry and wet baseline, in order to calculate the degree of liquid reflection detected by the LDI, the various solutions were introduced to the test wells, which were then repeatedly scanned every minute.

This entire procedure was routinely carried out in a temperature-controlled environment of 19°C.

3.5 Forearm control experiments with SNAG [5]

By way of a control, the change in blood flow (measured in arbituary perfusion units, PU) due to 0.75% (20.58mM) SNAG [5], was monitored in parallel with equimolar concentrations of its precursor [4] and degradation product [6]. In addition, the effect of ethanol : water (1:1) alone was studied. This involved the use of nitrosated ethanol, flushed with nitrogen in the same manner as the *S*-nitrosothiol solutions (see section 2.1). On the basis of this work we can be completely certain that the enhanced blood flow was due to the *S*-nitrosothiol. In the following figure [Fig.24], this difference is presented. With practising physicians on hand, the enhanced response (Well 4) was confirmed to be that of a genuine vasodilatory response rather than an inflammatory response. The latter is often referred to as a 'wheal response', which characteristically gives a reddening of the skin over an extended area and for a prolonged time period.

Fig.24 *Images seen by the LDI from initial control experiments.*

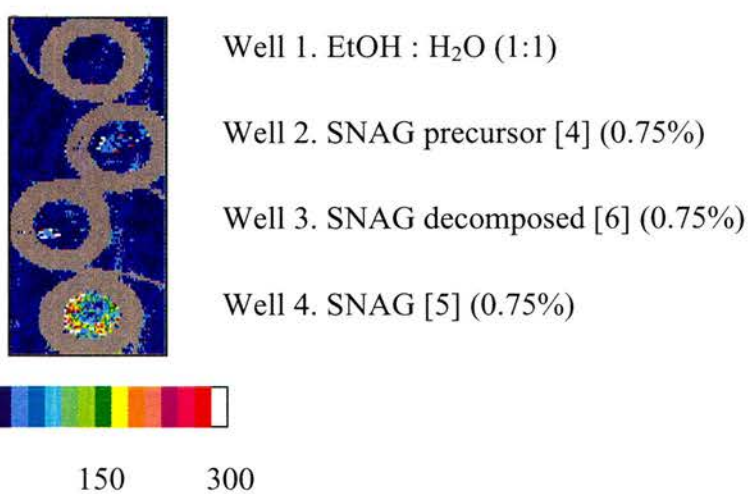

The colour change refers to a change in blood flux. A shift from blue to red illustrates an increase in flux, though obviously, a change as extreme as this is not observed. The scan shown illustrates a

typical forearm blood flow response seen for a healthy volunteer using the MoorLDI scanning laser-Doppler imager. Such scans are repeatedly recorded every minute during each experimental run. The usual duration is between 30-40 minutes.

From the scan shown in Fig. 24, the blood flux data is tabulated. Using these results we are able to produce a profile for each test well [Fig.25], over the entire experimental time course. Using this control plot [Fig.25], many preliminary questions were answered. For instance, in addition to the obvious observation regarding the need for NO, the lack of blood flux in all of the control wells shows that local skin warming from the test solutions does not have any significant bearing upon the overall response when studied over a period of time. The profile, (shown below) also illustrates a rapid onset of the response in agreement with the idea of a slow, yet continuous, supply of NO, independent of any biological or external requirements other than an environment temperature ranging from 25-37°C. The independent manner in which SNAG [5] functions will also explain why no tolerance to the compound is seen over the 27 minutes of testing.

Fig. 25 *A Control plot for a healthy volunteer.*

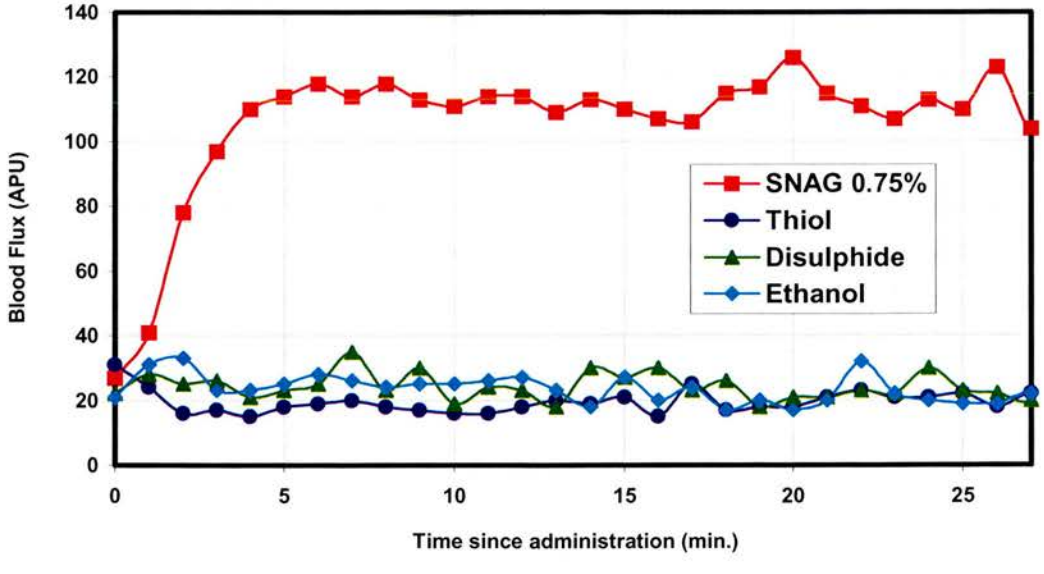

The above plot shows the typical control data recorded for a single healthy volunteer. This highlights the requirement for the SNO functionality in order to see an improvement in blood flow. In addition, the rapid onset and prolonged duration of the vasodilation, due to SNAG [5], can be clearly observed.

Fig. 26 supports the individual scan data presented previously [Fig. 25]. When shown in this graphical form, for a group of healthy individuals, there can be no confusion that the consistent vasodilatory response is a result of the NO donor activity of SNAG [5]. This eliminates any suggestion that the thiol [4], disulphide [6], ethanol, water or a combination of these components may be responsible for the observed flux increases.

Fig. 26 *Control data presented as the area under the curve in 10 minute intervals for a group of healthy male subjects.*

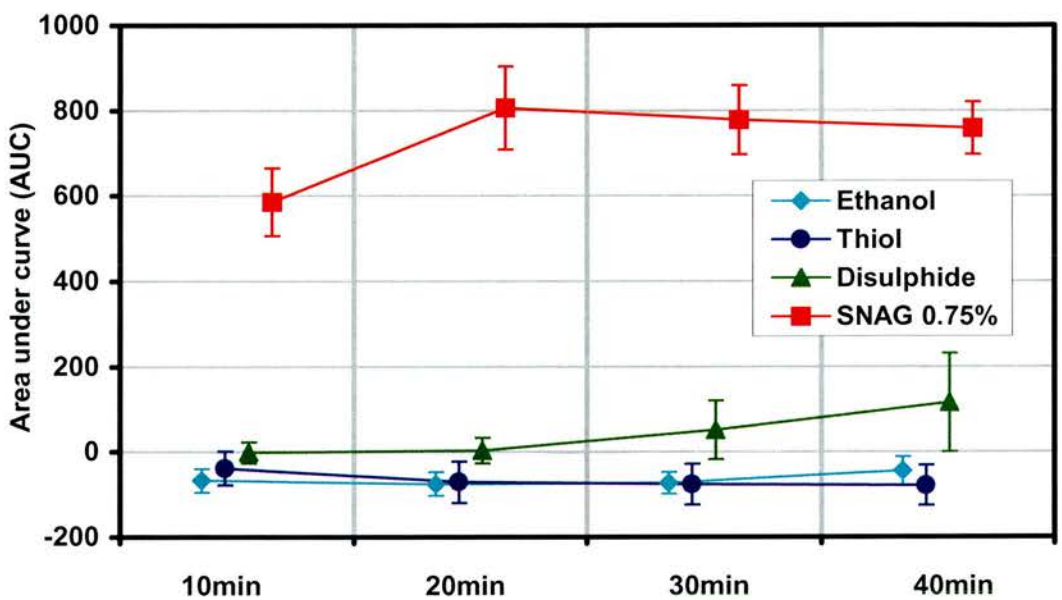

This collated data was obtained from a study on eight healthy male individuals and reinforces the profile seen in figure 25. All values were referenced with respect to data obtained from the initial dry baseline readings. The deviation between subjects, illustrated by the error bars, shows the high level of reproducibility between each experimental run.

For five of the subjects used in the previously described study, repeat visits were possible. This enabled the degree of reproducibility to be better appreciated. As illustrated in Fig. 27, the experimental data obtained for duplicate runs highlights that certain individuals produced more consistent data than others. Overall, reproducibility was considered adequate to allow further work using SNAG [5] and related compounds. Thus throughout the rest of the work, the synthetic and testing protocols, already described (sections 2.1 and 3.4), were carefully maintained without further modifications.

Fig. 27 *Reproducibility of the control SNAG [5] data from five healthy subjects.*

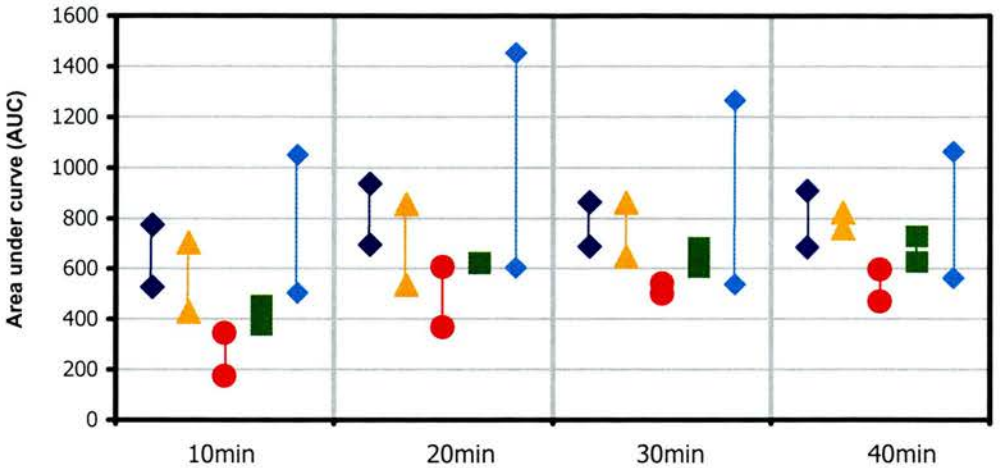

Control SNAG [5] data from five subjects who agreed to a second experimental run. The various colours indicate that certain subjects showed closer agreement between visits than others. When considering how emotional and environmental factors can greatly alter a subject's response on a given day, the data presented above was considered to be sufficiently reproducible thus validating the protocol.

3.6 Probing experiments to rationalise the mechanism of action.

3.6.1 The duration of the vasodilation and the secondary response.

When administering 0.75% (20.58mM) SNAG [5] the peak response was obtained so quickly that changing the duration of drug application does not significantly alter the general profile of blood flux with time. The different profiles outlined in figures 28a-c are as a result of subject variability rather than as a consequence of different dosing regimens. The profile observed in Fig. 28a is particularly interesting since it was consistently observed in several individuals. The explanation for the initial rise followed by a transient drop before the flux recovers to a plateau resulted in much speculation. In physiological terms this is explainable. For instance, it is reasonable

to assume an initial relaxation of the most superficial blood vessels due to NO donation, before the larger underlying A-V shunts also become dilated. This would have the effect of producing an initial rise in blood flux followed by a delayed drop. The rate at which NO can diffuse from the skin's surface to the deeper layers of the dermis will determine the time lag between the initial rise and subsequent fall in flux. Obviously the dilation of the A-V shunts will result in a drop in blood pressure downstream of the shunts thus explaining the lower blood flux measured by the LDI in the most superficial vascular network. The quick recovery in flux may be as a consequence of neuronal activation in the shunts, producing vasoconstriction and allowing the local homeostasis of blood pressure to be preserved. This would obviously have the effect of allowing the flux in the capillary loops to increase once again.

Using a different line of thought, the transient drop in flux may be the result of the test solution producing some initial cooling upon the skin's surface, in the face of an initial upsurge in flux due to NO donation. This purely physical explanation is less likely however, since the control wells do not show any appreciable drop in flux, suggesting that there is no significant degree of skin cooling upon the addition of the ethanol : water (1:1) solutions.

The most fascinating observation from the profiles presented (Fig. 28a-c), is the secondary response, so called, as it is the response seen following complete removal of all test solution from the wells. Whilst the size of this response is again subject-dependent, all individuals who show a significant secondary response, first show a drop in blood flux upon removal of the test solutions. This is thought to be in response to local skin cooling, since the solution on the skin is known to act as a protective layer to heat loss over a prolonged period. Such an idea is reinforced by the reduced flux observed in the control wells, upon removal of well contents, though this is obviously a much more subtle drop since the measured flux is already at a baseline level.

The mechanism behind the secondary response has opened up a debate as to the pathway by which SNAG [5] acts following initial contact with the forearm. While it tends to suggest that SNAG [5] is not simply decomposing within the well and diffusing into the skin, it does not necessarily follow that SNAG [5] is entering the skin and releasing NO. Instead SNAG [5] may be entering the skin and performing

transnitrosation reactions (section 4.1.2d) with endogenous thiols which then go on to act as NO reservoirs (Scheme 21). Thus the events taking place are clearly not straight forward, particularly when the rapid rate of the initial response is considered, since this suggests that the direct diffusion of NO from the test well may indeed be a viable pathway. Of course a combination of these processes might be responsible for the biological response. This clearly illustrated the need for further studies with SNAG [5] to better appreciate its mechanism of action, before considering other NO donors.

Fig. 28a *Control data for SNAG [5] (0.75%, 20.58mM) when administered for 10 minutes.*

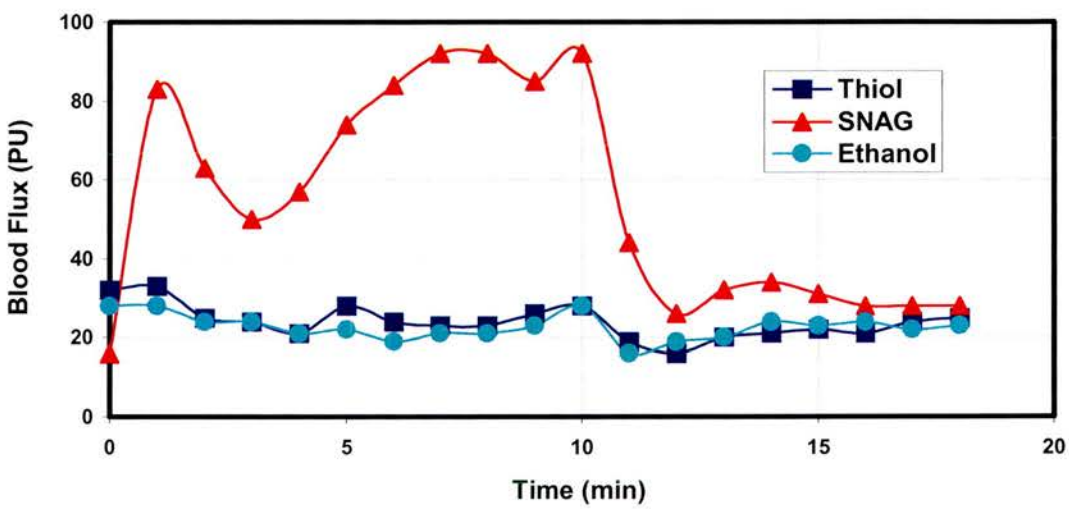

Fig. 28b *Control data for SNAG [5] (0.75%, 20.58mM) when administered for 20 minutes.*

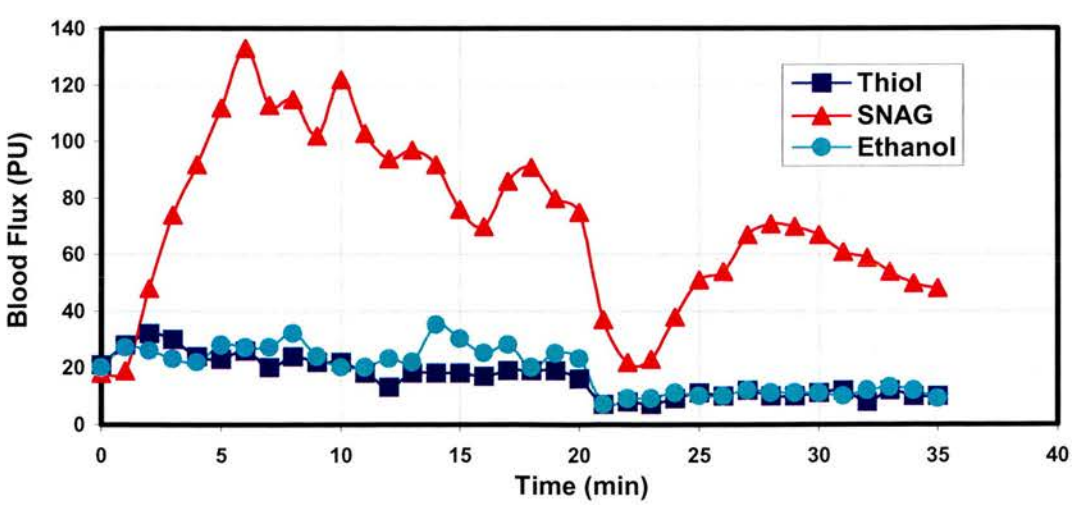

Fig. 28c *Control data for SNAG [5] (0.75%, 20.58mM) when administered for 44 minutes.*

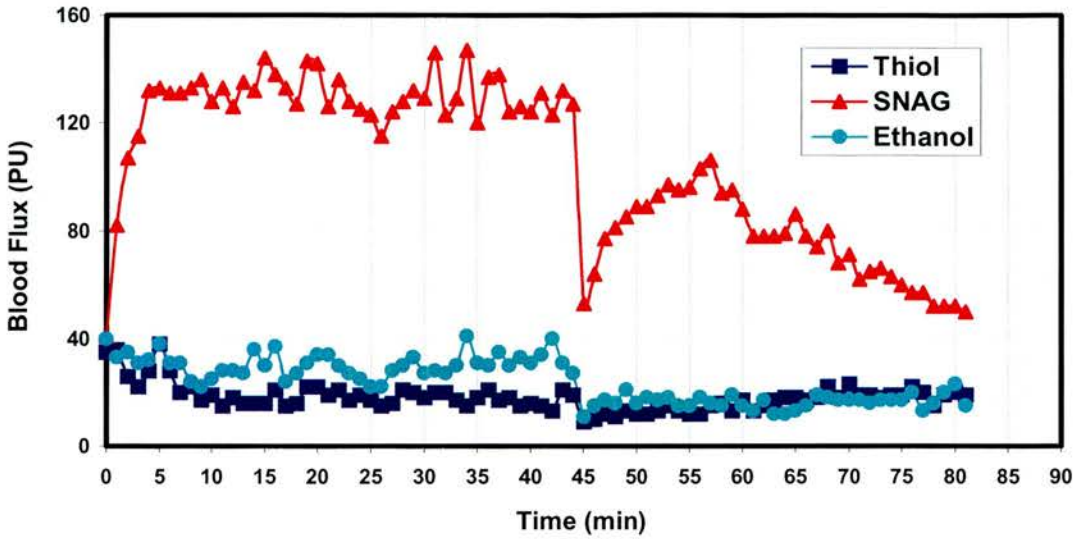

To healthy male volunteers, 0.75% (20.58mM) SNAG [5] was administered for a period of (a) 10 minutes, (b) 20 minutes and (c) 44 minutes, whilst being compared against control wells which were ran in parallel over the same time courses. LDI recordings performed after the removal of the well contents, suggests the existence of a secondary response.

Scheme 21 *The proposed transnitrosation reaction which may occur in the skin.*

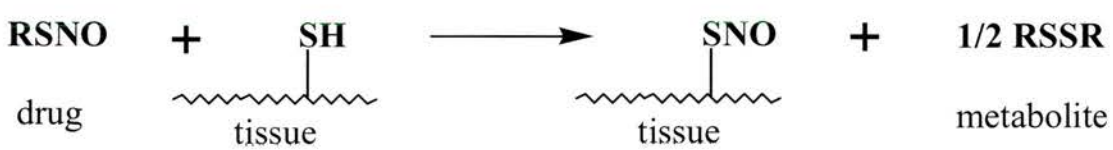

The above scheme relies on the inhabitation of endogenous thiols in the skin, such as, cysteine and glutathione. Many dermatologists[10,11] predict such a presence at the skin's envelope region where the dermal papillae are found (Section 1.3.1). Whether the NO remains bound to its parent compound or in combination with other thiols, the existence of an NO pool in the skin is an attractive possibility that is difficult to prove or eliminate from the debate.

3.6.2 Dose response data.

Dose response profiles were obtained using 0.25, 0.50 and 0.75% (6.86mM, 13.72mM and 20.58mM, respectively) SNAG [5]. While the different doses plateau to the same increased level of flux, the time to reach such a response strongly

suggests a dependence on concentration. This is clearly outlined in figure 29, where the three concentrations (0.25, 0.50 and 0.75%) all plateau to the same level after a period of 30 minutes upon the forearm. Such a finding is a major development upon the preliminary results[3] mentioned previously (section 3.3).

Fig. 29 *A dose-response profile obtained from a healthy subject.*

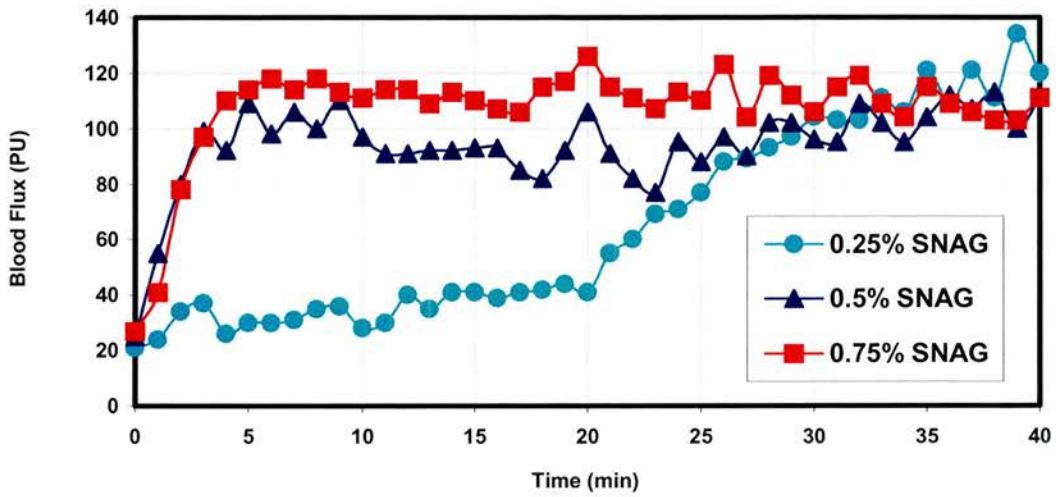

The three doses of SNAG [5] (0.25, 0.50 & 0.75%) were administered to the same forearm of a healthy male volunteer. The data suggests the time taken to reach plateau is concentration driven.

Since the dose-response data was so encouraging, we conducted a further study on eight healthy individuals. The same three concentrations were administered in randomised order upon the forearm, to establish if the initial work was reproducible. Figure 30 shows this to be clearly the case.

Fig. 30 *Collated dose-response data from a study on eight healthy subjects.*

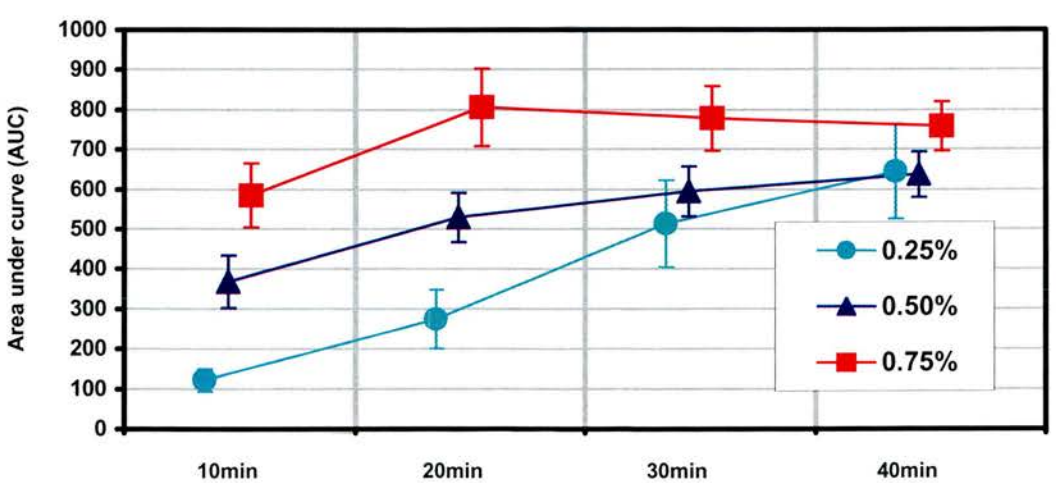

Taking the area under the curve in 10 minute blocks, following the administration of three different

doses of SNAG [5] (0.25, 0.50 & 0.75%) to eight healthy male volunteers, produced the plots shown. The incorporation of error bars helps confirm that the response is concentration dependent.

The major difference between the data presented here and that published in 1997,[3] is the heightened flux despite the administration of smaller doses. This further supports the idea that a more reliable protocol and NO donor are now in place.

3.6.3 The role of photochemical decomposition.

As already described (section 1.4.2, scheme 7), the decomposition of *S*-nitrosothiols can be driven by one of three processes, thermal,[12,13] photochemical[13,14] or copper (I) catalysis.[15,16] Of course there is also the potential for more than one of these processes to operate at any one given time. In attempting to grasp an understanding of SNAG's mechanism of action *in vivo*, the potential for the photochemical decomposition of SNAG [5], whilst within the testing wells, was studied by scanning two identical concentrations of SNAG [5] in parallel. One well was intermittently covered and the other was completely exposed to the environmental conditions and the laser (λ = 638nm) of the Doppler imager. As illustrated in Fig. 31, it would be difficult to argue that restricting the degree of light exposure had any bearing on the biological response.

Fig. 31 *The effect of light exposure upon the vasodilatory response of SNAG [5] (0.75%) when administered to the forearm of a healthy individual.*

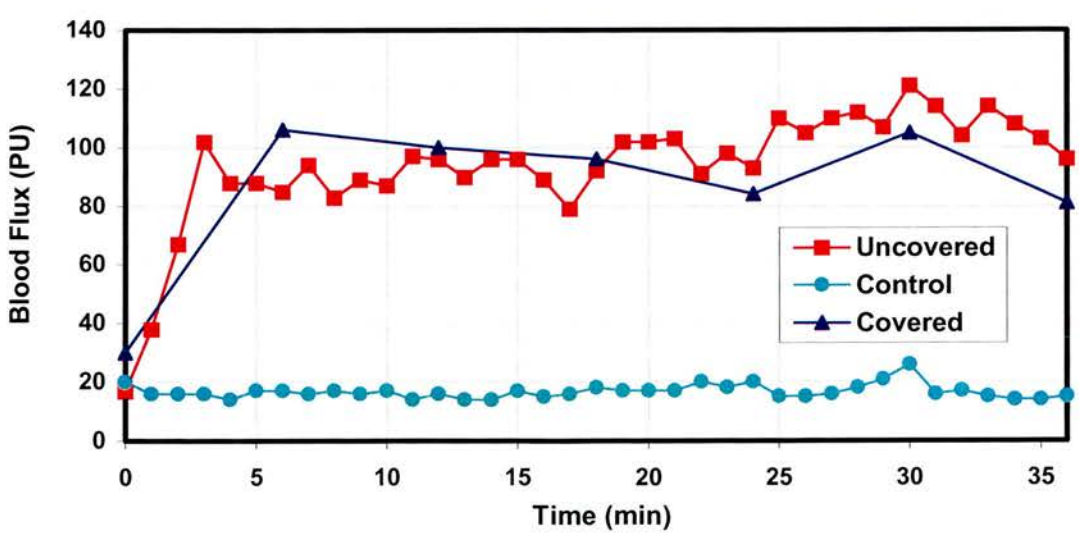

To a healthy male volunteer, SNAG [5] (0.75%) was administered, to the forearm, in two separate

wells along with a control well (ethanol : water, 1:1). Whilst one of the wells containing SNAG [5] was left exposed to air and the laser, as in the normal procedure, the other was covered for 5 minute periods followed by a single scanning period of 1 minute. No significant difference was seen between the two SNAG wells, labelled covered and uncovered, when monitored over 36 minutes.

However, conclusions drawn from these data must be made with caution. As a result, *in vitro* data were also obtained (section 4.1.2a). These suggested that the photochemical decomposition of SNAG [5] is not a dominant pathway by which NO is liberated from our compounds. With this additional data the similarities in blood flux can be attributed to SNAG's chemical properties rather than attempting to explain the results solely in a biological sense.

3.6.4 The effect of copper.

The introduction of copper to the testing wells was seen as an obvious experiment. Since copper sulphate is itself capable of producing hypotension at high concentrations,[17-19] a low but significant amount was introduced to selected wells (2ppm). Any enhancement in blood flux from SNAG [5] in the presence of copper, compared to SNAG [5] in the absence of copper, would clearly suggest the possibility of direct NO diffusion from the well. As shown in Fig. 32, the plateau response was unchanged by the presence of copper. However the initial rate with which the flux increased was governed by this variable. Consequently the protocol was extended to a bigger group of healthy male volunteers. When the study was performed concurrently with the dose response work, the beneficial effects of copper [Fig. 33] were fully appreciated. The clear increase in initial blood flux suggests that direct NO diffusion from the test wells is at least one of the possible mechanisms in operation. Since this does not explain the secondary response illustrated by Fig. 28b-c, other mechanisms can also be assumed.

Fig. 32 *How vasodilation due to SNAG [5] (0.75%) is effected by the addition of copper to the testing well.*

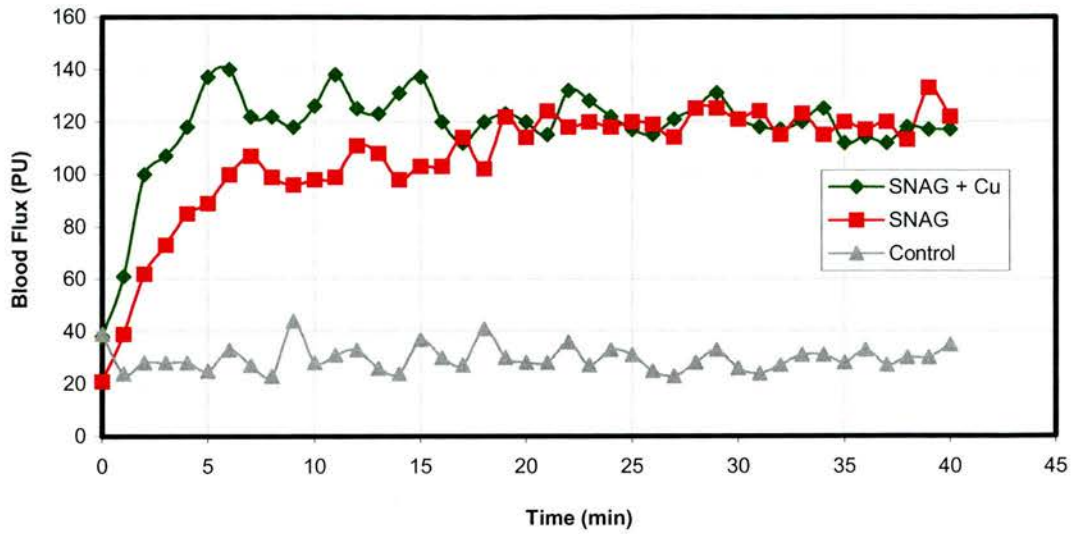

Using the forearm of a healthy male volunteer we were able to show the beneficial effect of adding a copper sulphate solution (2ppm) to a test well containing SNAG [5] (0.75%, 20.58mM).

Fig. 33 *The increase in blood flux seen in eight healthy male volunteers following the addition of a copper sulphate solution (2ppm) to SNAG [5] (0.75%, 20.58mM).*

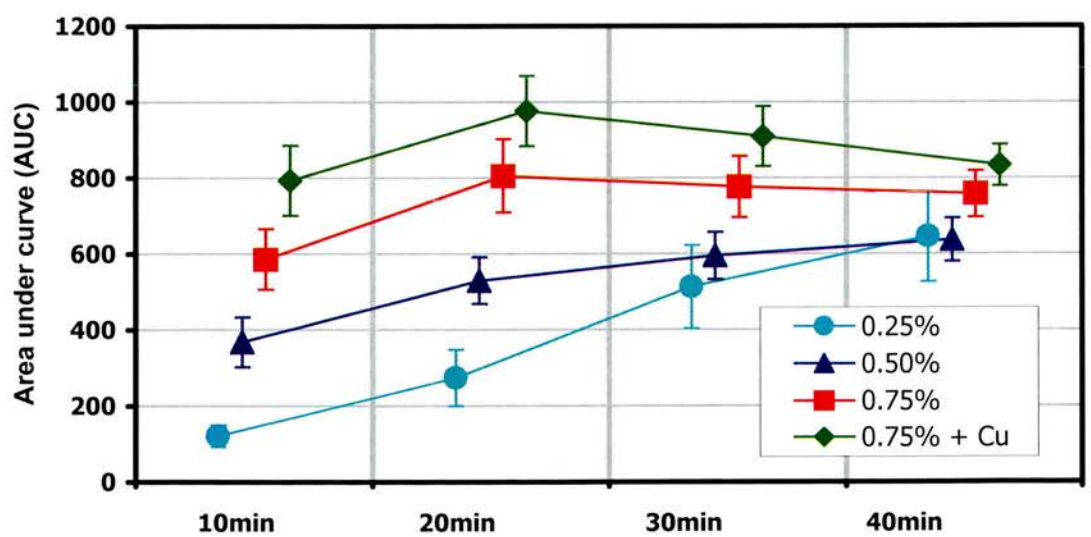

In eight healthy male volunteers the effect of all three concentrations of SNAG [5] (0.25, 0.50 & 0.75%) was compared against SNAG [5] (0.75%) in the presence of a copper sulphate solution (2ppm). The increase in blood flux is consistent with the idea of direct NO diffusion from the test well to the capillary loops under examination by the LDI. Since copper sulphate is itself a hypotensive

agent, it was also added to control wells to ensure that any response was only due to the action of Cu(I) on the SNO group rather than the result of $CuSO_4$ itself.

Using identical concentrations and conditions in an *in vitro* model suggested that copper decomposition was not hugely significant in terms of NO release. Obviously this is in conflict with our biological data. Revision of the biological protocol uncovered how the copper sulphate solution was added as an extra component to SNAG [5] which was already diluted to 0.75% (ethanol : water, 1:1). Thus despite no change in decomposition due to the presence of copper sulphate, the change in ethanol : water proportions was shown by *in vitro* data to be a crucial variable and ultimately the one responsible for the change in blood flux (section 4.1.2b). This can be rationalised since SNAG [5] is not at all soluble in the water. So despite the SNAG [5] solution being diluted, more NO is still released.

On the basis of the reported decompositions when the SNO compounds are not fully able to dissolve into solution, the effect of increasing the water content, and thus reducing the solubility, can be seen as a crucial factor in this instance. Such an idea is exemplified by the profiles obtained when the ethanol : water proportions were altered whilst maintaining the concentration of the SNAG [5] solution (0.25%, 6.86mM) (Fig. 34). This lower concentration of SNAG [5] was purposely chosen since the slower time to onset allows the various rates of increased flux to be more easily observed. The reduction in flux observed after 25 minutes for the two wells containing most water (1:2.5 and 1:4 in Fig.33) is clearly seen.

A change in blood flux, after reaching a level of plateau, could be attributed to the fact that the greater water content renders the SNAG [5] unstable, thus after 25 minutes perhaps very little SNAG [5] is still remaining within the well. Such a theory would also explain the faster time to onset at these two ethanol : water ratios. Although the initial biological data involving copper sulphate [see figures 32 and 33] suggested the faster onset to the wrong variable, the idea of direct NO transfer from the well to the skin, remains valid, since in addition to the data presented in Fig. 34, the decomposition data (section 4.1.2b) correlate very well with this line of thought.

Fig. 34 *How the water proportion in the SNAG [5] solution (0.25%, 6.86mM) effects the blood flux when administered to the forearm of a healthy male volunteer.*

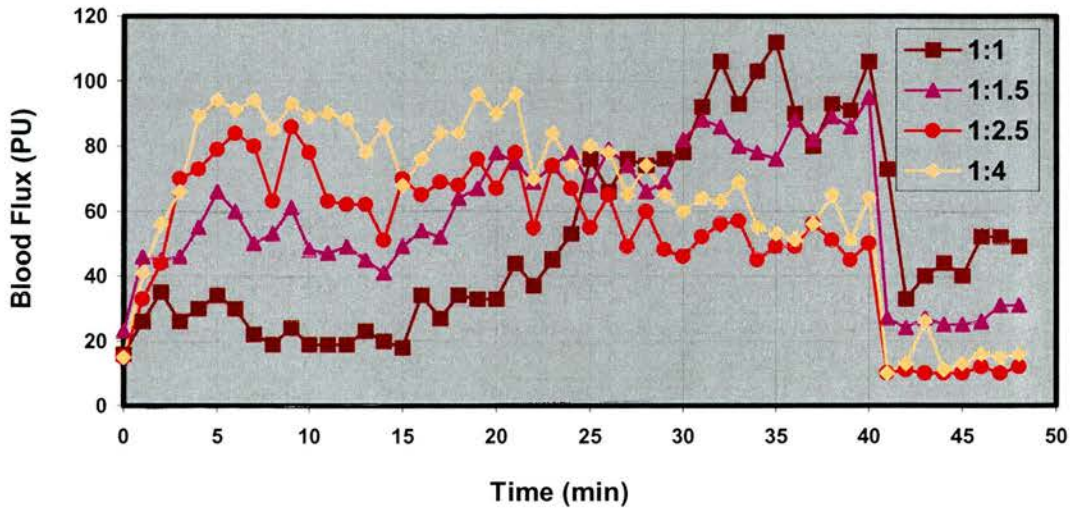

A low concentration of SNAG [5] (0.25%, 6.86mM) was applied to the forearm of a healthy male subject to see the effect of water proportion upon blood flux. The faster rate of SNAG [5] decomposition at higher water levels is seen visually in the above blood flux profile by a faster onset and fall from plateau with time. After 40 minutes the solutions were removed from the test wells so that the secondary effect could be recorded.

As chapter 4 illustrates, the major factor governing SNAG [5] decomposition is temperature. This is one factor, which we cannot alter in the biological work due to temperature increases invalidating the readings by the LDI due to elevation of the baseline. However, altering the water proportion is clearly an alternative handle for manipulating the vasodilatory potential of SNAG [5]. It could be envisaged that such a simple task could indeed be incorporated into a patient's application procedure depending upon the urgency with which the beneficial properties of SNAG [5] were required. However, there must of course be a stage at which dilution of the SNAG [5] solution becomes so great that its optimum effect is no longer observed due to excessive dilution.

3.7 Novel sugar data.

All of the *S*-nitrosated sugar compounds, described in chapter 2, were tested. Their selection for synthesis and biological testing was based on the rationale presented in section 1.4.4. As a consequence of earlier discussion, the reasoning behind the inclusion of each compound will only resurface in attempting to explain significant differences seen in blood flux. Due to limited quantities of material, much of this work was only performed once, though all of the testing was limited to the forearm of the same healthy individual in an attempt to limit variability between subjects. The subject was selected after exhibiting a good degree of reproducibility to SNAG [5] [Fig. 27]. However, it is accepted that the results in this section can, at best, only provide guidance on the importance of altering the sugar.

In the first of the comparative studies, SNAG [5] was administered along side SAGA [15] and SNAGAL [25]. Based on stability properties alone (section 4.1.3), the slower onset seen for the D-galactose and D-glucosamine compounds [Fig. 35] is expected. Such logic relies on the idea of direct NO transfer as a prominent mechanistic route by which vasodilation is achieved. However, after scanning for 23 minutes, all three-test solutions give virtually identical blood flux readings, with all plateauing to a level of approximately 112 PU.

One of the most intriguing ideas was to compare the D and L-isomers from xylose and arabinose [Fig. 36]. A significant difference would have at least left open the possibility of an enzymatic involvement in the pathway by which this group of compounds act. Of course any difference is based on the assumption that an enzyme would preferentially interact with one isomer form over the other.

Fig. 35 *Comparing the vasodilatory potential of SNAG [5] (20.58mM) with that of its sister compounds, SAGA [15] (20.58mM) and SNAGAL [25] (20.58mM), from D-glucosamine and D-galactose, respectively.*

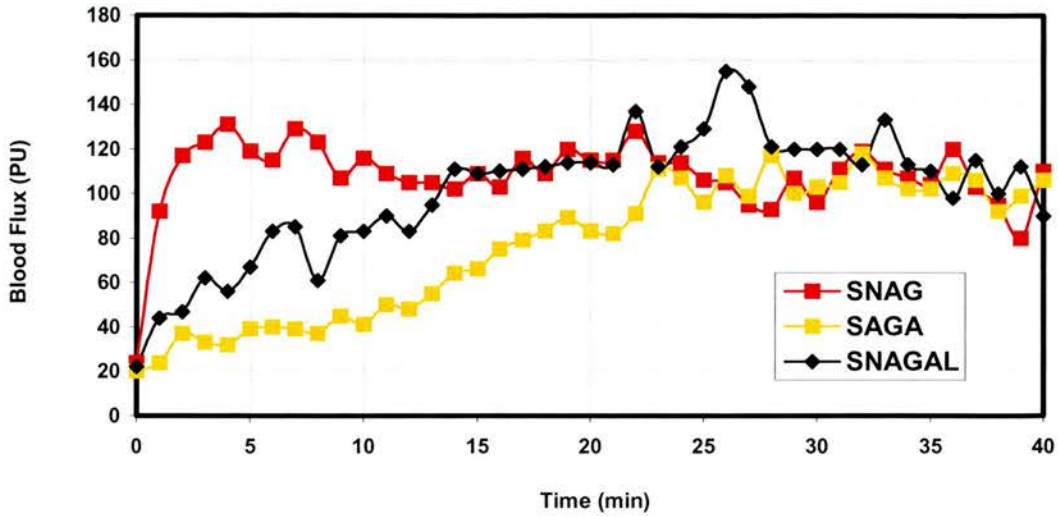

All three test compounds were applied to the same forearm of a healthy male volunteer, as ethanol : water (1:1) solutions (20.58mM). The duration of testing was 40 minutes. After this time there was no appreciable difference seen between the three NO donors since all produced a blood flux of over 100 PU (perfusion units).

Fig. 36 *Comparing the vasodilatory potential of SNAG [5] (20.58mM) with that of its (a) D and L-arabinose [38][42] and (b) D and L-xylose derivatives [30][34].*

(a)

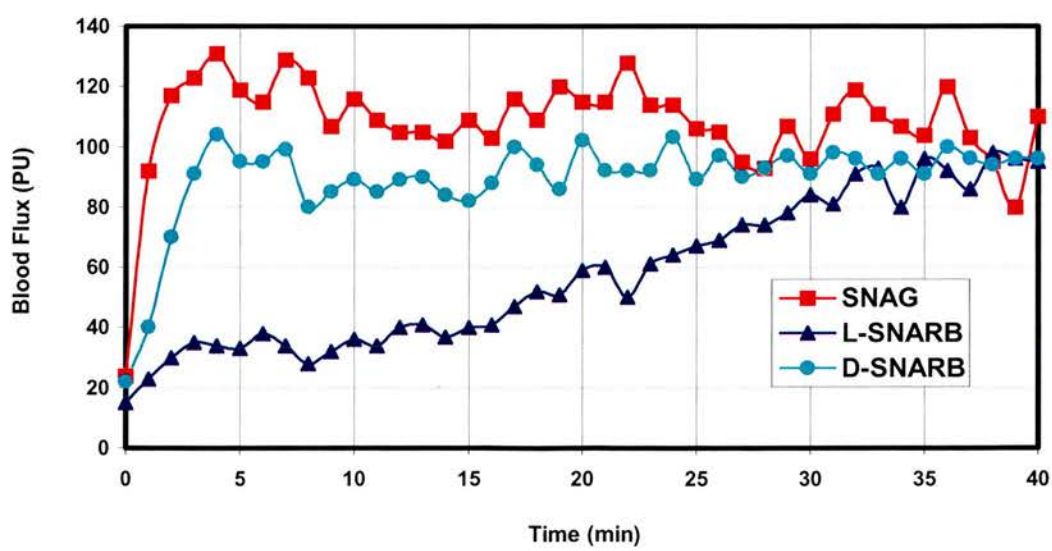

(b)

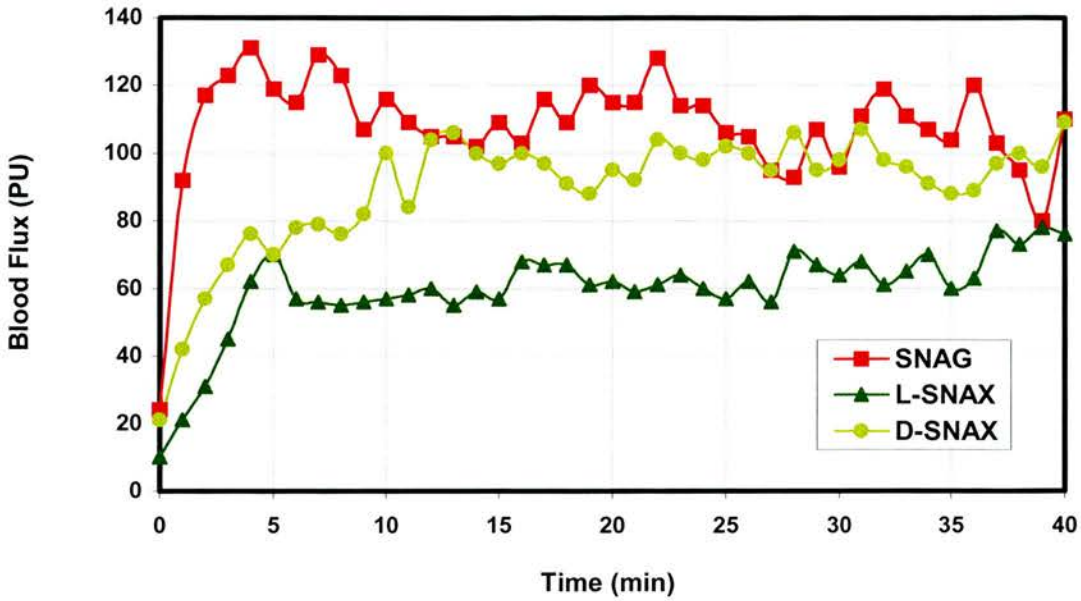

From the routine dosing regimen of ethanol : water (1:1) solutions (20.58mM), the title compounds were tested. Again using the forearm of a healthy male volunteer their progress as vasodilators was monitored over a period of 40 minutes. For ease in interpretation the same SNAG profile as that presented in figure 35 was included, to allow parallels to be drawn.

It is interesting to see that the D-form of both arabinose [38] and xylose [30] produced a quicker time to onset relative to the respective L-forms [42][34]. These variations in response cannot be explained by decomposition differences (section 4.1.3) since, as expected, the two isomeric forms of each sugar have comparable stability.

The possibility of an enzyme preferentially metabolising one form of the sugar, over another, is an attractive, alternative explanation. At the most ambition end of the spectrum, the selective recognition of just one isomer at the active site of guanylate cyclase could be considered. However, from designating sugar name with ring conformation, the L-series of arabinose is most closely related to the D-series of xylose. Such confusion is based on nomenclature rules surrounding the projection at the anomeric centre relative to that at the C-4 position. As a result the D-series for arabinose is the mirror image of the D-series for xylose, should the axial-equatorial position at C-4 be ignored (section 1.4.4, Fig. 18). Consequently, the two sets of data [Fig. 36 (a-b)] do not provide any direct evidence to link improvements in blood flux with a common similarity in the sugar structure of the NO donor. Thus, the data can

in no way reinforce the idea that an enzymatic process is taking place. Instead the results show, as with the other sugars [Fig. 35], the variability in the time to onset between similar drugs administered in identical dosing regimens. The ability of all wells to plateau to the same blood flux level over the 40 minutes of LDI scanning would also appear to be a re-occurring observation.

Similar data was seen for SNAL [46], the D-lactose derived NO donor [Fig. 37]. In contrast, SNAM [51], originating from D-maltose, was not able to give the standard profile of an increasing initial flux followed by a sustained plateau. This difference is the result of maltose exhibiting very different solubility in ethanol : water to that seen for the other sugar derivatives under examination (section 6.12.5). Due to this, after dilution, a dose some 12-fold lower in concentration was administered (1.71mM). For comparative purposes an identical dosing regimen was followed for SNAG [5] (0.0625%, 1.71mM). Not surprisingly, no significant deviation from baseline measurements was observed from these two wells [Fig. 37].

Fig. 37 *Comparing the vasodilatory potential of SNAG with that of its D-lactose [46] and D-maltose [51] derivatives.*

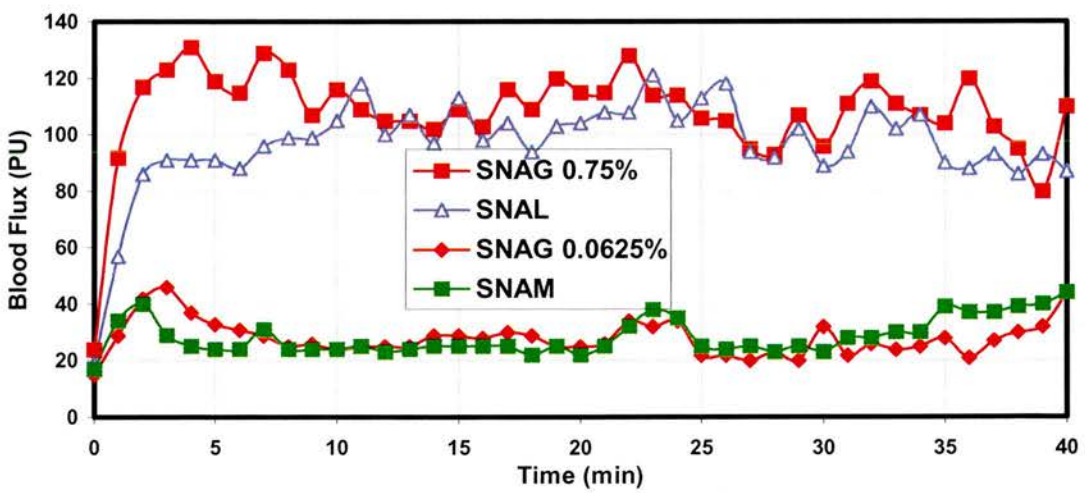

To the forearm of a healthy male subject, 0.75% SNAG (20.58mM) was compared against SNAL (20.58mM), whilst 0.0625% SNAG (1.71mM) was compared against SNAM (1.71mM). The profiles from the wells of the latter mentioned test solutions undoubtedly tells us more about the effect of lowering the dose rather the effect of using a larger NO sugar donor, such as maltose. On the other hand, SNAL (0.75%) showed a similar profile to SNAG (0.75%), in keeping with responses seen for other novel compounds at concentrations of 0.75%.

The slower onset in vasodilation for SNAL [46] compared against SNAG [5] is at least, in part, explainable by *in vitro* work. This shows a slower rate of NO release for the lactose derivative [46] when tracked relative to SNAG [5] (section 4.1.3). However, as for all of the sugar compounds, testing on a larger group of subjects is a necessary requirement before even attempting to provide an explanation to any obvious trends or differences. For now, all we can conclude from these novel tests is that when given in a suitable dose (20.58mM) a fully acetylated *S*-nitrosothiol, with a sugar backbone, will produce an increase in blood flux (of at least five-fold) that is sustainable for at least 40 minutes. In other words, the vasodilation observed is not unique to the addition of SNAG [5] to the forearm.

3.8 Hand data.

The administration of ethanol : water solutions into 2cm diameter test wells to measure changes in hand blood flux proved to be impractical. As a result it quickly became apparent that the NO donors would require incorporation into a gel or cream. Only using such methodology could their response upon the peripheral circulation of the dorsum and pulp of the finger be adequately explored by LDI. Substituting the water proportion from the test solutions with KY jelly enabled the generation of a gel with the correct consistency to remain at the site of administration yet of sufficient fluidity to enable the laser of the LDI to freely permeate and thus measure the RBC flux.

To understand if this system would operate as efficiently as the ethanol : water (1:1) solutions, the KY jelly mixtures were first tested upon the forearm of healthy volunteers. Such individuals were selected if they had already shown good responses to SNAG using the protocol described for the forearm work. From the recorded data we were also keen to identify whether clear dose-response and secondary response profiles would be observed. In relation to the first of these objectives the answer would appear to be no [Fig.38]. Alternatively, the dampening of the secondary response and indeed the level at which the blood flux plateaus, would appear to suggest that the delivery of SNAG in this manner is less favourable in terms of skin

permeation than that involving the use of ethanol : water (1:1). However, compromising the magnitude of the response is off weighed by the benefits of using KY jelly. For instance, the ease of application and the redundancy of the test wells in experiments focusing solely on the hands has enabled our understanding of hand blood flow to be greatly improved.

Fig. 38 *The dose response profile for SNAG when administered to the forearm of a healthy individual in a KY jelly : ethanol (1:1) mixture.*

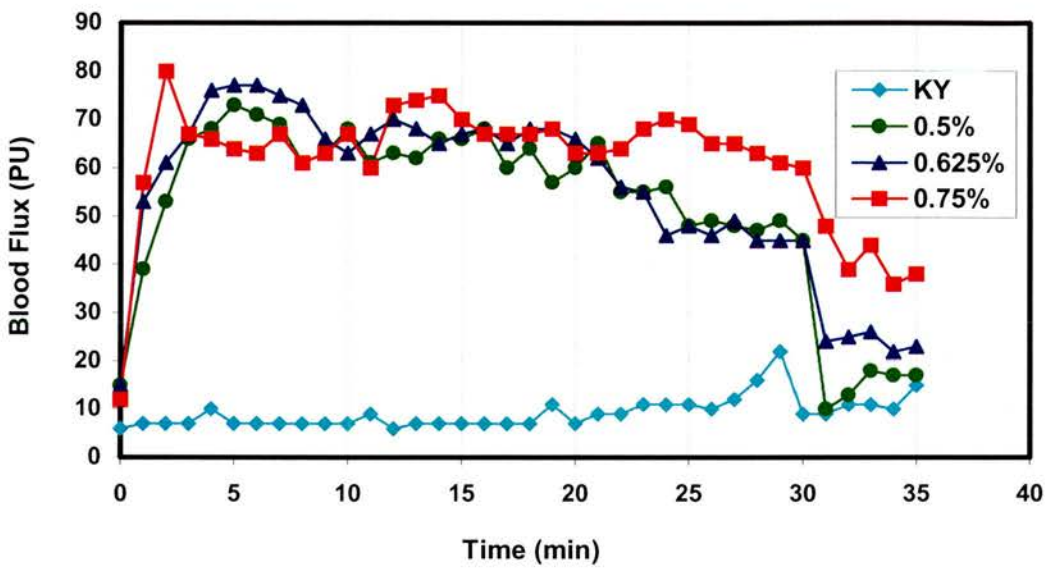

To the forearm of a healthy male subject, 0.50% (13.72mM), 0.625% (17.15mM) and 0.75% (20.58mM) SNAG was administered in the form of KY jelly : ethanol (1:1) mixtures. Comparing the response from all three wells, against that seen for the control well (KY jelly : ethanol, 1:1), suggests the three different concentrations of SNAG have very similar biological activity. Consequently, no typical dose-response profiles were observed from the above set of data. Substituting ethanol for KY jelly clearly lowered the plateau response in all three wells containing NO donor. The removal of the well contents after 30 minutes gave secondary responses, which although lower than in previous work, did show some evidence of dose-response behaviour.

This modification to the protocol allowed many different experiments to be carried out in a relatively short time period. This was in part due to the fact that the drawbacks encountered from the protocol involving the use of SNAG solutions were avoided. Thus the major problem of well leakage is obviously removed when using SNAG in the form of a gel. In all forearm work, the progress of SNAG and related compounds was often monitored over 40 minutes thus any such leaks during this

time proved to be frustrating in terms of lost data and, of course, the requirement for even more test compound.

From early work, the use of SNAG (0.75%, 20.58mM) upon the dorsum of the fingers produced some very encouraging data [Fig. 39].

Fig. 39 *The beneficial effect of SNAG (0.75%), in KY jelly, when administered to the dorsum of the fingers (healthy subject).*

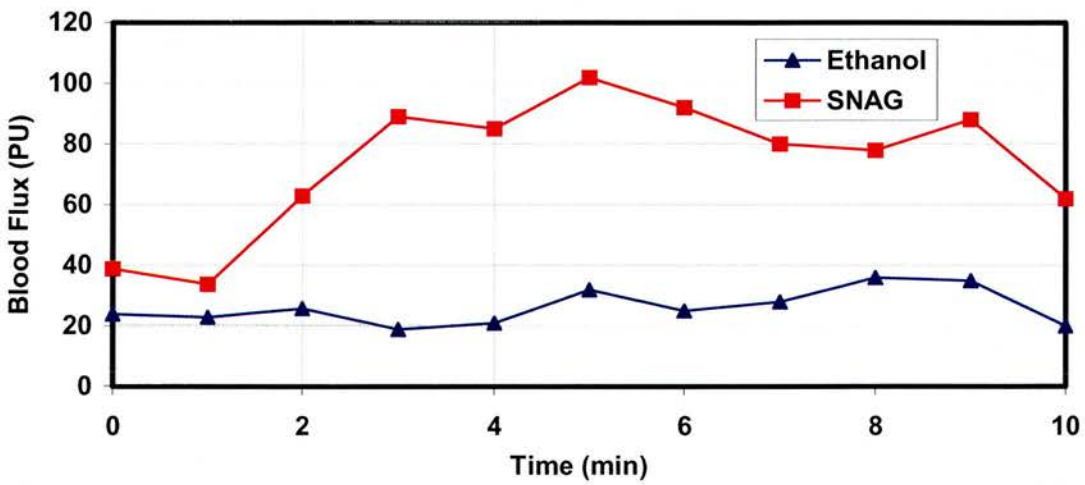

To a healthy male volunteer, SNAG (0.75%, 20.58mM) in KY jelly was administered to the dorsum of one finger. In parallel and as a control, ethanol in KY jelly was applied to the adjacent finger. Scanning by LDI over 10 minutes shows the vasodilatory potential of SNAG, since a four-fold increase over the baseline recording is observed.

As administration of SNAG in this form is particularly easy, its response in a single healthy male volunteer was also tracked along the entire distance of the hand, starting at the wrist and finishing at the finger nail. It was hoped that this would highlight any changes in microcirculation morphology as we moved away from the arm as a test site. As illustrated in figure 40, SNAG (0.75%, 20.58mM) produced an abrupt increase in dorsal hand blood flow.

Fig. 40 *A hand scan produced by LDI, showing the vasodilatory ability of SNAG (0.75%, 20.58mM) when compared with an ethanol control.*

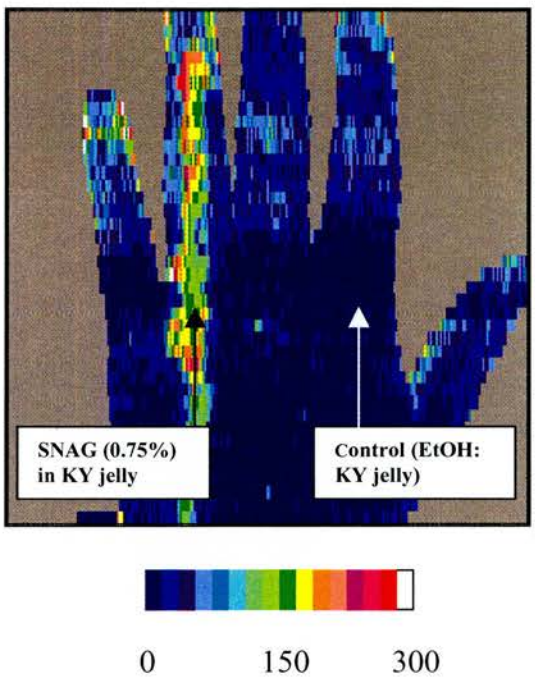

To the same healthy male volunteer used to produce the data in figure 39, SNAG (0.75%, 20.58mM) was applied along the entire length of the dorsum of the hand. The data above shows how an ethanol control gel was run in parallel so that the vasodilatory effects of SNAG could be fully appreciated. The changes in colour show the change in blood flux. As in figure 24, blue refers to a low blood flux whilst red/white represents a very high level of flux. This scan was completed in just under one minute allowing the plot in figure 39 to be obtained by computer manipulation.

While the data presented in figures 39 and 40 were as we had hoped, further studies on healthy male individuals were less promising. As a result of these findings it quickly became apparent that subject variability would make a detailed study, using this protocol, impossible. Figure 41 clearly illustrates this point, since the blood flux following the addition of SNAG (0.75%, 20.58mM) is not significantly different to that seen at the control site where ethanol in KY jelly was applied.

Fig. 41 *The common response of SNAG (0.75%), in KY jelly, when administered to the dorsum of the fingers (healthy subject).*

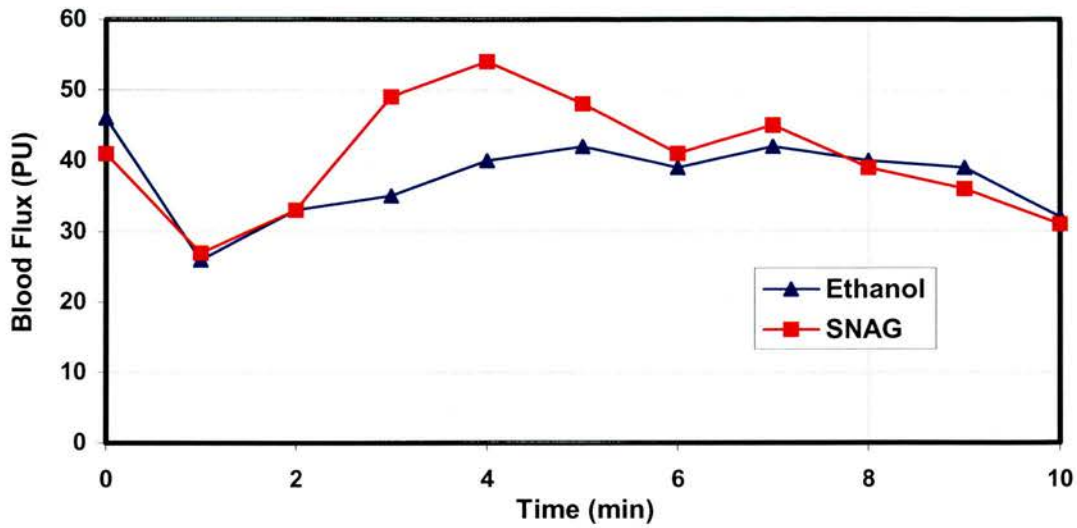

Administration of SNAG (0.75%, 20.58mM) in KY jelly, did not produce a significant difference in blood flux over baseline, when applied to the dorsum of the finger. The data presented above was obtained from a single healthy male volunteer though represents the standard profile seen from this type of study. Thus the data presented in figures 39-40, although favourable, does not portray the common response.

On accepting the above plot [Fig. 41] to represent the common response to the treatment of SNAG (0.75%, 20.58mM) upon the dorsum of the hand, we can also conclude that figures 39-40, although encouraging, are only applicable to a minor group of individuals. The similar blood flux responses seen between SNAG and control treated sites was also observed when the finger pulp became the major focus of the work. As already described (section 3.3) the finger pulps are essentially under thermoregulatory control,[6] making responses due to NO donation at best difficult to observe, since baseline readings are naturally so much higher (100-120 PU) than those observed in other body regions studied in this work (15-40 PU). Consequently, figure 42 shows how the LDI detected only very slight blood flux differences between NO treated and NO absent sites on the finger pulps.

In an attempt to see if the lack of blood flux variation is purely due to the heightened baseline reading, a cold challenge was attempted upon the test hand. This involved submerging the whole hand under cold tap water (12°C) for five minutes. Initially ice-water (0-4°C) was used. However, such extensive cooling produced a great deal

of discomfort to the subjects and instead of observing a slow steady increase in blood flux, an emergency wheal type response was seen. This completely masked any response of SNAG. In contrast the cold tap water allowed a slow increase in blood flux, over 8 minutes, to be observed. Since the blood flux was of a significantly lower level over this time, any response due to SNAG would clearly be evident as its time to onset is almost immediate (as shown by all previous figures). All subjects who agreed to this protocol wore a glove during the cooling process so that no physical stimulus, such as drying the hand, would interfere with the observed response. Figure 43 clearly highlights that even under this manipulated state, SNAG (0.75%, 20.58mM) had no effect in enhancing the microcirculatory flux of the finger pulps, in healthy individuals.

Fig. 42 *The common response of SNAG (0.75%, 20.58mM) in KY jelly, when administered to the pulp of the fingers (healthy subject).*

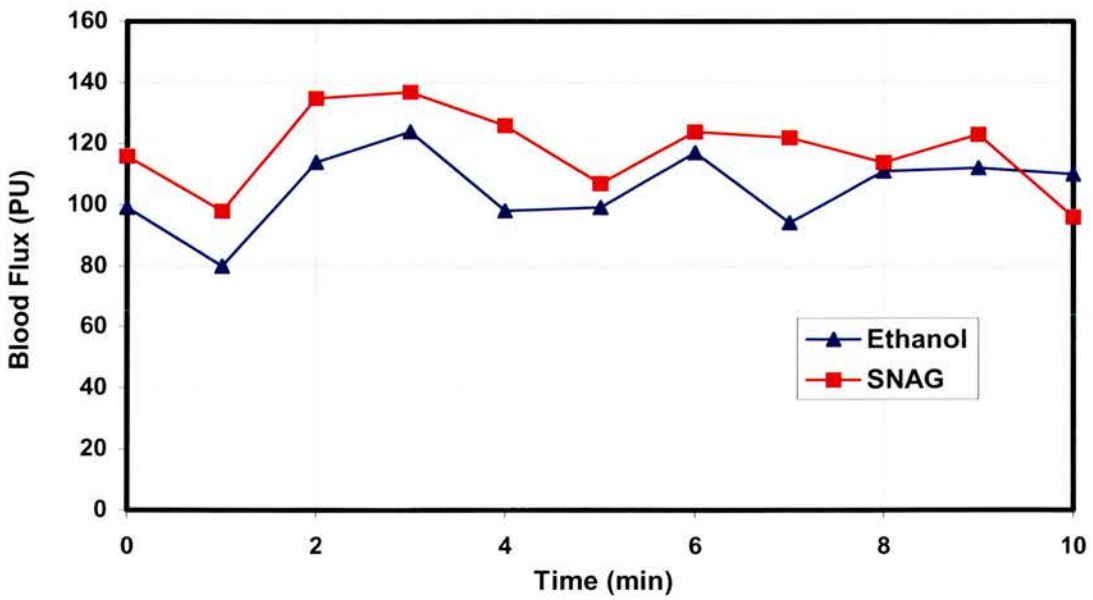

The above plot illustrates the similarity in blood flux response when SNAG (0.75%, 20.58mM) in KY jelly was administered in parallel to ethanol in KY jelly (control). This data was obtained from a single healthy male volunteer though represents the standard profile seen in all other healthy individuals that were studied.

Fig.43 *The effect of SNAG (0.75%, 20.58mM) in KY jelly, upon the finger pulp of a healthy individual after a 5 minute period of hand cooling.*

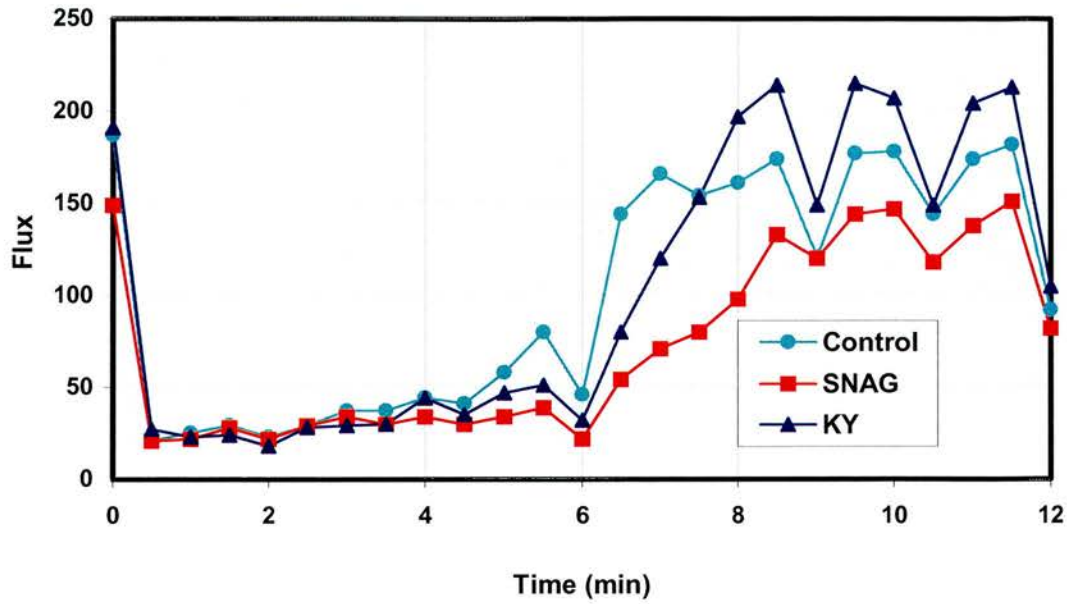

The above plot compares the effect of SNAG (0.75%, 20.58mM) in KY jelly, with ethanol in KY jelly (control) and KY jelly alone. Prior to administration, the hand from which all finger blood flux measurements were taken, was cooled for a period of 5 minutes. The flux readings presented at time zero, represent the blood flow before cooling, whilst those at time 0.5 minutes relate to the start of the blood flow scanning immediately after the cooling period. The recovery in flux over approximately 8 minutes on all test sites indicates that SNAG (0.75%, 20.58mM) has no significant role in enhancing this process.

As a result of the above data being so conclusive, no further work on the finger pulps was attempted. Whilst we were disappointed that SNAG (0.75%, 20.58mM) did not produce an enhanced blood flux, the result is at least consistent with what has been reported previously by our group.[3-5] It does however remain something of a mystery as to how Benjamin and co-workers[7] were able to report enhanced blood flow responses in both the forearm and finger pulps of healthy individuals and Raynaud's sufferers. This again brings into the question whether their system represents a genuine source of NO donor or instead illustrates an immune type response. Evidence to support the latter hypothesis stems from work by Ormerod and co-workers,[20] who report, in the same year, how a histological study uncovered edema, and a swelling of keratinocytes and endothelial cells after exposure to an NO releasing cream on normal skin. What is of particular interest from this study is the news that the NO releasing cream was in fact the exact same system of sodium nitrite

and ascorbic acid that Benjamin and his colleagues used. Thus the observed adverse effects of the cream are far more likely to represent the toxic nature of sodium nitrite than that of free nitric oxide. With this knowledge we remain convinced that our data represents the true reflection of NO's activity at both the level of the forearm and of that at the finger dorsum and pulp.

3.9 Lipophilic study upon the forearm.

The inconsistencies seen in the finger work may, at least in part, be as a consequence of subject variability at the level of skin type and thickness. Whereas the skin on the forearm is often found to be of similar thickness and texture between individuals, that upon the hands can vary considerably since it is highly driven by environmental factors such as life style and in particular with an individual's occupation. We have already discussed the importance of occupation in understanding the microcirculation (section 1.2.6). However, to improve our understanding of how skin penetration might influence the observed blood flow responses to SNAG, a whole series of *S*-nitroso-1-thio-glucose compounds of increasing lipophilicity were synthesised (section 2.3) for biological testing.

As outlined in section 1.3.1, the outmost layer of the skin, the stratum corneum, is the body's major protective coating to foreign agents and is therefore especially lipophilic in character. This property was the sole reason for the inclusion of the lipophilic target molecules [59][65][70] and [76] in this work (section 1.4.4). In comparing the LDI responses of each compound in the series it was hoped that a pattern would emerge suggesting the preferential uptake of compounds of a particular lipophilicity. This would in turn highlight the significance of the entire donor molecule crossing the skin. Such a result could then also reinforce the idea that skin type and skin penetration are fundamental to explaining the differences seen in response to SNAG when applied to the fingers.

In figure 44, SNAG (0.75%, 20.58mM) is compared against all four of its related compounds, these being the propionylated [59], butyrionylated [65], valerionylated [70] and hexanionylated [76] derivatives. All were administered in doses equivalent

to that reported previously for SNAG [5] (0.75%, 20.58mM). The order in which the compounds are listed in the legend of figure 44, are in accordance with their ascending lipophilic character (section 4.2). As the data suggests [Fig. 44], the two most lipophilic of all the test compounds, [70] (VAL) and [76] (HEX), gave responses that initially increased faster than the propionylated [59] (PROP) and butyrionylated [65] (BUT) compounds, though such data was still inferior to the profile given for SNAG [5]. This trend was observed throughout the complete 35 minutes of scanning by the LDI, as all of the more lipophilic derivatives of SNAG plateaued to the same lower level of blood flux after 30 minutes. Whilst the lower response was disappointing from the point of view of establishing a new lead compound, the data, albeit from a single test run, suggests that lipophilicity is a crucial determinant in the design of a successful NO donor. Alternatively, the dampened responses could be explained on the basis of differences in SNO stability within the series (section 4.3). From chapter 4, the varied Log P and kinetic data for the series, indicate that a combination of these parameters could realistically be contributing to the observed biological profiles. [Fig. 44].

Fig. 44 *How vasodilation is affected by the lipophilicity of SNAG (20.58mM).*

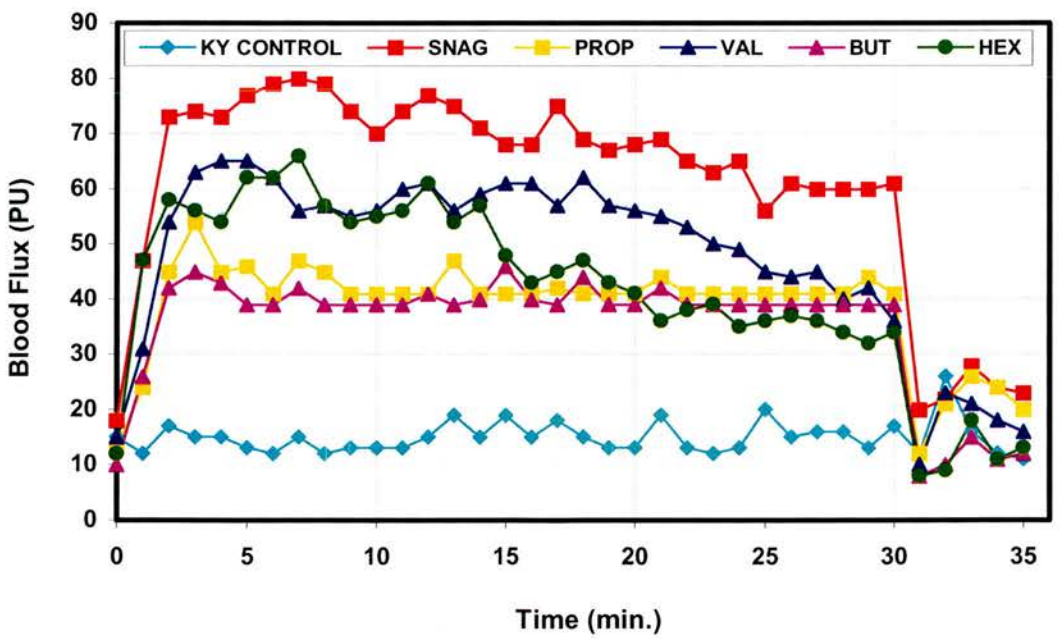

To a single healthy male volunteer, in one visit, using both forearms, SNAG [5] (0.75%, 20.58mM) was compared against its propionylated [59] (PROP), butyrionylated [65] (BUT), valerionylated [70] (VAL) and hexionylated [76] (HEX) compounds, diluted to equivalent concentrations (0.75%,

20.58mM). All applications were made in KY jelly, with randomised administration of SNAG, its derivatives and the control (EtOH : KY jelly, 1:1) upon the forearm test sites. The compounds administered at t = 0 minutes, were removed from the forearm after 30 minutes. The data strongly implies that the acetylated form of the S-nitrosothiol-sugar (SNAG [5]) is the best compromise when in the search for a transdermally acting NO donor compound.

Taking the work to the other extreme continued to highlight SNAG [5] as the most potent NO donor in this study. Initial tests with a hydrophilic derivative of SNAG, containing four free hydroxyl sites (see section 1.4.4), clearly illustrated this point [Fig. 45]. The compound, *S*-nitroso-1-thioglucose, SNOG [79], could not match the standard biological profile of SNAG [5] (0.75%, 20.58mM). In combination with the data from the lipophilic compounds [Fig. 44], there is ample evidence to suggest that SNAG with its acetylated side arms exhibits the optimum properties for good vasodilatory activity upon the forearm, both in terms of stability and Log P value.

Fig. 45 *How vasodilation is effected by the hydrophilicity of SNAG [5] (20.58mM).*

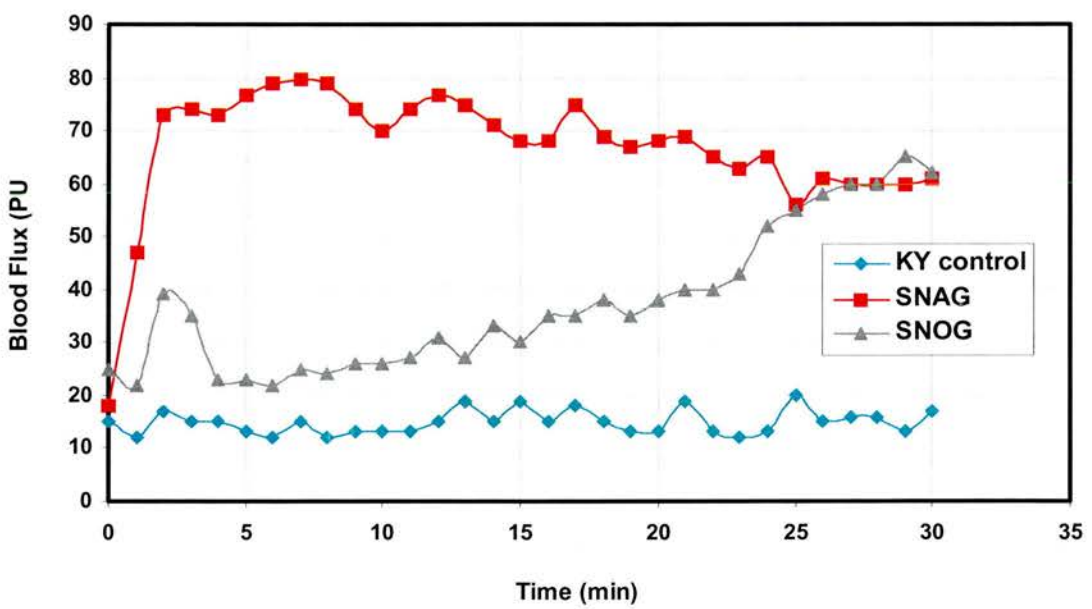

Comparing the vasodilatory ability of SNAG [5] (0.75%, 20.58mM) with that of its hydrophilic sister compound, SNOG [79] (0.75%, 20.58mM) when administered in KY jelly to a healthy male volunteer. Despite reaching the same level of vasodilation as SNAG, after 30 minutes upon the forearm, the slow onset of the response, illustrates the different characteristics of SNOG [79] both in terms of stability and log P value. To the control site, ethanol : KY jelly (1:1) was applied.

The slower onset of the response from SNOG [79] (0.75%, 20.58mM), may, at least in part, be explained by its highly unusual stability over many hours (section 4.1.3). On the basis of this we can propose that the slow but steady rise in blood flux due to SNOG [79], represents solely that of the parent molecule entering into the skin and releasing NO at some later stage *in vivo*. Although this idea may carry some weight, it should also be treated with caution, since the decomposition of SNOG [79], was followed in the same manner as for all the other compounds, by UV studies at 345nm and therefore in the millimolar range. As reported by Weller,[21] the many origins of NO in the skin, produce levels only in the nano and picomolar range. Thus direct extrapolations from the kinetic data (section 4.1.2-3 and 4.3) to the biological profiles presented here should be made with extreme care.

3.10 Comparing healthy volunteers with Raynaud's sufferer's (forearm & hand).

3.10.1 Forearm data.

After many probing experiments (sections 3.6-3.9) as well as many repetitive studies (see figures 30 & 33), all of the data on healthy subjects pointed towards SNAG as the best of the *S*-nitrosothio-sugars under examination. With a rigid protocol in place, attention was diverted to the effects of SNAG [5], if indeed any, on Raynaud's patients. As described in section 3.1 a heterogeneous group of Raynaud's sufferer's were recruited following approval from their respective clinicians.

From the forearm dose-response plots obtained from the sufferers, differences between these profiles and those seen for healthy individuals are clearly visible. The most striking feature from the data collected, was the loss of the plateau region suggesting at a very early stage, differences in SNAG's duration of action. Figure 46 is typical of the profile seen for a Raynaud's patient after administration of the three standard doses of SNAG [5] along side a control well.

Fig. 46 *A typical forearm dose-response profile for a Raynaud's sufferer.*

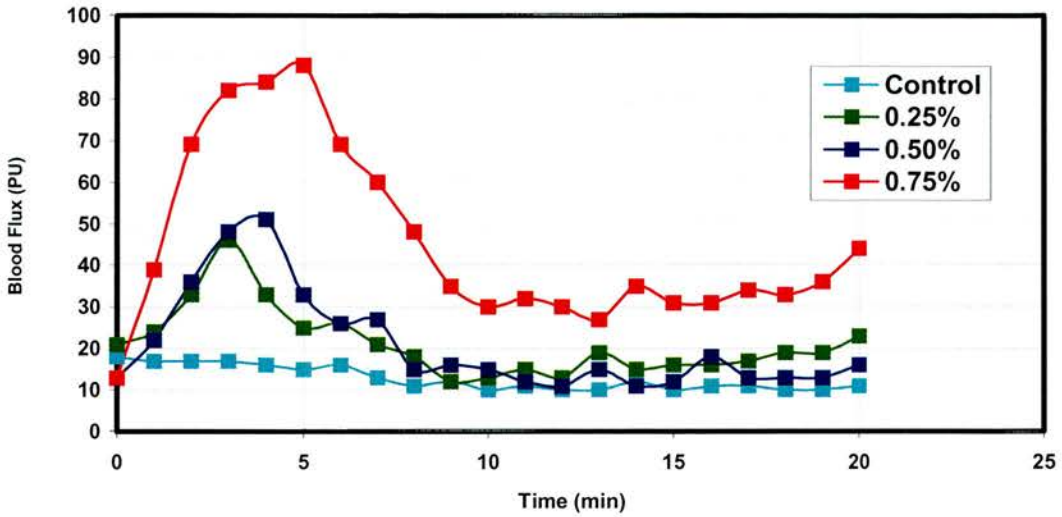

In separate wells, three doses of SNAG [5] (0.25%, 6.86mM; 0.50%, 13.72mM and 0.75%, 20.58mM) and an ethanol : water (1:1) control, were administered to the forearm of a diagnosed Raynaud's sufferer for 20 minutes. The profile is very noticeably different to that seen for a healthy subject.

The patients quick rise and fall in blood flux due to SNAG, is further emphasised by the plot below [Fig. 47]. This shows the collated data from a heterogenous group of eight Raynaud's sufferers.

Fig. 47 *The total blood flow response, over 20 minutes, with respect to baseline, for healthy subjects and Raynaud's patients.*

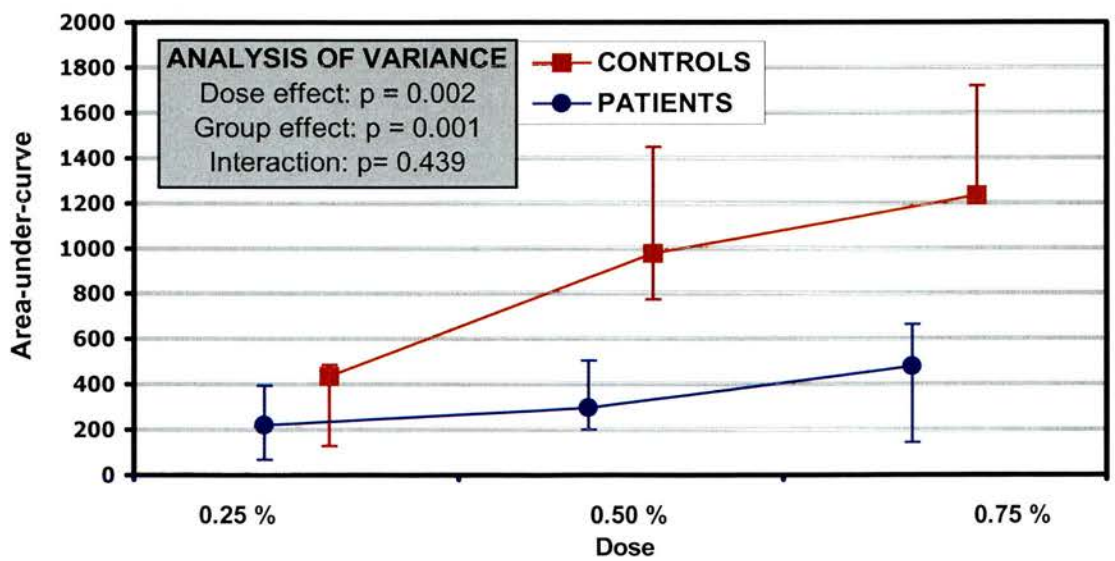

In the above plot, the blue line (labelled PATIENTS) represents the collated data from a heterogeneous group of eight Raynaud's sufferer's. Alternatively the red line (labelled CONTROLS)

represents the combined data from eight healthy subjects. All data is presented as the area under the curve (AUC), for each test well, over the 20 minutes of scanning. The dose effect: p=0.002 (small value) shows there is a significant difference between the three doses administered. We can therefore state that there is a dose effect. Group effect: p=0.001 (small value) highlights that there is a significant difference, overall, between the control's and the sufferer's. Interaction: p>0.05 (significantly large) illustrating that the difference seen between the two groups is not dependent on the dose.

For each patient, the area under the curve (AUC) with respect to baseline, was recorded (see previous Fig. 46) for the three dose-response profiles of SNAG [5] (0.75%, 0.50% and 0.25%). Over 20 minutes of testing, the low responsiveness to SNAG when compared with data obtained from eight healthy subjects is obvious to see. This is further emphasized by the statistical data on variance.

At first glance the peak blood flux responses appear to be significantly reduced in the Raynaud's patients. However, when plotted relative to baseline and superimposed on the data for healthy subjects, it was found that the combined maxima were only marginally lower in the Raynaud's group. As shown in figure 48, the similarity in peak response is particularly noticeable at the higher SNAG doses (0.50%, 13.72mM & 0.75%, 20.58mM).

Fig. 48 *Peak blood flow responses, over 20 minutes, with respect to baseline, for Raynaud's patients and healthy subjects.*

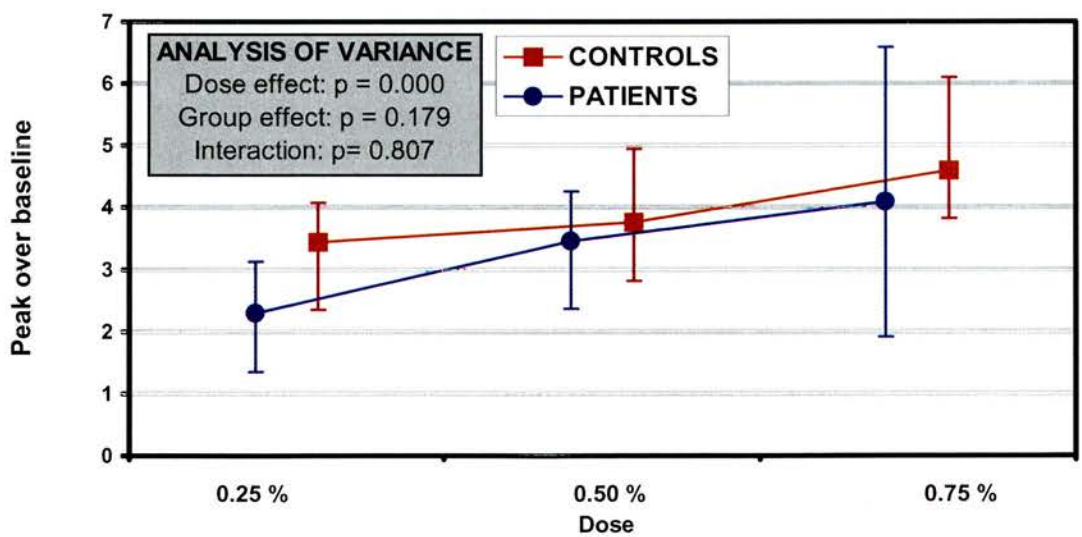

In the above plot, the blue line (labelled PATIENTS) again represents the collated data from a heterogeneous group of eight Raynaud's sufferers. The red line (labelled CONTROLS) represents the combined data from eight healthy subjects. The dose effect: p=0.000 shows there is a significant

difference between the three doses administered. We can therefore state that there is a dose effect. The group effect: p>0.05 (significantly large) highlights that there is not a significant difference, overall, between the control's and the sufferer's. Interaction: p>0.05 (significantly large) illustrating that the similarities in peak response for the two groups is not dependent on the dose.

Presenting the data, relative to baseline [Fig. 49(b), (d) & (f)] should be treated with some caution. This is exemplified by direct comparison with absolute responses to SNAG [5] [Fig. 49(a), (c) & (e)] which show that the blood vessels, in no way, dilate to the same extent in the two subject groups.

Fig. 49 *Illustrating respectively, the absolute and relative differences seen in response to SNAG [5], (a-b) 0.25%, 6.86mM, (c-d) 0.50%, 13.72mM and (e-f) 0.75%, 20.58mM, when administered to the forearm of healthy subjects and Raynaud's patients.*

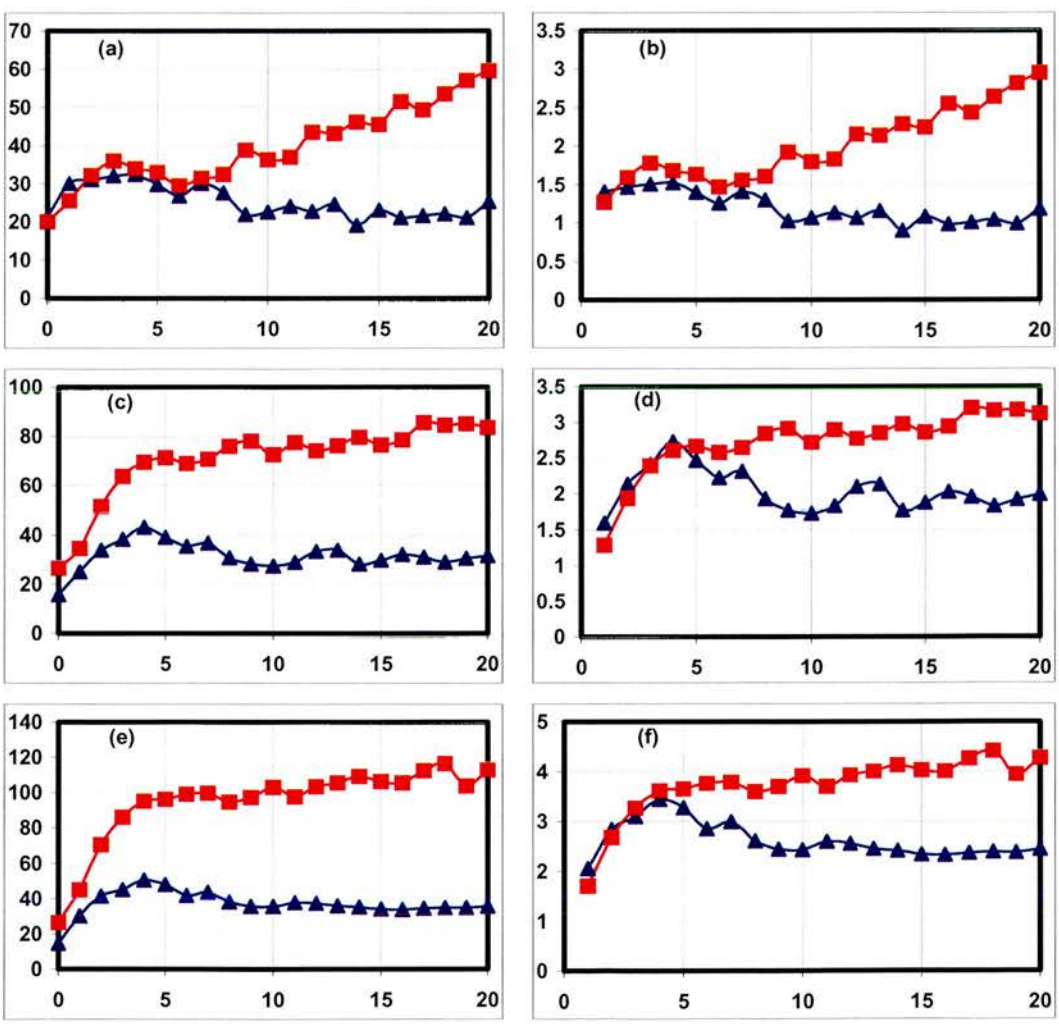

In all of the above plots the blue lines represent the collated responses from Raynaud's patients whilst the red lines show the data from healthy subjects. Each group consisted of eight volunteers. For all

plots the y axis is a measure of blood flux in arbitrary perfusion units while the x axis shows the duration of administration in minutes. The data presented previously in figure 48, was obtained from the relative plots (labelled (b),(d) and(f)). As can be seen plots (a), (c) and (e), illustrating the absolute data, tell a somewhat different story.

Interpretation of figures 48 and 49, in combination, show that the major difference between the two groups of individuals lies in the resting, baseline response. The low blood flow measured from the control wells of the Raynaud's sufferers [Fig. 46] results in the relative peak responses to SNAG [5] appearing artificially high. Whilst this shows that SNAG [5] is capable of bringing about the same relative increase in blood flux to that seen in healthy subjects, the elasticity of the blood vessel wall is brought into question. Thus a physical problem at the level of the microcirculation of sufferers may be responsible for the distinct differences in absolute response, seen between the two subject groups.

3.10.2 Hand data

By way of a modification to the standard hand protocol (section 3.8), SNAG [5] (0.75%, 20.58mM) was administered to the dorsum of sufferers hands as an ethanol : water (1:1) solution. This was possible since a region between the thumb and the index finger, which was flat enough to successfully house a testing well, was identified. Preliminary data such as that presented in figure 50 was encouraging. With such data it was postulated that the poor responses seen earlier, whilst using KY jelly, might have been as a result of the absence of ethanol. This would suggest that ethanol has a role in enhancing the uptake of SNAG/NO.

Despite this experiment being routinely included during a patients visit, the responses were highly variable and consequently no conclusive remarks or graphical representations can be made. In the majority of cases no response over baseline was observed when SNAG [5] (0.75%, 20.58mM) was present. Whilst it is disappointing that SNAG [5] did not prove to be a beneficial blood flux enhancer on the hands of Raynaud's sufferers, this does at least fit with the results from the similar study on healthy subjects using KY jelly (section 3.8). Other supporting evidence is found from work by Noon and co-workers[22]. Following the infusion of the competitive NOS inhibitor, L-NMMA, into the brachial artery, they report how forearm blood

flow was reduced, consistent with a NO pathway, whilst that in the dorsum of the hand was unaffected, in line with a NO independent mechanism. From a different viewpoint, it could be again argued that the poor responsiveness to SNAG [5] upon the hand, tells us more about differences in skin morphology and thickness as you move from the forearm to the hand, than differences concerned with the microcirculation in such body regions.

Fig. 50 *The response to SNAG [5] (0.75% 20.58mM), in a Raynaud's sufferer, when administered to the dorsum of the hand.*

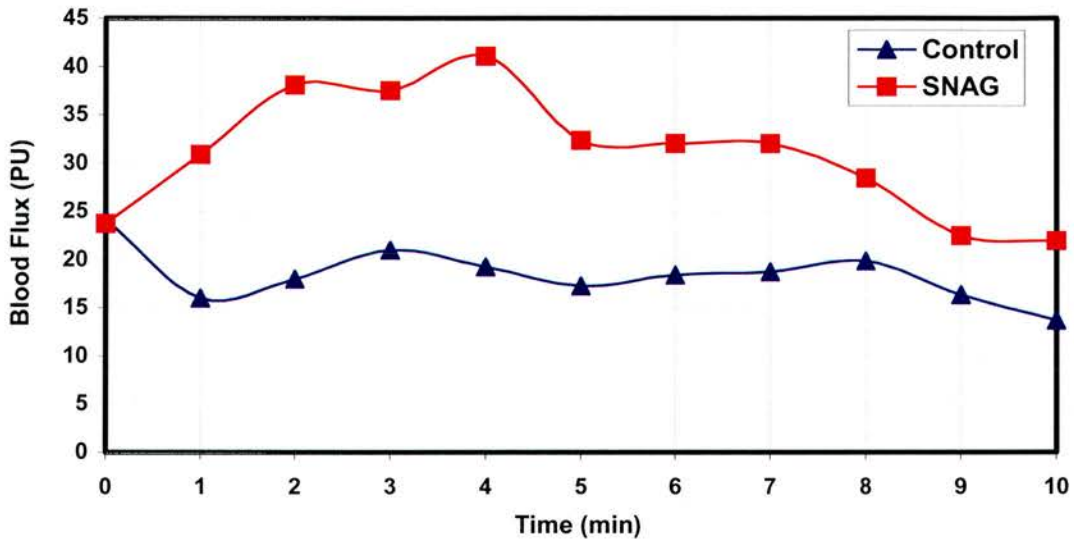

A single profile obtained from the hand of a Raynaud's sufferer. The blue line represents the control well (ethanol : water, 1:1) whilst the red line shows the response from a well containing SNAG [5] (0.75%, 20.58mM), administered as an ethanol : water (1:1) solution. The flat region between the thumb and the index finger was used in this instance as the test site. Thus for each run of this particular experiment, the need for two wells meant that both hands were required.

3.11 Incorporation of transdermal enhancers.

Remaining on the theme of skin penetration, the addition of transdermal enhancers to the drug formulation was investigated. In order to see the effects of any transdermal promotor, a system with the potential for improvement in biological responsiveness

was required. Such a scenario was fulfilled, using SNO-GLY [90] (0.75%, 20.58mM). Following preliminary tests [Fig. 51], SNO-GLY [90] showed a vasodilation approximating to 50% of that seen for a SNAG [5] solution of the same concentration.

Fig. 51 *Comparing the response of SNO-GLY [90] with that of SNAG [5] when administered to the forearm of a healthy male volunteer.*

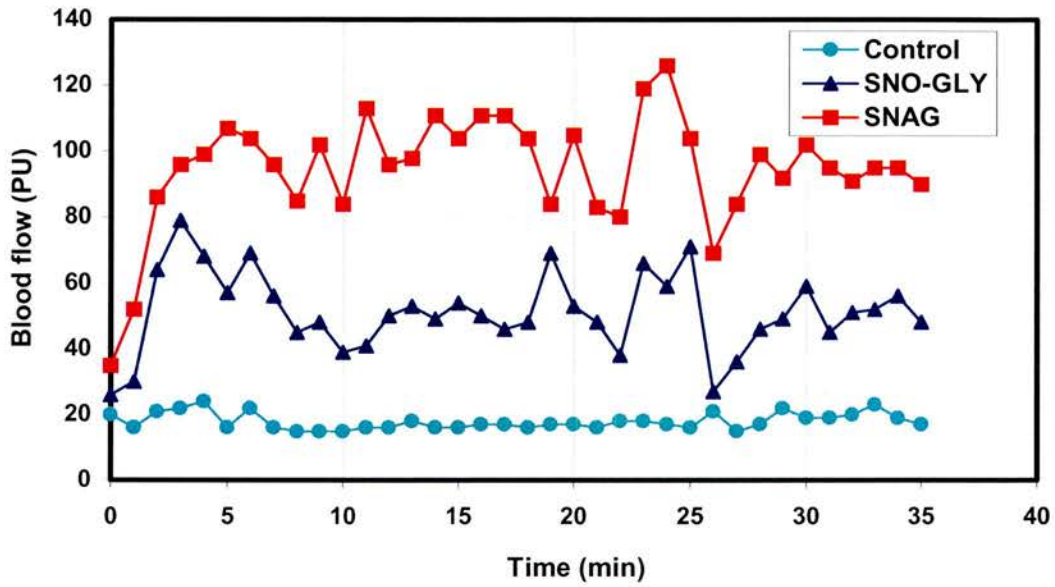

Using ethanol : water (1:1) solutions, SNO-GLY [90] (20.58mM) was compared against SNAG [5] (0.75%, 20.58mM) and a standard control well. SNO-GLY [90] tends to plateau around 50 PU. This is approximately half the size of the blood flux plateau seen for SNAG [5] (0.75%, 20.58mM). After scanning the forearm for 25 minutes all three wells were removed and the secondary response was monitored over a further 10 minutes. As can be clearly observed, the data from this latter time period follows very closely with that seen over the previous time course.

One of the prominent chemical differences between the two compounds centres upon the presence of free hydroxyls exclusively in SNO-GLY [90]. Such groups obviously make a dramatic difference to the lipophilicity of the NO donor. This difference is particularly noticeable when directly comparing the structure of SNO-GLY [90] against the fully acetylated molecule of SNAG [5] [Fig. 52].

Fig. 52 *Comparing the structure of SNO-GLY [90] with that of SNAG [5].*

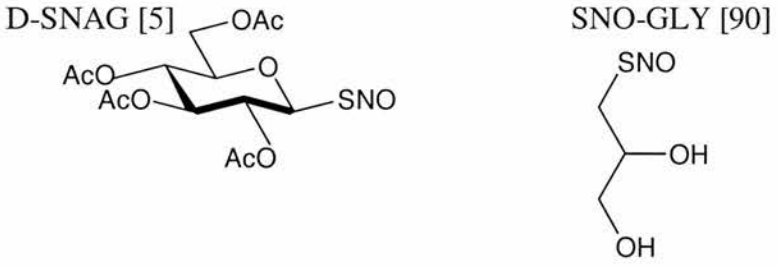

The free hydroxyls in SNO-GLY [90] provide the major difference in hydrophilicity/lipophilicity, when compared structurally against SNAG [5].

To see if skin penetration is one of the determining factors that governs the degree of vasodilation in the forearm, the incorporation of three clinically proven transdermal enhancers into the SNO-GLY [90] formulation was studied [Fig. 53]. As described by Godwin and Michniak,[23] the standard penetration enhancers, used to date, have been the sulfoxides, pyrrolidinones, fatty acids and alcohols. The major concern with all of these compounds is in relation to systemic and localised toxicity. With this in mind Godwin and Michniak turned their attention to the terpene series, as such compounds are constituents of essential oils found in flowers, fruits and the leaves of plants.

In using natural products to avoid toxicity problems, in a manner analogous to our own way of thinking with regard to the NO-donors (sections 1.4.3 and 3.1), the enhancer properties of α-terpineol and geraniol upon caffeine and hydrocortisone respectively, were shown to be significant.[23] As caffeine is hydrophilic and hydrocortisone is a polar steroid, we were interested to see the effects of α-terpineol and geraniol, when added to our SNO-GLY [90] test solution. For comparative purposes the incorporation of (+)-limonene was also investigated, since this terpene found in orange peel, was reported[23] to be very ineffective as a transdermal enhancer. Thus, based on the assumption that skin penetration is a key property by which our NO-donors function, we expected to see major differences in biological response depending upon the particular terpene applied.

Why certain terpenes should be more beneficial than others in enhancing skin penetration raises many theories. To address this issue a group, led by Arellano,[24] suggested that α-terpineol and geraniol are particularly effective at promoting the skin's uptake of hydrophilic compounds due to their possessing hydroxyl groups

capable of forming hydrogen bonding interactions. The exact mechanism of action involved here is unclear. Godwin and Michniak propose that the disruption of intracellular lipids of the stratum corneum is the most likely explanation for the compromised barrier resistance. However, contrary to this line of thought limonene, which is known[23] to attack the skins outermost surface very rapidly, is not a good penetration enhancer.

Fig. 53 The three terpenes chosen for transdermal enhancer studies.

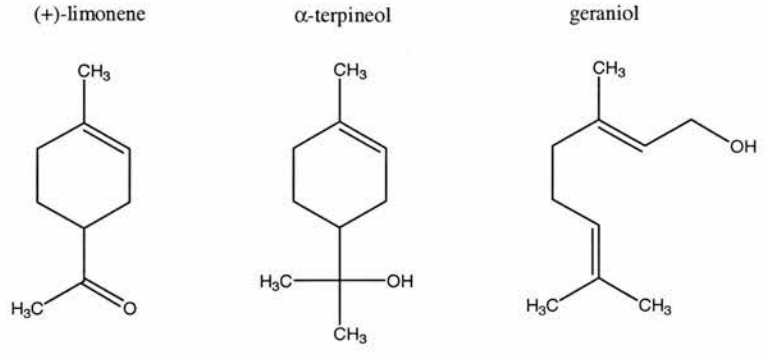

Limonene, α-terpineol and geraniol, from the terpene family, are all reported[23] to be transdermal enhancers. The effectiveness of the three in promoting skin uptake is highly variable, though appears to be governed by the presence of hydroxyl groups. As can be clearly seen above, only limonene is deficient in hydroxyl sites. This may explain why the literature reports that α terpineol and geraniol are more effective in enhancing the transdermal uptake of hydrophilic and polar therapeutic agents.

Since the terpene series have been generally recognised as safe (GRAS) by the FDA, we were able to incorporate the above work into our own protocol. In accordance with the procedures outlined by Godwin and Michniak[23] all the terpenes were diluted in propylene glycol (PG) to a concentration of 0.4M. These solutions, along with a control containing PG alone, were then applied to the forearm of the subject to pre-treat the site of administration. After a period of 20 minutes, during which the forearm was continually scanned by the LDI, an equivalent amount of SNO-GLY [90] in ethanol was added, to give an overall NO donor concentration of 0.75% (20.58mM). This latter description is a modification to the Godwin and Michniak protocol, which simply involved the addition of the therapeutic agent in PG on top of the previous application containing the enhancer. Despite this, the idea of using ethanol as 50% of the drug vehicle is not a new one.[25] Further scanning by the LDI produced the findings illustrated in figure 54.

The absence of data from the well containing (+)-limonene is a consequence of this terpene being a skin irritant and therefore producing a wheal response which would mask any effect of the NO donor. This adverse effect was detected after 17 minutes upon the forearm. From the three remaining wells, geraniol was shown to increase the vasodilatory response to the greatest extent. (α)-Terpineol, on the other hand, had a negative effect on the size of the biological response with respect to that seen for SNO-GLY (0.75%, 20.58mM) in the presence of PG alone (control well).

Fig. 54 *The effect of transdermal enhancers on the vasodilatory response to SNO-GLY [90], when tested upon the forearm of a healthy male subject.*

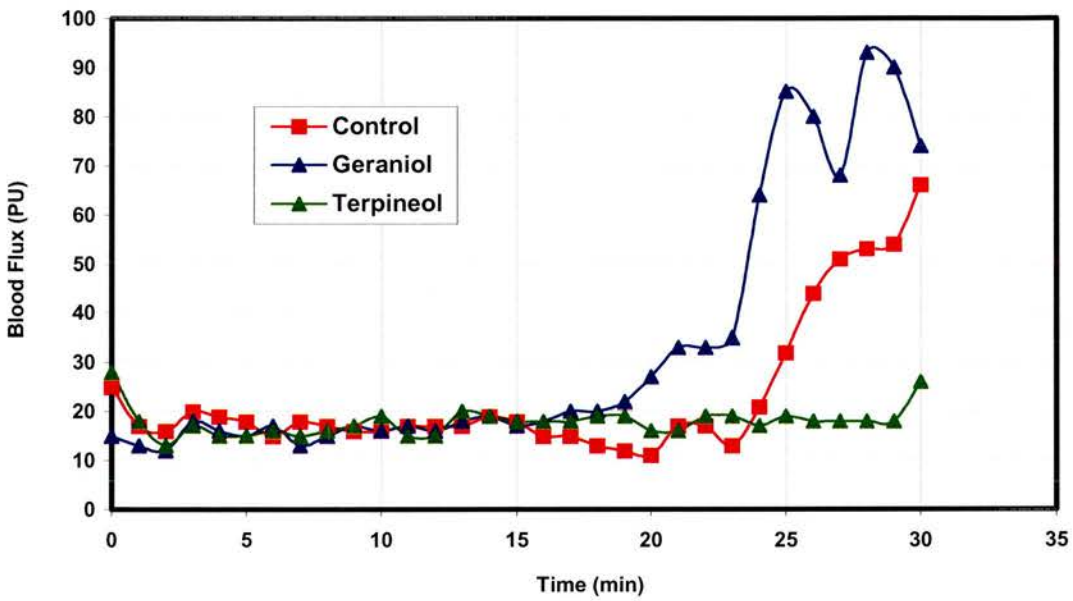

To the same healthy male subject used to obtain the data presented in figure 51, geraniol (0.4M) and α-terpineol (0.4M) in propylene glycol (PG), were used to pretreat the forearm. The control well contained PG alone. After the pre-treatment phase (time point = 20 minutes), SNO-GLY [90], in ethanol, was added to all wells (giving a NO-donor concentration of 0.75% (20.58mM) overall). The initial rise in flux was then studied over 10 minutes. As described previously, the well containing (+)-limonene had to be abandoned after the pre-treatment phase, due to substantial reddening of the skin and reports of skin irritation.

From their comprehensive work, Godwin and Michniak report[23] how micromolar quantities of therapeutic agent can penetrate the skin following the addition of the transdermal enhancers. However, in our work, concentrations of NO in the

nanomolar region are sufficient to bring about vasodilation of blood vessels, thus our protocol is far too sensitive to provide any meaningful data with regard to the activity of the terpenes. As a consequence, rationalising these results is difficult. Overall it is impossible to either dismiss or confirm the importance of altering the degree of skin penetration. There is of course the added confusion here in distinguishing between the uptake of free NO and the uptake of the NO-donor itself. Thus the story is a complicated one, yet essential in determining the mechanism of action of SNAG [5] and all the other compounds discussed in this chapter. The work presented under the heading of pharmacokinetics (chapter 4), aims to answer the many questions raised in relation to the mode of action of these NO-donors. In combination with the results shown in this chapter we have summarised the key points that we believe this work has identified (see chapter 5).

3.12 References.

1 G.R. Fenwick, R.K. Heaney and W.J. Mullin, *CRC Crit. Rev. Food Sci. Nutr.*, 1983, **18**, 123.

2 P. Oberg, *Crit. Rev. Biomed. Eng.*, 1990, **18**, 125.

3 A.R. Butler, R.A. Field, I.R. Greig, F.W. Flitney, S.K. Bisland, F. Khan and J.J.F. Belch, *Nitric Oxide: Biol. Chem.*, 1997, **1**, 211.

4 F. Khan, I.R. Greig, D.J. Newton, A.R. Butler and J.J.F. Belch, *Lancet*, 1997, **350**, 410.

5 I.R. Greig, Ph. D. Thesis, University of St Andrews, UK, 1997.

6 J.D. Coffman, *Am. J. Physiol.*, 1994, **267**, H2087.

7 A.T. Tucker, R.M. Pearson, E.D. Cooke and N. Benjamin, *Lancet*, 1999, **354**, 1670.

8 J.B.J. Hardwick, A.T. Tucker, M. Wilks, A. Johnston and N. Benjamin, *Clin. Sci.*, 2001, **100**, 395.

9 C. Harvsch, P. Scemmes and J. Taylor, *Comp. Med. Chem.*, 1990, **5**, 645.

10 V. Kolb-Bachofen, discussion following seminar at Edinburgh University, UK, November 1999.

11 R. Weller, presented in part at the 3rd Scottish NO meeting, University of St Andrews, UK, November 2000.

12 H. Rheinboldt and F. Mott, *J. Prakt. Chem.*, 1932, **133**, 328.

13 D.J. Sexton, A. Muruganandam, D.J. McKenny and B. Mutus, *Photochem. Photobiol.*, 1994, **59**, 463.

14 J. Barrett, L.J. Fitzgibbons, J. Glauser, R.H. Still and P.N.W. Young, *Nature*, 1966, **211**, 848.

15 J. McAninly, D.L.H. Williams, S.C. Askew, A.R. Butler and C. Russell, *Chem. Comm.*, 1993, **23**, 1758.

16 A.P. Dicks, H.R. Swift, D.L.H. Williams, A.R. Butler, H.H. Al-Sa'doni and B.G. Cox, *J. Chem. Soc. Perkin Trans 2*, 1996, 481.

17 E. Schwartz and E. Schmidt, *Ann. Emerg. Med.*, 1986, **15**, 952.

18 S.K. Agarwal, S.C. Tiwari and S.C. Dash, *Int. J. Artif. Organs*, 1993, **16**, 20.

19 T. Nakatani, L. Spolter and K. Kobayashi, *Life Sci.*, 1994, **54**, 967.

20 A.D. Ormerod, P. Copeland, I. Hay, A. Husain and S.W.B. Ewen, *J. Invest. Dermatol.*, 1999, **113**, 393.

21 R. Weller, *Br. J. Dermatol.*, 1997, **137**, 665.

22 J.P. Noon, W.G. Haynes, D.J. Webb and A.C. Shore, *J. Physiol.*, 1996, **490**, 501.

23 D.A. Godwin and B.B. Michniak, *Drug Dev. Industr. Pharmacy*, 1999, **25**, 905.

24 A. Arellano, S. Sontoya, C. Martin and P. Ygartua, *Int. J. Pharm.*, 1996, **130**, 141.

25 S. Gao and J. Singh, *Int. J. Pharm.*, 1997, **154**, 67.

Chapter 4 Discussion & Results.

Pharmacokinetics

In vitro work to determine the stability, absorption & distribution of the NO donors.

4.1 UV decomposition data.

4.1.1 X-ray crystallography

One explanation for the *S*-nitrosothio-sugars being unstable as solids is the suggestion of a solvent dependence, as outlined by the potential for crystal hopping.[1] This theory was contemplated after the appearance of pre-SNAG [4] crystals, obtained in methanol, differed significantly, by the human eye, to those from ethanol. Such differences were also identified when altering variables such as solvent cooling, crystal seeding and glass surface scratching. To understand if the phenomenon of crystal hopping is indicative of acetylated thio-sugar compounds, the crystal structure, packing arrangements and powder diffraction data of pre-SNAG [4] was studied. All such work was performed on the thiols as opposed to the *S*-nitrosothiols due to the inherent instability of the latter functionality when incorporated into the glucose molecule at the anomeric position (as already described in section 2.1).

From altering the crystallisation conditions, including the solvent itself (from methanol to ethanol, in the case of pre-SNAG [4], section 6.2.4), identical powder diffraction data was obtained from various crops of pre-SNAG [4] crystals. This categorically dismissed the existence of more than one crystalline form of the compound.

The crystal structure of pre-SNAG was successfully resolved and is presented in Fig. 55. This provides further insight into the crystalline nature of the acetylated thio-sugars, by highlighting the importance of the anomeric position of the sugar in the packing interactions. The proposed intermolecular hydrogen bonding between S(1) of one molecule to O(11) and O(13A/B) of two other molecules is illustrated in

figure 55. From this, the effect of nitrosating the thiol, on reducing the overall crystal stability, can be fully appreciated. This may explain the problems encountered in isolating SNAG [5] as a solid.

Fig. 55 *The crystal structure (left) and packing interactions (right) for 1-thio-2,3,4,6-tetra-O-acetyl-β-D-glucopyranose [4] (the precursor to SNAG).*

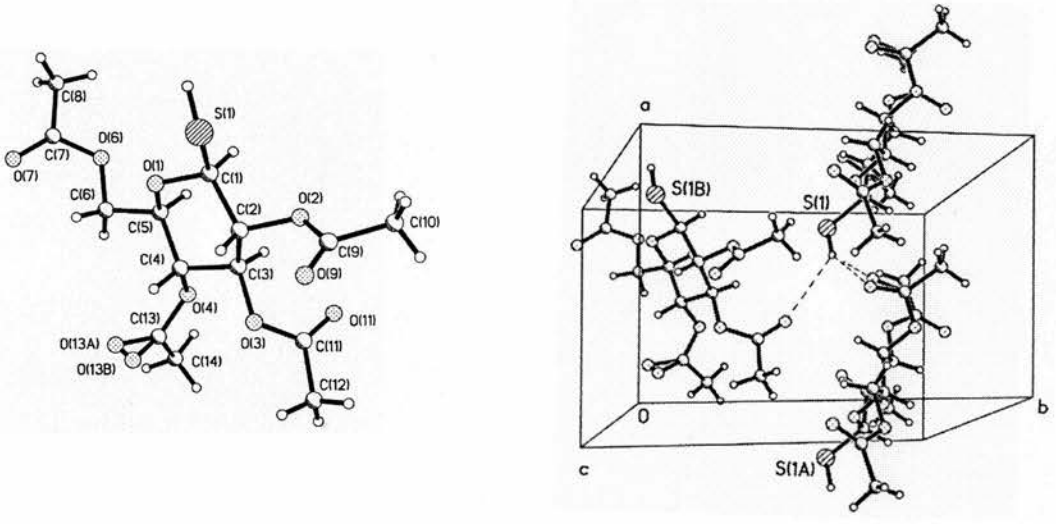

Note: The oxygen forming the carbonyl of the acetyl attached to the C-4 position of the sugar ring is labelled as O(13A) and O13(B) due to it existing in two different space groups. See appendices A for the resolved data.

4.1.2 The kinetics of SNAG [5] decomposition by UV.

Since all the biological testing was performed in ethanol : water (1:1), this solvent system was applied to all *in vitro* work in order to provide a fair comparison. As already reported (section 1.4.2), *S*-nitrosothiols can decompose in one of three ways; photochemically,[2,3] thermally[2,4] or by copper (I) catalysis.[5,6] To establish which had the most pronounced effect, all of these degradative pathways were investigated independently upon SNAG [5], by monitoring the disappearance of the UV absorption maxima at 345nm [Fig. 21], which is characteristic for *S*-nitrosothiols. In addition, decompositions were performed at various concentrations and pH.

4.1.2a Temperature and photochemical decomposition.

As illustrated by figure 56, temperature has a highly significant effect upon the decomposition of SNAG [5] over a period of 2.5 hours. Photolysis, on the other hand [Fig.57] had very little or no effect. Such findings accompany the knowledge that SNAG [5] must be cooled and maintained to -80°C when stored, to ensure that an infinite shelf life is maintained. Thus the importance of the thermal environment is perhaps not surprising. This is further substantiated by work involving the use of the NO electrode (section 4.3).

Fig.56 *The thermal decomposition of SNAG*

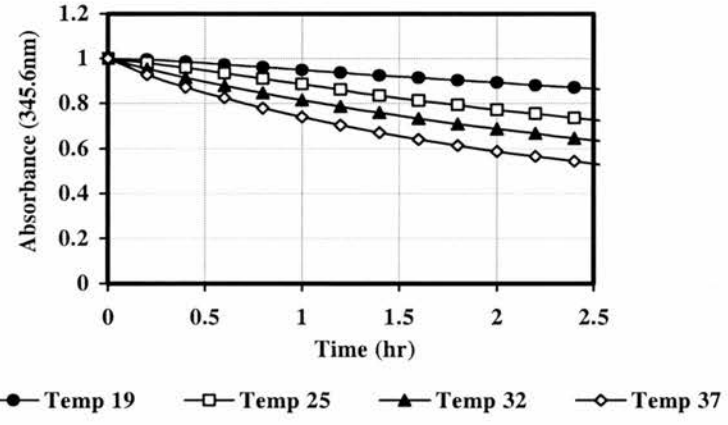

Four different temperatures were studied to see the effect upon the decomposition of SNAG [5] (2.4mM), in EtOH : H_2O, (1:1). 19°C, 25°C, 32°C & 37°C relate to the temperature of the biological testing suite, standard room temperature, skin temperature & body temperature, respectively.

Fig.57 *The photochemical decomposition of SNAG*

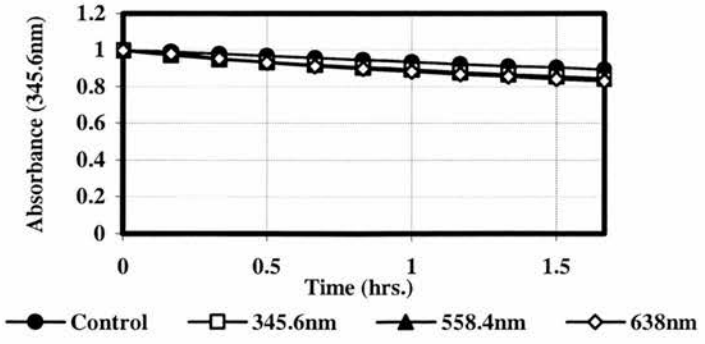

The decomposition of SNAG [5] (2.4mM) in EtOH : H_2O, (1:1) was followed under controlled conditions (with no light), & in the presence of continuous light. Three different wavelengths were studied, 345.6nm, 558.4nm & 638nm, which relate to the wavelength of the SNO peak, the visible peak

for S-nitrosothiols & the wavelength of the helium-neon laser of the Doppler flowmeter, respectively. All tests were carried out at 19°C to reduce the effect of thermal decomposition.

4.1.2b Copper catalysed decomposition

Initially, much of the kinetic work centred on the effect of copper ions, so that suitable water and ethanol quality could be established and maintained throughout the study. Interestingly, despite the addition of copper sulphate enhancing the biological response *in vivo*, all work undertaken *in vitro* suggested that the copper effect was insignificant. The use of EDTA (1mM) and millipure water, as opposed to standard distilled water, also had no effect upon the decomposition. Eventually it was rationalised that the proportion of water to ethanol, which increased in the biological testing well, upon the addition of the copper sulphate solution, was the significant factor. Although it may be envisaged that increasing the water volume could explain a greater presence of copper (even without copper sulphate present) and hence increase decomposition, atomic absorption spectroscopy proved this theory to be incorrect. Instead it was actually found that the copper content of ethanol (14ppm) was by far in excess of that observed in the water (0.02ppm). Consequently HPLC grade ethanol was routinely used, though this did not alter the kinetic or biological data. This highlighted the insignificance of copper to the overall rate of decomposition.

From further *in vitro* kinetic work [Fig.58], it is obvious to see the importance of the ethanol : water proportion. This was substantiated by comparison with the biological work, as already described (section 3.6.4, Fig. 34), where the same range of proportions were used. Using a low dose of SNAG (0.25%), the time to onset was significantly slow enough to enable any differences to be observed. Preliminary work strongly supports the idea that the greater the water volume the greater the release of nitric oxide. Clearly the degree of solubility of the *S*-nitrosothiols is crucial to their stability, with a 50% increase in water volume greatly enhancing the decomposition rate. The whole rationale for introducing copper to the testing wells was to try and understand if the mechanism responsible for the vascular relaxation was as a result of free nitric oxide diffusing across the skin. Despite the initiator for NO liberation being wrongly assigned, the diffusion mechanism remains viable. What is more debatable is whether alternative mechanisms are also operating concurrently.

Fig.58 *Illustrating how water proportion has more of an effect upon SNAG [5] (2.4mM) decomposition than copper.*

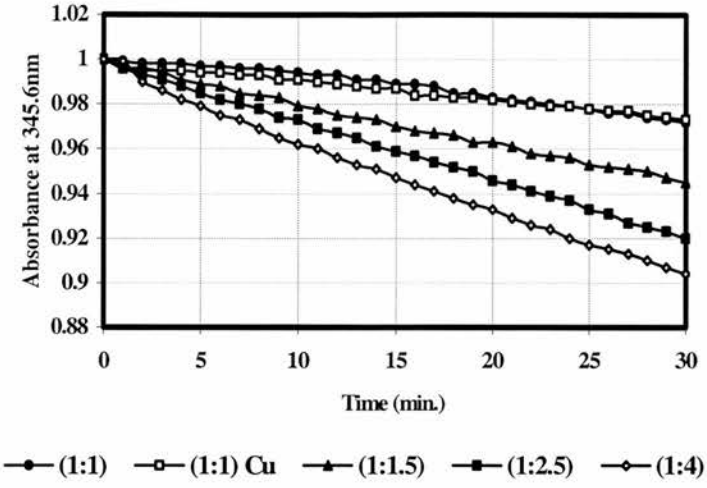

Using a copper sulphate concentration of 10ppm (represented by non-shaded squares), it is clear to see that water proportion is more dominant in effecting SNAG decomposition. The copper content of the water is negligible since the levels have been calculated to be less than that in the ethanol layer.

4.1.2c Concentration dependent decomposition.

The degree of NO release is certainly governed by *S*-nitrosothio-sugar concentration. This is exemplified by the *in vitro* [Fig.59] work and the biological data that highlights a very clear dose-response relationship (section 3.6.2). From the kinetic data, presented in figure 59, we can also suggest there is a critical concentration at which NO release is initiated. This concentration dependence may be explainable if scheme 22 is indeed an authentic NO degradative pathway. Such thinking relies on the idea that enough *S*-nitrosothiol must initially decompose in a spontaneous manner for there to be free thiol present to then react with a further molecule of RSNO. Further to this line of thought, if one is to propose that the biological response is the result of NO decomposition and diffusion from the wells alone, the *in vitro* data [Fig.59] becomes inadequate in explaining the vasodilatory responses seen for low doses of SNAG (0.25%) [Scheme 3.6.2, Fig.29-30].

To answer, what appears to be, conflicting *in vitro* and *in vivo* data, the detectable level (millimolar) of the UV spectrophotometer must be brought into question. As hinted in the footnote of figure 59, the lack of SNAG [5] decomposition observed by UV analysis, at concentrations of 0.25% and lower, does in no way eliminate the

possibility that sufficient NO is released to bring about vasodilation. As discussed recently by Garthwaite,[7] levels of NO in the nanomolar range are more than adequate to elicit biological changes in a human subject. Consequently we should not rule out the prospect of NO diffusion, from wells containing 0.25% SNAG [5], as a mechanism for producing noticeable increases in forearm blood flow.

Scheme 22 *The decomposition of an S-nitrosothiol to give two equivalents of free NO with every molecule of disulphide formed.*

$$\mathbf{RSNO \rightarrow RS\cdot + NO\cdot}$$

$$\mathbf{RS\cdot + RSNO \rightarrow RS{-}SR + NO\cdot}$$

Fig.59 *Showing how SNAG decomposition is concentration dependent.*

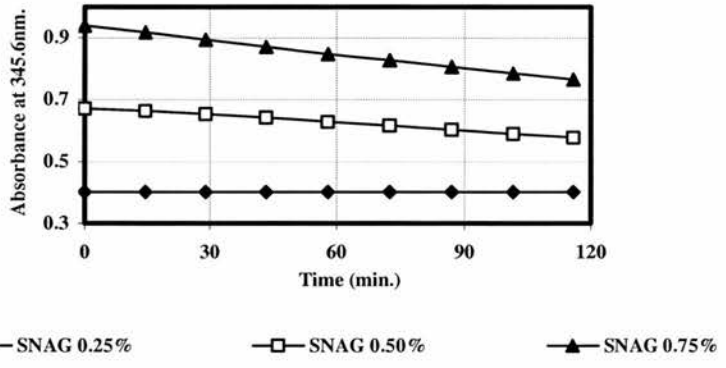

Studying the three concentrations (0.25, 0.50 & 0.75%) of SNAG [5] that were used in vivo (section 3.6.2), there is a clear relationship between decomposition rate and concentration. At the lowest concentration NO degradation may be below the detectable level of the UV spectrophotometry (millimolar range).

4.1.2d Transnitrosation

Since we observe a secondary effect upon the removal of SNAG [5] from the forearm (section 3.6.1) and with the knowledge of the short half-life of NO *in vivo*, the idea of transnitrosation to endogenous thiols, acting as NO stores, was considered. Since *S*-nitrosocysteine, made *in situ* due to isolation problems (section 6.3.3), has the same λ_{max} as SNAG [5] yet decays rapidly in the presence of copper (10ppm), a model was devised using SNAG [5] (2.4mM) in the presence of an

equivalent amount of copper (10ppm). As described already (section 4.1.2b), SNAG [5] decomposition is unaffected by such levels of copper, thus any rate enhancement with the addition of cysteine is evidence of transnitrosation. Fig.60 supports this theory and may therefore explain the biological observations presented in section 3.6.1.

Fig.60 *Evidence of Transnitrosation.*

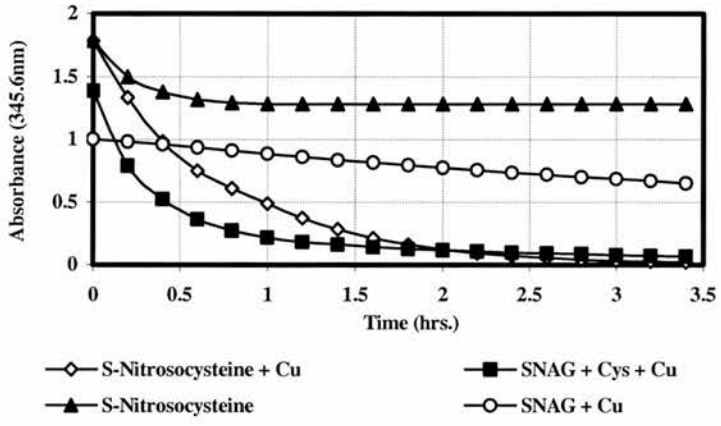

Due to the very different rate at which cysteine (2.4mM) and SNAG [5] (2.4mM) decompose in the presence of copper (10ppm), we are able to study whether the NO from SNAG can transnitrosate cysteine. The rate enhancement observed for SNAG in the presence of copper & cysteine strongly supports this idea, which in a biological sense may explain the secondary effect seen upon drug removal. All work was carried out using ethanol : water, (1:1) solutions.

4.1.2e The effect of pH

For completeness and since all biological work involves transdermal delivery, the effect of pH on the decomposition rate of SNAG [5] was investigated. The pH of skin is approximately 5.5, thus in comparison to physiological pH of 7.4, differences in NO release could be predicted. As illustrated by figure 61, this is clearly the case. Whilst it is interesting to see the effects of weakly acidic and basic mediums, the data should be treated with caution since the use of buffers in this work introduces a whole array of metal ions into the cuvette. Whilst we are convinced, from the work presented in section 4.1.2b, that copper ions have no effect on *S*-nitrosothiol decomposition, we can be less confident of how other metal ions may interfere, without a comprehensive study on each individually. For instance, both mercury and

silver salts have been linked with *S*-nitrosothiol decomposition.[8] Thus from this particular study we can merely propose that pH may be an important consideration in how rapidly the *S*-nitrosothiols decompose.

Fig.61 *The effect of pH on the decomposition of SNAG [5] (2.4mM)*

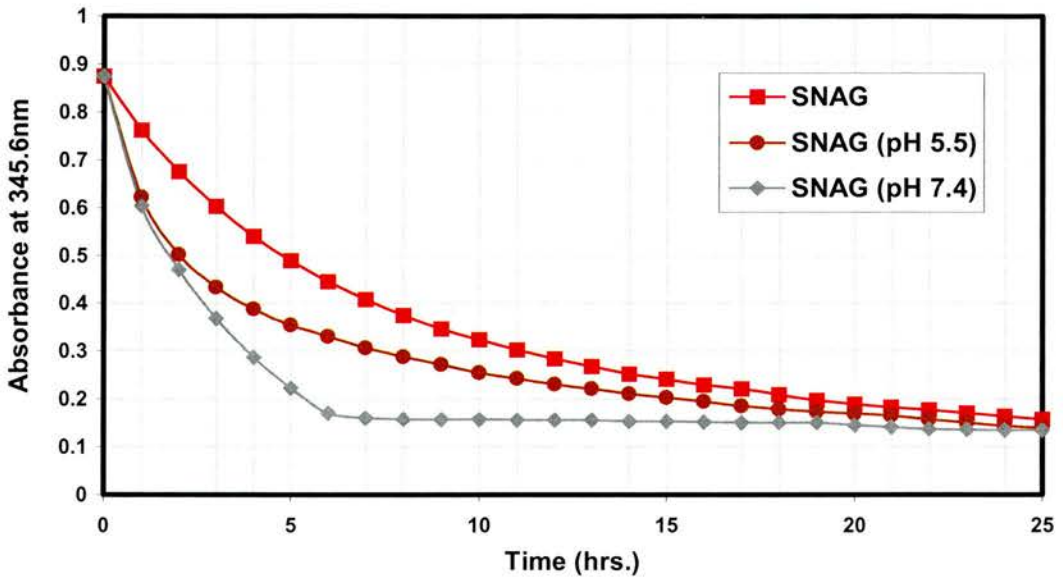

The decomposition of SNAG [5] in ethanol : water, (1:1) was compared against that of SNAG in the same ethanol : water ratios, using water of pH 5.5 (brown) and 7.4 (grey). In all of this work SNAG [5] was present at a concentration of 2.4mM for consistency.

4.1.3 Other *S*-nitrosothio-sugars.

Using SNAG [5] as the lead compound, many similar sugar based *S*-nitrosothiols were chosen for synthesis (Section 1.4.4 & chapter 6) and biological testing. The *in vitro* behaviour of each compound listed in figure 62, was therefore investigated in a comparative sense to SNAG [5] before allowing any of the work presented in section 3.7, to proceed.

As illustrated by figure 63, UV decomposition data was only possible for compounds [5], [15], [25], [30], [34], [38], [42] and [46]. The *S*-nitrosothiols labelled [51], [59], [65], [70], [76] and [84] were all too lipophilic to allow their decomposition rates in the standard ethanol : water (1:1) solution, to be adequately studied. *S*-nitrosothio-D-glucose (SNOG) [79] was also omitted from the plot [Fig.62] due to exhibiting no decomposition at all over 25 hours making it the most stable NO-donor in the study.

Fig.62 *The range of S-Nitroso-1-thio-acetylated sugars investigated.*

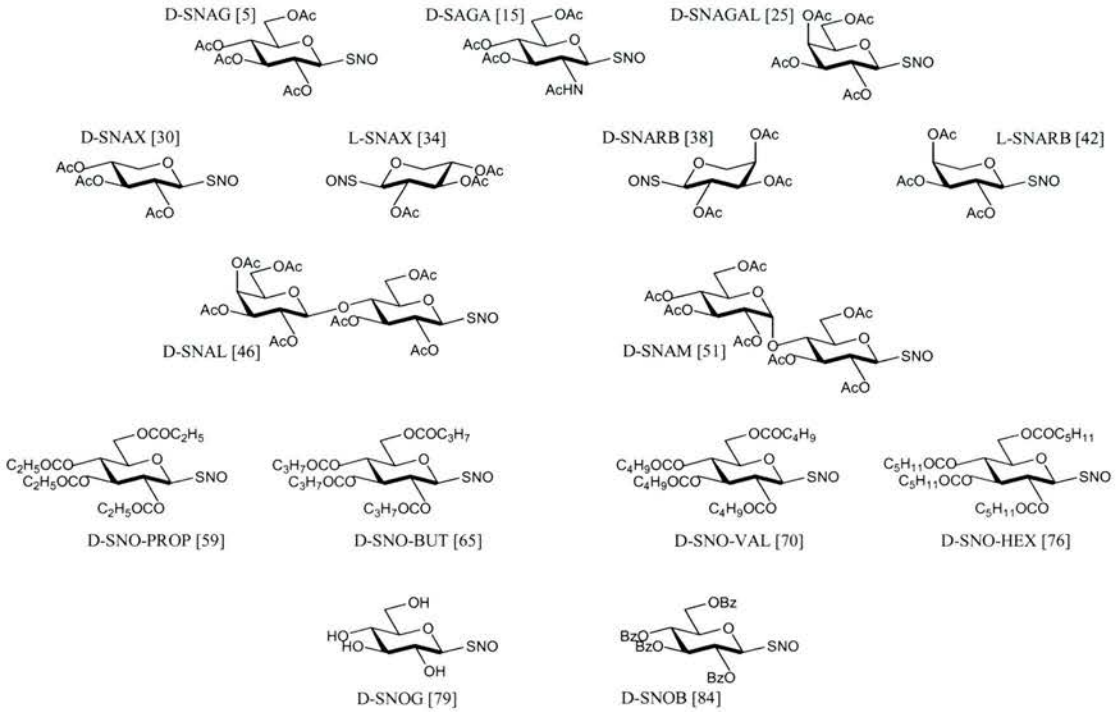

The above compounds were all synthesised according to procedures outlined in chapter 6. Attempts were then made to compare their in vitro performances as NO donors in a comparative manner to SNAG [5].

Fig.63 *Comparing the UV decomposition data of seven S-Nitroso-1-thio-acetylated sugars (2.4mM) relative to SNAG [5] (2.4mM).*

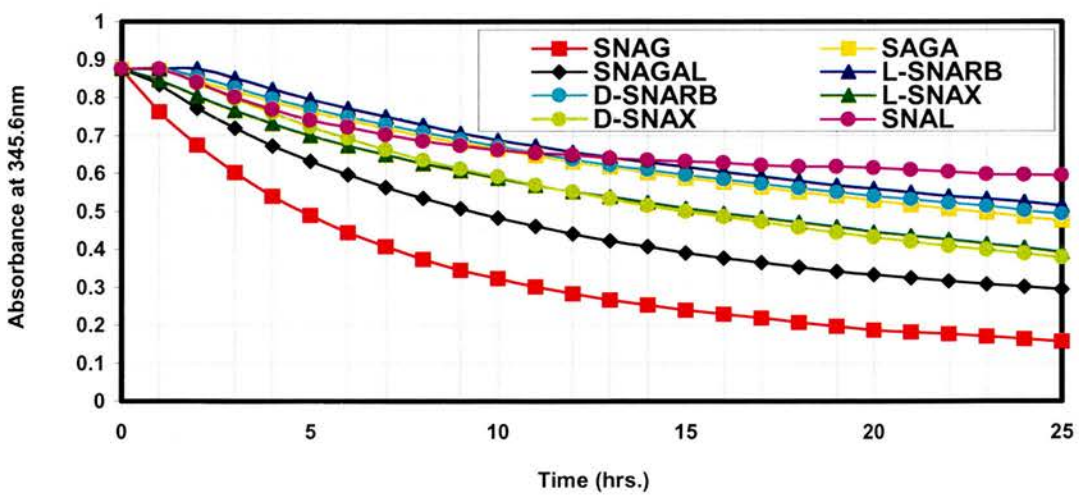

Using the UV spectrophotometer set at a fixed wavelength of 345.6nm, allowed the rate of decomposition of the S-nitrosothiols listed (legend), to be compared against SNAG [5]. In all of the work ethanol : water, 1:1 solutions were used and all NO donors were studied at a concentration of 2.4mM. In addition a constant temperature of 25°C was maintained using a PYE UNICAM cell temperature controller.

Whilst the slow release of NO from SNOG [79] is at least reflected in a slower onset of vasodilation, when applied to the forearm, relative to SNAG [5] (section 3.9, Fig. 45), the *in vivo* results for the majority of the *S*-nitrosothiols are more difficult to interpret using the kinetic results shown here. From the compounds studied *in vitro* (Fig. 63), all appear to be more stable than SNAG [5] itself. Due to this we would expect all such NO-donors ([5], [15], [25], [30], [34], [38], [42] and [46]) to have a slower time to onset, when studied *in vivo*, against SNAG [5]. Such thinking is based on the assumption that decomposition in the testing well followed by NO diffusion, is the only mechanism in operation. Whilst the data in section 3.7 does not highlight any major differences in biological activity between compounds tested, SNAG is shown to remain as potent as any other sugar based vasodilator, with a time to onset that is more than equal to the rest.

As described previously (section 3.7), similar decomposition profiles were recorded for D and L-isomers of the same sugar, as we would expect. The trend of greater stability in changing the sugar backbone was shown to be lactose < glucose < galactose < xylose < *N*-acetyl glucosamine < arabinose, respectively. Such relative stability was determined based upon the half-life ($t_{1/2}$) of each test compound. To accurately calculate this value the absorbance for each compound at infinity (t_∞) is required. Since this value is only found after ten half-life's, we assume that all profiles obey first order kinetics, thus allowing the use of Swinbourne plots to calculate $t_{1/2}$ (see appendix B),[9,10] from the raw data in figure 63.

Using this kinetic extrapolation, all of the compounds from which kinetic data was obtained could have a half-life ($t_{1/2}$) assigned. From comparing the profiles with the calculated half-lifes, it can be seen how misleading figure 63 is when taken alone. This highlights the importance of the absorbance reading at infinity (A_∞), since this varies between compounds quite significantly which, in turn provides a vast array of different half-lifes as presented in table 2. Thus the mere fact that the sugar backbone can influence the overall stability of the molecule, further highlights the complexity with which S-NO bond strength is governed.

Table 2 *Examining the results of the in vivo and in vitro work*

TEST COMPOUND	TIME TO PLATEAU (min)	DURATION OF RESPONSE (min.)	MAX. RESPONSE (PU)	HALF-LIFE ($t_{1/2}$) in hours
	From in vivo work	From in vivo work	From in vivo work	From in vitro work
D-SNAG 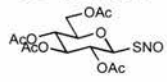	**2**	**>40**	**131**	**4.4**
D-SAGA 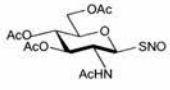	**23**	**>40**	**121**	**13.2**
D-SNAGAL 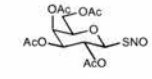	**14**	**>40**	**155**	**6.6**
D-SNAX 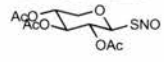	**10**	**>40**	**109**	**9.8**
L-SNAX 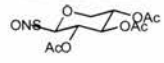	**6**	**>40**	**78**	**9.5**
D-SNARB 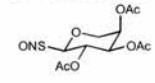	**32**	**>40**	**104**	**13.5**
L-SNARB 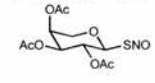	**4**	**>40**	**98**	**14.0**
D-SNAL 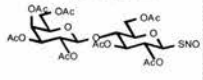	**8**	**>40**	**121**	**4.0**

This table aims to draw together the highlights from the in vivo (20.56mM) (see section 3.7) and in vitro (2.4mM) (see Fig.63) data. The time to plateau is the time taken (in minutes), after administration of the test compound, for the vasodilatory response to reach a steady state. The duration of the response is the time over which the test compound produces vasodilation at the level of plateau. The maximum response, measured in perfusion units (PU) by the laser Doppler imager (LDI), is the peak response measured during the entire recording of superficial blood flow in the

forearm. The half-life (in hours) is the time taken for half of the test compound to decompose, releasing free NO, whilst being maintained at 25°C in an ethanol : water (1:1) solution.

From the above table, four major observations can be made. The first two are perhaps the most obvious, since the data clearly show that all of the S-nitrosothiols listed are of reasonable stability in solution, which in turn could explain the prolonged duration of action when tested *in vivo*. The third major feature is the lack of correlation between a test compound's half-life and the time taken by it to produce a vasodilatory plateau. However, the fourth observation is perhaps the most interesting to note, since the compounds with the three shortest half-lifes (D-SNAG [5], D-SNAGAL [25] and D-SNAL [46]) also give the three highest maximum vasodilatory responses. The exception to this rule is D-SAGA [15], which shows a maximum response, which is equal to that of D-SNAL [46] despite having a half-life over three fold greater [Fig. 63].

Introducing the non-sugar based NO-donor, *S*-nitroso-*N*-acetyl-penicillamine, SNAP [8] (sections 1.4.4 and 6.3.2) highlights a further conflict to this latter idea. Using the data presented in figure 64 together with Swinbourne calculations (appendix B), a half-life of 0.9 hours was identified for this commonly used *S*-nitrosothiol. As a consequence and with the knowledge of our findings from table 2, we were encouraged to study its ability to increase forearm blood flow. However from *in vivo* work, where its biological activity was compared directly against SNAG [5], both the time to reach plateau (21 minutes) and the maximum response (117 PU) were less impressive (see table 2) than that of SNAG [5]. Thus the observations from table 2 must be viewed with a great deal of caution and indeed suggest the need for a more comprehensive study using all of these novel NO-donors, before attempting to interpret the data in a detailed fashion.

There are obviously many possible UV studies that we could have performed for this section of the work. Since we are particularly interested in determining the mechanism of action by which these donors function, our attention will now turn to other analytical tools such as log P, NO electrodes and X-ray photoelectron spectroscopy (XPS). For future work in this particular area, transnitrosation (section 4.1.2d) would appear to be one of the most exciting, at least in terms of the data that we were able to collect. Indeed in the last seven years there have been several

publications on this topic, suggesting a role for endogenous thiols as very real NO stores.[11-13]

Fig.64 *Comparing the stability of SNAG [5] against a non-sugar NO-donor (SNAP [8]).*

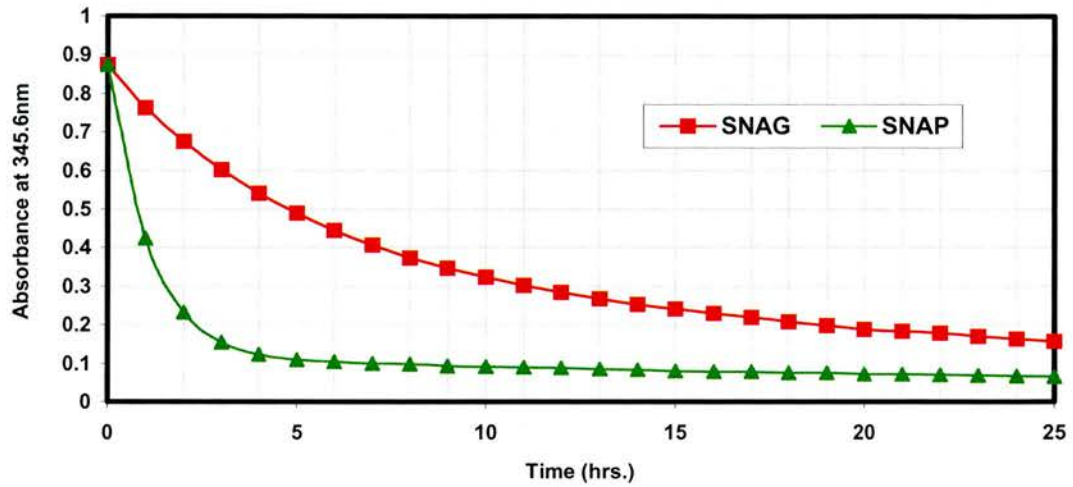

In ethanol : water, (1:1) the decomposition of SNAG [5] (red) was compared against that of SNAP [8] (green). Such a comparison was necessary to highlight how non-sugar related NO-donors are not necessarily more stable in solution, despite showing superior shelf life in the solid state. For fair comparison a concentration of 2.4mM was used in both kinetic runs.

4.2 Log P data.

To better understand the transdermal delivery properties of SNAG, propionylated [59] (section 6.13.8), butrionylated [65] (section 6.14.5), valerionylated [70] (section 6.15.5) and hexionylated [76] (section 6.16.5) relatives of SNAG [5] were applied to Log P testing. The sole purpose of this work was to try and establish if there was an appreciable difference in lipophilicity between the five compounds. Ultimately this work was deemed necessary as it was hoped that the results would help determine if increasing the lipophilicity improves the transdermal uptake of the sugar molecules. In an attempt to see a significant difference, the unprotected form of SNAG, referred to as SNOG [79], was included in the work.

Fig. 65 *The Sirius PCA101 apparatus for measuring LogP by potentiometric titration*

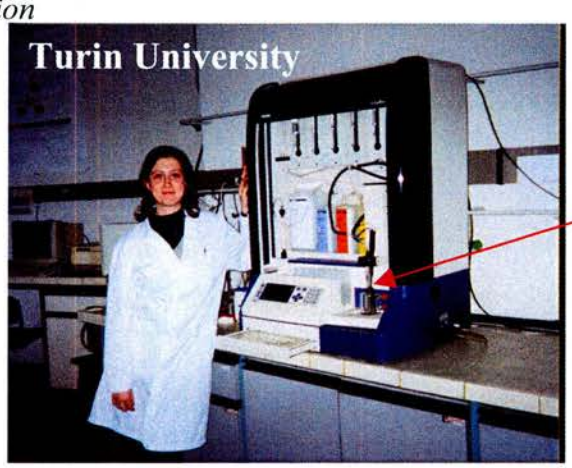

The pH electrode is also equipped with an Ag/AgCl double-junction pH electrode, a temperature probe, an overhead stirrer, a precision dispenser and a six-way valve for distribution reagents and titrants.

Using potentiometric titration[14-15] (Sirius PCA101, Sirius Analytical Instruments Ltd, UK) [Fig. 65 and appendix C] and shake flask techniques[16] (appendice D), we were able to confidently attribute Log P values to the thiol derivatives of this lipophilic series of compounds [Fig.66]. The thiols were studied rather than the *S*-nitrosated species to avoid complications with compound decomposition during the analysis. However, using computational predictions (CLOGP), it was possible to calculate a value for the pre and post nitrosated species, which showed the former agreeing well with the experimental data. Thus we can be confident that the CLOGP data for the *S*-nitrosated compounds also closely resembles the actual values, particularly since the SNO functionality is known to have very little bearing on a molecule's overall lipophilicity. This explains why the thiol and SNO compounds have such similar CLOGP values (as illustrated in figure 66, by the blue and yellow bars).

As a result of the very abrupt increases in lipophilicity as we move through this series [Fig.66], it was not surprising that UV analysis, using ethanol : water (1:1), was not possible for these compounds, due to solubility problems. Instead an NO electrode monitored the rate of NO release (see section 4.3). Increased lipophilicity also prevented the use of an aqueous ethanolic solution when testing their vasodilatory activity (see sections 2.3 and 3.9). This protocol was consequently replaced by dissolving the compounds in KY jelly, as described in chapter 3, to enable the helium-neon laser, of the LDI, to penetrate through the administered compound (a clear gel) to the depth of the microcirculatory vessels.

Fig. 66 *Log P & CLOGP data for SNAG [5], SNOG [79] and more lipophilic derivatives of SNAG.*

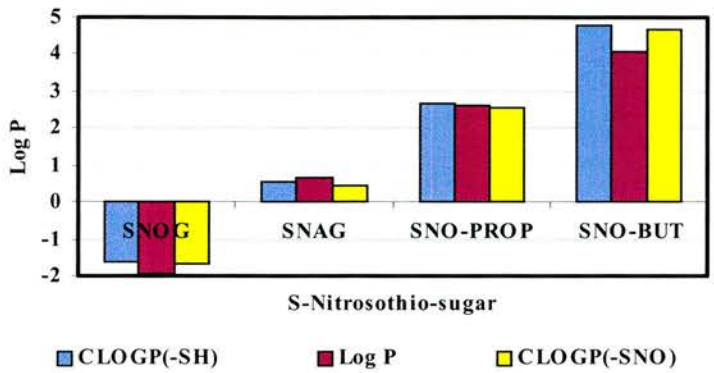

CLOGP (-SH) *(in blue) refers to Log P data calculated for the thiols by computational methods.* ***CLOGP (-SNO)*** *(in yellow) refers to data calculated in the same way but for the S-nitrosothiol, whilst* ***Log P*** *data (in purple) was obtained experimentally by shake flask & potentiometric titration, using the Sirius PCA101 instrument. From left to right, the compounds for which Log P data were obtained were, SNOG [79], SNAG [5], SNO-PROP [59] and SNO-BUT [65]. With the exception of SNOG [79] (determined by shake flask) all the rest were experimentally obtained by potentiometric titration.*
NB. Compounds of greater chain length than SNO-BUT [65] were too lipophilic for measurement by this means.

It was hoped that from this series of compounds there would be some correlation between Log P value [Fig.66] and the observed vasodilatory response (section 3.9, figures 44 and 45). From the *in vivo* results, we found that SNAG [5] and SNOG [79], the two most hydrophilic in the series, both gave equally higher plateau responses, than any of the more lipophilic derivatives. Whilst this might suggest that the actual uptake of the sugar molecules, across the skin, is an important factor that is strictly governed by lipophilicity, or lack there of, it could equally be explained if a significant difference in NO release, exists within this series. Attention was therefore moved to the NO probe.

4.3 NO probe data.

In an attempt to try and establish if the lipophilic series would release NO at a different rate to SNAG [5] an ISO-NOP sensor (World Precision Instruments, UK)

was used. The data presented in figure 67 highlight a very clear difference in NO release, with SNO-VAL [70] decomposing more slowly than SNAG [5]. Such findings bode well with the idea that SNAG [5] is a better vasodilator than its lipophilic relatives. However, what is less readily understood is how SNOG [79], the most stable of all the *S*-nitrosothio-sugars, in solution at least, has the ability to plateau to the same level as SNAG [5], albeit more slowly.

Fig. 67 *A plot to show how SNAG releases NO more quickly than its lipophilic relative, SNO-VAL [70].*

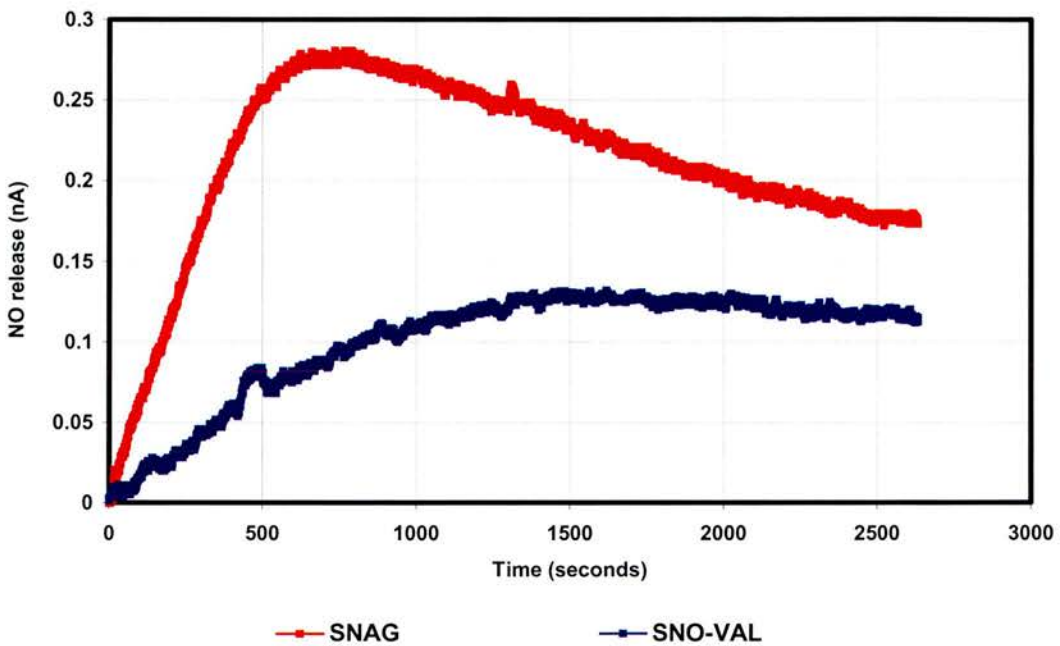

In an ethanol : water, 1:1 medium, thermostatically controlled to 25°C, we were able to show how SNAG [5] releases NO significantly faster than its lipophilic relative SNO-VAL [70]. From calibration plots an NO-oxidation current of 1nA roughly corresponds to an NO concentration of 1μM.

The above result can be rationalised if we envisage how the *S*-nitrosated anomeric position may have improved protection from decomposition, due to an increased steric bulk, provided by the introduction of longer side arms upon the glucose molecule. Such an idea is displayed below in figure 68.

Fig. 68 *Increasing the lipophilicity of SNAG [5]*

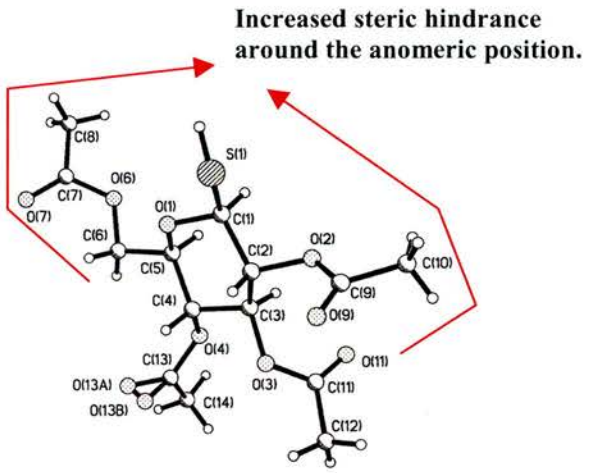

Using the resolved crystal structure of pre-SNAG [4], we can model the effects of increasing the lipophilicity of SNAG [5] and as highlighted, propose further protection to the highly important anomeric position.

To reinforce the work presented in section 4.1.2a and to appreciate just how much more NO is released from SNAG [5] should it enter into an *in vivo* environment (37°C), the NO probe was used to study how *S*-nitrosothiol decomposition varies with temperature [Fig.69].

Fig. 69 *Using the NO probe to further emphasise the effect of temperature on the decomposition of SNAG [5].*

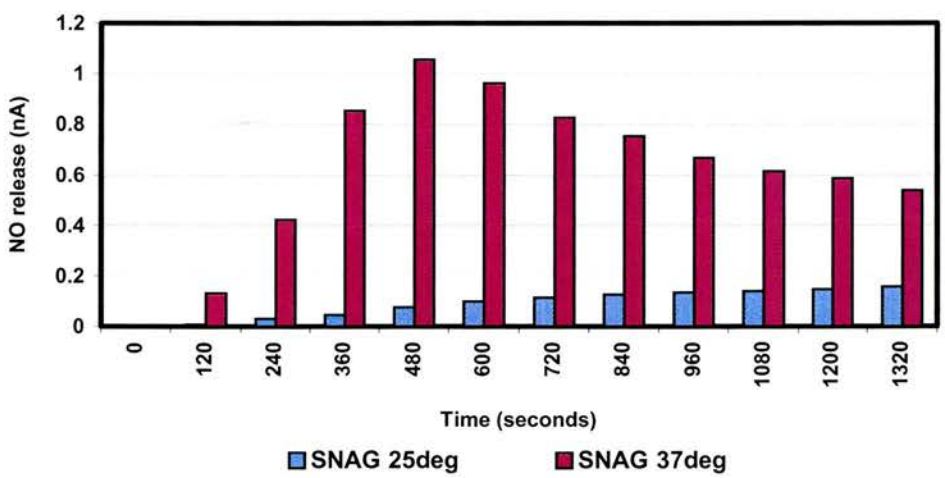

Further to the work reported in section 4.1.2a (Fig.56), where we identified the importance of temperature, the above plot shows just how NO release can significantly increase when raising the temperature to that found in a biological model (37°C). As in Fig. 67, calibration plots show the NO-oxidation current (plotted on the y axis), to relate almost exactly to that of absolute NO concentration

(μM). As in the system used previously (Fig. 67), an ethanol : water (1:1) medium was used. Temperature was regulated by a thermostatically controlled water bath.

Since SNAG [5] at physiological temperature does release NO more efficiently than at room temperature, identifying whether the entire molecule can readily penetrate the skin, becomes all the more important in terms of understanding the mechanism of action. With this in mind, the use of XPS to study skin layers after testing with SNAG [5], was the next obvious study.

4.4 XPS and skin stripping experiments.

Fig. 70 *The X-ray photoelectron spectrometer (XPS).*

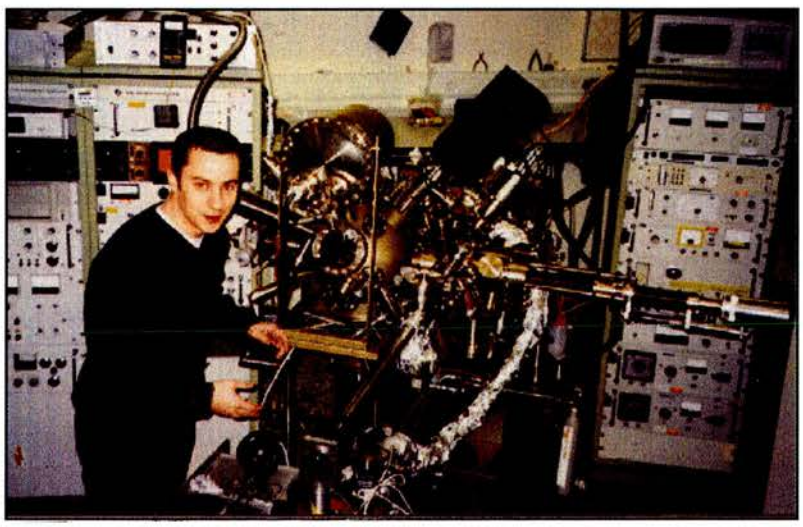

Time on this VG ESCALAB-3 spectrometer (Vacuum Generators, UK) was made possible courtesy of the Surface chemistry group based at the University of St Andrews.

In an attempt to identify if skin penetration is part of a viable mechanism by which SNAG [5] and related compounds perform biologically, a protocol involving X-ray Photoelectron Spectroscopy (XPS) together with progressive skin stripping, was devised. XPS is a powerful technique[17] for studying surfaces [Fig.70], and more precisely, the atomic content of these (Appendices E). In this work the surface is the adhesive tape used repeatedly to strip one layer of stratum corneum cells,[18] after prolonged exposure (40 minutes) to SNAG [5]. Fortunately, XPS is particularly

responsive to qualitatively and quantitatively detecting sulphur. Thus any enhancement, over baseline (control), in sulphur content, positively identifies the compound in that particular layer of skin. Whether the compound is as the RSNO or the corresponding disulphide (RSSR) is insignificant. Consequently what this technique provides is a handle by which we can trace the movement of compound across the skin.

The data obtained from this process suggest that SNAG [5] does partially penetrate the skin, at least to a superficial level [Fig. 71]. Thus, we have the possibility of NO release within the skin, followed by either diffusion to the active site or transnitrosation to endogenous thiols which then act as reservoirs of nitric oxide within the outermost layers of the skin.

Fig.71 *The XPS results showing five skin strips, taken after applying SNAG [5] to the forearm for 40 minutes.*

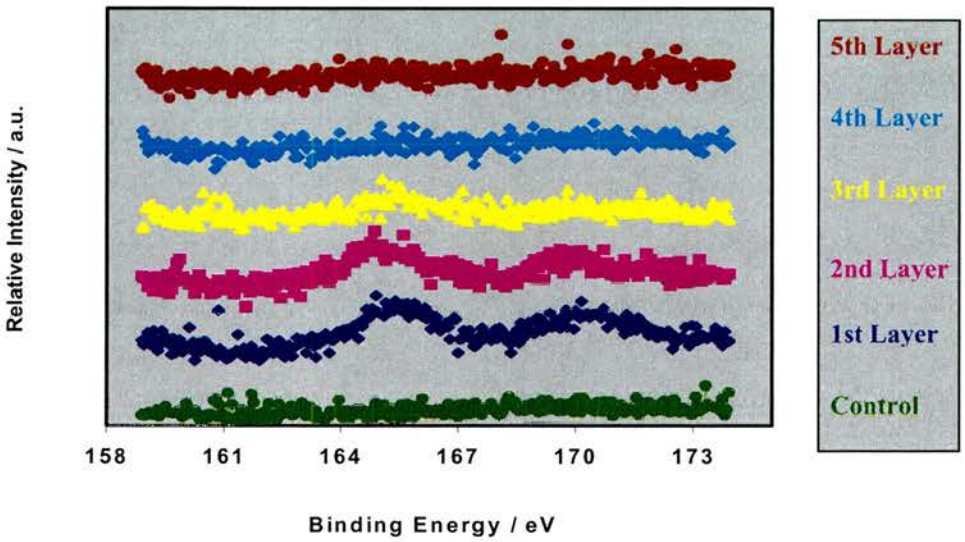

Having administered SNAG [5] (0.75%, 20.58mM) to the forearm of a healthy subject for 40 minutes, successive skin strips were taken along with a control strip (green) from a site free from SNAG [5]. On the basis of skin stripping experiments performed elsewhere,[18] it is assumed that each adhesive strip removes one further layer of dead keratinocytes (a depth of 1μm) from the skin's outermost surface. Before analysis the XPS apparatus was baked out to 160°C at a pressure of 5 x 10^{-10} Torr.

The colours in the above plot [Fig. 71], relate to the different skin layers removed. The outermost three layers, represented as dark blue, pink and yellow, all show a

peak at approximately 165.5eV. No such peak is observed in the control strip (green) or any of the deeper layers, represented as light blue and brown. The two most superficial layers also show a slight peak at 170eV. This latter binding energy corresponds to that of sulphate, suggesting the possibility that SNAG is in some way oxidised at the skins surface. For any disulphide or thiol present, we would expect to see a binding energy of 163.7eV. This suggests that the peak at 165.6 is instead that of an *S*-nitrosothiol (SNAG [5]).

4.5 References.

1 J. Gigg, R. Gigg, S. Payne and R. Conant, *J. Chem. Soc. Perkin trans. I*, 1987, 2411.

2 D.J. Sexton, A. Muruganandam, D.J. McKenny and B. Mutus, *Photochem. Photobiol.*, 1994, **59**, 463.

3 J. Barrett, L.J. Fitzgibbons, J. Glauser, R.H. Still and P.N.W. Young, *Nature*, 1966, **211**, 848.

4 H. Rheinboldt and F. Mott, *J. Prakt. Chem.*, 1932, **133**, 328.

5 J. McAninly, D.L.H. Williams, S.C. Askew, A.R. Butler and C. Russell, *Chem. Comm.*, 1993, **23**, 1758.

6 A.P. Dicks, H.R. Swift, D.L.H. Williams, A.R. Butler, H.H. Al-Sa'doni and B.G. Cox, *J. Chem. Soc. Perkin Trans 2*, 1996, 481.

7 J. Garthwaite of University College London, oral presentation at the 4th Scottish NO meeting, University of St Andrews, November 2001.

8 H.R. Swift and D.L.H. Williams, *J. Chem. Soc. Perkin Trans. 2*, 1997, **10**, 1933.

9 F.J. Kezdy, J. Jaz and A. Bruylants, *Bull. Soc. Chem. Belg.*, 1958, **67**, 687.

10 E.S. Swinbourne, *J. Chem. Soc.*, 1960, 2371.

11 D.J. Barnett, J. McAninly and D.L.H. Williams, *J. Chem. Soc. Perkin Trans. 2*, 1994, **6**, 1131.

12 A.P. Dicks, P.H. Beloso and D.L.H. Williams, *J. Chem. Soc. Perkin Trans. 2*, 1997, **8**, 1429.

13 A.P. Dicks, E. Li, A.P. Munro, H.R. Swift and D.L.H. Williams, *Can. J. Chem.*, 1998, **76**, 789.

14 A. Avdeef, *Quant. Struct. -Act. Relat.*, 1992, **11**, 510.

15 G. Caron, Ph.D. Thesis, The University of Lausanne, 1997.

16 J.C. Dearden and G.M. Bresnen, *Quant. Struct. –Act. Relat.*, 1988, **7**, 133.

17 C.D. Wagner, *Handbook of X-ray Photoelectron Spectroscopy*, Perkins-Elmer Corporation, Physical Electronic Division, 1979.

18 F. Pirot, Y.N. Kalia, A.L. Stinchcomb, G. Keating, A. Bunge and R.H. Guy, *Proc. Natl. Acad. Sci. USA*, 1997, **94**, 1562.

Chapter 5. Conclusions

Conclusions drawn from the chemical, pharmacokinetic & biological findings.

From the seventeen target compounds listed in figure 18 of section 1.4.4, only *S*-nitroso-6-thio-2,3,4,6-tetra-*O*-acetyl-β-D-glucopyranose, (6-SNAG) [89], was not successfully synthesised (section 6.19). This non-anomerically based *S*-nitrosothio-sugar would have provided particular interest in an *in vitro* system, due to the potential for it to complex to copper and thus release free NO (section 1.4.4, Fig. 20). However, from the other target molecules (shown in section 4.1.3, Fig. 62) many interesting pharmacokinetic and biological results were possible.

Of the extensive UV work undertaken, the most important finding was that of raised temperature, which we have shown to be a dominant contributor to the decomposition of this type of compound. We have also shown the inability of copper and light in effecting the stability of SNAG [5], though such observations are likely to hold true for all the sugar targets that were synthesised. Taking these observations together with the evidence of transnitrosation and the significance of the water to ethanol ratio we have illustrated the complexity surrounding the S-NO bond.

Biologically, three major points emerged from the testing. The first and most obvious was in identifying that all of the target compounds are able to bring about prolonged vasodilation. Altering the site of application, from the forearm to the hand, then highlighted the importance of skin type, which we were able to reinforce through work with NO-donors of different lipophilicity. Using the healthy volunteers in a parallel study to that of a heterogeneous group of Raynaud's sufferers, the third and most noticeable result was possible. This illustrated a clear distinction between the two subject groups. Whilst both produced equivalent peak blood flow responses, the inability of the Raynaud's patients to sustain a strong vasodilation, posed many questions with regard to the physical nature of their microcirculatory vessels.

In terms of Raynaud's phenomenon itself, this work is merely suggestive due to the small number of subjects involved. However, the differences between group data cannot be ignored. The improvement in blood flow, seen superficially in the forearm

of the patients, compared with that seen on control sites, by SNAG [5], dismisses any question of a fault in the NO pathway. Therefore the results may instead be highlighting a problem at the level of the peripheral blood vessels themselves and more precisely their inability to remain in a state of prolonged relaxation.

Putting aside the issue of what actually causes the disorder that is Raynaud's phenomenon, our attempts to improve peripheral blood flux have been fruitful. For future work to succeed beyond what has been achieved here, understanding the exact pathway by which these compounds function will be essential. Using the decomposition, Log P, XPS and probing biological work together with the group studies, we can, at the very least, summarise the possible mechanisms that operate [Fig. 72]. Such possibilities all remain viable, both in an individual sense, or alternatively in combination with others. Only once this puzzle has been unravelled will we be able to design a highly efficient transdermal NO-donor and at the same time hopefully understand better the deficiencies involved in Raynaud's and associated vascular disorders.

Fig. 72 *The possible mechanism(s) by which SNAG [5] and related compounds are able to dilate superficial forearm blood vessels.*

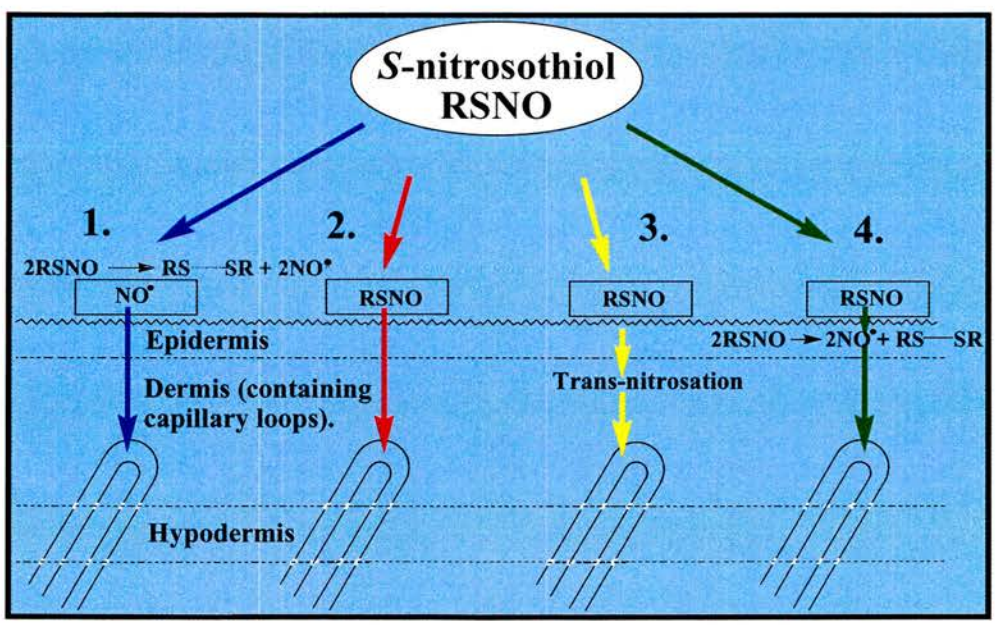

The above scheme (not to scale) represents a cross-section through the superficial layers of a human forearm. The rectangular boxes illustrate the testing wells in which S-nitrosothiol (RSNO), usually SNAG [5], is administered. 1. Shows decomposition of RSNO followed by direct NO diffusion to the blood vessel, 2. Suggests RSNO permeates the skin and travels to the active site, 3. Proposes RSNO permeates the skin only to undergo a transnitrosation reaction, thus forming a more stable RSNO which later releases NO when needed, and finally 4. Represents RSNO decomposing in the outer skin layers to generate free NO that diffuses to the active site.

Chapter 6. Experimental

Synthesis, yield optimisation, purification & characterisation of the test compounds.

6.1 *Materials*

- Commercial solvents were used. These were dried where appropriate.
- The T.L.C. plates used were silica gel 60-F_{254} (Merck). Detection was by charring, using a dilute ethanolic solution of sulphuric acid.
- Column chromatography involved the use of silica gel 60 (Fluka).
- Melting point determination was performed on a Gallenkamp melting point apparatus (uncorrected).
- Optical rotation was measured at the sodium D-line (at ambient temperature). An optical activity AA-1000 polarimeter was used and $[\alpha]_D$ values were calculated in units of 10^{-1}deg cm^2 g^{-1}.
- UV-VIS spectra were recorded on a Philips PU8700 UV-VIS scanning spectrophotometer fitted with a PYE UNICAM cell temperature controller.
- IR spectra were recorded on an Avatar 360 FT-IR (Nicolet, Madison, USA).
- ^1H NMR and ^{13}C NMR analysis was performed on a Varian Gemini 2000 spectrometer at 300MHz and 75MHz respectively.
  ^1H NMR spectra were referenced to the following internal standards: δ_H 7.26ppm in $CDCl_3$, δ_H 3.31ppm in CD_3OD, δ_H 4.79ppm in D_2O.
  ^{13}C NMR spectra were referenced to the following internal standards: δ_C

77.16ppm in $CDCl_3$, δ_C 49.0ppm in CD_3OD.

The reporting of all chemical shifts (δ) are in ppm and coupling constants (J) are calculated in Hz.

- EI,CI and FAB Mass Spectroscopy was performed on a VG AutoSpec, (Fisons Instruments, Manchester, UK). The calibration reference for both CI and EI was perfluorokerosene and for CI isobutane was used as the carrier gas.
  FAB required a matrix of nitrobenzylalcohol.

- Electrospray Mass Spectroscopy was performed on a VG Platform, (Fisons Instruments, Manchester, UK). The carrier liquid of choice being methanol.

- MALDI-TOF spectra were obtained on a TOFSpec 2E equipped with a nitrogen laser (337nm), (Micromass, Manchester, UK). Mass spectra were acquired in reflection mode (positive mode).

- Blood flow studies were possible using the MoorLDI scanning laser - doppler imager (Moor Instruments, Axminster, UK) based at Ninewells hospital, Dundee. This involved the use of a low power laser beam. (1.5mW helium-neon, wavelength 632.8nm).

All chromatography was performed using long thin columns. The silica 60, 70-230 mesh (63-200μm) was then solvated with the mobile phase of choice and thoroughly flushed dry prior to loading the crude material, which was pre-absorbed onto silica. Purification involving the use of hexane, albeit chromatography or crystallisation, required distillation of the solvent before use. This was due to NMR analysis showing trace amounts of unwanted hydrocarbon in ^{13}C spectra.

Characterisation by CI, EI and Electrospray mass spectroscopy was found to be too harsh for many of the compounds synthesised. Consequently, high resolution MALDI-TOF spectroscopy was routinely employed.

Thiols and *S*-nitroso- containing compounds were always subjected to Ellman's test[1] and the Griess test[2,3] (section 2.1), respectively. This was to ensure that only purities

greater than 95% were ever carried forward without the need for further crystallisation / chromatography. Even then, it was important to establish, by NMR, that any impurity was that of the corresponding disulphide. These two established colorimetric analyses proved very useful handles with which to ensure only high quality material was ever tested biologically.

6.2 Synthesis of *S*-Nitroso-1-thio-2,3,4,6-tetra-*O*-acetyl-β-D-glucopyranose, (SNAG) [5].

6.2.1 Preparation of 2,3,4,6-Tetra-*O*-acetyl-α-D-glucopyranosyl bromide[4] [1].

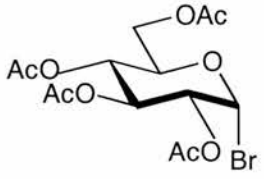

HBr/acetic acid (45%, 20ml) was added at room temperature and with stirring, to a closed system containing anhydrous glucose (20.0g, 0.11mol), in acetic anhydride (100ml). After 10 minutes, all of the solid material had dissolved to give a clear pale yellow solution. This indicated complete acetylation, which was confirmed by TLC analysis [R_f = 0.25, ethyl acetate : hexane, 2:3. Solvent front: 49mm]. To form the bromide a further addition of HBr/acetic acid (45%, 100ml) was made. Following a 17 hour period of stirring, the resulting clear yellow solution was concentrated, before being repeatedly co-evaporated with copious amounts of toluene (10 x 250ml). The red tar that formed was then dissolved in dichloromethane and washed thoroughly with 10% $NaHCO_3$ (3 x 250ml). After concentrating to a yellow oil, this was dissolved in diethyl ether (350ml), which was removed under suction, after filtering through a charcoal bed. A bright white crystalline solid (41.5g) was produced, giving a 91% yield, mp 85-86°C [lit.[5] 87-88°C], $[\alpha]_D^{25}$ +194.8° (c, 2.4 in chloroform) [lit.[6] $[\alpha]_D^{20}$ +197.8 (c, 2.4 in chloroform)], [R_f = 0.34, ethyl acetate : hexane, 2:3. Solvent front: 55mm]. δ_H(300MHz; $CDCl_3$) 2.02-2.12 (12H, 4x s, 4x CH_3CO), 4.15 (1H, dd, $J_{5,6a}$ 1.92, J_{gem} 12.36Hz, *H*-6(a)), 4.28-4.37 (2H, m, *H*-5 & *H*-6(b)), 4.86 (1H, dd, $J_{1,2}$ 3.85, $J_{2,3}$ 9.89Hz, *H*-2), 5.18 (1H, t, *J* 9.89Hz, *H*-3), 5.58 (1H, t, *J* 9.61Hz, *H*-4), 6.63 (1H, d, $J_{1,2}$ 3.85Hz, *H*-1). δ_C(75MHz; $CDCl_3$) 20.5, 20.6 & 20.7 (4x CH_3CO), 61.5 (*C*-6), 67.8, 70.3, 72.7 & 72.8 (*C*-2,3,4,5), 91.8 (*C*-1),

169.4, 169.6, 170.2 & 170.8 (4x *C*OCH$_3$). MALDI-TOF, M+Na 433 (+/- 3.5ppm).

6.2.2 Preparation of 2,3,4,6-Tetra-*O*-acetyl-*β*-D-glucopyranosyl isothiouronium bromide[7] [2].

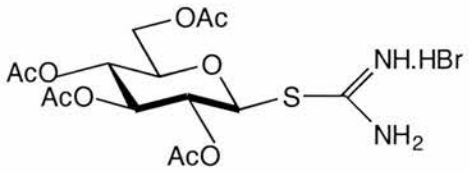

Under dry conditions, 2,3,4,6-tetra-*O*-acetyl-α-D-glucopyranosyl bromide [1] (6.90g, 16.8mmol) was added to 1.5 equivalents of thiourea (1.92g, 25.2mmol) in dry 2-propanol (45ml). After refluxing and stirring vigorously, for 15 minutes, a clear amber solution was produced. Upon standing at room temperature for 1.5 hours, a white crystalline solid formed. This was transferred to the refrigerator and left overnight, yielding 5.63g, 69% of the desired product, after washing with ice-cold 2-propanol (50ml). This material was recrystallised using the same solvent to give white crystals in 60% overall yield, mp 190-192°C [lit.[7] 205°C (from 2-propanol)], $[\alpha]_D^{25}$ -4.0 (c, 1 in water) [lit.[7] $[\alpha]_D^{23}$ -7.6 (c, 1.443 in water)]. δ_H(300MHz; D_2O) 2.11-2.18 (12H, 4x s, 4x C*H*$_3$CO), 4.24-4.29 (1H, ddd, $J_{5,6a}$ 2.47, $J_{5,6b}$ 4.39 & $J_{4,5}$ 9.89 Hz, *H*-5), 4.32 (1H, dd, $J_{5,6a}$ 2.47 & J_{gem} 12.91 Hz, *H*-6(a)), 4.44 (1H, dd, $J_{5,6b}$ 4.39, J_{gem} 12.90 Hz, *H*-6(b)), 5.26 (1H, t, $J_{2,3}$ 9.34 $J_{1,2}$ 9.89 Hz, *H*-2), 5.37 (1H, t, *J* 9.61 Hz, *H*-3/*H*-4), 5.49 (1H, t, *J* 9.61 Hz, *H*-3/*H*-4), 5.52 (1H, d, $J_{1,2}$ 9.89 Hz, *H*-1). δ_C(75MHz; D_2O) 18.1, 18.2 (4x *C*H$_3$CO), 59.9 (*C*-6), 65.6, 67.2, 71.4 & 73.9 (*C*-2,3,4,5), 79.2 (*C*-1), 165.5 (S-*C*(NH$_2$)NH.HBr), 170.4, 170.6, 171.0 & 171.6 (4x *C*OCH$_3$). MALDI-TOF, M+Na (-HBr) 429 (+/- 7.0ppm)

6.2.3 Preparation of 2,3,4,6-Tetra-*O*-acetyl-1-*S*-acetyl-1-thio-*β*-D-glucopyranose[8] [3].

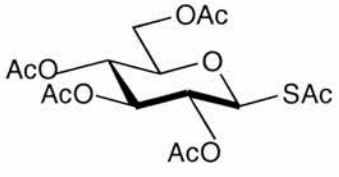

Four equivalents of potassium thioacetate (3.33g, 29.2mmol) with 2,3,4,6-tetra-*O*-acetyl-α-D-glucopyranosyl bromide [1] (3.00g, 7.30mmol), dissolved in dry acetone (100ml), was stirred as a closed system for 24 hours. After this time, TLC analysis showed one pink spot, indicative for the presence of sulfur. Dilution into

dichloromethane (100ml) was followed by aqueous washes, first with 10% $Na_2S_2O_3$ (250ml) and then with 10% Na_2CO_3 (2x 300ml). The red organic layer was then passed through a charcoal bed before being dried ($MgSO_4$) and concentrated to an orange oil (2.76g, 93%). This crude material was purified by column chromatography (distilled hexane : ethyl acetate, 2:1) to give a pink solid (1.97g, 66%) which was then successfully recrystallised from methanol. After filtering and washing with ice cold methanol, bright white crystals were obtained (1.103g, 37%), mp 119-120°C [lit.[8] 121°C (from methanol)], $[\alpha]_D^{25}$ +1.1° (c, 1 in 1,1,2,2-tetrachloroethane) [lit.[8] $[\alpha]_D^{25}$ +9.0°, +0.5° (c, 2,1 in 1,1,2,2-tetrachloroethane)], [R_f = 0.15, hexane : ethyl acetate, 2:1, solvent front: 55mm]. δ_H(300MHz; $CDCl_3$) 1.98-2.05 (12H, 4x s, 4x OCOC*H*$_3$), 2.36 (3H, s, SCOC*H*$_3$), 3.82 (1H, ddd, $J_{5,6a}$ 2.20, $J_{5,6b}$ 4.67, $J_{4,5}$ 9.90Hz, *H*-5), 4.08 (1H, dd, $J_{5,6a}$ 2.20, J_{gem} 12.64Hz, *H*-6(a)), 4.24 (1H, dd, $J_{5,6b}$ 4.67, J_{gem} 12.63Hz, *H*-6(b)), 5.09 (1H, t, *J* 9.61, *J* 9.89Hz, *H*-3/*H*-4), 5.10 (1H, dd, $J_{2,3}$ 9.06, $J_{1,2}$ 10.44Hz, *H*-2), 5.24 (1H, d, $J_{1,2}$ 10.7Hz, *H*-1), 5.25 (1H, t, *J* 8.79, *J* 9.33Hz, *H*-3/*H*-4). δ_C(75MHz; $CDCl_3$) 20.6 (3x OCO*C*H$_3$), 20.7 (OCO*C*H$_3$), 30.9 (SCO*C*H$_3$), 61.8 (*C*-6), 68.0, 69.1, 74.1 & 76.5 (*C*-2,3,4,5), 80.3 (*C*-1), 169.6 (2x O*C*OCH$_3$), 170.3 & 170.9 (O*C*OCH$_3$), 192.3 (S*C*OCH$_3$). MS (CI), M+1 407 (+/-2.0ppm).

6.2.4 Preparation of 1-Thio-2,3,4,6-tetra-*O*-acetyl-β-D-glucopyranose[8] [4].

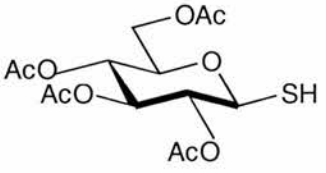

(a) 2,3,4,6-Tetra-*O*-acetyl-β-D-glucopyranosyl isothiouronium bromide [2] (2.00g, 4.10mmol), with 2 equivalents of potassium metabisulphite (1.825g, 8.20mmol), in water (25ml), was heated to reflux. The N_2 flushed system was then allowed to reflux for 5 minutes. After cooling, dichloromethane (100ml) was added. The organic layer was washed thoroughly with water and dried over $MgSO_4$. When concentrated a clear colourless oil was obtained (quantitative yield) which was crystallised and recrystallised from methanol, producing white crystals, 1.21g, 81% (from 2 crops), mp 113-114°C [lit.[8] mp 115°C], $[\alpha]_D^{25}$ +6.4° (c, 2.2 in chloroform) [lit.[8] $[\alpha]_D^{20}$ +5.8° (c, 2.2 in chloroform)], [R_f = 0.62, dichloromethane : methanol, 95:5, solvent front:

61mm]. ν_{max}/cm^{-1} 2587(w) (-SH) and 1740(br, s) (C=O). δ_H(300MHz; $CDCl_3$) 1.99-2.08 (12H, 4x s, 4x C*H*$_3$CO), 2.30 (1H, d, $J_{1,SH}$ 9.89Hz, S*H*) confirmed by D_2O, 3.71 (1H, ddd, $J_{5,6a}$ 2.20, $J_{5,6b}$ 4.67, $J_{4,5}$ 9.62Hz, *H*-5), 4.11 (1H, dd, $J_{5,6a}$ 2.20, J_{gem} 12.36Hz, *H*-6(a)), 4.24 (1H, dd, $J_{5,6b}$ 4.67, J_{gem} 12.36Hz, *H*-6(b)), 4.54 (1H, t, $J_{1,SH}$ 9.89Hz, *H*-1), 4.96 (1H, t, *J* 9.34Hz, *H*-3), 5.09 (1H, t, $J_{1,2}$ 9.89, $J_{2,3}$ 9.34Hz, *H*-2), 5.18 (1H, t, *J* 9.34Hz, *H*-4). δ_C(75MHz; $CDCl_3$) 20.6 & 20.8 (4x OCO*C*H$_3$), 62.1 (*C*-6), 68.3, 73.7 & 76.5 (*C*-2,3,4,5), 78.9 (*C*-1), 169.6, 169.9, 170.4 & 170.9 (4x O*C*OCH$_3$). MALDI-TOF, M+Na 387 (+/-8.0ppm).

(b) Under a nitrogen flushed environment, benzylamine (216μL, 1.97mmol) was added to 2,3,4,6-tetra-*O*-acetyl-1-*S*-acetyl-1-thio-*β*-D-glucopyranose [3] (400mg, 0.98mmol) in dry THF (10ml). The reaction was continually monitored by TLC and was halted after 1 hour due to the first indication of disulphide formation, [R_f 0.05, ethyl acetate : hexane, 2:3. Solvent front: 55mm]. After dilution with dichloromethane (125ml), successive washes with 1M HCl (100ml), 10% $NaHCO_3$ (100ml) and water (100ml) gave a yellow oil, in quantitative yield, upon drying ($MgSO_4$) and concentrating, [R_f 0.11, ethyl acetate : hexane, 2:3. Solvent front 55mm]. This material was passed through a long thin silica column (distilled hexane : ethyl acetate, 2:1) before being crystallised and recrystallised from ethanol. Characterisation of this white crystalline solid, 168mg, 47%, gave identical data to that recorded previously.

6.2.5 Preparation of *S*-Nitroso-1-thio-2,3,4,6-tetra-*O*-acetyl-*β*-D-glucopyranose, (SNAG) [5].

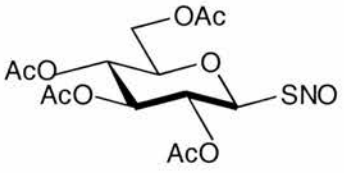

1-Thio-2,3,4,6-tetra-*O*-acetyl-β-D-glucopyranose [4] (75mg, 0.205mmol) was dissolved in HPLC grade ethanol (5ml). To this solution (41.2mM), under low light conditions, nitrous fumes were generated by reacting concentrated HCl with ground $NaNO_2$ in an adjacent flask. The orange solution produced was then filtered, under gravity, through dry potassium carbonate and then flushed for 4 minutes with nitrogen. The ethanol volume was corrected, to allow for any solvent evaporation,

before the compound was immediately stored in dry ice, with no light exposure. λ_{max}(EtOH:H_2O, 1:1)/nm 345.6 & 558.4 (ε/dm^3 mol^{-1} cm^{-1} 416.7 & 10.8 respectively). As for all *S*-nitrosothio-sugars, no correct Maldi-TOF data could be obtained for SNAG [5].

6.2.6 Preparation of 2,3,4,6,2',3',4',6'-Octa-*O*-acetyl-di-β,β'-D-glucopyranosyl disulphide[8,9] [6].

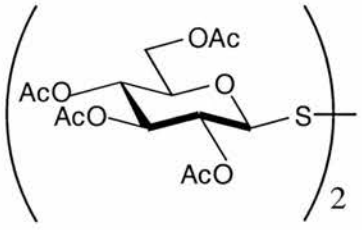

1-Thio-2,3,4,6-tetra-*O*-acetyl-β-D-glucopyranose [4] (400mg, 1.10mmol) in methanol (24ml) was stirred for 1 hour with 10% hydrogen peroxide (2ml). Following the addition of water (30ml) to initiate turbidity, the flask was left to stand in the refrigerator overnight. Upon standing, bright white needles formed, these were washed with ice cold water to give, 317mg, 80%, mp 142-3°C [lit.[8] 143-4°C], $[\alpha]_D^{25}$ -156.2° (c, 0.6 in chloroform) [lit.[8] $[\alpha]_D^{25}$ -160.3° +/-1.7° (c, 0.6 in chloroform)], [R_f 0.55, dichloromethane : methanol, 95:5. Solvent front: 60mm]. Loss of IR signals seen for thiol at ν_{max}/cm^{-1} 2587(w) (-SH) and 1740(br, s) (C=O), diagnostic of disulphide formation. δ_H(300MHz; $CDCl_3$) 1.99-2.11 (12H, 4x s, $COCH_3$), 3.77 (1H, ddd, $J_{5,6a}$ 2.20, $J_{5,6b}$ 4.39, $J_{4,5}$ 9.89Hz, *H*-5), 4.20 (1H, dd, $J_{5,6a}$ 2.20, J_{gem} 12.64Hz, *H*-6(a)), 4.32 (1H, dd, $J_{5,6b}$ 4.39, J_{gem} 12.63Hz, *H*-6(b)), 4.64 (1H, d, $J_{1,2}$ 9.61Hz, *H*-1), 5.08 (1H, t, *J* 9.34, *J* 9.89Hz, *H*-2/3/4), 5.17 (1H, t, *J* 9.34Hz, *H*-2/3/4), 5.25 (1H, t, *J* 9.06Hz, *H*-2/3/4). δ_C(75MHz; $CDCl_3$) 20.6 (2x $COCH_3$), 20.7 & 20.8 ($COCH_3$), 61.6 (*C*-6), 68.0, 69.8, 74.0 & 76.3 (*C*-2,3,4,5), 87.4 (*C*-1), 169.4, 169.5, 170.3 & 171.0 (4x $COCH_3$). MALDI-TOF, M+Na 749 (+/-1.73ppm).

6.3 Synthesis of *S*-Nitrosoglutathione (GSNO) [7], *S*-Nitrosothio-*N*-acetyl-DL-penicillamine (SNAP) [8], *S*-Nitrosothio-L-cysteine (SNOC) [9] and *S*-Nitrosothio-*N*-acetyl-L-cysteine (SNAC) [10].

6.3.1 Synthesis of *S*-Nitrosoglutathione, (GSNO)[10] [7].

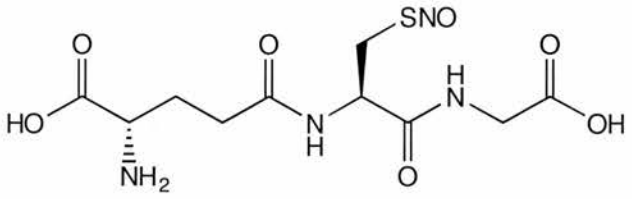

(a) To glutathione (2.5g, 8.13mmol) dissolved in 2M HCl (4ml), 1 equivalent of sodium nitrite (0.561g, 8.13mmol) was added, under reduced light conditions and at 5°C. A deep red solution was immediately observed upon the introduction of the nitrite. After stirring for 30 minutes a pink solid formed. At this stage acetone (16.5ml) was added to the system, which was then allowed to stir for a further 10 minutes. Having filtered the pink solid it was then washed with ice cold water (10ml), acetone (60ml) and ether (60ml), to give the titled compound in 57% yield (1.56g) [lit.[10] 76%], $[\alpha]_D^{25}$ +46.0° (c, 1.31 in H_2O) [lit.[8] $[\alpha]_D^{24}$ +47.0° (c 1.31 in H_2O)], λ_{max}(EtOH : H_2O, 1:1)/nm 336.0 & 545.6 (ε/dm^3 mol^{-1} cm^{-1} 841.2 & 29.6) [Lit.[10] λ_{max}(H_2O)/nm 335.0 & 545.0 (ε/dm^3 mol^{-1} cm^{-1} 922 & 15.9)].

(b) Under minimal light, glutathione (2.50g, 8.13mmol) was dissolved in a minimum volume of distilled water. Nitrous fumes from an adjacent flask were then introduced as in procedure 6.2.5. Water was removed on the freeze drier, yielding quantitatively, a red fluffy solid (2.74g, ~100%) with identical analytical data to the product from the literature protocol reported previously.

6.3.2 Synthesis of *S*-Nitrosothio-*N*-acetyl-DL-penicillamine, (SNAP)[11,12] [8].

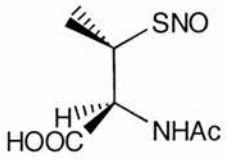

N-Acetyl-DL-penicillamine (1g, 5.23mmol) was dissolved in a minimum quantity of dry THF. The nitrous fuming method (section 6.2.5) was then performed. Upon concentrating this resulted in a green precipitate in quantitative yield, λ_{max}(EtOH : H_2O, 1:1)/nm 340.8 & 594.4 (ε/dm^3 mol^{-1} cm^{-1} 724.6 & 21.7) [lit.[11,12] λ_{max}(H_2O)/nm 590 (ε/dm^3 mol^{-1} cm^{-1} 12.4)].

6.3.3 Synthesis of *S*-Nitrosothio-L-cysteine, (SNOC) [9].

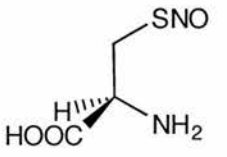

Water was added to L-cysteine (0.5g, 4.13mmol) until all of the thiol was in solution. After nitrosating (section 6.2.5) the water was removed on the freeze drier. The resulting precipitate was deep orange in colour. However, on exposure to air this decomposed dramatically, with the production of a brown, pungent gas, (presumably NO_2).

6.3.4 Synthesis of *S*-Nitrosothio-*N*-acetyl-L-cysteine, (SNAC) [10].

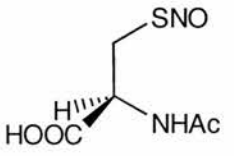

The nitrosation of *N*-acetyl-L-cysteine when dissolved in methanol, produced an intensely coloured orange solution which proved impossible to characterise due to stability problems similar to those outlined previously (section 6.3.3).

6.4 Synthesis of *S*-Nitroso-1-thio-2-acetamido-3,4,6-tri-*O*-acetyl-2-deoxy-β-D-glucopyranose, (SAGA.) [15].

6.4.1 Preparation of 2-Acetamido-3,4,6-tri-*O*-acetyl-2-deoxy-α-D-glucopyranosyl chloride[13] [11].

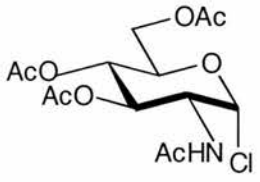

Originally, the HCl gas required to catalyse this reaction, was generated by reaction of concentrated H_2SO_4 and ammonium chloride moistened with concentrated HCl. This gas was then flushed through acetyl chloride, which was subsequently added to the reaction vessel. However, it was later observed that a better yield was obtained using a HCl gas cylinder.

N-Acetylglucosamine (20.0g, 90mmol) was added to acetyl chloride (40ml), in a HCl saturated atmosphere. With vigorous stirring and continuous HCl flushing, the mixture initially refluxed spontaneously. The HCl supply was removed after 15 minutes, but stirring at room temperature was continued for a total of 38 hours, during which time the progress of the reaction was followed continually by TLC (ethyl acetate : hexane, 2:1).

Work-up of the reaction involved dilution with dichloromethane (200ml). Ice (200g) and water (50ml) were then added with stirring. The organic layer, was then washed with more ice and saturated sodium bicarbonate solution (300ml). The resulting orange organic layer was dried ($MgSO_4$) and concentrated to 75ml, before sodium dried diethyl ether (300ml) was added with continuous swirling. Thirty seconds later, the formation of crystals was observed. The vessel was left closed for 12 hours, before the crystals were washed with dry diethyl ether (3 x 50ml). The fine beige crystals (23.61g, 72%) [lit.[13] 67-79%], were then dried under suction and stored over sodium hydroxide and phosphorus pentaoxide. TLC analysis highlighted traces of the corresponding hemiacetyl [R_f 0.14, ethyl acetate : hexane, 2:1. Solvent front: 57mm]. As a consequence, the product was purified using column chromatography (Gradient system, ethyl acetate : distilled hexane, 1:10 → 1:1), mp 125°C (from ethanol) [lit.[13] 127-128°C (from ethanol)], $[\alpha]_D^{25}$ +115.8 (c, 1 in chloroform) [lit.[13] $[\alpha]_D^{24}$ +110 (c, 1 in chloroform)], [R_f = 0.32, ethyl acetate : hexane, 2:1. Solvent

front: 57mm]. δ_H(300MHz; $CDCl_3$) 1.97-2.09 (12H, 4x s, 3x OCOCH_3 & 1x NCOCH_3), 4.10-4.14 (1H, m, *H*-6(a)), 4.24-4.35 (2H, m, *H*-5 & *H*-6(b)), 4.48-4.56 (1H, m, *H*-2), 5.20 (1H, t, *J* 9.7Hz, *H*-3/*H*-4), 5.32 (1H, t, *J* 9.9Hz, *H*-3/*H*-4), 5.83 (1H, br d, $J_{2,NH}$ 8.5Hz, N-*H*), 6.18 (1H, d, $J_{1,2}$ 3.85Hz, *H*-1). δ_C(75MHz; $CDCl_3$) 20.5, 20.6 (3x OCO*C*H_3), 23.0 (NCO*C*H_3), 53.5 (*C*-2), 61.2 (*C*-6), 67.0, 70.2 & 70.9 (*C*-3,4,5), 93.7 (*C*-1), 169.3, 170.3, 170.7 & 171.6 (3x O*C*OCH$_3$ & 1x N*C*OCH$_3$).

6.4.2 Preparation of 2-Acetamido-3,4,6-tri-*O*-acetyl-2-deoxy-β-D-glucopyranosyl isothiouronium chloride[7,14] [12].

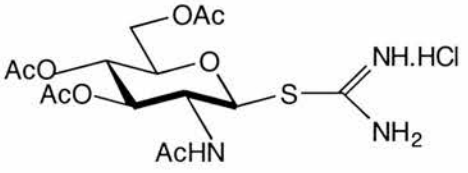

Using the same procedure as described in 5.2.2, 2-acetamido-3,4,6-tri-*O*-acetyl-2-deoxy-α-D-glucopyranosyl chloride [11] (4.0g, 10.9mmol), was added to 1.1 equivalents of thiourea (0.913g, 12.0mmol), in dry acetone (10ml). The system was allowed to reflux for 15 minutes and was then immersed in an ice bath for a further 15 minutes. A white precipitate was produced. This was filtered and thoroughly washed with ice cold acetone (200ml) to give a 70% yield (3.4g) of white crystals, [lit.[14] 82%], mp 174°C [lit.[14] mp 179-181°C (from methanol-acetone)], $[\alpha]_D^{25}$ -26.9° (c, 1.1 in methanol) [lit.[14] $[\alpha]_D^{22}$ -29.2 (c, 1.1 in methanol)]. δ_H(300MHz; D_2O) 2.04-2.17 (12H, 4x s, 3x OCOCH_3 & 1x NCOCH_3), 4.24 (1H, ddd, $J_{5,6a}$ 2.20, $J_{5,6b}$ 4.40, $J_{4,5}$ 9.90Hz, *H*-5), 4.32 (1H, dd, $J_{5,6a}$ 2.47, J_{gem} 12.63Hz, *H*-6(a)), 4.44 (1H, dd, $J_{5,6b}$ 4.39, J_{gem} 12.63Hz, *H*-6(b)), 4.82-5.22 (2H, m, *H*-2 & *H*-3/*H*-4), 5.40 (1H, t, *J* 9.61, *J* 9.89Hz, *H*-3/*H*-4), 5.49 (1H, d, $J_{1,2}$ 10.71Hz, *H*-1). δ_C(75MHz; D_2O) 18.0, 18.1, 18.2 & 19.9 (3x OCO*C*H_3 & 1x NCO*C*H_3), 49.8 (*C*-2), 60.0 (*C*-6), 66.0, 71.0, 73.8 (*C*-3,4,5), 80.1 (*C*-1), 165.8 (S*C*(NH_2)NH.HCl), 170.7, 171.0, 171.6 & 172.7 (3x O*C*OCH$_3$ & 1x N*C*OCH$_3$).

6.4.3 Preparation of 2-Acetamido-3,4,6-tri-*O*-acetyl-1-*S*-acetyl-2-deoxy-1-thio-β-D-glucopyranose[14] [13].

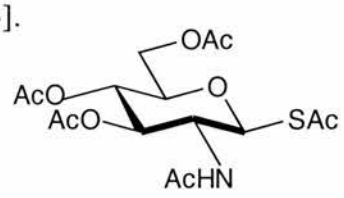

Into a stirred, closed system containing 2-acetamido-3,4,6-tri-*O*-acetyl-2-deoxy-α-D-glucopyranosyl chloride [11] (1.63g, 4.46mmol), in dry acetone (20ml), a four-fold excess of potassium thioacetate (2.03g, 17.8mmol) was added. The reaction was followed by TLC (dichloromethane : methanol, 95:5) and shown to be complete after 3 hours. Dilution of the reaction mixture in dichloromethane (150ml), followed by an aqueous wash (375ml), yielded a precipitate upon drying ($MgSO_4$) and concentrating (1.53g, 85%). The product was purified by column chromatography (dichloromethane : methanol, 95:5) followed by recrystallisation from distilled hexane : ethyl acetate. This resulted in fluffy white crystals in 35% yield, mp 188-196°C [lit.[14] mp 199-200°C (from methanol-ether), lit.[15] mp 196-7°C (from 2-propanol)], $[\alpha]_D^{25}$ -3° (c, 1 in chloroform) [lit.[14] $[\alpha]_D^{23}$ -2 +/-0.2° (c 1.29 in chloroform)], [R_f = 0.29, dichloromethane : methanol, 95:5. Solvent front: 53mm]. δ_H(300MHz; $CDCl_3$) 1.90 (3H, s, OCOCH_3), 2.00-2.06 (9H, 2x s, 2x OCOCH_3 & 1x NCOCH_3), 2.36 (3H, s, SCOCH_3), 3.78-3.80 (1H, m, *H*-5), 4.08 (1H, dd, $J_{5,6a}$ 1.92, J_{gem} 12.36Hz, *H*-6(a)), 4.23 (1H, dd, $J_{5,6b}$ 4.67, J_{gem} 12.36Hz, *H*-6(b)), 4.33-4.36 (1H, m, *H*-2), 5.10-5.17 (3H, m, *H*-1, *H*-3 & *H*-4), 5.80 (1H, br d, $J_{2,NH}$ 9.61Hz, N-*H*). δ_C(75MHz; $CDCl_3$) 20.4, 20.5, 20.6 (3x OCO*C*H_3), 23.0 (NCO*C*H_3), 30.7 (SCO*C*H_3), 52.1 (*C*-2), 61.8 (*C*-6), 67.8, 74.0, 76.5 (*C*-3,4,5), 81.6 (*C*-1), 169.3, 170.1, 170.8, 171.4 (3x O*C*OCH$_3$ & 1x N*C*OCH$_3$), 193.7 (S*C*OCH$_3$).

6.4.4 Preparation of 2-Acetamido-3,4,6-tri-*O*-acetyl-2-deoxy-1-thio-β-D-glucopyranose[9] [14].

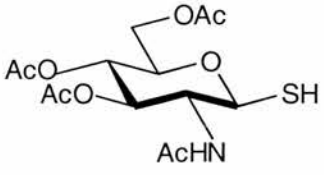

2-Acetamido-3,4,6-tri-*O*-acetyl-2-deoxy-β-D-glucopyranosyl isothiouronium chloride [12] (1.50g, 3.39mmol) was reacted with an excess of potassium metabisulphite (1.51g, 6.79mmol) in water (16.5ml). The reflux conditions and

duration were kept identical to that in section 6.2.4. After cooling and the addition of dichloromethane (50ml), the organic phase was washed with water (350ml) and dried ($MgSO_4$). Concentration gave a white solid product (0.61g, 50%), that could be recrystallised using ethanol, mp 151-152°C [lit.[15] mp 167-8°C (from ethyl acetate-petroleum ether)], $[\alpha]_D^{25}$ -12° (c, 0.9 in chloroform) [lit.[15] $[\alpha]_D^{25}$ -14.5° (c, 0.9 in $CHCl_3$)], [R_f = 0.30, dichloromethane : methanol, 95:5. Solvent front: 50mm]. ν_{max}/cm^{-1} 2555(w) (-SH), 1741(br, s) (C=O), 3322 (w, 2 bands) (-CONH-). δ_H(300MHz; $CDCl_3$) 1.98-2.09 (12H, 4x s, 3x OCOC*H*$_3$ & 1x NCOC*H*$_3$), 2.56 (1H, d, $J_{1,SH}$ 9.27Hz, S*H*), 3.68 (1H, ddd, $J_{5,6a}$ 2.22, $J_{5,6b}$ 4.64, $J_{4,5}$ 9.48Hz, *H*-5), 4.12 (1H, dd, $J_{5,6a}$ 2.22, J_{gem} 12.29Hz, *H*-6(a)), 4.13-4.18 (1H, m, *H*-2), 4.24 (1H, dd, $J_{5,6b}$ 4.83, J_{gem} 12.48Hz, *H*-6(b)), 4.57 (1H, t, *J* 9.67Hz, *H*-1/3/4), 5.07 (1H, t, *J* 9.47, *J* 9.87Hz, *H*-1/3/4), 5.12 (1H, t, *J* 9.67, *J* 9.27Hz, *H*-1/3/4), 5.59 (1H, br d, $J_{2,NH}$ 9.47Hz, N*H*). δ_C(75MHz; $CDCl_3$) 20.7, 20.8, 20.9 (OCO*C*H$_3$), 23.4 (NCO*C*H$_3$), 56.9 (*C*-2), 62.3 (*C*-6), 68.3, 73.6, 76.4 (*C*-3,4,5), 80.4 (*C*-1), 169.3, 170.5, 170.8, 171.3 (3x O*C*OCH$_3$ & 1x N*C*OCH$_3$). MALDI-TOF, M+Na 386 (+/-1.04ppm).

6.4.5 Preparation of *S*-Nitroso-1-thio-2-acetamido-3,4,6-tri-*O*-acetyl-2-deoxy-*β*-D-glucopyranose, (SAGA) [15].

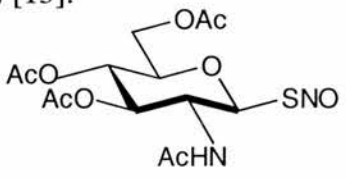

Using the methodology described in section 5.2.5, nitrous fumes were bubbled into a flask containing 2-acetamido-3,4,6-tri-*O*-acetyl-2-deoxy-1-thio-β-D-glucopyranose (75mg, 2.06 x 10^{-4}mol), dissolved in HPLC grade ethanol (5ml). The observed orange solution (quantitative yield) was filtered, flushed with nitrogen and stored as already reported. λ_{max}(EtOH:H_2O, 1:1)/nm 344.0 & 556.7 ($\varepsilon/dm^3\ mol^{-1}\ cm^{-1}$ 553.7 & 17.5).

6.5 Synthesis of *S*-Nitroso-1-thio-2-acetamido-3,4,6-tri-*O*-acetyl-2-deoxy-β-D-galactopyranose, (SAGAL) [20].

6.5.1 Preparation of 2-Acetamido-1,3,4,6-tetra-*O*-acetyl-2-deoxy-α-D-glucopyranose[16] [16].

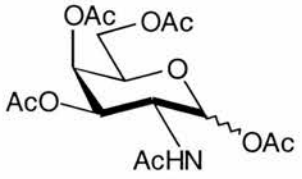

D-galactosamine hydrochloride (500mg, 2.32mmol) was left stirring at room temperature in acetic anhydride (2.5ml) and pyridine (5ml) for 20 hours. TLC analysis showed the reaction to be complete after this time. [R_f = 0.22, dichloromethane : methanol, 95:5. Solvent front: 52mm]. The mixture was co-evaporated with toluene (4x 50ml) to give a pink solid. This was dissolved in dichloromethane (50ml) and washed twice with 1M HCl (2x 100ml). After washing with 10% sodium carbonate (2x 100ml) the organic phase was dried ($MgSO_4$) and concentrated to a bright white solid, 650mg, 72% (second attempt gave 74%) [lit.[16] 55%], mp 236°C, $[\alpha]_D^{25}$ +20.5° (c, 0.4 in chloroform). δ_H(300MHz; $CDCl_3$) 1.94-2.17 (15H, 5x s, 4x OCOC*H*$_3$ & 1x NCOC*H*$_3$), 3.99-4.21 (3H, m, *H*-5, *H*-6(a) & *H*-6(b)), 4.44 (1H, dt, $J_{2,NH}$ 9.06, $J_{1,2}$ 9.27, $J_{2,3}$ 11.28Hz, *H*-2), 5.08 (1H, dd, $J_{3,4}$ 3.42, $J_{2,3}$ 11.28Hz, *H*-3), 5.32-5.43 (2H, m, *H*-4 & *H*-1), 5.70 (1H, br d, $J_{2,NH}$ 8.66Hz, N-*H*). δ_C(75MHz; $CDCl_3$) 20.7 (3x OCOC*H*$_3$), 20.9 (1x OCOC*H*$_3$), 23.3 (1x NCOC*H*$_3$), 49.8 (*C*-2), 61.3 (*C*-6), 66.3, 70.3, 71.9 (*C*-3,4,5), 93.0 (*C*-1), 169.5, 170.1, 170.2, 170.4, 170.7 (4x O*C*OCH$_3$ & 1x N*C*OCH$_3$). MALDI-TOF, M+Na 412 (+/-7.0ppm).

6.5.2 Preparation of 2-Acetamido-3,4,6-tri-*O*-acetyl-2-deoxy-α-D-galactopyranosyl chloride[17] [17].

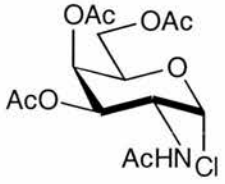

In an ice-water bath 2-acetamido-1,3,4,6-tetra-*O*-acetyl-2-deoxy-α-D-glucopyranose [16] (400mg, 1.03mmol) was dissolved in dry dichloromethane (210ml) and flushed vigorously with $HCl_{(g)}$ for 30 minutes. After flushing, the flask was firmly sealed and

transferred to the fridge. An aqueous wash with ice-cold water (2 x 250ml) and 10% sodium carbonate (250ml) was performed once the flask had stood at 4°C for 48 hours. Drying ($MgSO_4$) and concentrating gave a white solid, 349mg, 93% [lit.[17] 65%], mp 97-98°C (from ether) [lit.[17] mp 98-9°C (from ether), lit.[18] mp 131-6°C (from ethyl acetate-ether)], $[\alpha]_D^{25}$ +131.2° (c, 2 in chloroform) [lit.[17] $[\alpha]_D^{26}$ -12° (c, 2 in ether), lit.[18] $[\alpha]_D^{23}$ +134° +/-2 (c 2.09 in chloroform)]. δ_H(300MHz; $CDCl_3$) 1.99-2.05 (9H, 3x s, 3x OCOC*H*$_3$), 2.15 (3H, s, NCOC*H*$_3$), 4.08 (1H, dd, $J_{5,6a}$ 6.81, J_{gem} 11.42Hz, *H*-6(a)), 4.18 (1H, dd, $J_{5,6b}$ 6.37, J_{gem} 11.42Hz, *H*-6(b)), 4.48-4.53 (1H, m, *H*-2), 4.78-4.84 (1H, m, *H*-5), 5.28 (1H, dd, $J_{3,4}$ 3.30, $J_{2,3}$ 11.43Hz, *H*-3), 5.44-5.48 (1H, m, *H*-4), 5.76 (1H, br d, $J_{2,NH}$ 9.01Hz, N-*H*), 6.26 (1H, d, $J_{1,2}$ 3.74Hz, *H*-1 (100% α product)). δ_C(75MHz; $CDCl_3$) 20.7 (3x OCO*C*H$_3$), 23.2 (NCO*C*H$_3$), 49.4 (*C*-2), 61.2 (*C*-6), 66.7, 67.5, 70.0 (*C*-3,4,5), 95.2 (*C*-1), 170.3, 170.6 (3x O*C*OCH$_3$), 171.2 (N*C*OCH$_3$).

6.5.3 Preparation of 2-Acetamido-3,4,6-tri-*O*-acetyl-1-*S*-acetyl-2-deoxy-1-thio-*β*-D-galactopyranose [18].

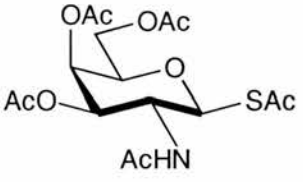

2-Acetamido-3,4,6-tri-*O*-acetyl-2-deoxy-*α*-D-galactopyranosyl chloride [17] (300mg, 8.20 x 10^{-4} mol) was dissolved in dry acetone (30ml) and stirred with 4 equivalents of potassium thioacetate (375mg, 3.28mmol). After 22 hours at room temperature, TLC analysis showed the reaction to be complete. [R_f = 0.11 (pink with charring), ethyl acetate : hexane, 2:1. Solvent front: 55mm]. Following the addition of dichloromethane (100ml) and an aqueous wash with 10% sodium carbonate (3 x 250ml), the organic layer was dried ($MgSO_4$) and concentrated to give a red/brown tar, 259mg, 78%. Column chromatography (ethyl acetate : distilled hexane, 2:1) gave a white solid, 114mg, 34% [lit.[19] 63%], mp 192°C [lit.[19] mp 197-8°C (from dichloromethane-diethyl ether)], $[\alpha]_D^{25}$ +13.5° (c, 1 in chloroform) [lit.[19] $[\alpha]_D^{20}$ +11.3° (c, 1 in chloroform)]. δ_H(300MHz; $CDCl_3$) 1.91-2.03 (9H, 3x s, 3x OCOC*H*$_3$), 2.15 (3H, s, NCOC*H*$_3$), 2.37 (3H, s, SCOC*H*$_3$), 3.98-4.03 (1H, m, *H*-6(a)), 4.04-4.14 (1H, m, *H*-5), 4.13 (1H, dd, $J_{5,6b}$ 6.87, J_{gem} 11.26Hz, *H*-6(b)), 4.50 (1H, q, *J* 10.77Hz, *H*-2), 5.06 (1H, dd, $J_{3,4}$ 3.30, $J_{2,3}$ 10.77Hz, *H*-3), 5.17 (1H, d, $J_{1,2}$

10.77Hz, *H*-1), 5.38 (1H, t, *J* 3.30Hz, *H*-4), 5.61 (1H, br d, $J_{2,NH}$ 9.89Hz, N-*H*). δ_C(75MHz; $CDCl_3$) 20.7 (3x $OCOCH_3$), 23.3 ($NCOCH_3$), 30.9 ($SCOCH_3$), 48.7 (*C*-2), 61.6 (*C*-6), 66.9, 71.1, 75.3 (*C*-3,4,5), 82.2 (*C*-1), 170.5, 170.7 (3x $OCOCH_3$), 171.0 ($NCOCH_3$), 194.1 ($SCOCH_3$). MALDI-TOF, M+Na 428 (+/-6.1ppm).

6.5.4 Preparation of 2-Acetamido-3,4,6-tri-*O*-acetyl-2-deoxy-1-thio-*β*-D-glucopyranose [19]. (Test reaction)

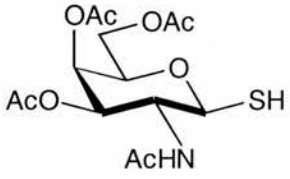

Under a nitrogen flushed environment, 2-acetamido-3,4,6-tri-*O*-acetyl-1-*S*-acetyl-2-deoxy-1-thio-*β*-D-galactopyranose [18] (31mg, 7.65 x 10^{-5}mol) dissolved in dry THF (5ml), was stirred with 2 equivalents of benzylamine (17μl, 1.53 x 10^{-4}mol). The reaction was followed at 5 minute intervals by TLC analysis. From plate intensity the reaction appeared to be 50% complete after 20 minutes. Upon adding a further equivalent of benzylamine (8.5μl, 7.65 x 10^{-5}mol) all starting material had reacted within 2 hours. Having diluted with dichloromethane (100ml) and washed successively with 1M HCl (200ml), 10% sodium hydrogen carbonate (200ml) and water (200ml), a clear, colourless oil was obtained upon drying ($MgSO_4$) and concentrating, (23mg, 83%). [R_f = 0.04, ethyl acetate : hexane, 3:1. Solvent front: 57mm]. Crude NMR showed: δ_H(300MHz; $CDCl_3$) 2.60 (1H, d, $J_{1,SH}$ 9.17Hz, S*H*). Low Resolution MALDI-TOF, M+Na 386.

6.6 Synthesis of *S*-Nitroso-1-thio-2,3,4,6-tetra-*O*-acetyl-*β*-D-galactopyranose, (SNAGAL) [25].

6.6.1 Preparation of 1,2,3,4,5-Penta-*O*-acetyl-*α*/*β*-D-galactopyranose[20] [21].

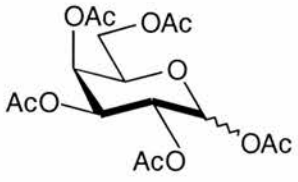

To a suspension of D-(+)-galactose (10g, 55.5mmol) in acetic anhydride (50ml), iodine (500mg, 4mmol) was added, whilst stirring under ice cold conditions. The reaction was followed by TLC and shown to be complete after 30 minutes. Isolation and purification of the product was possible upon the addition of the reaction mixture to an ice/water mixture (400ml), containing saturated sodium thiosulphate (50ml). With vigorous stirring the product precipitated out of solution. This was filtered and washed with further portions of ice cold water (1L), to give a white solid (19.15g, 88%), mp 94°C [lit.[21] 95.5°C for α-product, 142°C for β-product], $[\alpha]_D^{25}$ +100.3° (c, 1 in chloroform) [lit.[21] $[\alpha]_D^{20}$ +25°(β), +106.7°(α) (c, 1 in chloroform)], [R_f = 0.38, ethyl acetate : hexane, 1:1. Solvent front: 53mm]. α:β (93:7) δ_H(300MHz; $CDCl_3$) 2.00-2.04 (9H, 3x s, 3x OCOC*H*$_3$), 2.16 (6H, s, 2x OCOC*H*$_3$), 4.08-4.11 (2H, m, *H*-6(a) & *H*-6(b)), 4.34-4.39 (1H, m, *H*-5), 5.32-5.35 (2H, m, *H*-2 & *H*-3), 5.49-5.51 (1H, m, *H*-4), 5.70 (0.07H, d, $J_{1,2}$ 8.46Hz, *H*-1(β)), 6.36-6.39 (0.93H, m, *H*-1(α)). δ_C (75MHz; $CDCl_3$) 20.5, 20.6, 20.8 (5x OCO*C*H$_3$), 61.4 (*C*-6), 66.6, 67.5, 67.6, 68.9 (*C*-2,3,4,5), 89.9 (*C*-1(α)), 92.4 (*C*-1(β)), 169.2, 170.2, 170.5, 170.7 (5x O*C*OCH$_3$). MS(CI), M (-OAc) 331, MALDI-TOF, M+Na 413 (+/-9.20ppm).

6.6.2 Preparation of 2,3,4,6-Tetra-*O*-acetyl-*α*-D-galactopyranosyl bromide [22].

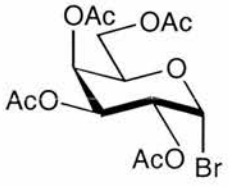

(a) Dissolved in dry dichloromethane (150ml), the crystalline material of 1,2,3,4,5-penta-*O*-acetyl-α/β-D-galactopyranose [21] (10.0g, 25.6mmol), generated previously

[section 6.6.1], was brominated using 45% HBr/acetic acid (50ml). Initially a large amount of heat was produced, therefore the stopper was periodically removed to allow the acidic fumes to escape. TLC analysis showed the reaction to be complete after 8.5 hours. This reaction time was reduced by nearly 3 hours when repeated on twice the scale reported here. Extraction from ice cold 10% sodium carbonate (3L in total) was repeated until a neutral pH was obtained. A clear yellow oil, in quantitative yield, resulted from drying ($MgSO_4$) and concentrating the organic layer. The addition of diethyl ether and distilled hexane afforded large white needles upon refrigeration (9.20g, 87%, from 2 crops), mp 83-84°C [lit.[22] mp 82-83°C (from petroleum ether)], $[\alpha]_D^{25}$ +224.1° (c, 1 in chloroform) [lit.[22] $[\alpha]_D^{20}$ +236.4° (c, 1 in chloroform)], [R_f = 0.49, ethyl acetate : hexane, 1:1. Solvent front: 54mm]. δ_H(300MHz; $CDCl_3$) 2.01-2.14 (12H, 4x s, 4x OCOC*H*$_3$), 4.10 (1H, dd, $J_{5,6a}$ 6.59, J_{gem} 11.26Hz, *H*-6(a)), 4.18 (1H, dd, $J_{5,6b}$ 6.32, J_{gem} 11.26Hz, *H*-6(b)), 4.48-4.54 (1H, m, *H*-5), 5.04 (1H, dd, $J_{1,2}$ 4.12, $J_{2,3}$ 10.44Hz, *H*-2), 5.40 (1H, dd, $J_{3,4}$ 3.57, $J_{2,3}$ 10.44Hz, *H*-3), 5.51-5.55 (1H, m, *H*-4), 6.69 (1H, d, $J_{1,2}$ 4.12Hz, *H*-1(α-product)). δ_C(75MHz; $CDCl_3$) 20.5, 20.6, 20.7 (4x OCO*C*H$_3$), 60.8 (*C*-6), 67.0, 67.8, 68.0, 71.1 (*C*-2,3,4,5), 88.2 (*C*-1), 169.9, 170.1, 170.2, 170.5 (4x O*C*OCH$_3$). MS(CI), M (-Br) 311.

(b) The one pot acetylation and bromination reaction (section 6.2.1) was applied to D-(+)-galactose (2g, 11.1mmol). On obtaining a clear solution after the initial addition of acetic anhydride (10ml) and HBr/acetic acid (45%, 2ml), a further addition of HBr/acetic acid (45%, 10ml) was made. The reaction was followed by TLC. After halting the reaction, co-evaporation with toluene (8x 200ml) generated a white solid. Crystallisation required cooling in diethyl ether and distilled hexane over a 24 hour period. The resulting large crystals (1.21g, 27%) were then washed in cold diethyl ether : distilled hexane, (1:1), mp 82-83°C [lit.[22] mp 82-83°C], $[\alpha]_D^{25}$ +222.4° (c, 1 in chloroform) [lit.[22] $[\alpha]_D^{20}$ +236.4° (c, 1 in chloroform)], [R_f = 0.51, ethyl acetate : hexane, 1:1. Solvent front: 53mm]. δ_H(300MHz; $CDCl_3$) & δ_C(75MHz; $CDCl_3$) as in section 6.6.2(a).

6.6.3 Preparation of 2,3,4,6-Tetra-*O*-acetyl-*β*-D-galactopyranosyl isothiouronium bromide[7] [23].

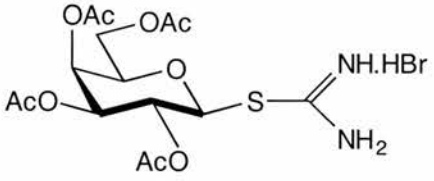

Using the method described by Bonner and Khan,[7] acetobromogalactose [22] (6.0g, 14.6mmol) was reacted with 1.5 equivalents of thiourea (1.67g, 21.9mmol) in dry 2-propanol (24ml). After refluxing for exactly 45 minutes, the reaction vessel was transferred to an ice-water bath. On addition of a few drops of hexane and with scratching, a white solid formed. This was filtered and washed with ice cold 2-propanol (30ml), to give the desired salt (3.48g, 49%, range in yield was 46-49% from 4 attempts), [lit.[7] 75%]. Using hot 2-propanol, the product was recrystallised, mp 161-162°C [lit.[7] mp 169.5°C (from 2-propanol)], $[\alpha]_D^{25}$ +19.6° (c, 1.56 in ethanol) [lit.[7] $[\alpha]_D^{25}$ +16° (c 1.56 in ethanol)]. Found: C, 36.85; H, 4.8; N, 5.5. $C_{15}H_{23}N_2O_9SBr$ requires C, 37.0; H, 4.8; N, 5.75%. δ_H(300MHz; D_2O) 2.08-2.28 (12H, 4x s, 4x CH_3CO), 4.31-4.35 (2H, m, *H*-6(a) & *H*-6(b)), 4.47-4.51 (1H, m, *H*-5), 5.39 (1H, dd, $J_{3,4}$ 3.02, $J_{2,3}$ 9.61Hz, *H*-3), 5.43-5.47 (1H, m, *H*-1), 5.55 (1H, t, $J_{2,3}$ 9.61, $J_{1,2}$ 9.89Hz, *H*-2), 5.63 (1H, t, *J* 3.02Hz, *H*-4). δ_C(75MHz; CD_3OD) 20.7, 20.9, 25.6 ($OCOCH_3$), 62.9 (*C*-6), 67.9, 68.9, 72.8, 77.1 (*C*-2,3,4,5), 83.2 (*C*-1), 170.0 (S-*C*(NH_2)NH.HBr), 171.4, 171.5, 171.8 & 172.3 (4x *C*OCH_3). MS(CI), M (-SC(NH_2)NH.HBr) 331.

6.6.4 Preparation of 1-Thio-2,3,4,6-tetra-*O*-acetyl-*β*-D-galactopyranose[23] [24].

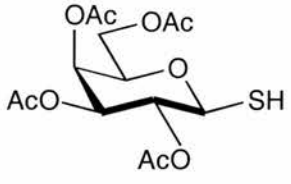

2,3,4,6-Tetra-*O*-acetyl-*β*-D-galactopyranosyl isothiouronium bromide [23] (1.0g, 2.05mmol) was refluxed under nitrogen, for 15 minutes, in water (12ml) containing 2 equivalents of potassium metabisulphite (0.912g, 4.10mmol). The reaction vessel was then cooled and the contents diluted with dichloromethane (30ml). After washing with water (100ml), the organic phase was dried ($MgSO_4$) and concentrated

to give a yellow oil, 0.623g, 83% [lit.[23] 94%]. TLC analysis showed a small percentage of disulphide [R_f = 0.25, dichloromethane : methanol, 95:5. Solvent front: 48mm], therefore the material was purified on a long dry silica column (dichloromethane : methanol, 95:5) as attempts to crystallise the material, as reported[23], were unsuccessful. Chromatography gave the pure product as a clear, colourless oil, 287mg, 38% [lit.[23] 71.6%]. The addition of diethyl ether with cooling, eventually gave a white solid, mp 82-83°C (from ether), [lit.[23] mp 83°C (from methanol)], $[\alpha]_D^{25}$ +11.6° (c 3.5 in chloroform) [lit.[23] $[\alpha]_D^{25}$ +11.3° (c 3.5 in chloroform)], [R_f = 0.70, dichloromethane : methanol, 95:5. Solvent front: 48mm]. δ_H(300MHz; $CDCl_3$) 1.99-2.17 (12H, 4x s, 4x OCOC*H*$_3$), 2.37 (1H, d, $J_{1,SH}$ 9.89Hz, S*H*), 3.92-3.97 (1H, m, *H*-6(a)), 4.12-4.15 (2H, m, *H*-6(b) & *H*-5), 4.54 (1H, t, $J_{1,2}$ 9.61, $J_{1,SH}$ 9.89Hz, *H*-1), 5.02 (1H, dd, $J_{3,4}$ 3.30, $J_{2,3}$ 10.17Hz, *H*-3), 5.19 (1H, dd, $J_{1,2}$ 9.61, $J_{2,3}$ 10.17Hz, *H*-2), 5.44-5.48 (1H, m, *H*-4). δ_C(75MHz; $CDCl_3$) 20.6, 20.7, 20.9 (4x OCO*C*H$_3$), 61.6 (*C*-6), 67.4, 71.0, 71.7, 75.1 (*C*-2,3,4,5), 79.4 (*C*-1), 170.1, 170.3, 170.5, 170.7 (4x O*C*OCH$_3$). MALDI-TOF, M+Na 387 (+/-2.84ppm).

6.6.5 Preparation of *S*-Nitroso-1-thio-2,3,4,6-tetra-*O*-acetyl-*β*-D-galactopyranose, (SNAGAL) [25].

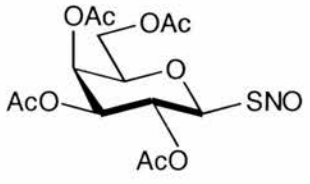

Using the nitrous fumes described earlier [section 6.2.5], 1-thio-2,3,4,6-tetra-*O*-acetyl-*β*-D-galactopyranose [24] (75mg, 2.06 x 10^{-4}mol) dissolved in ethanol (5ml), gave the characteristic orange solution in almost quantitative yield (according to Griess test). λ_{max}(EtOH:H_2O, 1:1)/nm 344.8 & 558.2 (ε/dm^3 mol^{-1} cm^{-1} 474.6 & 17.1).

6.6.6 Preparation of 2,3,4,6,2',3',4',6'-Octa-*O*-acetyl-di-β,β'-D-galactopyranosyl disulphide[24] [26].

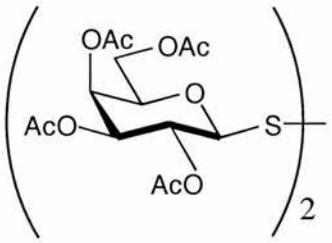

From a failed nitrosation step, the disulphide was obtained from 1-thio-2,3,4,6-tetra-*O*-acetyl-β-D-galactopyranose [24] (90mg, 2.47 x 10^{-4}mol) in dry dichloromethane (5ml). After bubbling through nitrous fumes, the orange solution was concentrated for 1 minute on the rotary evaporator. This resulted in a white powder in quantitative yield, 89.5mg, mp 72-4°C (from ethanol), $[\alpha]_D^{25}$ -117.0° (c, 0.6 in chloroform), [R_f = 0.25, dichloromethane : methanol, 95:5. Solvent front: 50mm]. δ_H(300MHz; $CDCl_3$) 1.99, 2.05, 2.09, 2.17 (12H, 4x s, 4x OCOCH_3), 4.03 (1H, dd, $J_{4,5}$ 0.96Hz, $J_{5,6}$ 7.24Hz, *H*-5), 4.11 (1H, dd, $J_{5,6a}$ 7.24, J_{gem} 10.62Hz, *H*-6(a)), 4.24 (1H, dd, $J_{5,6b}$ 7.24, J_{gem} 10.62Hz, *H*-6(b)), 4.58 (1H, d, $J_{1,2}$ 9.65Hz, *H*-1), 5.09 (1H, dd, $J_{3,4}$ 3.38, $J_{2,3}$ 10.13Hz, *H*-3), 5.36 (1H, t, *J* 10.13Hz, *H*-2), 5.45 (1H, dd, $J_{4,5}$ 0.96Hz, $J_{3,4}$ 3.37Hz, *H*-4). δ_C(75MHz; $CDCl_3$) 20.4, 20.5, 20.6, 20.7 (8x OCO*C*H_3), 60.8 (*C*-6), 66.9, 67.5, 71.7, 74.7 (*C*-2,3,4,5), 88.4 (*C*-1), 169.3, 169.9, 170.0, 170.2 (8x O*C*OCH$_3$). MALDI-TOF, M+Na 749 (+/-8.3ppm).

6.7 Synthesis of *S*-Nitroso-1-thio-2,3,4-tri-*O*-acetyl-β-D-xylo-pyranose, (D-SNAX) [30].

6.7.1 Preparation of 2,3,4-Tri-*O*-acetyl-α-D-xylopyranosyl bromide[4] [27].

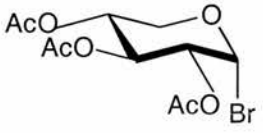

The one pot acetylation/bromination procedure,[4] already described [sections 6.2.1 & 6.6.2(b)], was applied to D-xylose (2g, 13,32mmol). Heat was generated after the initial addition of 45% HBr/acetic acid (2ml) in acetic anhydride (10ml), consequently the acetylation, characterised by all the sugar dissolving, only required

40 minutes of continuous stirring at room temperature. Having added the second portion of 45% HBr/acetic acid (10ml), the reaction was stirred for 17 hours before TLC analysis showed complete bromination. Co-evaporation with toluene (600ml in all) was followed by dilution into dichloromethane (50ml) and an aqueous wash with ice-cold water (200ml) and 10% sodium hydrogen carbonate (1L in all). Drying ($MgSO_4$) and concentrating gave a yellow oil, 4.30g, 95% (96% on second attempt). For crystallisation and recrystallisation diethyl ether was the solvent of choice, giving in 2 crops, 1.795g, 40% (51% on second attempt), mp 98-100°C [lit.[6] mp 101-2°C (from ether), lit.[25] mp 100-1°C (from ether) & lit.[26] mp 102°C (from ether)], $[\alpha]_D^{25}$ +216.3° (c, 2.4 in chloroform) [lit.[6] $[\alpha]_D^{20}$ +211.9° (c, 2.4 in chloroform)]. [R_f = 0.44, ethyl acetate : hexane, 1:1. Solvent front: 55mm]. δ_H(300MHz; $CDCl_3$) (100% α-product) 2.06-2.10 (9H, 3x s, 3x OCOCH_3), 3.88 (1H, t, $J_{4,5a}$ 10.99, J_{gem} 11.26Hz, *H*-5(a)), 4.06 (1H, dd, $J_{4,5b}$ 6.04, J_{gem} 11.26Hz, *H*-5(b)), 4.78 (1H, dd, $J_{1,2}$ 3.84, $J_{2,3}$ 9.88Hz, *H*-2), 5.00-5.09 (1H, m, *H*-4), 5.57 (1H t, *J* 9.89Hz, *H*-3), 6.58 (1H, d, $J_{1,2}$ 3.85Hz, *H*-1, α-product). δ_C(75MHz; $CDCl_3$) 20.6 (3x OCO*C*H_3), 62.5 (*C*-5), 68.1, 69.6, 70.9 (*C*-2,3,4), 87.6 (*C*-1), 169.9, 170.0 (3x O*C*OCH$_3$).

6.7.2 Preparation of 2,3,4-Tri-*O*-acetyl-β-D-xylopyranosyl isothiouronium bromide [28].

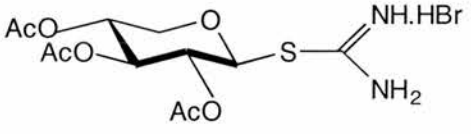

As previously described[7] [section 6.2.2, 6.4.2, & 6.6.4], acetobromo-D-xylose [27] (4.0g, 11.79mmol) with 1.5 equivalents of thiourea (1.35g, 17.69mmol) in dry 2-propanol (21ml) was refluxed. After 45 minutes the faintly brown reaction mixture was passed through a charcoal pad before being cooled and scratched with a trace amount of hexane to initiate turbidity. Crystallisation was not observed, however when re-dissolved in a minimum of hot 2-propanol, crystal formation at room temperature occurred promptly. Upon standing, for 1 hour, the title compound was filtered and washed with ice-cold 2-propanol to give 2.245g, 49%. Recrystallisation from 2-propanol gave 1.10g, 24% from 4 crops, mp 180°C [lit.[7] 181°C (from 2-propanol)], $[\alpha]_D^{25}$ -72.0° (c, 0.6 in ethanol) [lit.[7] $[\alpha]_D^{25}$ -71.5° (c, 0.587 in EtOH)]. δ_H(300MHz; CD_3OD) 2.05-2.09 (9H, 3x s, 3x OCOCH_3), 3.72 (1H, dd, $J_{4,5a}$ 7.91,

J_{gem} 12.01Hz, *H*-5(a)), 4.30 (1H, dd, $J_{4,5b}$ 4.69, J_{gem} 12.02Hz, *H*-5(b)), 5.01 (1H, ddd, $J_{4,5b}$ 4.69, $J_{3,4}$ 7.62, $J_{4,5a}$ 7.91Hz, *H*-4), 5.10 (1H, t, $J_{2,3}$ 7.33, $J_{1,2}$ 7.62Hz, *H*-2), 5.27 (1H, t, $J_{2,3}$ 7.33, $J_{3,4}$ 7.62Hz, *H*-3), 5.58 (1H, d, $J_{1,2}$ 7.62Hz, *H*-1). δ_C(75MHz; CD_3OD) 20.8, 20.85 (3x OCO*C*H_3), 66.3, 69.2, 70.2, 72.1 (*C*-2,3,4,5), 83.4 (*C*-1), 170.3 (S*C*(NH_2)NH.HBr), 171.2 (2x O*C*OCH_3), 171.6 (O*C*OCH_3). MALDI-TOF, M+Na (-HBr) 357 (+/-9.8ppm).

6.7.3 Preparation of 1-Thio-2,3,4-tri-*O*-acetyl-*β*-D-xylopyranose [29].

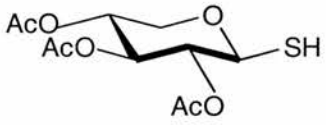

Following the hydrolysis protocol already described [section 6.2.2], 2,3,4-tri-*O*-acetyl-*β*-D-xylopyranosyl isothiouronium bromide [28] (1.0g, 2.41mmol) was dissolved in water (8ml) containing an equivalent of potassium metabisulphite (0.535g, 2.41mmol). After 15 minutes at reflux, with continuous nitrogen flushing, the mixture was cooled and diluted into dichloromethane (40ml). After washing with water (100ml), the organic layer was dried ($MgSO_4$) and concentrated to give a white solid, 0.691g, 98%. This was recrystallised from hot methanol, which having stood overnight in the refrigerator gave, in one crop, pure product, 400mg, 57%, mp 125°C [lit.[9] mp 123-9°C (from methanol)], $[\alpha]_D^{25}$ -13.1° (c, 0.54 in chloroform) [lit.[9] $[\alpha]_D^{25}$ -16.5° +/-2° (c, 0.542 in chloroform)], [R_f = 0.75, dichloromethane : methanol, 95:5. Solvent front: 58.5mm]. ν_{max}/cm^{-1} 2593(w) (-SH) and 1750(br, s) (C=O). δ_H(300MHz; $CDCl_3$) 2.03-2.075 (9H, 3x s, 3x OCOC*H*$_3$), 2.27 (1H, d, $J_{1,SH}$ 9.73Hz, S*H*) confirmed by D_2O, 3.38 (1H, dd, $J_{4,5a}$ 9.53, J_{gem} 11.56Hz, *H*-5(a)), 4.20 (1H, dd, $J_{4,5b}$ 5.27, J_{gem} 11.55Hz, *H*-5(b)), 4.58 (1H, dd, $J_{1,2}$ 8.71, $J_{1,SH}$ 9.52Hz, *H*-1), 4.90 (1H, t, *J* 8.71Hz, *H*-2), 4.99 (1H, dt, $J_{4,5b}$ 5.27, $J_{3,4}$ 8.92, $J_{4,5a}$ 9.53Hz, *H*-4), 5.16 (1H, t, *J* 8.71Hz, *H*-3). δ_C(75MHz; $CDCl_3$) 20.8, 20.9 (3x OCO*C*H_3), 66.4, 68.7, 72.5, 73.4 (*C*-2,3,4,5), 79.1 (*C*-1), 169.7, 169.8, 170.0 (3x O*C*OCH_3). MALDI-TOF, M+Na 315 (+/-4.10ppm).

6.7.4 Preparation of *S*-Nitroso-1-thio-2,3,4-tri-*O*-acetyl-*β*-D-xylopyranose, (D-SNAX) [30].

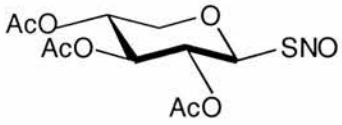

Using nitrous fumes [section 6.2.5] 1-thio-2,3,4-tri-*O*-acetyl-*β*-D-xylopyranose [29] (30.1mg, 1.03 x 10^{-4}mol) was nitrosated in ethanol (5ml) to give the characteristic orange solution (41.2mM), in quantitative yield (by Griess test). λ_{max}(EtOH:H_2O, 1:1)/nm 343.2 & 558.6 (ε/dm^3 mol^{-1} cm^{-1} 450.4 & 14.2).

6.8 Synthesis of *S*-Nitroso-1-thio-2,3,4-tri-*O*-acetyl-*β*-L-xylo-pyranose, (L-SNAX) [34].

6.8.1 Preparation of 2,3,4-Tri-*O*-acetyl-*α*-L-xylopyranosyl bromide [31].

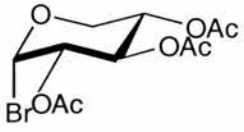

The titled compound was synthesised from the one pot acetylation/bromination procedure,[4] using, in the first instance, L-xylose (2.0g, 13.3mmol) combined with acetic anhydride (10ml) and 45% HBr/acetic acid (2ml). The second addition of 45% HBr/acetic acid (10ml) was possible after just 1 hour and 20 minutes, since a large amount of heat was produced during the initial stirring process, allowing complete acetylation to occur swiftly [R_f = 0.33, ethyl acetate : hexane, 2:3. Solvent front: 55mm]. On the basis of TLC analysis, the bromination was left overnight, before the mixture was co-evaporated with toluene (200ml), diluted in dichloromethane (100ml) and washed with ice-cold sodium hydrogen carbonate (2x 250ml). Drying ($MgSO_4$) and concentrating gave a yellow oil, containing crystals, in quantitative yield. The addition of diethyl ether enabled the isolation of a white crystalline material, 2.22g, 49.5% (from 2 crops), mp 94°C [lit.[27] 102°C (from ether)], $[\alpha]_D^{25}$ -209.4° (c, 3.5 in chloroform) [lit.[27] $[\alpha]_D^{23}$ -211.6° (c, 3.5 in chloroform)], [R_f = 0.46, ethyl acetate : hexane, 2:3. Solvent front: 52.5mm]. δ_H(300MHz; $CDCl_3$) 2.05, 2.09 (9H, 3x s, 3x OCOC*H*$_3$), 3.88 (1H, dt, $J_{4,5a}$ 10.77, J_{gem} 11.42Hz, *H*-5(a)), 4.05 (1H, dd, $J_{4,5b}$ 5.93, J_{gem} 11.42Hz, *H*-5(b)), 4.77 (1H, dd, $J_{1,2}$ 3.96, $J_{2,3}$ 9.89Hz, *H*-2), 5.04

(1H, ddd, $J_{4,5b}$ 5.93, $J_{3,4}$ 9.67, $J_{4,5a}$ 10.77Hz, *H*-4), 5.56 (1H, t, $J_{3,4}$ 9.67, $J_{2,3}$ 9.89Hz, *H*-3), 6.58 (1H, d, $J_{1,2}$ 3.96Hz, *H*-1, (α-product)). δ_C(75MHz; $CDCl_3$) 20.6 (3x $OCOCH_3$), 62.5 (*C*-5), 68.1, 69.6, 70.9 (*C*-2,3,4), 87.6 (*C*-1), 170.0 (3x $OCOCH_3$).

6.8.2 Preparation of 2,3,4-Tri-*O*-acetyl-β-L-xylopyranosyl isothiouronium bromide[9] [32].

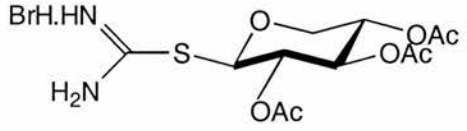

Using the Stanek protocol,[9] acetobromo-L-xylose [31] (2.10g, 6.20mmol) was refluxed with 1.5 equivalents of thiourea (0.708g, 9.30mmol) in dry acetone (5ml). Within 15 minutes, a large bright white solid had formed and therefore the reaction was halted and the flask was cooled. After washing with ice-cold acetone (50ml) the white solid (1.845g, 72%) was recrystallised in hot acetone (250ml) to give a pure crystalline product, 1.055g, 42% (from 3 crops), mp 154-5°C (from acetone), $[\alpha]_D^{25}$ +117.4° (c, 0.2 in methanol). δ_H(300MHz; CD_3OD) 2.05, 2.06, 2.09 (9H, 3x s, 3x $OCOCH_3$), 3.71 (1H, dd, $J_{4,5a}$ 8.20, J_{gem} 12.06Hz, *H*-5(a)), 4.29 (1H, dd, $J_{4,5b}$ 4.82, J_{gem} 12.06Hz, *H*-5(b)), 5.01 (1H, dt, $J_{4,5b}$ 4.82, $J_{3,4}$ 7.72, $J_{4,5a}$ 8.20Hz, *H*-4), 5.09 (1H, t, *J* 7.72Hz, *H*-2/*H*-3), 5.27 (1H, t, *J* 7.72Hz, *H*-2/*H*-3), 5.565 (1H, d, $J_{1,2}$ 7.72Hz, *H*-1). δ_C(75MHz; CD_3OD) 20.1 (3x $OCOCH_3$), 63.0 (*C*-5), 67.0, 68.2, 68.4 (*C*-2,3,4), 81.4 (*C*-1), 171.0 ($SC(NH_2)NH.HBr$), 172.2 (3x $OCOCH_3$). MALDI-TOF, M+Na (-HBr) 357 (+/-5.32ppm).

6.8.3 Preparation of 1-Thio-2,3,4-tri-*O*-acetyl-β-L-xylopyranose[9] [33].

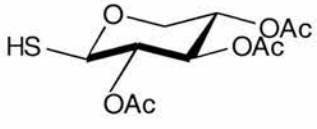

The thiouronium salt [32] (500mg, 1.20mmol) was refluxed in water (4ml) containing one equivalent of potassium metabisulphite (268mg, 1.20mmol) for 5 minutes. After this time, a white solid precipitated out of the clear, colourless solution. Dilution with dichloromethane (20ml) was followed by an aqueous wash (50ml). Drying ($MgSO_4$) and concentrating the organic phase gave a clear colourless oil. Using a minimum of hot methanol a white crystalline material was obtained. This

was washed with ice-cold methanol, 165mg, 47%, mp 122-4°C (from methanol), $[\alpha]_D^{25}$ +83.1° (c, 0.4 in chloroform), [R_f = 0.61, dichloromethane : methanol, 95:5. Solvent front: 51mm]. ν_{max}/cm^{-1} 2588(w) (-SH) and 1750(br, s) (C=O). δ_H(300MHz; $CDCl_3$) 2.04-2.08 (9H, 3x s, 3x OCOC*H*$_3$), 2.275 (1H, d, $J_{1,SH}$ 9.67Hz, S*H*), 3.38 (1H, dd, $J_{4,5a}$ 9.47, J_{gem} 11.69Hz, *H*-5(a)), 4.21 (1H, dd, $J_{4,5b}$ 5.24, J_{gem} 11.69Hz, *H*-5(b)), 4.57 (1H, dd, $J_{1,2}$ 8.86, $J_{1,SH}$ 9.67Hz, *H*-1), 4.91 (1H, t, $J_{2,3}$ 8.66, $J_{1,2}$ 8.86Hz, *H*-2), 4.99 (1H, dt, $J_{4,5b}$ 5.24, $J_{3,4}$ 8.87, $J_{4,5a}$ 9.47Hz, *H*-4), 5.165 (1H, t, $J_{2,3}$ 8.66, $J_{3,4}$ 8.86Hz, *H*-3). δ_C(75MHz; $CDCl_3$) 20.8, 20.9 (3x OCO*C*H$_3$), 66.4, 68.8, 72.5, 73.5 (*C*-2,3,4,5), 79.1 (*C*-1), 169.7, 169.8, 170.0 (3x O*C*OCH$_3$). MALDI-TOF, M+Na 315 (+/-5.40ppm).

6.8.4 Preparation of *S*-Nitroso-1-thio-2,3,4-tri-*O*-acetyl-*β*-L-xylopyranose, (L-SNAX) [34].

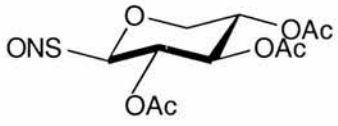

Using the nitrosation procedure outlined [section 6.2.5], an orange solution was obtained from 1-thio-2,3,4-tri-*O*-acetyl-*β*-L-xylopyranose [33] (30.1mg, 1.03 x 10^{-4}mol) dissolved in ethanol (2.5ml). λ_{max}(EtOH:H_2O, 1:1)/nm 344.6 & 557.6 ($\varepsilon/dm^3\ mol^{-1}\ cm^{-1}$ 460.4 & 12.1).

6.9 Synthesis of *S*-Nitroso-1-thio-2,3,4-tri-*O*-acetyl-*α*-D-arabinopyranose, (D-SNARB) [38].

6.9.1 Preparation of 2,3,4-Tri-*O*-acetyl-*β*-D-arabinopyranosyl bromide[4] [35].

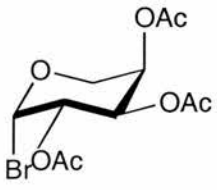

D-Arabinose (20.0g, 0.133mol) in acetic anhydride (100ml) and 45% HBr/acetic acid (20ml), completely dissolved after 35 minutes of stirring. TLC analysis confirmed complete acetylation, thus a second portion of HBr/acetic acid (100ml) was added. The bromination reaction was left for 22 hours before co-evaporation with toluene

(1L in all). The yellow oil that formed was diluted in dichloromethane (200ml) and washed with ice-water (500ml) and ice cold 10% sodium carbonate. After drying ($MgSO_4$) and concentrating, a yellow oil was still observed in quantitative yield. Addition of diethyl ether initiated crystallisation. This was then recrystallised from the same solvent (200ml). Following refrigeration over-night, white crystals were obtained after filtering and washing, 23.97g, 53.3%, mp 136-7°C [lit.[28] mp 139°C (from ether)], $[\alpha]_D^{25}$ -281.0° (c, 1 in chloroform) [lit.[28] $[\alpha]_D^{22}$ -283.4° (c, 1 in chloroform)], [R_f = 0.44, ethyl acetate : hexane, 1:1. Solvent front: 55mm]. δ_H(300MHz; $CDCl_3$) 2.02-2.14 (9H, 3x s, 3x OCOC*H*$_3$), 3.92 (1H, dd, $J_{4,5a}$ 1.92, J_{gem} 13.46Hz, *H*-5(a)), 4.20-4.26 (1H, m, *H*-5(b)), 5.05-5.11 (1H, m, $J_{1,2}$ 3.57Hz, *H*-2), 5.37-5.42 (2H, m, *H*-3 & *H*-4), 6.69 (1H, d, $J_{1,2}$ 3.57Hz, *H*-1 (β-product)). δ_C(75MHz; $CDCl_3$) 20.65, 20.8, 20.85 (3x OCO*C*H$_3$), 64.7 (*C*-5), 67.6, 67.8, 67.9 (*C*-2,3,4), 89.6 (*C*-1), 169.8, 170.0, 170.1 (3x O*C*OCH$_3$).

6.9.2 Preparation of 2,3,4-Tri-*O*-acetyl-α-D-arabinopyranosyl isothiouronium bromide[8] [36].

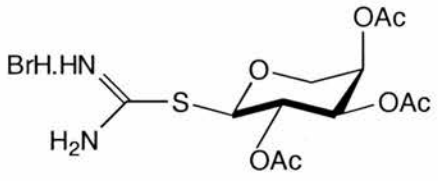

In dry acetone (8ml), 2,3,4-tri-*O*-acetyl-β-D-arabinopyranosyl bromide [35] (10.0g, 29.49mmol) was refluxed with one equivalent of thiourea (2.245g, 29.49mmol). A large amount of white material precipitated out of solution after 5 minutes. Reflux was continued for a further 10 minutes before the solid was filtered and washed with ice-cold acetone. The crude product was then dissolved in a minimum of hot ethanol[8] and then allowed to slowly cool to room temperature, giving a crystalline material, 6.875g, 56% (from 1 crop) [lit.[8] 50% yield], mp 172-4°C [lit.[8] mp 172°C (from ethanol)], $[\alpha]_D^{25}$ -29.5° (c, 2.1 in ethanol) [lit.[8] $[\alpha]_D^{25}$ -26.5 +/-0.8° (c 2.1 in ethanol)]. δ_H(300MHz; CD_3OD) 2.04-2.13 (9H, 3x s, 3x OCOC*H*$_3$), 4.00 (1H, dd, $J_{4,5a}$ 1.93, J_{gem} 13.03Hz, *H*-5(a)), 4.16 (1H, dd, $J_{4,5b}$ 4.34, J_{gem} 13.02Hz, *H*-5(b)), 5.25-5.375 (3H, m, *H*-2, *H*-3 & *H*-4), 5.50 (1H, d, $J_{1,2}$ 7.72Hz, *H*-1). δ_C(75MHz; CD_3OD) 20.5 (2x OCO*C*H$_3$), 20.7 (OCOC*H*$_3$), 67.3, 68.6, 71.1 (*C*-2,3,4,5), 83.2 (*C*-1), 170.2 (S*C*(NH$_2$)NH.HBr), 171.0, 171.05, 171.4 (3x O*C*OCH$_3$). MALDI-TOF, M+Na (-HBr) 357 (+/-9.0ppm).

6.9.3 Preparation of 1-Thio-2,3,4-tri-*O*-acetyl-α-D-arabinopyranose[8] [37].

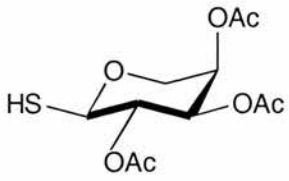

As reported by Cerny,[8] 2,3,4-tri-*O*-acetyl-α-D-arabinopyranosyl isothiouronium bromide [36] (2g, 4.816mmol) was refluxed with 1.3 equivalents of sodium sulphite (800mg, 6.35mmol) in water (25ml). By way of modifying this protocol, nitrogen gas was bubbled through the mixture continuously to try and preserve the thiol and prevent its oxidation. After a reaction time of 5 minutes the flask was submerged in an ice-water bath and diluted with dichloromethane (100ml). Washing with water (100ml) was followed by drying ($MgSO_4$) and concentrating the organic phase to a clear, colourless oil, 532mg, 38%. The recommended use of petroleum ether for crystallisation proved to be unsuccessful, as did the use of diethyl ether, methanol, ethanol and 2-propanol. Consequently column chromatography was employed (dichloromethane : methanol, 95:5) to obtain the desired compound still as an oil, 314mg, 22%, $[\alpha]_D^{25}$ +0.8° (c, 1.2 in chloroform) [lit.[8] $[\alpha]_D^{25}$ +2.2° +/-0.2° (c, 1.2 in chloroform)]. [R_f = 0.68 (charred red), dichloromethane : methanol, 95:5. Solvent front: 56mm], ν_{max}/cm^{-1} 2588(w) (-SH) and 1738(br, s) (C=O). δ_H(300MHz; $CDCl_3$) 2.02-2.14 (9H, 3x s, 3x OCOC*H*$_3$), 2.36 (1H, d, $J_{1,SH}$ 9.67Hz, S*H*), 3.68 (1H, dd, $J_{4,5a}$ 1.61, J_{gem} 13.09Hz, *H*-5(a)), 4.07 (1H, dd, $J_{4,5b}$ 3.22, J_{gem} 13.09Hz, *H*-5(b)), 4.56 (1H, dd, $J_{1,2}$ 8.46, $J_{1,SH}$ 9.67Hz, *H*-1), 5.04 (1H, dd, $J_{3,4}$ 3.42, $J_{2,3}$ 9.06Hz, *H*-3), 5.18 (1H, t, $J_{1,2}$ 8.46, $J_{2,3}$ 9.06Hz, *H*-2), 5.29 (1H, dt, $J_{4,5a}$ 1.61, $J_{4,5b}$ 3.22, $J_{3,4}$ 3.42Hz, *H*-4). δ_C(75MHz; $CDCl_3$) 20.9 (3x OCO*C*H$_3$), 67.2, 68.0, 70.9, 71.4 (*C*-2,3,4,5), 79.2 (*C*-1), 170.0, 170.2, 170.5 (3x O*C*OCH$_3$). MALDI-TOF, M+Na 315 (+/-7.9ppm).

6.9.4 Preparation of *S*-Nitroso-1-thio-2,3,4-tri-*O*-acetyl-α-D-arabinopyranose, (D-SNARB) [38].

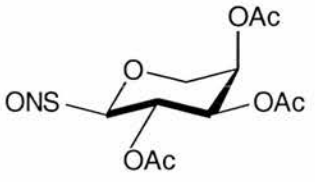

1-Thio-2,3,4-tri-*O*-acetyl-α-D-arabinopyranose [37] (30.1mg, 1.03 x 10^{-4}mol) dissolved in HPLC grade ethanol (2.5ml), was nitrosated by the reported procedure

[section 6.2.5]. λ_{max}(EtOH:H_2O, 1:1)/nm 343.5 & 558.6 (ε/dm^3 mol^{-1} cm^{-1} 461.7 & 12.4).

6.10 Synthesis of *S*-Nitroso-1-thio-2,3,4-tri-*O*-acetyl-α-L-arabinopyranose, (L-SNARB) [42].

6.10.1 Preparation of 2,3,4-Tri-*O*-acetyl-β-L-arabinopyranosyl bromide[4] [39].

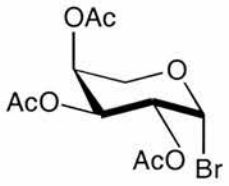

L-Arabinose (5.0g, 33.3mmol) stirred with acetic anhydride (25ml) and 45% HBr/acetic acid (5ml) gave a clear solution in under 1 hour, signifying the complete conversion to the penta-acetylated sugar. After the second portion of 45% HBr/acetic acid was introduced, the mixture was stirred for 24 hours. Co-evaporation with toluene (2x 250ml) was followed by dilution into dichloromethane (200ml) and an aqueous wash with ice-water (700ml in all) and then ice-cold 10% sodium carbonate (2x 250ml). Drying ($MgSO_4$) and concentrating gave an off-white solid. Crystallisation and recrystallisation was possible with a minimum of hot diethyl ether. Upon filtering and washing with ice-cold ether, white crystals were obtained, 4.85g, 43%, mp 135°C [lit.[28] mp 139°C (from ether)], $[\alpha]_D^{22}$ +278.2° (c, 1 in chloroform) [lit.[28] $[\alpha]_D^{22}$ +283.6° (c, 1 in chloroform)], [R_f = 0.44, ethyl acetate : hexane, 1:1. Solvent front: 55.5mm]. δ_H(300MHz; $CDCl_3$) 2.03-2.15 (9H, 3x s, 3x OCOCH_3), 3.93 (1H, dd, $J_{4,5a}$ 1.61, J_{gem} 13.29Hz, *H*-5(a)), 4.21-4.25 (1H, m, J_{gem} 13.29Hz, *H*-5(b)), 5.06-5.12 (1H, m, $J_{1,2}$ 3.83Hz, *H*-2), 5.38-5.43 (2H, m, *H*-3 & *H*-4), 6.70 (1H, d, $J_{1,2}$ 3.83Hz, *H*-1 (β-product)). δ_C(75MHz; $CDCl_3$) 20.7, 20.8, 20.9 (3x OCO*C*H_3), 64.8 (*C*-5), 67.7, 68.0, 68.1 (*C*-2,3,4), 89.8 (*C*-1), 170.0 (O*C*OCH$_3$), 170.3 (2x O*C*OCH$_3$).

6.10.2 Preparation of 2,3,4-Tri-*O*-acetyl-α-L-arabinopyranosyl isothiouronium bromide[8,29] [40].

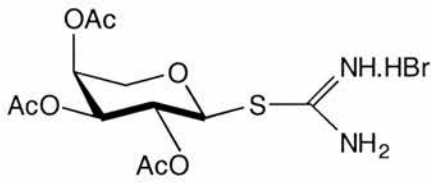

2,3,4-Tri-*O*-acetyl-β-L-arabinopyranosyl bromide [39] (4.0g, 11.8mmol) in dry acetone (5ml) was refluxed with 1.2 equivalents of thiourea (1.08g, 14.15mmol) for 5 minutes. The product quickly precipitated out of solution and therefore the reaction was cooled and the solid extracted. Crystallisation and recrystallisation in a minimum of hot ethanol (150ml) gave, after cooling and scratching, a white crystalline compound, 3.34g, 68% (from 2 crops), mp 162°C [lit.[29] mp 169-171°C (from acetone)], $[\alpha]_D^{25}$ + 3.9° (c, 1.3 in water) [lit.[29] $[\alpha]_D^{21}$ +8.8° (c, 1.3 in water)]. δ_H(300MHz; CD_3OD) 2.04, 2.115, 2.13 (9H, 3x s, 3x OCOCH_3), 4.00 (1H, dd, $J_{4,5a}$ 1.93, J_{gem} 13.03Hz, *H*-5(a)), 4.16 (1H, dd, $J_{4,5b}$ 4.34, J_{gem} 13.02Hz, *H*-5(b)), 5.27 (1H, dd, $J_{3,4}$ 3.38, $J_{2,3}$ 8.69Hz, *H*-3), 5.32 (1H, t, $J_{1,2}$ 7.72, $J_{2,3}$ 8.68Hz, *H*-2), 5.35-5.375 (1H, m, *H*-4), 5.50 (1H, d, $J_{1,2}$ 7.72Hz, *H*-1). δ_C(75MHz; CD_3OD) 20.5, 20.7 (3x OCO*C*H_3), 67.3, 68.6, 71.1 (*C*-2,3,4,5), 83.2 (*C*-1), 170.95, 171.05, 171.4 (3x O*C*OCH$_3$). Electrospray M^+(-Br) 335. MALDI-TOF, M+Na (-HBr) 357 (+/-2.0ppm).

6.10.3 Preparation of 1-Thio-2,3,4-tri-*O*-acetyl-α-L-arabinopyranose[8] [41].

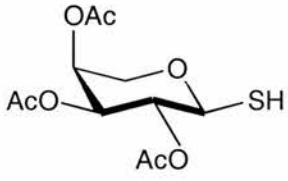

Based on the literature protocol used earlier [section 6.9.3], 2,3,4-tri-*O*-acetyl-α-L-arabinopyranosyl isothiouronium bromide [40] (1.20g, 2.89mmol) was refluxed, under nitrogen, in water (15ml) containing 1.3 equivalents of sodium sulphite (473mg, 3.76mmol). After heating for 5 minutes the reaction vessel was cooled and dichloromethane was added (125ml in all). After washing with water (125ml), the organic layer was dried ($MgSO_4$) and concentrated to give a yellow oil, 473mg, 56%. Due to difficulties in crystallising, the material was purified on a long dry silica column (dichloromethane : methanol, 95:5), giving a clear colourless oil, 264mg, 31%, $[\alpha]_D^{25}$ +31.5° (c, 2.2 in chloroform) [lit.[29] $[\alpha]_D^{20}$ +39.4° (c, 2.2 in chloroform)],

[R_f = 0.66 (charred red), dichloromethane : methanol, 95:5. Solvent front: 56mm], ν_{max}/cm^{-1} 2588(w) (-SH) and 1737(br, s) (C=O). δ_H(300MHz; $CDCl_3$) 2.02-2.14 (9H, 3x s, 3x OCOC*H*$_3$), 2.36 (1H, d, $J_{1,SH}$ 9.87Hz, S*H*), 3.68 (1H, dd, $J_{4,5a}$ 1.61, J_{gem} 13.09Hz, *H*-5(a)), 4.08 (1H, dd, $J_{4,5b}$ 3.22, J_{gem} 13.09Hz, *H*-5(b)), 4.56 (1H, dd, $J_{1,2}$ 8.46, $J_{1,SH}$ 9.87Hz, *H*-1), 5.04 (1H, dd, $J_{3,4}$ 3.42, $J_{2,3}$ 9.27Hz, *H*-3), 5.18 (1H, t, $J_{1,2}$ 8.46, $J_{2,3}$ 9.27Hz, *H*-2), 5.295 (1H, dt, $J_{4,5a}$ 1.61, $J_{4,5b}$ 3.22, $J_{3,4}$ 3.42Hz, *H*-4). δ_C(75MHz; $CDCl_3$) 21.0 (3x OCO*C*H$_3$), 67.2, 68.0, 70.9, 71.4 (*C*-2,3,4,5), 79.2 (*C*-1), 170.0 (3x O*C*OCH$_3$). MALDI-TOF, M+Na 315 (3.5ppm).

6.10.4 Preparation of *S*-Nitroso-1-thio-2,3,4-tri-*O*-acetyl-α-L-arabinopyranose, (L-SNARB) [42].

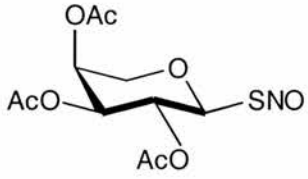

1-Thio-2,3,4-tri-*O*-acetyl-α-L-arabinopyranose [41] (30.1mg, 1.03 x 10^{-4}mol) dissolved in HPLC grade ethanol (2.5ml) was nitrosated by the method described [section 6.2.5]. λ_{max}(EtOH:H_2O, 1:1)/nm 343.1 & 558.0 (ε/dm^3 mol^{-1} cm^{-1} 453.3 & 11.0).

6.11 Synthesis of *S*-Nitroso-1-thio-2,2',3,3',4',6,6'-hepta-*O*-acetyl-4-*O*-(β-D-galactopyranosyl)-β-D-glucopyranose, (SNAL) [46].

6.11.1 Preparation of 2,2',3,3',4',6,6'-Hepta-*O*-acetyl-4-*O*-(β-D-galactopyranosyl)-α-D-glucopyranosyl bromide [43].

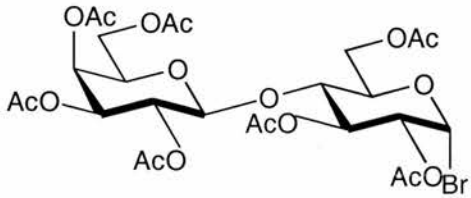

Using the procedure already outlined [section 6.2.1], D-lactose (5g, 5.48mmol) was initially acetylated (acetic anhydride (25ml) and 45% HBr/acetic acid (5ml)) and then brominated (45% HBr/acetic acid (25ml)). The first step required stirring overnight [R_f = 0.15, ethyl acetate : hexane, 1:1. Solvent front: 55mm] whilst the

second required 9 hours. After a toluene work-up (3x 200ml), a white solid formed (quantitative yield). This solid was then diluted in dichloromethane (75ml) and washed with ice-cold water (100ml) and 10% sodium hydrogen carbonate (100ml). Drying ($MgSO_4$) and concentrating again gave a white solid. Recrystallisation was possible using diethyl ether (250ml) alone, which after filtering and washing with ice-cold diethyl ether gave white crystals, 9.51g, 93%, mp 140-141°C [lit.[30] mp 141-2°C (from ethanol)], $[\alpha]_D^{25}$ +100.8° (c, 1 in chloroform) [lit.[31] $[\alpha]_D^{23}$ +108.7 (c, 1.01 in chloroform)], [R_f = 0.20, ethyl acetate : hexane, 1:1. Solvent front: 55mm]. ν_{max}/cm^{-1} 2573(w) (-SH) and 1746(br, s) (C=O). δ_H(300MHz; $CDCl_3$) 1.96-2.15 (21H, 7x s, 7x OCOCH_3), 3.86 (1H, t, *J* 9.67Hz, *H*-3/*H*-4), 3.88-3.91 (1H, m, *H*-5'), 4.08 (1H, dd, $J_{5,6a/6a'}$ 7.07, J_{gem} 11.20Hz, *H*-6(a)/*H*-6'(a)), 4.15 (1H, dd, $J_{5,6b/6b'}$ 6.60, J_{gem} 11.20Hz, *H*-6(b)/*H*-6'(b)), 4.15-4.21 (2H, m, *H*-6(a) & *H*-6(b)/ *H*-6'(a) & *H*-6'(b)), 4.47-4.51 (1H, m, *H*-5), 4.51 (1H, d, $J_{1',2'}$ 7.69Hz, *H*-1'), 4.76 (1H, dd, $J_{1,2}$ 4.17, $J_{2,3}$ 9.89Hz, *H*-2), 4.96 (1H, dd, $J_{3',4'}$ 3.52, $J_{2',3'}$ 10.33Hz, *H*-3'), 5.12 (1H, dd, $J_{1',2'}$ 7.91, $J_{2',3'}$ 10.55Hz, *H*-2'), 5.35 (1H, dd, $J_{4',5'}$ 1.10, $J_{3',4'}$ 3.52Hz, *H*-4'), 5.55 (1H, t, *J* 9.67Hz, *H*-3/*H*-4), 6.52 (1H, d, $J_{1,2}$ 4.17Hz, *H*-1). δ_C(75MHz; $CDCl_3$) 20.4, 20.6, 20.7 (OCO*C*H_3), 60.9, 61.1 (*C*-6,6'), 66.7, 69.1, 69.7, 70.8, 70.9, 71.0, 73.0, 75.0 (*C*-2,2',3,3',4,4',5,5'), 86.5 (*C*-1), 100.9 (*C*-1'), 169.1, 169.4, 170.1, 170.2, 170.3, 170.5 (7x *C*OCH$_3$).

6.11.2 Preparation of 2,2',3,3',4',6,6'-Hepta-*O*-acetyl-1-*S*-acetyl-1-thio-4-*O*-(*β*-D-galactopyranosyl)-*β*-D-glucopyranose[8,32] [44].

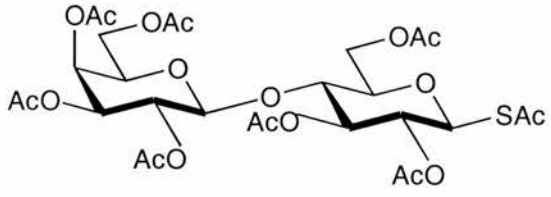

2,2',3,3',4',6,6'-Hepta-*O*-acetyl-4-*O*-(*β*-D-galactopyranosyl)-*α*-D-glucopyranosyl bromide [43] (2.0g, 2.86mmol) with four equivalents of potassium thioacetate (1.306g, 11.4mmol) was stirred at room temperature in acetone (25ml). After 12 hours TLC analysis showed that the reaction had gone to completion. Consequently the red reaction mixture was diluted into dichloromethane (150ml) and washed with water (250ml) before drying ($MgSO_4$) and concentrating to give an orange foam. The smell and colour of the product suggested the presence of thioacetic acid and so

column chromatography (ethyl acetate : distilled hexane, 1:1) was required. The desired compound was subsequently obtained as a yellow oil, 1.99g, quantitative yield [lit.[32] 81%], $[\alpha]_D^{25}$ +134.3° (c, 0.5 in chloroform), [R_f = 0.18 (charred red), ethyl acetate : hexane, 1:1. Solvent front: 55mm] [lit.[32] R_f = 0.17, ethyl acetate : hexane, 1:1]. δ_H(300MHz; $CDCl_3$) 1.94, 1.99, 2.015, 2.02, 2.08, 2.13 (21H, 7x s, 7x OCOCH_3), 2.34 (3H, 3x s, 3x SCOCH_3), 3.70-3.80 (2H, m, *H*-6(a) & (b)/*H*-6'(a) & (b)), 3.85 (1H, dt, $J_{4',5'}$ 0.88, $J_{5',6'}$ 7.03Hz, *H*-5'), 4.025-4.15 (3H, m, *H*-3/*H*-4 & *H*-6(a) & (b)/*H*-6'(a) & (b)), 4.40-4.45 (1H, m, *H*-5), 4.45 (1H, d, $J_{1',2'}$ 7.70Hz, *H*-1'), 4.92 (1H, dd, $J_{3',4'}$ 3.52, $J_{2',3'}$ 10.33Hz, *H*-3'), 5.015 (1H, dd, $J_{2,3}$ 9.23, $J_{1,2}$ 10.55Hz, *H*-2), 5.08 (1H, dd, $J_{1',2'}$ 7.70, $J_{2',3'}$ 10.55Hz, *H*-2'), 5.19 (1H, d, $J_{1,2}$ 10.55Hz, *H*-1), 5.23 (1H, t, *J* 8.57, *J* 9.01Hz, *H*-3/*H*-4), 5.32 (1H, dd, $J_{4',5'}$ 0.88, $J_{3',4'}$ 3.52Hz, *H*-4'). δ_C(75MHz; $CDCl_3$) 20.6 (7x OCO*C*H_3), 61.0, 62.1 (*C*-6,6'), 66.8, 69.1, 69.4, 70.9, 71.1, 73.8, 75.8, 77.3 (*C*-2,2',3,3',4,4',5,5'), 80.2 (*C*-1), 101.0 (*C*-1'), 169.2, 169.8, 170.3, 170.4, 170.55, 170.6 (7x O*C*OCH$_3$), 192.1 (S*C*OCH$_3$). Electrospray M^+ (+Na) 717. MALDI-TOF, M+Na 717 (+/-5.40ppm).

6.11.3 Preparation of 1-Thio-2,2',3,3',4',6,6'-hepta-*O*-acetyl-4-*O*-(*β*-D-galactopyranosyl)-*β*-D-glucopyranose [45].

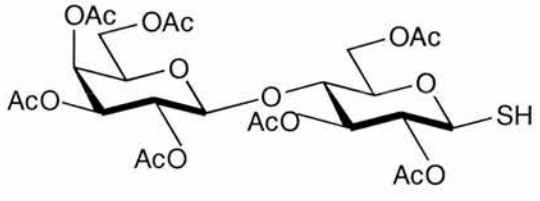

Under nitrogen conditions, 2,2',3,3',4',6,6'-hepta-*O*-acetyl-1-*S*-acetyl-1-thio-4-*O*-(*β*-D-galactopyranosyl)-*β*-D-glucopyranose [44] (500mg, 7.20 x 10^{-4}mol) dissolved in dry tetrahydrofuran (10ml) was stirred with two equivalents of benzylamine (157.5µl, 1.44mmol). The clear, lime coloured solution was monitored by TLC. Completion was observed after 4 hours and 15 minutes, thus the reaction was diluted into dichloromethane (100ml) and washed with 1M HCl (2x 100ml), 10% sodium carbonate (100ml) and water (100ml) as already described [section 6.2.4b]. A clear colourless oil (quantitative yield) was obtained after drying ($MgSO_4$) and concentrating. A long dry column of ethyl acetate : hexane (distilled), 1:1, gave an oil (276mg, 59%) of the same appearance as the crude product, $[\alpha]_D^{25}$ +3.8° (c, 0.51, in chloroform), [lit.[9] $[\alpha]_D^{25}$ +7.8° +/-2° (c, 0.51, in chloroform)], [R_f = 0.16 (charred

pink), ethyl acetate : hexane, 1:1. Solvent front: 55mm]. δ_H(300MHz; $CDCl_3$) 1.94, 2.02, 2.025, 2.04, 2.05, 2.11, 2.13 (21H, 7x s, 7x OCOC*H*$_3$), 2.24 (1H, d, $J_{1,SH}$ 9.61Hz, S*H*), 3.61 (1H, ddd, *J* 1.92, *J* 5.22, *J* 9.89Hz, *H*-5/*H*-5'), 3.78 (1H, t, *J* 9.06, *J* 9.89Hz, *H*-3/*H*-4), 3.85 (1H, t, $J_{1',2'}$ 7.70, $J_{2',3'}$ 6.59Hz, *H*-2'), 4.045 (1H, dd, *J* 4.67, J_{gem} 11.26Hz, *H*-6(a)/*H*-6'(a)), 4.06-4.10 (1H, m, *H*-3'), 4.12 (1H, dd, *J* 2.47, J_{gem} 11.26Hz, *H*-6(b)/*H*-6'(b)), 4.44-4.48 (1H, m, *H*-5/*H*-5'), 4.45 (1H, d, $J_{1',2'}$ 7.70Hz, *H*-1'), 4.51 (1H, t, *J* 9.89, *J* 9.61Hz, *H*-1/*H*-2), 4.86 (1H, t, *J* 9.61Hz, *H*-1/*H*-2), 4.93 (1H, dd, *J* 3.57, J_{gem} 10.44Hz, *H*-6(a)/*H*-6'(a)), 5.08 (1H, dd, *J* 7.97, J_{gem} 10.44Hz, *H*-6(b)/*H*-6'(b)), 5.16 (1H, t, *J* 9.34Hz, *H*-3/*H*-4), 5.33 (1H, dd, $J_{4',5'}$ 1.10, $J_{3,4}$ 3.30Hz, *H*-4'). δ_C(75MHz; $CDCl_3$) 20.6 (7x OCO*C*H$_3$), 60.9, 62.3 (*C*-6,6'), 66.7, 69.2, 70.8, 71.1, 73.6, 74.0, 76.1, 77.3 (*C*-2,2',3,3',4,4',5,5'), 78.5 (*C*-1), 101.2 (*C*-1'), 169.3, 169.8, 170.1, 170.2, 170.35, 170.6 (7x O*C*OCH$_3$). MALDI-TOF, M+Na 675 (+/-1.5ppm).

6.11.4 Preparation of *S*-Nitroso-1-Thio-2,2',3,3',4',6,6'-hepta-*O*-acetyl-4-*O*-(*β*-D-galactopyranosyl)-*β*-D-glucopyranose, (SNAL) [46].

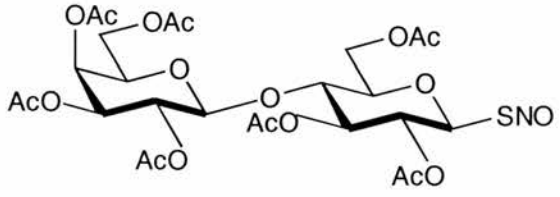

Using the procedure already outlined [section 6.2.5], 1-thio-2,2',3,3',4',6,6'-hepta-*O*-acetyl-4-*O*-(*β*-D-galactopyranosyl)-*β* -D-glucopyranose [45] (67.2mg, 1.03 x 10^{-4}mol) was nitrosated in HPLC grade ethanol (2.5ml) to give the desired orange solution. λ_{max}(EtOH:H_2O, 1:1)/nm 343.2 & 557.4 (ε/dm^3 mol^{-1} cm^{-1} 381.7 & 25).

6.12 Synthesis of *S*-Nitroso-1-thio-2,2',3,3',4',6,6'-Hepta-*O*-acetyl-4-O-(α-D-glucopyranosyl)-β-D-glucopyranose, (SNAM) [51].

6.12.1 Preparation of 2,2',3,3',4',6,6'-Hepta-*O*-acetyl-4-O-(α-D-glucopyranosyl)-α-D-glucopyranosyl bromide[4] [47].

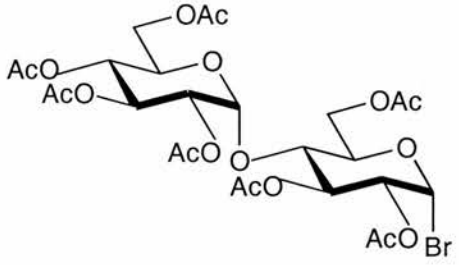

D-(+)-Maltose-monohydrate (5.0g, 13.88mmol) was subjected to the one pot synthesis already outlined (section 6.2.1). The acetylation and bromination required 2.5 and 4 hours respectively. Having co-evaporated with toluene (600ml in all) the yellow oil was diluted in dichloromethane (75ml) and was extracted from ice cold water (125ml). After washing with ice cold 10% sodium hydrogen carbonate (125ml), the organic layer was dried ($MgSO_4$) and concentrated. Crystallisation from diethyl ether was difficult, but upon evaporation a bright white solid was obtained (9.146g, 94%), mp 82-3°C [lit.[33,34] mp 84°C (from ligroin)], $[\alpha]_D^{25}$ +186.1° (c, 0.4 in chloroform) [lit.[33] $[\alpha]_D^{20}$ +180.1 (c, 0.387 in chloroform)], [R_f = 0.56 (after 3 runs), ethyl acetate : hexane, 1:1. Solvent front: 54.5]. δ_H(300MHz; $CDCl_3$) 1.985, 2.01, 2.02, 2.06, 2.075, 2.12 (21H, 7x s, 7x OCOC*H*$_3$), 3.93 (1H, dt, *J* 2.62, *J* 3.22, *J* 10.27Hz, *H*-5/*H*-5'), 4.06 (1H, dd, *J* 2.22, *J* 2.62, *J* 10.28Hz, *H*-5/*H*-5'), 4.20-4.275 (1H, m, *H*-6(a)/*H*-6'(a)), 4.23 (1H, t, *J* 9.88Hz, *H*-3/*H*-3'/*H*-4/*H*-4'), 4.235 (2H, dd, *J* 3.63, *J* 6.25, J_{gem} 12.30Hz, *H*-6(a)&(b)/*H*-6'(a)&(b)), 4.50 (1H, dd, *J* 3.63, J_{gem} 13.70Hz, *H*-6(b)/*H*-6'(b)), 4.695 (1H, dd, *J* 4.03, *J* 9.87Hz, *H*-2/*H*-2'), 4.85 (1H, dd, *J* 4.03, *J* 10.48Hz, *H*-2/*H*-2'), 5.05 (1H, t, *J* 9.67, *J* 10.07Hz, *H*-3/*H*-3'/*H*-4/*H*-4'), 5.35 (1H, dd, *J* 9.47, *J* 10.48Hz, *H*-3/*H*-3'/*H*-4/*H*-4'), 5.40 (1H, d, $J_{1',2'}$ 4.43Hz, *H*-1'), 5.59 (1H, t, *J* 9.27, *J* 9.67Hz, *H*-3/*H*-3'/*H*-4/*H*-4'), 6.48 (1H, d, $J_{1,2}$ 4.03Hz, *H*-1). δ_C(75MHz; $CDCl_3$) 20.6 (7x OCO*C*H$_3$), 61.45, 61.95 (*C*-6,6'), 68.05, 68.75, 69.4, 70.1, 71.1, 71.7, 72.45, 72.7 (*C*-2,2',3,3',4,4',5,5'), 86.2 (*C*-1), 95.9 (*C*-1'), 169.7, 169.75, 170.1, 170.5, 170.7, 170.9 (7x O*C*OCH$_3$).

The bromination step was stopped as soon as the TLC suggested the reaction was complete since the desired product can degrade to give acetobromoglucose. NMR

provided the diagnostic data to illustrate the presence of two different acetobromo-sugars when a toluene work-up was not immediately performed: 70% acetobromomaltose, δ_H(300MHz; $CDCl_3$) 6.50 (1H, d, $J_{1,2}$ 4.1Hz, *H*-1) and 30% acetobromoglucose, δ_H(300MHz; $CDCl_3$) 6.60 (1H, d, $J_{1,2}$ 4.1Hz, *H*-1). δ_C(75MHz; $CDCl_3$) 86.1, 86.6 (2x *C*-1), 95.9, (*C*-1').

6.12.2 Preparation of 2,2',3,3',4',6,6'-Hepta-*O*-acetyl-4-O-(α-D-glucopyranosyl)-β-D-glucopyranosyl isothiouronium bromide[9] [48].

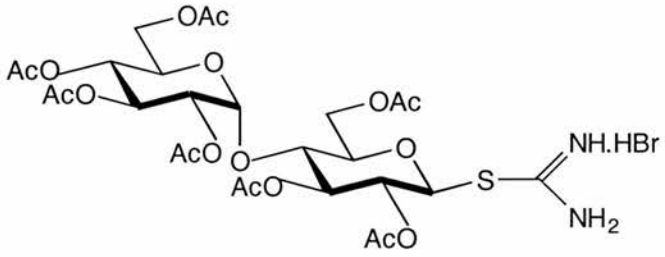

2,2',3,3',4',6,6'-Hepta-*O*-acetyl-4-O-(α-D-glucopyranosyl)-α-D-glucopyranosyl bromide [47] (3.0g, 4.29mmol) in dry acetone (3.5ml) was refluxed with a slight excess of thiourea (335mg, 4.405mmol). After 15 minutes the reaction flask was cooled in an ice-water bath. However, even with scratching the clear yellow solution gave no precipitate. Despite signs of turbidity an aqueous work-up was necessary. The water was then removed by co-evaporating with ethanol to give a white solid. This was crystallised from diethyl ether to give a white solid, 1.17g, 36% [lit.[9] 79.6%], δ_H(300MHz; D_2O) & δ_C(75MHz; D_2O) suggests a mixture of products and the presence of thiourea. MALDI-TOF, (Low Res.) M+Na (-HBr) 717.

6.12.3 Preparation of 2,2',3,3',4',6,6'-Hepta-*O*-acetyl-1-*S*-acetyl-1-thio-4-O-(α-D-glucopyranosyl)-β-D-glucopyranose [49].

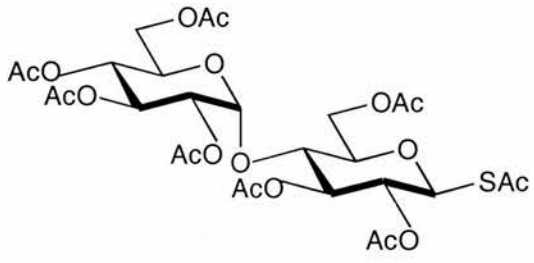

2,2',3,3',4',6,6'-Hepta-*O*-acetyl-4-O-(α-D-glucopyranosyl)-α-D-glucopyranosyl bromide [47] (2.568g, 3.67mmol) was stirred with four equivalents of potassium thioacetate (1.68g, 14.7mmol) in dry acetone (35ml), as already described [6.2.3].

After 12 hours TLC analysis showed the reaction to be complete. The bright orange reaction mixture was diluted in dichloromethane (150ml) and washed with 10% sodium carbonate (3x 250ml). Drying ($MgSO_4$) and concentrated to give an orange oil, 2.4g, 94%. Crude NMR showed the presence of thioacetic acid and so the compound was columned using the same solvent system as for the lactose derivative. Purification gave a white oil, 1.992g, 78%, $[\alpha]_D^{25}$ +143.1° (c, 0.5 in chloroform) [lit.[35] $[\alpha]_D^{20}$ +139° (c, 0.5 in chloroform)], [R_f = 0.50 (charred red), ethyl acetate : hexane, 1:1. Solvent front: 54.5mm. Run 3 times]. δ_H(300MHz; $CDCl_3$) 1.97, 1.98, 2.00, 2.03, 2.07, 2.10 (21H, 7x s, 7x OCOC*H*$_3$), 2.35 (3H, s, SCOC*H*$_3$), 3.80 (1H, ddd, $J_{5',6a'}$ 2.42, $J_{5',6b'}$ 3.96, $J_{4',5'}$ 9.89Hz, *H*-5'), 3.92 (1H, dt, $J_{5,6a}$ 2.42, $J_{5,6b}$ 3.52, $J_{4,5}$ 10.33Hz, *H*-5), 3.94 (1H, t, *J* 9.23Hz, *H*-3), 4.01 (1H, dd, $J_{5,6a}$ 2.42, J_{gem} 12.30Hz, *H*-6(a)), 4.18 (1H, dd, $J_{5',6a'}$ 2.42, J_{gem} 9.00Hz, *H*-6'(a)), 4.22 (1H, dd, $J_{5',6b'}$ 3.96, J_{gem} 8.57Hz, *H*-6'(b)), 4.42 (1H, dd, $J_{5,6b}$ 3.52, J_{gem} 12.31Hz, *H*-6(b)), 4.83 (1H, dd, $J_{1',2'}$ 4.17, $J_{2',3'}$ 10.55Hz, *H*-2'), 4.95 (1H, dd, $J_{2,3}$ 9.23, $J_{1,2}$ 9.01Hz, *H*-2), 5.03 (1H, t, $J_{3',4'}$ 9.67, $J_{4',5'}$ 9.89Hz, *H*-4'), 5.26 (1H, d, $J_{1,2}$ 9.01Hz, *H*-1), 5.275 (1H, dd, $J_{3,4}$ 9.23, $J_{4,5}$ 10.33Hz, *H*-4), 5.33 (1H, t, $J_{3',4'}$ 9.67, $J_{2',3'}$ 10.55Hz, *H*-3'), 5.37 (1H, d, $J_{1',2'}$ 4.17Hz, *H*-1'). δ_C(75MHz; $CDCl_3$) 20.6, 20.7, 20.8, 20.9 (7x OCO*C*H$_3$), 30.8 (SCO*C*H$_3$), 61.5, 62.8 (*C*-6,6'), 68.1, 68.7, 69.4, 69.9, 70.1, 72.7, 76.4, 76.7 (*C*-2,2',3,3',4,4',5,5'), 79.9 (*C*-1), 95.8 (*C*-1'), 169.7, 169.8, 170.1, 170.2, 170.7, 170.8 (7x O*C*OCH$_3$), 192.1 (S*C*OCH$_3$). Electrospray (Low Res.) M+Na 717. MALDI-TOF, M+Na 717 (+/-5.7ppm).

6.12.4 Preparation of 1-Thio-2,2',3,3',4',6,6'-Hepta-*O*-acetyl-4-O-(*α*-D-glucopyranosyl)-*β*-D-glucopyranose [50].

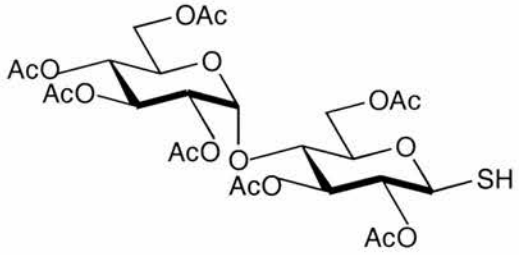

By the reported protocol [section 6.2.4(b)], 2,2',3,3',4',6,6'-hepta-*O*-acetyl-1-*S*-acetyl-1-thio-4-O-(*α*-D-glucopyranosyl)-*β*-D-glucopyranose [49] (400mg, 5.76 x 10^{-4}mol) was de-*S*-acetylated with 2 equivalents of benzylamine (126µl, 11.52 x 10^{-4}mol) in nitrogen flushed, dry, tetrahydrofuran (8ml). The reaction was halted

after 5 hours and 45 minutes. Work-up was as already described to give a clear, colourless oil (quantitative yield). Unlike previous procedures the pure product was retrieved by crystallisation and recrystallisation from ethanol rather than by column chromatography. Washing with ice-cold ethanol gave white crystals, 257mg, 68%, mp 149-152°C (from ethanol) [lit.[9] 149-152°C (from methanol), $[\alpha]_D^{25}$ +72.2° (c, 0.5 in chloroform), [lit.[9] $[\alpha]_D^{25}$ +78.5° +/-2° (c, 0.498 in chloroform)], [R_f = 0.14 (charred pink), ethyl acetate : hexane, 1:1. Solvent front: 54.5mm]. ν_{max}/cm^{-1} 2564(w) (-SH) and 1755(br, s) (C=O). δ_H(300MHz; $CDCl_3$) 1.98, 1.99, 2.01, 2.03, 2.035, 2.08, 2.14 (12H, 7x s, 7x OCOC*H*$_3$), 2.24 (1H, d, $J_{1,SH}$ 9.61Hz, S*H*), 3.68-3.74 (1H, m, *H*-5/*H*-5'), 3.89-3.94 (1H, m, *H*-5/*H*-5'), 3.99 (1H, t, $J_{3,4}$ 8.51, $J_{2,3}$ 9.89Hz, *H*-3), 4.03 (1H, dd, *J* 2.10, J_{gem} 12.09Hz, *H*-6(a)/*H*-6'(a)), 4.19 (1H, dd, *J* 4.39, J_{gem} 8.51Hz, *H*-6(a)/*H*-6'(a)), 4.23 (1H, dd, *J* 4.94, J_{gem} 8.51Hz, *H*-6(b)/*H*-6'(b)), 4.44 (1H, dd, *J* 2.20, J_{gem} 12.09Hz, *H*-6(b)/*H*-6'(b)), 4.575 (1H, t, $J_{1,SH}$ 9.61Hz, *H*-1), 4.79 (1H, t, $J_{3,4}$ 8.51, $J_{4,5}$ 9.34Hz, *H*-4), 4.84 (1H, dd, $J_{1',2'}$ 4.12, $J_{2',3'}$ 10.17Hz, *H*-2'), 5.03 (1H, t, $J_{1,2}$ 9.61, $J_{2,3}$ 9.89Hz, *H*-2), 5.23 (1H, t, $J_{4',5'}$ 8.79, $J_{3',4'}$ 9.89Hz, *H*-4'), 5.34 (1H, t, $J_{3',4'}$ 9.89, $J_{2',3'}$ 10.16Hz, *H*-3'), 5.39 (1H, d, $J_{1',2'}$ 4.12Hz, *H*-1'). δ_C(75MHz; $CDCl_3$) 20.5, 20.8 (7x OCO*C*H$_3$), 61.5, 63.0 (*C*-6,6'), 68.0, 68.6, 69.3, 70.0, 72.7, 74.4, 76.1, 76.6 (*C*-2,2',3,3',4,4',5,5'), 78.3 (*C*-1), 95.7 (*C*-1'), 169.6, 170.0, 170.1, 170.2, 170.6, 170.7 (7x O*C*OCH$_3$). MALDI-TOF, M+Na 675 (+/-5.8ppm).

6.12.5 Preparation of *S*-Nitroso-1-thio-2,2',3,3',4',6,6'-Hepta-*O*-acetyl-4-O-(*α*-D-glucopyranosyl)-*β*-D-glucopyranose, (SNAM) [51].

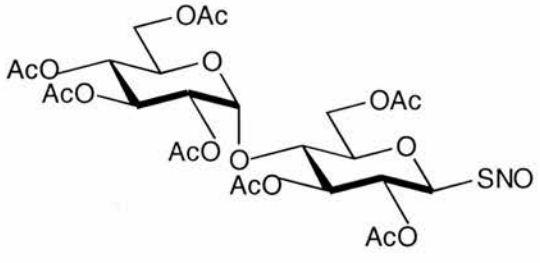

Due to solubility problems in ethanol, a lower concentration of 1-thio-2,2',3,3',4',6,6'-hepta-*O*-acetyl-4-O-(*α*-D-glucopyranosyl)-*β*-D-glucopyranose [50] (22.4mg, 3.43 x 10^{-5}mol, in ethanol (10ml)) was nitrosated using the procedure already described [section 6.2.5]. λ_{max}(EtOH:H_2O, 1:1)/nm 345.6 & 558.0 (ε/dm^3 mol^{-1} cm^{-1} 675.0 & 39.8).

6.13 Synthesis of *S*-Nitroso-1-thio-2,3,4,6-tetra-*O*-propionyl-*β*-D-glucopyranose, (SNO-PROP) [59].

6.13.1 Preparation of 1,2,3,4,6-Penta-*O*-propionyl-*α*/*β*-D-glucopyranose[20] [52].

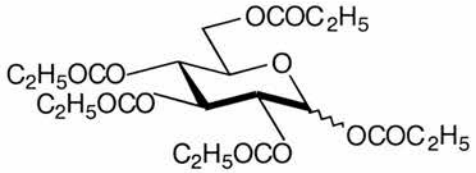

A catalytic amount of iodine (250mg, 9.85 x10^{-4}mol) was added to D-glucose (5.0g, 27.75mmol) in an excess of propionic anhydride (25ml), this initially generated a lot of heat. TLC analysis showed the reaction to be complete after 5 hours. The reaction mixture was poured onto a vigorously stirred solution of crushed ice (400ml) containing sodium thiosulphate (10ml). The product formed an oil rather then a solid so consequently an aqueous wash of 10% sodium carbonate (125ml) with dichloromethane (500ml) was necessary. The organic layer was then dried ($MgSO_4$) and concentrated to give a yellow oil in greater than quantitative yield due to the unreacted excess of propionic anhydride. Co-evaporation with toluene (200ml), on the cold finger, removed some of the anhydride, however column chromatography was essential for full purity (ethyl acetate : distilled hexane, 1:3). Crystallisation with diethyl ether and separately with ethanol : water (95:5) was unsuccessful, therefore the product remained as a lime coloured viscous oil, in quantitative yield. $[\alpha]_D^{25}$ +15.1° (c, 3.95 in chloroform), [lit.[36] $[\alpha]_D^{25}$ +14.29° (c, 3.955 in chloroform)]. [R_f = 0.50, ethyl acetate : hexane, 2:3. Solvent front : 55.5mm]. δ_H(300MHz; $CDCl_3$) 1.03 (6H, t, *J* 7.65Hz, 2x $OCOCH_2CH_3$), 1.05 (3H, t, *J* 7.45, *J* 7.65Hz, $OCOCH_2CH_3$), 1.09 (3H, t, *J* 7.45, *J* 7.65Hz, $OCOCH_2CH_3$), 1.15 (3H, t, *J* 7.45, *J* 7.65Hz, $OCOCH_2CH_3$), 2.21, 2.22, 2.25, 2.32 (8H, 4x q, *J* 7.65Hz, 4x $OCOCH_2CH_3$), 2.40 (2H, q, *J* 7.45Hz, $OCOCH_2CH_3$), 4.03-4.10 (2H, m, *H*-5, *H*-6(a)), 4.22 (1H, dd, $J_{5,6b}$ 4.50, J_{gem} 12.37Hz, *H*-6(b)), 5.07 (1H, dd, $J_{1,2}$ 3.63, $J_{2,3}$ 10.28Hz, *H*-2), 5.115 (1H, t, $J_{3,4}$ 10.07, $J_{2,3}$ 10.28Hz, *H*-3), 5.45 (1H, t, $J_{3,4}$ 9.87Hz, *H*-4), 5.70 (0.1H, d, $J_{1,2}$ 8.06Hz, *H*-1(β)), 6.30 (0.9H, d, $J_{1,2}$ 3.83Hz, *H*-1(α)). δ_C(75MHz; $CDCl_3$) 8.75, 8.8, 8.9, 9.0 (5x $OCOCH_2CH_3$), 27.1, 27.2, 27.4 (5x $OCOCH_2CH_3$), 61.3 (*C*-6), 67.65, 69.2, 69.7, 70.0 (*C*-2,3,4,5), 89.0 (*C*-1(β)), 91.75 (*C*-1(α)), 172.4, 173.0, 173.1, 173.7, 174.1 (5x $OCOCH_2CH_3$). MALDI-TOF, M+Na 483.18 (7.0ppm).

6.13.2 Preparation of 2,3,4,6-tetra-*O*-propionyl-α-D-glucopyranosyl chloride[17] [53].

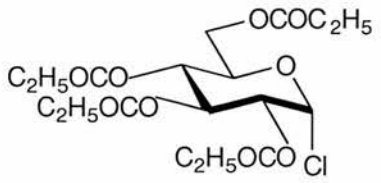

(a) 1,2,3,4,6-Penta-*O*-propionyl-α/β-D-glucopyranose [52] (3.07g, 6.67mmol) in dry diethyl ether (35ml) was flushed for 20 minutes with HCl fumes. The system was vented through anhydrous calcium chloride during this period of flushing. After 20 minutes, the system was sealed with film and the flask was submerged in ice-water. TLC analysis (ethyl acetate : hexane, 1:3 & 2:3) was inconclusive, so after sitting at 0°C for 12 hours, the reaction was halted by dilution into diethyl ether (100ml). This was then washed with ice/water (2x 250ml) followed by one wash with 10% sodium carbonate (250ml). The organic phase was dried ($MgSO_4$) and concentrated to give a clear, colourless oil in quantitative yield. The R_f of the product matched that of the starting material. ^1H and ^{13}C nmr analysis also showed the compound to still be the fully propionylated sugar. Diagnostic data: δ_H(300MHz; $CDCl_3$) 1.025 (15H, 5x t, *J* 7.5Hz, 5x $OCOCH_2CH_3$), 2.19-2.46 (10H, m, 5x $OCOCH_2CH_3$), 6.32 (1H, d, $J_{1,2}$ 3.74Hz, *H*-1(α)). δ_C(75MHz; $CDCl_3$) 89.1 (*C*-1), 172.5, 173.05, 173.2, 173.8, 174.3 (5x $OCOCH_2CH_3$).

(b) The reaction was repeated using dry dichloromethane (as in section 6.5.2) and the reaction time was extended to 48 hours. However after an aqueous work-up identical to that described here, the starting material was again retrieved in quantitative yield.

6.13.3 Preparation of Methyl 2,3,4,6-tetra-*O*-propionyl-1-thio-β-D-gluco-pyranoside[37] [54].

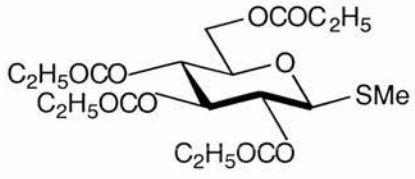

To 1,2,3,4,6-Penta-*O*-propionyl-α/β-D-glucopyranose [52] (460.5mg, 1mmol) in dry dichloromethane (4ml), iodine (305mg, 1.2mmol), hexamethyldisilane (104µl, 0.51mmol) and methyl disulphide (46µl, 0.51mmol) were added, in that order. The

mixture was stirred at room temperature. TLC analysis (dichloromethane : acetone, 97:3) suggested the reaction to be complete after 1 hour and 45 minutes. After dilution into dichloromethane (100ml) the reaction was washed with 10% sodium thiosulphate (150ml) and 10% sodium carbonate (100ml), before a final wash with water (100ml). Drying ($MgSO_4$) and concentrating gave a clear, pale yellow oil. Due to by-products, the yield was more than quantitative. This was confirmed by crude nmr. As a result the material was columned (dichloromethane : acetone, 97:3). This gave the pure product as a clear, colourless oil, 383mg, 88%, $[\alpha]_D^{25}$ +52.9° (c, 0.4 in chloroform), [R_f = 0.57 (chars pink), dichloromethane : acetone, 97:3. Solvent front: 53.5mm]. δ_H(300MHz; $CDCl_3$) 1.04-1.19 (12H, 4x t, *J* 7.5Hz, 4x $OCOCH_2CH_3$), 2.16 (3H, s, SCH_3), 2.21-2.46 (8H, m, 4x $OCOCH_2CH_3$), 3.74 (1H, ddd, $J_{5,6a}$ 2.42, $J_{5,6b}$ 4.84, $J_{4,5}$ 10.12Hz, *H*-5), 4.15 (1H, dd, $J_{5,6a}$ 2.42, J_{gem} 12.31Hz, *H*-6(a)), 4.25 (1H, dd, $J_{5,6b}$ 4.61, J_{gem} 12.30Hz, *H*-6(b)), 4.40 (1H, d, $J_{1,2}$ 10.11Hz, *H*-1), 5.08 (1H, t, *J* 8.86, *J* 10.23Hz, *H*-2/3/4), 5.10 (1H, t, *J* 9.54, *J* 10.50Hz, *H*-2/3/4), 5.25 (1H, t, *J* 8.86, *J* 10.23Hz, *H*-2/3/4). δ_C(75MHz; $CDCl_3$) 8.9, 9.0 (4x $OCOCH_2CH_3$), 11.2 (SCH_3), 27.3, 27.4 (4x $OCOCH_2CH_3$), 62.0 (*C*-6), 68.1, 68.9, 73.7, 76.2 (*C*-2,3,4,5), 83.0 (*C*-1), 173.05, 173.1, 173.7, 174.3 (4x $OCOCH_2CH_3$). MALDI-TOF, M+Na 457.15 (5.9ppm).

6.13.4 Preparation of 2,3,4,6-Tetra-*O*-propionyl-α-D-glucopyranosyl bromide[38] [55].

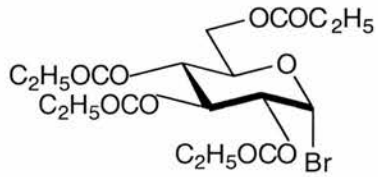

(a) Methyl 2,3,4,6-tetra-*O*-propionyl-1-thio-β-D-glucopyranoside [54] (339mg, 7.802 x10^{-4}mol) in dry dichloromethane (25ml) was reacted with 2.56 equivalents of 1M IBr in dichloromethane (2ml, 2mmol). The mixture was left stirring in an ice bath for 3.5 hours. The reaction progress by TLC analysis (ethyl acetate : hexane, 1:3) was difficult due to poor separation from the starting material. Consequently the mixture was diluted in dichloromethane (100ml), after the reported stirring time, and washed with 10% sodium thiosulphate (100ml) followed by 10% sodium carbonate (100ml). The combined organic layer was dried ($MgSO_4$) and concentrated to give an amber oil, 278mg, 76%, [R_f = 0.53 + 0.14-0.48 (streak), ethyl acetate : hexane, 2:3.

Solvent front: 55mm]. NMR showed a mixture of products, but suggested the desired compound was achieved as the major component. δ_H(300MHz; $CDCl_3$) 6.55 (1H, d, $J_{1,2}$ 4.17Hz, *H*-1(α)). δ_C(75MHz; $CDCl_3$) 94.2 (*C*-1).

(b) D-glucose (2.0g, 11.1mmol) was dissolved in propionic anhydride (10ml) and stirred with 45% HBr in acetic acid (2ml) for 17 hours. After this period the clear, pale yellow solution gave 1 spot by TLC [R_f = 0.54, ethyl acetate : hexane, 1:1. Solvent front: 55mm]. A second portion of 45% HBr in acetic acid (10ml) was added before a further period of stirring. After 24 hours, TLC analysis [R_f = 0.64 + 0.29-0.45, ethyl acetate : hexane, 1:1. Solvent front: 55mm] showed more than one compound. The same plate was observed following a further 24 hours of stirring. At this point the clear red solution was co-evaporated with toluene (700ml in all) before dilution into dichloromethane (75ml). This organic layer was then washed with ice-cold water (125ml) and 10% sodium hydrogen carbonate (125ml). Drying ($MgSO_4$) and concentrating gave a yellow oil. Attempted crystallisation from diethyl ether was unsuccessful. NMR showed partial acetylation and propionylation, thus the material was not columned. Diagnostic data: δ_H(300MHz; $CDCl_3$) 1.04-1.16 (11.5H, m, $OCOCH_2CH_3$), 1.99-2.08 (3.5H, m, $OCOCH_3$), 6.59 (1H, m, *H*-1 (OAc/$OCOCH_2CH_3$/mixture)). δ_C(75MHz; $CDCl_3$) 8.9, 9.1 ($OCOCH_2CH_3$), 20.6 ($OCOCH_3$), 27.3, 27.4 ($OCOCH_2CH_3$), 169.6, 170.0, 170.3, 170.7 ($OCOCH_3$), 173.1, 173.4, 173.5, 174.2 ($OCOCH_2CH_3$).

6.13.5 Preparation of 2,3,4,6-Tetra-*O*-propionyl-α-D-glucopyranosyl iodide[39] [56].

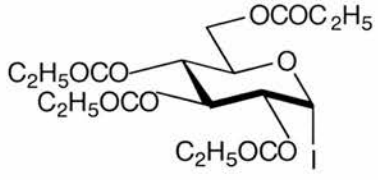

1,2,3,4,6-Penta-*O*-propionyl-α/β-D-glucopyranose [52] (1.50g, 3.26mmol) was dissolved in dry dichloromethane (13ml) before 1 equivalent of iodine (826.5mg, 3.26mmol) and hexamethyldisilane (667μl, 3.26mmol) was introduced. After 2 hours TLC analysis (ethyl acetate : hexane, 1:3) showed the reaction to be complete. Work-up involved dilution into dichloromethane (100ml) followed by aqueous washes with 10% sodium thiosulphate (150ml) and 10% sodium carbonate (2x 150ml) before a wash with water alone (100ml). The combined dichloromethane layer was dried

($MgSO_4$) and concentrated to give the pure product as a yellow syrup, 1.76g, quantitative yield, $[\alpha]_D^{25}$ +386.5° (c, 0.68 in chloroform), [R_f = 0.50, ethyl acetate : hexane, 1:3. Solvent front: 55.5mm]. δ_H(300MHz; $CDCl_3$) 1.075, 1.09, 1.12, 1.13 (12H, 4x t, *J* 7.5Hz, 4x $OCOCH_2CH_3$), 2.22-2.40 (8H, m, 4x $OCOCH_2CH_3$), 4.05 (1H, ddd, $J_{5,6a}$ 1.65, $J_{5,6b}$ 3.85, $J_{4,5}$ 10.16Hz, *H*-5), 4.11 (1H, dd, $J_{5,6a}$ 1.92, J_{gem} 12.36Hz, *H*-6(a)), 4.21 (1H, dd, $J_{1,2}$ 4.12, $J_{2,3}$ 9.88Hz, *H*-2), 4.33 (1H, dd, $J_{5,6b}$ 4.12, J_{gem} 12.36Hz, *H*-6(b)), 5.19 (1H, t, $J_{3,4}$ 9.61, $J_{4,5}$ 10.16Hz, *H*-4), 5.48 (1H, t, $J_{3,4}$ 9.61, $J_{2,3}$ 9.89Hz, *H*-3), 6.98 (1H, d, $J_{1,2}$ 4.12Hz, *H*-1). δ_C(75MHz; $CDCl_3$) 9.0 (3x $OCOCH_2CH_3$), 9.1 ($OCOCH_2CH_3$), 27.3 (2x $OCOCH_2CH_3$), 27.4, 27.6 ($OCOCH_2CH_3$), 60.85 (*C*-6), 66.8, 70.3, 71.7, 73.4 (*C*-2,3,4,5), 75.2 (*C*-1), 173.2, 173.3, 173.5, 174.2 ($OCOCH_2CH_3$). MALDI-TOF, M+Na 537.06 (0.6ppm).

6.13.6 Preparation of 2,3,4,6-Tetra-*O*-propionyl-1-*S*-acetyl-1-thio-β-D-glucopyranose [57].

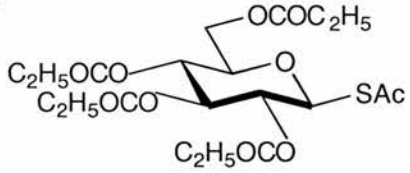

2,3,4,6-Tetra-*O*-propionyl-α-D-glucopyranosyl iodide [56] (800mg, 1.55mmol) was dissolved in dry acetone (50ml) before the addition of 4 equivalents of potassium thioacetate (710mg, 6.22mmol). Having stirred the mixture for 2 hours, at room temperature, TLC analysis (ethyl acetate : hexane, 1:3) showed the reaction to be complete. Work-up involved diluting the red/brown mixture in dichloromethane (100ml) and washing three times with 10% sodium carbonate (750ml in all). Drying ($MgSO_4$) and concentrating gave a red oil (751mg, quantitative). The product was purified by column chromatography (ethyl acetate : distilled hexane, 1:3) to give the desired compound as a yellow oil (600mg, 84%), $[\alpha]_D^{25}$ +17.15° (c, 0.8 in chloroform), [R_f = 0.23, ethyl acetate : hexane, 1:3. Solvent front: 56mm]. δ_H(300MHz; $CDCl_3$) 1.06 (3H, t, *J* 7.69Hz, $OCOCH_2CH_3$), 1.09 (6H, t, *J* 7.41, *J* 7.69Hz, 2x $OCOCH_2CH_3$), 1.13 (3H, t, *J* 7.42, *J* 7.69Hz, $OCOCH_2CH_3$), 2.21-2.35 (8H, m, 4x $OCOCH_2CH_3$), 2.37 (3H, s, $SCOCH_3$), 3.85 (1H, ddd, $J_{5,6a}$ 2.20, $J_{5,6b}$ 4.67, $J_{4,5}$ 10.16Hz, *H*-5), 4.11 (1H, dd, $J_{5,6a}$ 1.92, J_{gem} 12.36Hz, *H*-6(a)), 4.26 (1H, dd, $J_{5,6b}$ 4.67, J_{gem} 12.36Hz, *H*-6(b)), 5.13 (1H, t, $J_{2,3}$ 9.34, $J_{1,2}$ 10.43Hz, *H*-2), 5.14 (1H, dd, $J_{3,4}$ 8.79, $J_{4,5}$ 10.16Hz, *H*-4), 5.27 (1H, d, $J_{1,2}$ 10.43Hz, *H*-1), 5.30 (1H, t, $J_{3,4}$

8.79, $J_{2,3}$ 9.34Hz, *H*-3). δ_C(75MHz; $CDCl_3$) 8.9, 9.0, 9.1 (4x $OCOCH_2CH_3$), 27.35, 27.4 (4x $OCOCH_2CH_3$), 30.8 ($SCOCH_3$), 61.7 (*C*-6), 67.8, 69.0, 73.9, 76.7 (*C*-2,3,4,5), 80.4 (*C*-1), 173.05, 173.1, 173.7, 174.3 (4x $OCOCH_2CH_3$), 192.3 ($SCOCH_3$). MALDI-TOF, M+Na 485.15 (+/-2.1ppm).

6.13.7 Preparation of 1-Thio-2,3,4,6-tetra-*O*-propionyl-β-D-glucopyranose [58].

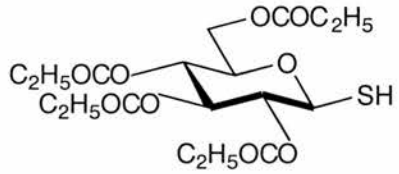

Under a nitrogen flushed environment, 2,3,4,6-tetra-*O*-propionyl-1-*S*-acetyl-1-thio-β-D-glucopyranose [57] (194mg, 4.19 $x10^{-4}$ mol) was dissolved in dry tetrahydrofuran (7ml). The addition of 2 equivalents of benzylamine (92µl, 8.38 $x10^{-4}$ mol) produced a clear, bright amber solution. This was stirred and continually monitored by TLC analysis (ethyl acetate : hexane, 1:3) which showed the reaction to be complete after exactly 1 hour. The mixture was diluted in dichloromethane (75ml) and washed successively with 1M HCl (100ml), 10% sodium carbonate (100ml) and water (100ml). The organic phase was dried ($MgSO_4$) and concentrated to a clear colourless oil. This was purified by column chromatography (ethyl acetate : distilled hexane, 1:3) to give the title compound, still as a colourless oil, 97.4mg, 55%, [R_f = 0.18, ethyl acetate : hexane, 1:3. Solvent front: 54mm]. δ_H(300MHz; $CDCl_3$) 1.04-1.17 (12H, m, 4x $OCOCH_2CH_3$), 2.21-2.42 (9H, m, 4x $OCOCH_2CH_3$ & S*H*), 3.73 (1H, ddd, $J_{5,6a}$ 2.20, $J_{5,6b}$ 4.67, $J_{4,5}$ 9.89Hz, *H*-5), 4.14 (1H, dd, $J_{5,6a}$ 2.20, J_{gem} 12.36Hz, *H*-6(a)), 4.255 (1H, dd, $J_{5,6b}$ 4.67, J_{gem} 12.36Hz, *H*-6(b)), 4.55 (1H, t, *J* 9.89Hz, *H*-1/*H*-4), 4.99 (1H, t, *J* 9.34Hz, *H*-2/3/4), 5.13 (1H, t, *J* 9.61Hz, *H*-1/2/3/4), 5.22 (1H, t, *J* 9.06, *J* 9.34Hz, *H*-2/3/4). δ_C(75MHz; $CDCl_3$) 8.9, 9.0, 9.05 (4x $OCOCH_2CH_3$), 27.35, 27.45 (4x $OCOCH_2CH_3$), 62.0 (*C*-6), 67.9, 73.1, 73.9, 76.7 (*C*-2,3,4,5), 79.1 (*C*-1), 173.1, 173.15, 173.7, 174.4 (4x $OCOCH_2CH_3$). MS (EI), M (-SH) 387. MALDI TOF, M+Na 443.13 (+/-9.95ppm).

6.13.8 Preparation of *S*-Nitroso-1-thio-2,3,4,6-tetra-*O*-propionyl-*β*-D-glucopyranose, (SNO-PROP) [59].

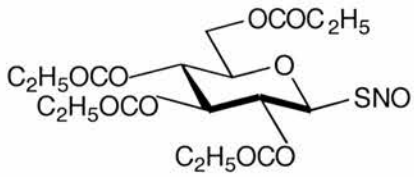

As with all the other sugars, the fuming method [section 6.2.5] was employed to nitrosate 1-thio-2,3,4,6-tetra-*O*-propionyl-*β*-D-glucopyranose [58] (43.3mg, 1.03 x 10^{-4} mol) in HPLC grade ethanol (2.5ml). As in all other cases, an orange solution was produced. λ_{max}(EtOH:H_2O, 1:1)/nm 345.6 & 560.0 (ε/dm^3 mol^{-1} cm^{-1} 375.0 & 10.6 respectively).

6.13.9 Preparation of 2,3,4,6,2',3',4',6'-Octa-*O*-propionyl-di-*β*,*β*'-D-glucopyranosyl disulphide [60].

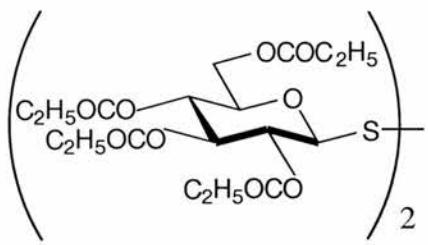

Following exactly the same protocol as already outlined [section 6.13.7], 2,3,4,6-tetra-*O*-propionyl-1-*S*-acetyl-1-thio-*β*-D-glucopyranose [58] (200mg, 4.32 x10^{-4} mol) gave the corresponding disulphide when the reaction time was extended to 4 hours and 45 minutes. Using the work-up and purification procedure described [section 6.13.7], the title compound was obtained, 151mg, 83%, $[\alpha]_D^{25}$ -946.4° (c, 0.2 in chloroform), [R_f = 0.11, ethyl acetate : hexane, 1:3. Solvent front: 57.5mm]. δ_H(300MHz; $CDCl_3$) 1.06, 1.08, 1.15, 1.16 (12H, 4x t, *J* 7.5Hz, 4x $OCOCH_2CH_3$), 2.20-2.45 (8H, m, 4x $OCOCH_2CH_3$), 3.79 (1H, ddd, $J_{5,6a}$ 2.20, $J_{5,6b}$ 4.67, $J_{4,5}$ 10.17Hz, *H*-5), 4.17 (1H, dd, $J_{5,6a}$ 1.92, J_{gem} 12.36Hz, *H*-6(a)), 4.37 (1H, dd, $J_{5,6b}$ 4.67, J_{gem} 12.36Hz, *H*-6(b)), 4.66 (1H, d, $J_{1,2}$ 9.61Hz, *H*-1), 5.11 (1H, t, *J* 9.34, *J* 9.89Hz, *H*-3/*H*-4), 5.20 (1H, t, $J_{2,3}$ 9.34, $J_{1,2}$ 9.61Hz, *H*-2), 5.28 (1H, t, *J* 9.06, *J* 9.34Hz, *H*-3/*H*-4). δ_C(75MHz; $CDCl_3$) 9.0, 9.1 (4x $OCOCH_2CH_3$), 27.3, 27.35, 27.4 (4x $OCOCH_2CH_3$), 61.5 (*C*-6), 67.6, 69.5, 73.6, 76.3 (*C*-2,3,4,5), 87.4 (*C*-1), 172.6, 172.7, 173.5, 174.1 (4x $OCOCH_2CH_3$). MALDI-TOF, M+Na 861.26 (+/-5.3ppm).

6.14 Synthesis of *S*-Nitroso-1-thio-2,3,4,6-tetra-*O*-butyrionyl-*β*-D-glucopyranose, (SNO-BUT) [65].

6.14.1 Preparation of 1,2,3,4,6-Penta-*O*-butyrionyl-*α*/*β*-D-glucopyranose [61].

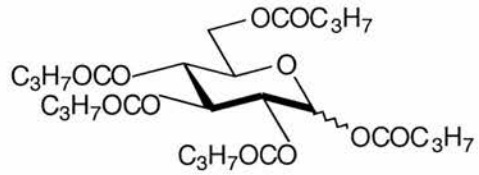

D-Glucose (2.5g, 13.88mmol) was fully butyrionylated using the protocol outlined for the propionylated derivative [section 6.13.1]. The sugar was stirred for 21 hours with 1.2 equivalents of anhydride, as opposed to 1.4 [section 6.13.1]. TLC analysis (ethyl acetate : hexane, 1:5) showed complete conversion. Dilution into dichloromethane (100ml) and washes with ice-cold 10% sodium thiosulphate (2x 250ml) and 10% sodium carbonate (2x 250ml) gave a pale yellow oil upon concentrating. To this, pyridine (10ml) and water (sparingly) were added. The flask was then left to sit in ice-water bath for 48 hours to enable the removal of any remaining anhydride by nucleophilic catalysis. After this period of time, a second work-up was performed by washing the dichloromethane layer (100ml) with 1M HCl (500ml in all), 10% sodium carbonate (500ml in all) and water (250ml). Drying ($MgSO_4$) and concentrating gave the desired compound, 8.47g, quantitative, $[\alpha]_D^{25}$ +45.5° (c, 2 in chloroform) [lit.[40] $[\alpha]_D^{25}$ +44.5° (c, 2 in chloroform)], [R_f = 0.34, ethyl acetate : hexane, 1:5. Solvent front: 56.5mm]. δ_H(300MHz; $CDCl_3$) 0.855-1.01 (15H, m, 5x $OCOCH_2CH_2CH_3$), 1.53-1.72 (10H, m, 5x $OCOCH_2CH_2CH_3$), 2.15-2.44 (10H, m, 5x $OCOCH_2CH_2CH_3$), 4.06-4.12 (1H, m, *H*-5), 4.095 (1H, dd, $J_{5,6a}$ 2.20, J_{gem} 12.91Hz, *H*-6(a)), 4.20 (1H, dd, $J_{5,6b}$ 4.94, J_{gem} 12.90Hz, *H*-6(b)), 5.09 (1H, dd, $J_{1,2}$ 3.85, $J_{2,3}$ 10.44Hz, *H*-2), 5.145 (1H, t, *J* 9.61, *J* 9.89Hz, *H*-3/*H*-4), 5.49 (1H, t, *J* 9.89Hz, *H*-3/*H*-4), 5.72 (3%H, d, $J_{1,2}$ 8.24Hz, *H*-1(β)), 6.34 (97%H, d, $J_{1,2}$ 4.12Hz, *H*-1(α)). δ_C(75MHz; $CDCl_3$) 13.5, 13.6 (5x $OCOCH_2CH_2CH_3$), 18.2, 18.25, 18.3, 18.4 (5x $OCOCH_2CH_2CH_3$), 35.7, 35.9, 36.0, 36.1 (5x $OCOCH_2CH_2CH_3$), 61.4 (*C*-6), 67.7, 69.3, 69.6, 70.2 (*C*-2,3,4,5), 89.0 (*C*-1(α)), 91.8 (*C*-1(β)), 171.6, 172.2, 172.5, 172.9, 173.5 (5x $OCOCH_2CH_2CH_3$). MALDI-TOF, M+Na 553.26 (+/-2.9ppm).

6.14.2 Preparation of 2,3,4,6-Tetra-*O*-butyrionyl-α-D-glucopyranosyl iodide [62].

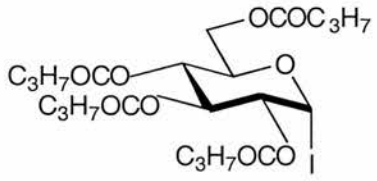

1,2,3,4,6-Penta-*O*-butyrionyl-α/β-D-glucopyranose [61] (5.0g, 9.42mmol) in dry dichloromethane (62.5ml) was reacted as in section 6.13.5, except that two equivalents of hexamethyldisilane (3.86ml, 18.85mmol) and iodine (4.78g, 18.85mmol) were used. The reaction was complete after stirring for 4 hours and 15 minutes. Following an aqueous work-up identical to that described (6.13.5), the desired compound was obtained as a pure yellow syrup, 4.90g, 91%, $[\alpha]_D^{25}$ +350.4° (c, 0.44 in chloroform), [R_f = 0.38, ethyl acetate : hexane, 1:5. Solvent front: 57.5mm]. δ_H(300MHz; $CDCl_3$) 0.90, 0.92, 0.93, 0.94 (12H, 4x t, *J* 7.42Hz, $OCOCH_2CH_2CH_3$), 1.58, 1.62, 1.64, 1.65 (8H, q, *J* 7.42Hz, 4x $OCOCH_2CH_2CH_3$), 2.20-2.35 (8H, m, $OCOCH_2CH_2CH_3$), 4.05 (1H, ddd, $J_{5,6a}$ 2.20, $J_{5,6b}$ 4.40, $J_{4,5}$ 10.44Hz, *H*-5), 4.13 (1H, dd, $J_{5,6a}$ 1.92, J_{gem} 12.36Hz, *H*-6(a)), 4.205 (1H, dd, $J_{1,2}$ 4.39, $J_{2,3}$ 9.88Hz, *H*-2), 4.29 (1H, dd, $J_{5,6b}$ 4.39, J_{gem} 12.63Hz, *H*-6(b)), 5.20 (1H, dd, $J_{3,4}$ 9.61, $J_{4,5}$ 10.43Hz, *H*-4), 5.50 (1H, t, $J_{3,4}$ 9.61, $J_{2,3}$ 9.88Hz, *H*-3), 6.99 (1H, d, $J_{1,2}$ 4.39Hz, *H*-1). δ_C(75MHz; $CDCl_3$) 13.6, 13.7 (4x $OCOCH_2CH_2CH_3$), 18.3, 18.35 (4x $OCOCH_2CH_2CH_3$), 35.9, 35.95, 36.0 (4x $OCOCH_2CH_2CH_3$), 60.8 (*C*-6), 66.7, 70.4, 71.5, 73.4 (*C*-2,3,4,5), 75.3 (*C*-1), 172.3, 172.5, 172.6, 173.4 (4x $OCOCH_2CH_2CH_3$).

6.14.3 Preparation of 2,3,4,6-Tetra-*O*-butyrionyl-1-*S*-acetyl-1-thio-β-D-glucopyranose [63].

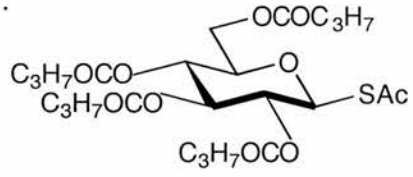

2,3,4,6-Tetra-*O*-butyrionyl-α-D-glucopyranosyl iodide [62] (4.749g, 8.32mmol), was reacted with four equivalents of potassium thioacetate (3.803g, 33.3mmol) in dry acetone (150ml), as described in section 6.13.6. TLC analysis (ethyl acetate : hexane, 1:3) showed the reaction to be complete after 17 hours. Work-up involved dilution into dichloromethane (100ml) and washing with 10% sodium thiosulphate (250ml), 10% sodium carbonate (2x 250ml) and water (250ml). The organic phase was dried

($MgSO_4$) and concentrated, after filtering through a charcoal bed, to give a golden yellow sirup, 4.21g, 98%. This was columned (ethyl acetate : distilled hexane, 1:6) to give the pure product, as a yellow solid, 1.145g, 26.5%, mp 62-3°C, $[\alpha]_D^{25}$ +22.7° (c, 1 in chloroform), [R_f = 0.37, ethyl acetate : hexane, 1:3. Solvent front: 57mm]. δ_H(300MHz; $CDCl_3$) 0.88, 0.90, 0.93 (12H, 3x t, *J* 7.42Hz, 4x $OCOCH_2CH_2CH_3$), 1.49-1.69 (8H, m, 4x $OCOCH_2CH_2CH_3$), 2.17-2.33 (8H, m, $OCOCH_2CH_2CH_3$), 2.36 (3H, s, $SCOCH_3$), 3.83 (1H, ddd, $J_{5,6a}$ 2.20, $J_{5,6b}$ 4.67, $J_{4,5}$ 10.17Hz, *H*-5), 4.11 (1H, dd, $J_{5,6a}$ 2.20, J_{gem} 12.36Hz, *H*-6(a)), 4.21 (1H, dd, $J_{5,6b}$ 4.67, J_{gem} 12.36Hz, *H*-6(b)), 5.12 (1H, t, $J_{3,4}$ 9.34, $J_{4,5}$ 10.16Hz, *H*-4), 5.13 (1H, dd, $J_{2,3}$ 9.07, $J_{1,2}$ 10.44Hz, *H*-2), 5.255 (1H, d, $J_{1,2}$ 10.44Hz, *H*-1), 5.30 (1H, t, $J_{2,3}$ 9.06, $J_{3,4}$ 9.34Hz, *H*-3). δ_C(75MHz; $CDCl_3$) 13.6, 13.65 (4x $OCOCH_2CH_2CH_3$), 18.3 (4x $OCOCH_2CH_2CH_3$), 30.8 ($SCOCH_3$), 35.9, 36.0 (4x $OCOCH_2CH_2CH_3$), 61.6 (*C*-6), 67.8, 68.95, 73.7, 76.7 (*C*-2,3,4,5), 80.4 (*C*-1), 172.2, 172.8, 173.5 (4x $OCOCH_2CH_2CH_3$), 192.4 ($SCOCH_3$). MALDI-TOF, M+Na 541.21 (+/-7.0ppm).

6.14.4 Preparation of 1-Thio-2,3,4,6-tetra-*O*-butyrionyl-*β*-D-glucopyranose [64].

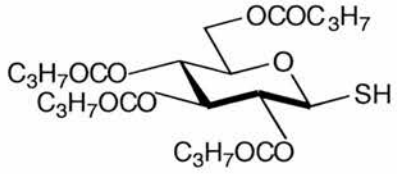

2,3,4,6-Tetra-*O*-butyrionyl-1-*S*-acetyl-1-thio-*β*-D-glucopyranose [63] (300mg, 5.78 $x10^{-4}$ mol) in dry tetrahydrofuran (6ml) flushed thoroughly with nitrogen, was stirred with two equivalents of benzylamine (127µl, 11.57 $x10^{-4}$mol). TLC analysis (ethyl acetate : hexane, 1:6) showed the reaction to be complete after 40 minutes. Work-up was as described in section 6.13.7, producing an amber oil, in quantitative yield. This material was purified by column chromatography (toluene : ethyl acetate, 100:2.5) giving the title compound in a highly clean form, as a clear colourless oil, 195mg, 71%, $[\alpha]_D^{25}$ +35.9° (c, 0.4 in chloroform), [R_f = 0.06, toluene : ethyl acetate, 100:2.5. Solvent front: 55mm]. ν_{max}/cm^{-1} 2559(w) (-SH) and 1746(br, s) (C=O). δ_H(300MHz; $CDCl_3$) 0.88, 0.89, 0.93, 0.94 (12H, 4x t, *J* 7.42Hz, 4x $OCOCH_2CH_2CH_3$), 1.485-1.70 (8H, m, 4x $OCOCH_2CH_2CH_3$), 2.17-2.35 (9H, m, 4x $OCOCH_2CH_2CH_3$ & S*H*), 3.70 (1H, ddd, $J_{5,6a}$ 2.20, $J_{5,6b}$ 4.67, $J_{4,5}$ 9.62Hz, *H*-5), 4.13 (1H, dd, $J_{5,6a}$ 2.20, J_{gem} 12.36Hz, *H*-6(a)), 4.20 (1H, dd, $J_{5,6b}$ 4.67, J_{gem} 12.36Hz, *H*-6(b)), 4.53 (1H, t, $J_{1,SH}$

9.61, $J_{1,2}$ 9.89Hz, *H*-1), 4.98 (1H, t, $J_{3,4}$ 9.34, $J_{2,3}$ 9.61Hz, *H*-3), 5.115 (1H, t, $J_{2,3}$ 9.61, $J_{1,2}$ 9.89Hz, *H*-2), 5.21 (1H, t, $J_{3,4}$ 9.34, $J_{4,5}$ 9.61Hz, *H*-4). δ_C(75MHz; $CDCl_3$) 13.6, 13.65 (4x $OCOCH_2CH_2\mathit{C}H_3$), 18.3 (4x $OCOCH_2\mathit{C}H_2CH_3$), 35.95, 36.0, 36.1 (4x $OCO\mathit{C}H_2CH_2CH_3$), 61.9 (*C*-6), 68.0, 73.3, 73.5, 76.7 (*C*-2,3,4,5), 79.0 (*C*-1), 172.2, 172.5, 172.8, 173.5 (4x $O\mathit{C}OCH_2CH_2CH_3$). MALDI-TOF, M+Na 499.20 (+/- 8.8ppm).

6.14.5 Preparation of *S*-Nitroso-1-thio-2,3,4,6-tetra-*O*-butyrionyl-*β*-D-glucopyranose, (SNO-BUT) [65].

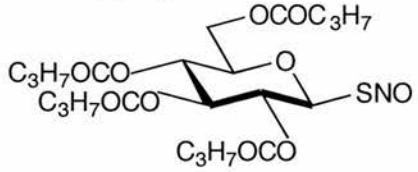

As described [section 6.2.5] 1-thio-2,3,4,6-tetra-*O*-butyrionyl-*β*-D-glucopyranose [64] (49mg, 1.03 $x10^{-4}$ mol) in HPLC grade ethanol (2.5ml) was nitrosated by the fuming method. λ_{max}(EtOH)/nm 345.0 & 561.0 (ε/dm^3 mol^{-1} cm^{-1} 408.5 & 8.8 respectively).

6.15 Synthesis of *S*-Nitroso-1-thio-2,3,4,6-tetra-*O*-valerionyl-*β*-D-glucopyranose, (SNO-VAL) [70].

6.15.1 Preparation of 1,2,3,4,6-Penta-*O*-valerionyl-*α*/*β*-D-glucopyranose [66].

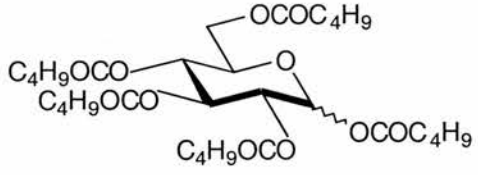

D-glucose (2.5g, 13.8mmol) was stirred in the presence of iodine (125mg, 0.5mmol) and 1.2 equivalents of valeric anhydride (16.46ml, 83.28mmol), until TLC analysis (ethyl acetate : hexane, 1:5) showed the reaction to be complete. Work-up involved the same procedure outlined in 6.14.1, in which a second aqueous wash was required, after submerging the flask overnight in an ice-water bath, following the addition of pyridine (10ml) and water (sparingly). Drying ($MgSO_4$) and concentrating gave a yellow syrup, 6.12g, 73%, $[\alpha]_D^{25}$ +68.0° (c, 1 in chloroform), [R_f = 0.42, ethyl

acetate : hexane, 1:5. Solvent front: 54mm]. δ_H(300MHz; $CDCl_3$) 0.845-0.95 (15H, m, 5x $OCOCH_2CH_2CH_2CH_3$), 1.24-1.44 & 1.47-1.69 (20H, m, 5x $OCOCH_2CH_2CH_2CH_3$), 2.19-2.46 (10H, m, 5x $OCOCH_2CH_2CH_2CH_3$), 4.055-4.12 (2H, m, *H*-5 & *H*-6(a)), 4.19 (1H, dd, $J_{5,6b}$ 4.67, J_{gem} 12.64Hz, *H*-6(b)), 5.085 (1H, dd, $J_{1,2}$ 3.85, $J_{2,3}$ 10.44Hz, *H*-2), 5.14 (1H, t, *J* 9.61, *J* 9.89Hz, *H*-3/*H*-4), 5.49 (1H, t, *J* 9.89Hz, *H*-3/*H*-4), 5.715 (0.06H, d, $J_{1,2}$ 8.51Hz, *H*-1(β)), 6.335 (0.94H, d, $J_{1,2}$ 3.85Hz, *H*-1(α)). δ_C(75MHz; $CDCl_3$) 13.6 (5x $OCOCH_2CH_2CH_2CH_3$), 22.15, 22.2 & 26.8, 26.85, 26.9 (5x $OCOCH_2CH_2CH_2CH_3$), 33.6, 33.7, 33.85, 33.9 (5x $OCOCH_2CH_2CH_2CH_3$), 61.5 (*C*-6), 67.8, 69.3, 69.7, 70.2 (*C*-2,3,4,5), 89.0 (*C*-1), 171.8, 172.4, 172.6, 173.1, 173.6 (5x $OCOCH_2CH_2CH_2CH_3$). MALDI-TOF, M+Na 623.34 (+/-2.4ppm).

6.15.2 Preparation of 2,3,4,6-Tetra-*O*-valerionyl-α-D-glucopyranosyl iodide [67].

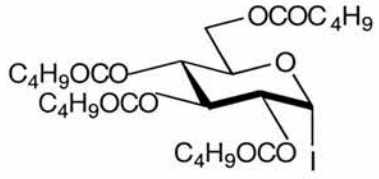

1,2,3,4,6-Penta-*O*-valerionyl-α/β-D-glucopyranose [66] (4.0g, 6.66mmol) in dry dichloromethane (50ml) was stirred with two equivalents of hexamethyldisilane (2.73ml, 13.32mmol) and iodine (3.38g, 13.32mmol), as described in section 6.14.2. TLC analysis (ethyl acetate : hexane, 1:10) showed the reaction to be complete after 23 hours. Work-up was identical to that outlined in section 6.13.5, giving a golden yellow oil/solid, 2.67g, 64%, $[\alpha]_D^{25}$ +243.2° (c, 0.26 in chloroform), [R_f = 0.26, ethyl acetate : hexane, 1:10. Solvent front: 56.5mm]. δ_H(300MHz; $CDCl_3$) 0.88, 0.90, 0.91, 0.92 (12H, 4x t, *J* 7.42Hz, 4x $OCOCH_2CH_2CH_2CH_3$), 1.235-1.42 & 1.48-1.69 (16H, m, 4x $OCOCH_2CH_2CH_2CH_3$), 2.21-2.47 (8H, m, 4x $OCOCH_2CH_2CH_2CH_3$), 4.045 (1H, ddd, $J_{5,6a}$ 2.20, $J_{5,6b}$ 4.40, $J_{4,5}$ 10.45Hz, *H*-5), 4.13 (1H, dd, $J_{5,6a}$ 1.92, J_{gem} 12.63Hz, *H*-6(a)), 4.20 (1H, dd, $J_{1,2}$ 4.39, $J_{2,3}$ 9.88Hz, *H*-2), 4.27 (1H, dd, $J_{5,6b}$ 4.39, J_{gem} 12.63Hz, *H*-6(b)), 5.20 (1H, t, *J* 9.61, *J* 10.16Hz, *H*-3/*H*-4), 5.49 (1H, t, *J* 9.61Hz, *H*-3/*H*-4), 6.98 (1H, d, $J_{1,2}$ 4.12Hz, *H*-1). δ_C(75MHz; $CDCl_3$) 13.6, 13.7 (4x $OCOCH_2CH_2CH_2CH_3$), 22.2 & 26.8, 26.85, 26.9 (4x $OCOCH_2CH_2CH_2CH_3$), 33.7, 33.75, 33.8, 33.85 (4x $OCOCH_2CH_2CH_2CH_3$), 60.85 (*C*-6), 66.7, 70.4, 71.5, 73.4 (*C*-2,3,4,5), 75.3 (*C*-1), 172.4, 172.65, 172.7, 173.55 (4x $OCOCH_2CH_2CH_2CH_3$).

6.15.3 Preparation of 2,3,4,6-Tetra-*O*-valerionyl-1-*S*-acetyl-1-thio-*β*-D-glucopyranose [68].

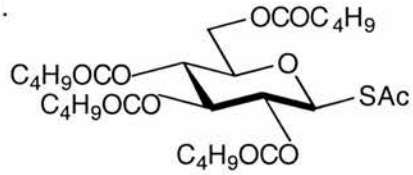

2,3,4,6-Tetra-*O*-valerionyl-*α*-D-glucopyranosyl iodide [67] (2.67g, 4.26mmol) dissolved in dry acetone (85ml) was reacted with four equivalents of potassium thioacetate (1.947g, 17.05mmol). TLC analysis (ethyl acetate : hexane, 1:10) showed the reaction to be complete after 12 hours of stirring. Work-up was as described in section 6.14.3 and resulted in a bright orange oil, 2.211g, 90%. This was purified by column chromatography (ethyl acetate : distilled hexane, 1:8) producing a yellow oil, 682mg, 28%, $[\alpha]_D^{25}$ +14.4° (c, 0.4 in chloroform), [R_f = 0.12 (charred pink), ethyl acetate : hexane, 1:8. Solvent front: 53mm]. δ_H(300MHz; $CDCl_3$) 0.85-0.92 (12H, m, 4x $OCOCH_2CH_2CH_2CH_3$) 1.21-1.39 & 1.45-1.63 (16H, m, 4x $OCOCH_2CH_2CH_2CH_3$), 2.18-2.37 (11H, m, 4x $OCOCH_2CH_2CH_2CH_3$ & $SCOCH_3$), 3.82 (1H, ddd, $J_{5,6a}$ 2.20, $J_{5,6b}$ 4.67, $J_{4,5}$ 10.17Hz, *H*-5), 4.10 (1H, dd, $J_{5,6a}$ 2.20, J_{gem} 12.36Hz, *H*-6(a)), 4.19 (1H, dd, $J_{5,6b}$ 4.39, J_{gem} 12.36Hz, *H*-6(b)), 5.11 (1H, t, $J_{3,4}$ 9.34, $J_{4,5}$ 10.17Hz, *H*-4), 5.12 (1H, dd, $J_{2,3}$ 9.34, $J_{1,2}$ 10.44Hz, *H*-2), 5.25 (1H, d, $J_{1,2}$ 10.44Hz, *H*-1), 5.29 (1H, t, *J* 9.34Hz, *H*-3). δ_C(75MHz; $CDCl_3$) 13.6, 13.7 (4x $OCOCH_2CH_2CH_2CH_3$), 22.15, 22.2 & 26.8 (4x $OCOCH_2CH_2CH_2CH_3$), 30.8 ($SCOCH_3$), 33.7, 33.75, 33.8 (4x $OCOCH_2CH_2CH_2CH_3$), 61.7 (*C*-6), 67.8, 68.9, 73.7, 76.7 (*C*-2,3,4,5), 80.4 (*C*-1), 172.3, 172.9, 173.6 (4x $OCOCH_2CH_2CH_2CH_3$), 192.3 ($SCOCH_3$). MALDI-TOF, M+Na 597.27 (+/-2.5ppm).

6.15.4 Preparation of 1-Thio-2,3,4,6-tetra-*O*-valerionyl-*β*-D-glucopyranose [69].

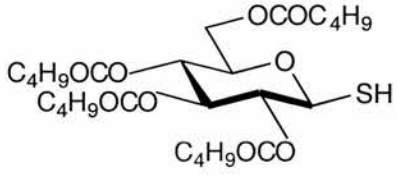

Under nitrogen, 2,3,4,6-tetra-*O*-valerionyl-1-*S*-acetyl-1-thio-*β*-D-glucopyranose [68] (250mg, 4.35 x10^{-4}mol) in dry tetrahydrofuran (5ml) was stirred with two equivalents of benzylamine (95µl, 8.70 x10^{-4} mol). After 1 hour and 15 minutes TLC

analysis showed the reaction to be complete. Work-up was as reported previously [section 6.13.7], giving a brown oil. Column chromatography (toluene : ethyl acetate, 100:1) gave a clear pale yellow oil, 113.5mg, 49%, $[\alpha]_D^{25}$ +72.0° (c, 0.2 in chloroform), [R_f = 0.05 (charred pink), toluene : ethyl acetate, 100:1. Solvent front: 55mm]. ν_{max}/cm^{-1} 2554(w) (-SH) and 1741(br, s) (C=O). δ_H(300MHz; $CDCl_3$) 0.875, 0.88, 0.90, 0.91 (12H, 4x t, *J* 7.42Hz, 4x $OCOCH_2CH_2CH_2CH_3$), 1.22-1.41 & 1.455-1.65 (16H, m, 4x $OCOCH_2CH_2CH_2CH_3$), 2.19-2.37 (9H, m, 4x $OCOCH_2CH_2CH_2CH_3$ & S*H*), 3.71 (1H, ddd, $J_{5,6a}$ 2.47, $J_{5,6b}$ 4.39, $J_{4,5}$ 9.61Hz, *H*-5), 4.13 (1H, dd, $J_{5,6a}$ 2.47, J_{gem} 12.36Hz, *H*-6(a)), 4.19 (1H, dd, $J_{5,6b}$ 4.67, J_{gem} 12.36Hz, *H*-6(b)), 4.53 (1H, t, $J_{1,SH}$ 9.61, $J_{1,2}$ 9.89Hz, *H*-1), 4.98 (1H, t, $J_{3,4}$ 9.34, $J_{4,5}$ 9.61Hz, *H*-4) 5.11 (1H, t, $J_{2,3}$ 9.34, $J_{1,2}$ 9.89Hz, *H*-2), 5.21 (1H, t, *J* 9.34Hz, *H*-3). δ_C(75MHz; $CDCl_3$) 13.6, 13.7 (4x $OCOCH_2CH_2CH_2CH_3$), 22.25, 26.8, 26.9 (4x $OCOCH_2CH_2CH_2CH_3$), 33.7, 33.8, 33.85. 33.9 (4x $OCOCH_2CH_2CH_2CH_3$), 62.0 (*C*-6), 68.1, 73.4, 73.5, 76.7 (*C*-2,3,4,5), 79.0 (*C*-1), 172.3, 172.7, 173.0, 173.7 (4x $OCOCH_2CH_2CH_2CH_3$). MALDI-TOF, M+Na 555.26 (+/-3.1ppm).

6.15.5 Preparation of *S*-Nitroso-1-thio-2,3,4,6-tetra-*O*-valerionyl -*β*-D-glucopyranose, (SNO-VAL) [70].

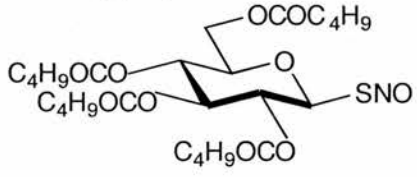

Nitrosation [section 6.2.5] of 1-thio-2,3,4,6-tetra-*O*-valerionyl-*β*-D-glucopyranose [69] (54.8mg, 1.03 $x10^{-4}$ mol), in HPLC grade ethanol (2.5ml), gave the characteristic orange solution for the title compound. λ_{max}(EtOH)/nm 344.9 & 566.0 ($\varepsilon/dm^3\ mol^{-1}\ cm^{-1}$ 417.5 & 7.6 respectively).

6.16 Synthesis of *S*-Nitroso-1-thio-2,3,4,6-tetra-*O*-hexionyl-β-D-glucopyranose, (SNO-HEX) [76].

6.16.1 Preparation of 1,2,3,4,6-penta-*O*-hexionyl-α/β-D-glucopyranose [71].

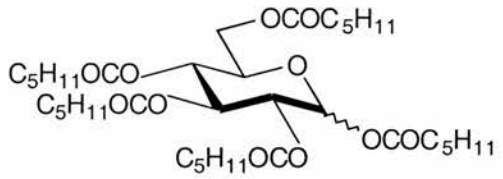

In the presence of 1.2 equivalents of hexanoic anhydride (38.54ml, 166.5mmol), D-glucose (5.0g, 27.75mmol) was stirred with a catalytic amount of iodine (250mg, 1mmol). After 12 hours there was still a small portion of solid material in the mixture. TLC analysis (ethyl acetate : hexane, 1:10) showed this to be starting material, thus more iodine was added (250mg, 1mmol). After 24 hours a work-up matching that described in section 6.13.1 was performed, though having obtained no precipitate after stirring rapidly in ice-water (400ml) with 10% sodium thiosulphate (20ml), 10% sodium carbonate (100ml) was also introduced. The beaker was then left to sit overnight in the refrigerator, to allow hydrolysis of the anhydride. Following dilution into dichloromethane (400ml), a further washing process was required with ice-cold 10% sodium carbonate (4x 500ml). Drying and concentrating gave a clear yellow oil which showed by nmr to still contain the anhydride, thus nucleophilic catalysis involving pyridine (10ml) and water (sparingly) [section 6.14.1] was performed to give the desired material in quantitative yield, $[\alpha]_D^{25}$ +82.0° (c, 2.42 in chloroform), [R_f = 0.22, ethyl acetate : hexane, 1:15. Solvent front: 52.5mm]. δ_H(300MHz; $CDCl_3$) 0.85-0.93 (15H, m, 5x $OCOCH_2CH_2CH_2CH_2CH_3$), 1.22-1.36 (20H, m, 5x $OCOCH_2CH_2CH_2CH_2CH_3$), 1.50-1.69 (10H, m, 5x $OCOCH_2CH_2CH_2CH_2CH_3$), 2.19-2.41 (10H, m, 5x $OCOCH_2CH_2CH_2CH_2CH_3$), 4.06-4.13 (2H, m, *H*-5, *H*-6(a)), 4.21 (1H, dd, $J_{5,6b}$ 4.82, J_{gem} 12.54Hz, *H*-6(b)), 5.10 (1H, dd, $J_{1,2}$ 3.86, $J_{2,3}$ 10.13Hz, *H*-2), 5.155 (1H, t, *J* 9.65, *J* 10.13Hz, *H*-3/*H*-4), 5.49 (1H, t, *J* 9.65, *J* 10.13Hz, *H*-3/*H*-4), 5.72 (0.07H, d, $J_{1,2}$ 8.20Hz, *H*-1(β)), 6.345 (0.93H, d, $J_{1,2}$ 3.86Hz, *H*-1(α)). δ_C(75MHz; $CDCl_3$) 13.5 (5x $OCOCH_2CH_2CH_2CH_2CH_3$), 24.1, 24.2, 24.25, 24.3, 30.9, 31.0 (5x $OCOCH_2CH_2CH_2CH_2CH_3$), 33.5, 33.6, 33.8 (5x $OCOCH_2CH_2CH_2CH_2CH_3$), 61.2 (*C*-6), 67.5, 69.1, 69.4, 69.9 (*C*-2,3,4,5), 88.7 (*C*-1(α)), 91.6 (*C*-1(β)), 171.3, 171.9,

172.2, 172.6, 173.1 (5x O*C*OCH$_2$CH$_2$CH$_2$CH$_2$CH$_3$). MALDI-TOF (Low resolution), M+Na 693.42.

A trace amount of hexanoic anhydride was also observed by ^{1}H & ^{13}C nmr.

6.16.2 Preparation of 2,3,4,6-tetra-*O*-hexionyl-α-D-glucopyranosyl iodide [72].

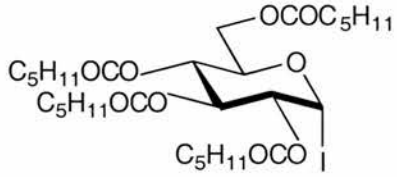

As already described [section 6.14.2], 1,2,3,4,6-penta-*O*-hexionyl-α/β-D-glucopyranose [71] (4.0g, 5.96mmol) in dry dichloromethane (50ml) was stirred with 2 equivalents of hexamethyldisilane (2.44ml, 11.93mmol) and iodine (3.03g, 11.93mmol). After 5 hours and 15 minutes, TLC analysis (ethyl acetate : hexane, 1:10) showed the reaction to be complete. Work-up, as already outlined [section 6.13.5], resulted in a yellow oil, 3.195g, 79%, $[\alpha]_D^{25}$ +6.8° (c, 1.6 in chloroform), [R_f = 0.31, ethyl acetate : hexane, 1:10. Solvent front: 55.5mm]. δ_H(300MHz; $CDCl_3$) 0.85-0.91 (12H, m, 4x OCOCH$_2$CH$_2$CH$_2$CH$_2$C*H*$_3$), 1.22-1.36 (16H, m, 4x OCOCH$_2$C*H*$_2$C*H*$_2$CH$_2$CH$_3$), 1.50-1.68 (8H, m, 4x OCOCH$_2$CH$_2$CH$_2$C*H*$_2$CH$_3$), 2.20-2.35 (8H, m, 4x OCOC*H*$_2$CH$_2$CH$_2$CH$_2$CH$_3$), 4.04 (1H, ddd, $J_{5,6a}$ 1.92, $J_{5,6b}$ 4.12, $J_{4,5}$ 10.16Hz, *H*-5), 4.125 (1H, dd, $J_{5,6a}$ 1.92, J_{gem} 12.63Hz, *H*-6(a)), 4.195 (1H, dd, $J_{1,2}$ 4.39, $J_{2,3}$ 9.61Hz, *H*-2), 4.27 (1H, dd, $J_{5,6b}$ 4.39, J_{gem} 12.63Hz, *H*-6(b)), 5.19 (1H, t, $J_{3,4}$ 9.61, $J_{4,5}$ 10.16Hz, *H*-4), 5.49 (1H, t, *J* 9.61Hz, *H*-3), 6.98 (1H, d, $J_{1,2}$ 4.39Hz, *H*-1(α)). δ_C(75MHz; $CDCl_3$) 13.8, 13.9 (4x OCOCH$_2$CH$_2$CH$_2$CH$_2$*C*H$_3$), 22.3, 22.35, 24.4, 24.5, 24.55, 31.2, (4x OCOCH$_2$*C*H$_2$*C*H$_2$*C*H$_2$CH$_3$), 33.9, 34.0, 34.1 (4x OCO*C*H$_2$CH$_2$CH$_2$CH$_2$CH$_3$), 60.85 (*C*-6), 66.7, 70.4, 71.5, 73.4 (*C*-2,3,4,5), 75.3 (*C*-1), 172.4, 172.65, 172.7, 173.5 (4x O*C*OCH$_2$CH$_2$CH$_2$CH$_2$CH$_3$). A trace amount of hexanoic anhydride was still observed by ^{1}H & ^{13}C nmr.

6.16.3 Preparation of 2,3,4,6-tetra-*O*-hexionyl-1-*S*-acetyl-1-thio-*β*-D-glucopyranose [73] & 2,3,4,6-tetra-*O*-hexionyl-1-*S*-hexionyl-1-thio-*β*-D-glucopyranose [74].

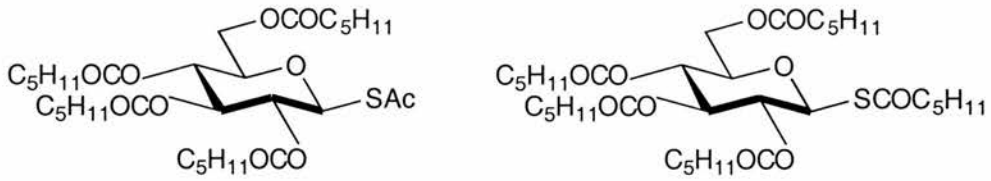

In dry acetone (70ml) 2,3,4,6-tetra-*O*-hexionyl-*α*-D-glucopyranosyl iodide [72] (1.49g, 2.18mmol) was stirred with four equivalents of potassium thioacetate (998mg, 8.74mmol). TLC analysis showed the reaction to be complete after 5.5 hours. Work-up was as already reported [section 6.14.3]. Column chromatography (ethyl acetate : distilled hexane, 1:10) gave two sugar compounds eluting in two separate fractions.

(i) The major product being the *S*-acetylated derivative, as a yellow oil, 522mg, 38%, $[\alpha]_D^{25}$ +15.2° (c, 1 in chloroform), [R_f = 0.11 (charred pink), ethyl acetate : hexane, 1:10. Solvent front: 54.5mm]. δ_H(300MHz; $CDCl_3$) 0.845-0.91 (12H, m, 4x $OCOCH_2CH_2CH_2CH_2CH_3$), 1.205-1.32 (16H, m, 4x $OCOCH_2CH_2CH_2CH_2CH_3$), 1.47-1.65 (8H, m, 4x $OCOCH_2CH_2CH_2CH_2CH_3$), 2.16-2.34 (8H, m, 4x $OCOCH_2CH_2CH_2CH_2CH_3$), 2.36 (3H, s, $SCOCH_3$), 3.82 (1H, ddd, $J_{5,6a}$ 2.20, $J_{5,6b}$ 4.40, $J_{4,5}$ 9.90Hz, *H*-5), 4.11 (1H, dd, $J_{5,6a}$ 1.92, J_{gem} 12.36Hz, *H*-6(a)), 4.19 (1H, dd, $J_{5,6b}$ 4.39, J_{gem} 12.36Hz, *H*-6(b)), 5.11 (1H, t, $J_{3,4}$ 9.61, $J_{4,5}$ 9.88Hz, *H*-4), 5.12 (1H, dd, $J_{2,3}$ 9.34, $J_{1,2}$ 10.43Hz, *H*-2), 5.25 (1H, d, $J_{1,2}$ 10.44Hz, *H*-1), 5.29 (1H, t, $J_{2,3}$ 9.34, $J_{3,4}$ 9.61Hz, *H*-3). δ_C(75MHz; $CDCl_3$) 13.8, 13.9 (4x $OCOCH_2CH_2CH_2CH_2CH_3$), 22.3, 22.35, 24.4, 24.5, 31.2, 31.25, 31.3 (4x $OCOCH_2CH_2CH_2CH_2CH_3$), 30.8 ($SCOCH_3$), 34.0, 34.1 (4x $OCOCH_2CH_2CH_2CH_2CH_3$), 61.7 (*C*-6), 67.8, 68.95, 73.8, 76.7 (*C*-2,3,4,5), 80.4 (*C*-1), 172.3, 173.0, 173.7 (4x $OCOCH_2CH_2CH_2CH_2CH_3$), 192.3 ($SCOCH_3$). MALDI-TOF, M+Na 653.33 (+/-2.4ppm).

(ii) The minor product was the hexionylated compound formed from trace amounts of hexanoic anhydride. This was observed as an orange oil, 181mg, 12%, $[\alpha]_D^{25}$ +16.9° (c, 0.26 in chloroform), [R_f = 0.21 (charred pink), ethyl acetate : hexane, 1:10. Solvent front: 54.5mm]. δ_H(300MHz; $CDCl_3$) 0.84-0.915 (15H, m, 5x $COCH_2CH_2CH_2CH_2CH_3$), 1.20-1.33 (20H, m, 5x $COCH_2CH_2CH_2CH_2CH_3$), 1.475-

1.67 (10H, m, 5x $COCH_2CH_2CH_2CH_2CH_3$), 2.17-2.36 (8H, m, 4x $OCOCH_2CH_2CH_2CH_2CH_3$), 2.56 (2H, t, *J* 7.3Hz, $SCOCH_2CH_2CH_2CH_2CH_3$), 3.82 (1H, ddd, $J_{5,6a}$ 2.20, $J_{5,6b}$ 4.40, $J_{4,5}$ 9.90Hz, *H*-5), 4.11 (1H, dd, $J_{5,6a}$ 1.92, J_{gem} 12.36Hz, *H*-6(a)), 4.20 (1H, dd, $J_{5,6b}$ 4.39, J_{gem} 12.36Hz, *H*-6(b)), 5.12 (1H, t, $J_{3,4}$ 9.62, $J_{4,5}$ 9.89Hz, *H*-4), 5.125 (1H, dd, $J_{2,3}$ 9.34, $J_{1,2}$ 10.44Hz, *H*-2), 5.26 (1H, d, $J_{1,2}$ 10.44Hz, *H*-1), 5.29 (1H, t, $J_{2,3}$ 9.34, $J_{3,4}$ 9.61Hz, *H*-3). δ_C(75MHz; $CDCl_3$) 13.8, 13.95 (5x $COCH_2CH_2CH_2CH_2CH_3$), 22.3, 24.4, 24.5, 24.9, 31.1, 31.25, 31.3 (5x $COCH_2CH_2CH_2CH_2CH_3$), 34.0, 34.05, 34.1 (4x $OCOCH_2CH_2CH_2CH_2CH_3$), 44.4 ($SCOCH_3$), 61.75 (*C*-6), 67.9, 69.1, 73.8, 76.7 (*C*-2,3,4,5), 80.2 (*C*-1), 172.4, 173.0, 173.7 (4x $OCOCH_2CH_2CH_2CH_2CH_3$), 196.1 ($SCOCH_3$). MALDI-TOF, M+Na 709.40 (+/-6.5ppm).

6.16.4 Preparation of 1-Thio-2,3,4,6-tetra-*O*-hexionyl-*β*-D-glucopyranose [75].

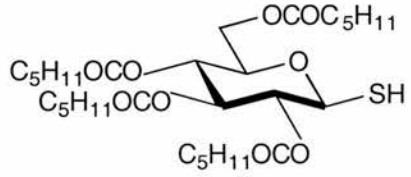

(a) 2,3,4,6-tetra-*O*-hexionyl-1-*S*-acetyl-1-thio-*β*-D-glucopyranose [73] (300mg, 4.75 x10^{-4}mol) in dry tetrahydrofuran (6ml) was stirred, under nitrogen, with 2 equivalents of benzylamine (104µl, 9.51 x10^{-4}mol). TLC analysis, after 30 minutes, showed a minor spot for the initial production of disulphide from the desired thiol. Consequently the reaction was halted. Work-up was as reported in section 6.13.7. Column chromatography (ethyl acetate : distilled hexane, 1:5) gave a clear, colourless oil, 120mg, 43%. On a second attempt of the reaction, performed on the same scale, the reaction time was extended to 1 hour. Following the work-up described earlier (section 6.13.7), crude nmr showed a favourable thiol to disulphide ratio (94:6). Column chromatography (toluene : ethyl acetate, 100:1) gave the desired compound, 178.5mg, 64%, $[\alpha]_D^{25}$ +17.2° (c, 0.62 in chloroform), [R_f = 0.21 (charred pink), ethyl acetate : hexane, 1:10. Solvent front: 54.5mm]. δ_H(300MHz; $CDCl_3$) 0.85-0.91 (12H, m, 4x $OCOCH_2CH_2CH_2CH_2CH_3$), 1.21-1.33 (16H, m, 4x $OCOCH_2CH_2CH_2CH_2CH_3$), 1.47-1.64 (8H, m, 4x $OCOCH_2CH_2CH_2CH_2CH_3$), 2.18-2.36 (8H, m, 4x $OCOCH_2CH_2CH_2CH_2CH_3$), 2.32 (1H, d, $J_{1,SH}$ 9.61Hz, S*H*), 3.705 (1H, ddd, $J_{5,6a}$ 2.47, $J_{5,6b}$ 4.67, $J_{4,5}$ 9.89Hz, *H*-5), 4.13 (1H, dd, $J_{5,6a}$ 2.47, J_{gem}

12.36Hz, *H*-6(a)), 4.19 (1H, dd, $J_{5,6b}$ 4.67, J_{gem} 12.36Hz, *H*-6(b)), 4.53 (1H, t, $J_{1,SH}$ 9.61, $J_{1,2}$ 9.89Hz, *H*-1), 4.97 (1H, t, $J_{3,4}$ 9.34, $J_{2,3}$ 9.61Hz, *H*-3), 5.11 (1H, t, $J_{2,3}$ 9.61, $J_{1,2}$ 9.89Hz, *H*-2), 5.21 (1H, t, $J_{3,4}$ 9.34, $J_{4,5}$ 9.89Hz, *H*-4). δ_C(75MHz; $CDCl_3$) 13.8, 13.9 (4x $COCH_2CH_2CH_2CH_2CH_3$), 22.3, 22.35, 24.4, 24.5, 31.25, 31.3 (4x $COCH_2CH_2CH_2CH_2CH_3$), 34.0, 34.1, 34.2 (4x $OCOCH_2CH_2CH_2CH_2CH_3$), 62.0 (*C*-6), 68.0, 73.4, 73.5, 76.7 (*C*-2,3,4,5), 79.0 (*C*-1), 172.3, 172.7, 173.0, 173.7 (4x $OCOCH_2CH_2CH_2CH_2CH_3$). MALDI-TOF, M+Na 611.32 (+/-3.4ppm).

(b) The title compound was also achieved from the same synthetic route [section 6.16.4(a)] using 2,3,4,6-tetra-*O*-hexionyl-1-*S*-hexionyl-1-thio-*β*-D-glucopyranose [74] (90mg, 1.31 $x10^{-4}$mol) as the starting material. This was clear from TLC analysis after 1 hour. [R_f = 0.24 (charred pink), ethyl acetate : hexane, 1:5. Solvent front: 56.5mm].

6.16.5 Preparation of *S*-Nitroso-1-thio-2,3,4,6-tetra-*O*-hexionyl-*β*-D-glucopyranose, (SNO-HEX) [76].

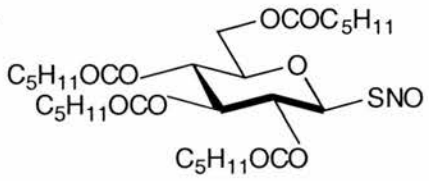

The title compound was obtained by nitrosation [section 6.2.5] of 1-thio-2,3,4,6-tetra-*O*-hexionyl-*β*-D-glucopyranose (60.6mg, 1.03 $x10^{-4}$mol) in HPLC grade ethanol (2.5ml). This gave an orange solution. λ_{max}(EtOH)/nm 344.8 & 560.5 (ε/dm^3 mol^{-1} cm^{-1} 402.9 & 9.3 respectively).

6.16.6 Preparation of 2,3,4,6,2',3',4',6'-Octa-*O*-hexionyl-di-*β*,*β*'-D-glucopyranosyl disulphide [77].

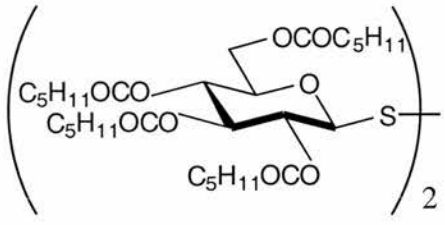

(a) Following the same protocol outlined in section 6.16.4(a), 2,3,4,6-tetra-*O*-hexionyl-1-*S*-acetyl-1-thio-*β*-D-glucopyranose [73] (250mg, 3.96 $x10^{-4}$mol) in dry tetrahydrofuran (6ml), was stirred, under nitrogen, with 2 equivalents of benzylamine

(87µl, 7.92 x10^{-4}mol) for 5 hours and 15 minutes. Work-up [section 6.13.7], was followed by column chromatography (ethyl acetate : distilled hexane, 1:5), to give a clear colourless oil, 134mg, 58%, $[\alpha]_D^{25}$ -231.4° (c, 1.2 in chloroform), [R_f = 0.23 (charred pink), ethyl acetate : hexane, 1:5. Solvent front: 52.5mm]. δ_H(300MHz; $CDCl_3$) 0.855-0.92 (12H, m, 4x $OCOCH_2CH_2CH_2CH_2CH_3$), 1.21-1.34 (16H, m, 4x $OCOCH_2CH_2CH_2CH_2CH_3$), 1.47-1.69 (8H, m, 4x $OCOCH_2CH_2CH_2CH_2CH_3$), 2.175-2.40 (8H, m, 4x $OCOCH_2CH_2CH_2CH_2CH_3$), 3.78 (1H, ddd, $J_{5,6a}$ 2.20, $J_{5,6b}$ 4.67, $J_{4,5}$ 9.89Hz, *H*-5), 4.16 (1H, dd, $J_{5,6a}$ 1.92, J_{gem} 12.36Hz, *H*-6(a)), 4.32 (1H, dd, $J_{5,6b}$ 4.67, J_{gem} 12.36Hz, *H*-6(b)), 4.64 (1H, d, $J_{1,2}$ 9.89Hz, *H*-1), 5.09 (1H, t, $J_{2,3}$ 9.61, $J_{1,2}$ 9.89Hz, *H*-2), 5.17 (1H, t, $J_{3,4}$ 9.34, $J_{2,3}$ 9.61Hz, *H*-3), 5.28 (1H, t, $J_{3,4}$ 9.34, $J_{4,5}$ 9.89Hz, *H*-4). δ_C(75MHz; $CDCl_3$) 13.8, 13.85, 13.9 (4x $OCOCH_2CH_2CH_2CH_2CH_3$), 22.2, 22.3, 24.4, 24.45, 24.5, 31.2, 31.25 (4x $OCOCH_2CH_2CH_2CH_2CH_3$), 33.9, 33.95, 34.0 (4x $OCOCH_2CH_2CH_2CH_2CH_3$), 61.5 (*C*-6), 67.7, 69.45, 73.4, 76.3 (*C*-2,3,4,5), 87.6 (*C*-1), 171.9, 172.7, 173.4 (4x $OCOCH_2CH_2CH_2CH_2CH_3$). MALDI-TOF (low resolution), M+Na 1197.64.

(b) When the reaction time was reduced to 1 hour and 40 minutes, crude nmr suggested a disulphide to thiol ratio of 2:1, when using the *H*-1 peak (doublet : triplet, at ~ 4.5ppm) as the diagnostic tool. These proportions were confirmed upon purification (ethyl acetate : distilled hexane, 1:5).

6.17 Synthesis of *S*-Nitroso-1-thio-*β*-D-glucopyranose, (SNOG) [79].

6.17.1 Preparation of 1-Thio-*β*-D-glucopyranose[41] [78].

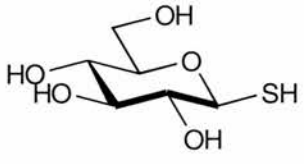

The sodium salt of 1-thio-β-D-glucose (207mg, 9.49 x10^{-4}mol) dissolved in methanol (40ml), was stirred with DOWEX/50WX8 100-200, H form, which had been previously washed with copious amounts of methanol (300ml). The ion-exchange resin was added until the solution was slightly acidic (1.248g of resin was

required in order to achieve this). The resin was then removed by filtration and thoroughly washed with methanol (50ml). Evaporation of the methanol gave a clear, colourless oil, 171mg, 92%, $[\alpha]_D^{25}$ +29.7° (c, 0.24 in methanol). ν_{max}/cm^{-1} 2544(w) (-SH) and 3362(br, s) (H-bonded -OH). δ_H(300MHz; D_2O) 3.31 (1H, t, *J* 9.06Hz, *H*-2/*H*-3/*H*-4), 3.47-3.55 (3H, m, *H*-5, *H*-2/*H*-3/*H*-4), 3.75 (1H, dd, $J_{5,6a}$ 4.78, J_{gem} 12.36Hz, *H*-6(a)), 3.93 (1H, dd, $J_{5,6b}$ 1.65, J_{gem} 12.36Hz, *H*-6(b)), 4.61 (1H, d, $J_{1,2}$ 9.89Hz, *H*-1). δ_C(75MHz; D_2O) 60.7 (*C*-6), 69.45, 75.8, 76.9 80.0 (*C*-2,3,4,5), 80.2 (*C*-1). MALDI-TOF, M+Na 219.03 (6.8ppm). No negligible peak at 413 therefore eliminates the possibility of disulphide formation.

6.17.2 Preparation of *S*-Nitroso-1-thio-*β*-D-glucopyranose, (SNOG) [79].

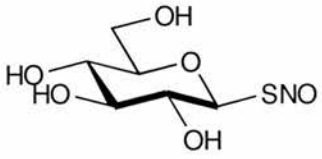

Nitrosation [section 6.2.5] of 1-thio-*β*-D-glucopyranose [78] (20.2mg, 1.03 $x10^{-4}$ mol) in HPLC grade ethanol (2.5ml) gave the characteristic orange solution (41.2mM). λ_{max}(EtOH:H_2O, 1:1)/nm 342.1 & 560.0 (ε/dm^3 mol^{-1} cm^{-1} 224.6 at 342.1nm).

6.18 Synthesis of *S*-Nitroso-1-thio-2,3,4,6-tetra-*O*-benzoyl-*β*-D-glucopyranose, (SNOB) [84].

6.18.1 Preparation of 1,2,3,4,6-Penta-*O*-benzoyl-*α*/*β*-D-glucopyranose[42] [80].

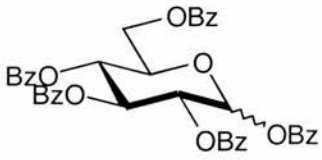

D-glucose (5.0g, 27.75mmol) was stirred in dry pyridine (30ml), whilst submerged in an ice-water bath. To this, 1.04 equivalents of benzoyl chloride (16.75ml, 144.32mmol) was added dropwise. Since this is an exothermic process, the addition was made at a sufficiently slow rate so as to prevent the temperature of the mixture rising above 4°C. A pink solid was observed once all the reagent had been introduced. Consequently more dry pyridine (20ml) was added whilst continuing to

stir the mixture in an ice-water bath. TLC analysis (ethyl acetate : hexane, 1:3) showed the reaction to be complete after 6 hours. Dilution into dichloromethane (100ml) and an aqueous wash with ice-cold 1M HCl (2x 100ml) was followed by a wash with ice-cold 10% sodium carbonate (2x 100ml). The organic layer was then given a final wash with water (100ml) before drying ($MgSO_4$) and concentrating to an off-white solid. As described by Fletcher,[42,43] this material was then diluted in ethanol (100ml) and re-concentrated to give a white solid which was then recrystallised in methanol. Upon washing with ice-cold methanol, the title compound was obtained as a fluffy, white crystalline material, 16.92g, 87% (from 2 crops), mp 164°C [lit.[42,43] mp 164-5°C (from methanol/glacial acetic acid) (for α) & mp 160-1°C (from methanol) (for β)], $[\alpha]_D^{25}$ -124.6° (c, 0.85 in chloroform) [lit.[42,43] $[\alpha]_D^{20}$ -114° (c, 0.85 in chloroform) (for α) & $[\alpha]_D^{20}$ -333° (c, 0.98 in chloroform) (for β)], [R_f = 0.65, ethyl acetate : hexane, 1:3. Solvent front: 54mm]. δ_H(300MHz; $CDCl_3$) 4.50 (1H, dd, $J_{5,6a}$ 5.22, J_{gem} 13.19Hz, *H*-6(a)), 4.62-4.67 (2H, m, *H*-5 & *H*-6(b)), 5.70 (1H, dd, $J_{1,2}$ 3.57, $J_{2,3}$ 10.16Hz, *H*-2), 5.87 (1H, t, $J_{4,5}$ 9.61, $J_{3,4}$ 9.89Hz, *H*-4), 6.05 (0.1H, d, $J_{1,2}$ 9.34Hz, *H*-1(β)), 6.34 (1H, t, $J_{3,4}$ 9.89, $J_{2,3}$ 10.16Hz, *H*-3), 6.87 (0.9H, d, $J_{1,2}$ 3.57Hz, *H*-1(α)), 7.26-7.69 (15H, m, 5x Ar (3,4,5 position)), 7.88-8.19 (10H, m, 5x Ar (2 & 6 position)). δ_C(75MHz; $CDCl_3$) 62.6 (*C*-6), 69.0, 70.6 (*C*-2,3,4,5), 90.2 (*C*-1(α)), 92.9 (*C*-1(β)), 128.6, 129.0 (5x Ar (3,4 & 5 position)), 129.95, 130.0, 130.05, 130.1, 130.25 (5x Ar (2 & 6 position)), 133.3, 133.6, 133.75, 134.1 (5x Ar (1 position)), 164.7, 165.4, 165.6, 166.2, 166.3 (5x O*C*OC_6H_5). MALDI-TOF, M+Na 723.18 (+/-2.5ppm).

6.18.2 Preparation of 2,3,4,6-Tetra-*O*-benzoyl-α-D-glucopyranosyl iodide [81].

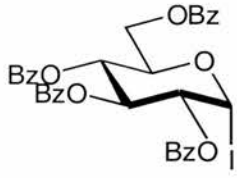

1,2,3,4,6-Penta-*O*-benzoyl-α/β-D-glucopyranose [80] (2.0g, 2.85mmol) in dry dichloromethane (25ml) was stirred with 2 equivalents of hexamethyldisilane (1.17ml, 5.71mmol) and iodine (1.45g, 5.71mmol), using the protocol already described [section 6.14.2]. TLC analysis (ethyl acetate : hexane, 1:3) showed the reaction to be complete after 1 hour and 30 minutes. Following work-up [section

6.13.5], a lime solid was obtained in quantitative yield, 2.01g, mp 139-40°C (from ether) [lit.[44] mp 141-2°C (from ether)], $[\alpha]_D^{25}$ +139.1° (c, 1 in chloroform) [lit.[44] $[\alpha]_D^{20}$ +139.5° (c, 1 in chloroform)], [R_f = 0.32, ethyl acetate : hexane, 1:3. Solvent front: 66.5mm]. δ_H(300MHz; $CDCl_3$) 4.49-4.57 (2H, m, *H*-5 & *H*-6(a)), 4.67 (1H, dd, $J_{5,6b}$ 2.20, J_{gem} 12.09Hz, *H*-6(b)), 4.75 (1H, dd, $J_{1,2}$ 4.12, $J_{2,3}$ 9.61Hz, *H*-2), 5.86 (1H, t, *J* 9.61, *J* 9.89Hz, *H*-3/*H*-4), 6.19 (1H, t, *J* 9.61, *J* 9.89Hz, *H*-3/*H*-4), 7.25-7.60 (13H, m, 4x Ar (3,4,5 position) & *H*-1), 7.86-8.09 (8H, m, 4x Ar (2 & 6 position)). δ_C(75MHz; $CDCl_3$) 62.0 (*C*-6), 67.85, 71.2, 72.4, 73.2 (*C*-2,3,4,5), 75.6 (*C*-1), 128.6, 128.7, 128.8 (4x Ar (3,4 & 5 position)), 129.95, 130.0, 130.2, 130.4 (4x Ar (2 & 6 position)), 133.5, 133.55, 133.85, 134.0 (4x Ar (1 position)), 165.3, 165.35, 165.8, 166.3 (4x O*C*OC_6H_5).

6.18.3 Preparation of 2,3,4,6-tetra-*O*-benzoyl-1-*S*-acetyl-1-thio-*β*-D-glucopyranose [82].

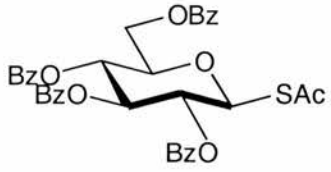

Using the 4 equivalents of potassium thioacetate (1.265g, 11.08mmol), 2,3,4,6-tetra-*O*-benzoyl-*α*-D-glucopyranosyl iodide [81] (1.957g, 2.77mmol) was stirred in dry acetone (50ml) for 12 hours. TLC analysis (ethyl acetate : hexane, 1:3) showed the reaction to be complete after this period of time, thus an aqueous work-up was performed [section 6.14.3]. From this a yellow foam was obtained, 1.776g, 98%. This was purified by column chromatography (ethyl acetate : distilled hexane, 1:5 to 1:3 gradient). From the resulting off-white precipitate, crystallisation and recrystallisation (ethyl acetate : distilled hexane) gave a white crystalline material, 556mg, 31%, mp 175-6°C, $[\alpha]_D^{25}$ +63.2° (c, 0.4 in chloroform), [R_f = 0.20, ethyl acetate : hexane, 1:3. Solvent front: 56mm]. δ_H(300MHz; $CDCl_3$) 2.32 (3H, s, SCO*C*H_3), 4.32 (1H, ddd, $J_{5,6b}$ 2.75, $J_{5,6a}$ 4.67, $J_{4,5}$ 10.17Hz, *H*-5), 4.47 (1H, dd, $J_{5,6a}$ 4.94, J_{gem} 12.36Hz, *H*-6(a)), 4.61 (1H, dd, $J_{5,6b}$ 2.75, J_{gem} 12.36Hz, *H*-6(b)), 5.62-5.69 (2H, m, *H*-1 & *H*-2/*H*-3 or *H*-4), 5.73 (1H, t, *J* 9.61, *J* 9.89Hz, *H*-2/*H*-3 or *H*-4), 6.00 (1H, t, *J* 9.34Hz, *H*-2/*H*-3 or *H*-4), 7.24-7.55 (12H, m, 4x Ar (3,4 & 5 position)), 7.80-8.06 (8H, m, 4x Ar (2 & 6 position)). δ_C(75MHz; $CDCl_3$) 30.9 (SCO*C*H_3), 63.0 (*C*-6), 69.3, 70.0, 74.3, 77.0 (*C*-2,3,4,5), 80.8 (*C*-1), 128.5, 128.55,

128.6, 128.9 (4x Ar (*C*-3,4,5)), 129.9, 130.05, 130.1 (4x Ar (*C*-2,6)), 133.3, 133.5, 133.7, 133.75 (4x Ar (*C*-1)), 165.35, 165.4, 165.9, 166.4 (4x O*C*OC$_6$H$_5$), 192.4 (S*C*OCH$_3$). MALDI-TOF, M+Na 677.15 (+/-9.6ppm).

6.18.4 Preparation of 1-Thio-2,3,4,6-tetra-*O*-benzoyl-*β*-D-glucopyranose [83].

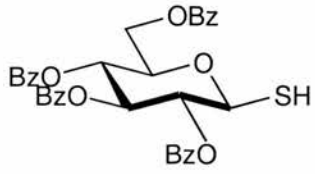

Under nitrogen, 2,3,4,6-tetra-*O*-benzoyl-1-*S*-acetyl-1-thio-*β*-D-glucopyranose (450mg, 6.87 x10^{-4}mol) in dry tetrahydrofuran (12ml) was stirred with 2 equivalents of benzylamine (151μl, 1.37mmol). TLC analysis (ethyl acetate : hexane, 1:3) suggested the initial production of disulphide after 1 hour and 30 minutes. Work-up [section 6.13.7] and column chromatography (ethyl acetate : distilled hexane, 1:3) gave the title compound as a clear colourless oil, 71mg, 17%, $[\alpha]_D^{25}$ +51.4° (c, 0.6 in deuterated chloroform), [R_f = 0.16, ethyl acetate : hexane, 1:3. Solvent front: 54.5mm]. ν_{max}/cm^{-1} 2655(w) (-SH) and 1727(br, s) (C=O). δ_H(300MHz; $CDCl_3$) 2.48 (1H, d, $J_{1,SH}$ 9.65Hz, S*H*), 4.18 (1H, ddd, $J_{5,6b}$ 2.89, $J_{5,6a}$ 4.82, $J_{4,5}$ 10.14Hz, *H*-5), 4.485 (1H, dd, $J_{5,6a}$ 5.31, J_{gem} 12.55Hz, *H*-6(a)), 4.64 (1H, dd, $J_{5,6b}$ 2.89, J_{gem} 12.54Hz, *H*-6(b)), 4.90 (1H, t, $J_{1,SH}$ 9.65, $J_{1,2}$ 10.13Hz, *H*-1), 5.505 (1H, t, *J* 9.65Hz, *H*-3/*H*-4), 5.71 (1H, t, $J_{2,3}$ 9.65, $J_{1,2}$ 10.13Hz, *H*-2), 5.89 (1H, t, *J* 9.17, *J* 9.65Hz, *H*-3/*H*-4), 7.25-7.58 (12H, m, 4x Ar (3,4 & 5 position)), 7.81, 7.89, 7.96, 8.04 (8H, dd, *J* 1.45, *J* 8.20Hz, 4x Ar (2 & 6 position)). δ_C(75MHz; $CDCl_3$) 63.3 (*C*-6), 69.5, 74.0, 74.4, 76.9 (*C*-2,3,4,5), 79.3 (*C*-1), 128.4, 128.5, 128.55 (4x Ar (*C*-3,4,5)), 129.8, 129.9, 130.0 (4x Ar (*C*-2,6)), 133.3, 133.4, 133.6 (4x Ar (*C*-1)), 165.2, 165.5, 165.8, 166.2 (4x O*C*OC$_6$H$_5$). MALDI-TOF, M+Na 635.13 (+/-9.3ppm).

The remainder of the crude material required re-columning due to co-eluting with the disulphide and the benzylamine adduct. However an alternative solvent system (ethyl acetate : hexane, 2:5) was equally unsuccessful in achieving good separation.

6.18.5 Preparation of *S*-Nitroso-1-thio-2,3,4,6-tetra-*O*-benzoyl-*β*-D-glucopyranose, (SNOB) [84].

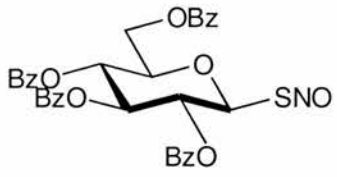

Nitrosation [section 6.2.5] of 1-thio-2,3,4,6-tetra-*O*-benzoyl-*β*-D-glucopyranose [83] (25mg, 4.08 $x10^{-5}$mol), in HPLC grade ethanol (1ml), gave an orange solution (41mM). λ_{max}(EtOH)/nm 346.4 & 560.0 (ε/dm^3 mol^{-1} cm^{-1} 254.6 & 6.8).

6.18.6 Preparation of 2,3,4,6,2',3',4',6'-Octa-*O*-benzoyl-di-*β*,*β*'-D-glucopyranosyl disulphide [85].

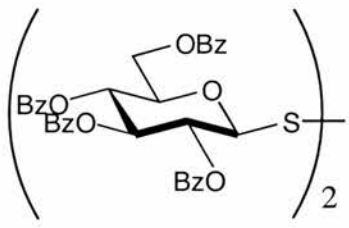

Dilution of the clear orange ethanolic solution of *S*-nitroso-1-thio-2,3,4,6-tetra-*O*-benzoyl-*β*-D-glucopyranose [83] (291µl, 41mM) with water (2.5ml) and more ethanol (2.209ml), gave a 1:1, ethanol : water mixture (2.4mM). Following the additions, a white suspension was observed. The white material was filtered and analysed by standard techniques. This showed 100% conversion to the disulphide. Such a result supports the theory that *S*-nitrosothio-sugar stability is governed by the degree of solvation. Diagnostic data: δ_H(300MHz; $CDCl_3$) 3.87-3.93 (1H, m, *H*-5), 4.50-4.545 (1H, m, *H*-6(a)), 4.60 (1H, dd, $J_{5,6b}$ 5.79, J_{gem} 12.09Hz, *H*-6(b)), 4.92 (1H, d, $J_{1,2}$ 10.13Hz, *H*-1), 5.55 (2H, t, *J* 9.65Hz, *H*-2/*H*-3/*H*-4), 5.97 (1H, t, *J* 9.17, *J* 9.65Hz, *H*-2/*H*-3/*H*-4), 7.26-7.55 (12H, m, 4x Ar (3,4 & 5 position)), 7.77-8.08 (8H, m, 4x Ar (2 & 6 position)). MALDI-TOF, M+Na 1245.265 (+/-7.5ppm).

6.19 Synthesis of *S*-Nitroso-6-thio-2,3,4,6-tetra-*O*-acetyl-*β*-D-glucopyranose, (6-SNAG) [89].

6.19.1 Preparation of 1,2,3,4-Tetra-*O*-acetyl-6-tosyl-*α*/*β*-D-glucopyranose[45] [86].

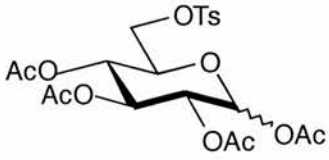

D-glucose (5.0g, 27.75mmol) dissolved in dry pyridine (75ml) was stirred for 24 hours with 1 equivalent of tosyl chloride (5.291g, 27.75mmol). After this time, 1.75 equivalents of acetic anhydride (18.53ml, 194.25mmol) was introduced. This addition was performed in an ice-water bath to prevent the exothermic process heating the mixture above 50°C. TLC analysis (ethyl acetate : hexane, 2:1) showed the reaction to be complete after a further 24 hours. Consequently the reaction mixture was concentrated to a syrup, before being co-evaporated with toluene (2x 200ml) to obtain a pink viscous slurry. This was dissolved in a minimum amount of ethanol (140ml), with heating, which was then left to cool to room temperature. Upon standing, a white solid formed. Filtering and washing with ice-cold ethanol gave a bright white solid, 3.382g, 24% [lit.[45] 40%]. Recrystallisation from ethanol (150ml) gave the pure product, 1.989g, 14%, mp 194-5°C [lit.[45] mp 194°C (from ethanol), lit.[46] mp 203-4°C (from pyridine)], $[\alpha]_D^{25}$ +22.7° (c, 0.7 in chloroform) [lit.[45] $[\alpha]_D^{20}$ +23° (c, 0.7 in chloroform), lit.[46] $[\alpha]_D^{25}$ +23.7° (c, 3.665 in chloroform)], [R_f = 0.54, ethyl acetate : hexane, 2:1. Solvent front: 57mm]. δ_H(300MHz; $CDCl_3$) 1.98, 1.985, 2.00, 2.07 (12H, 4x s, 4x OCOCH_3), 2.44 (3H, s, *p*-$SO_2C_6H_4CH_3$), 3.83 (1H, dt, $J_{5,6b}$ 3.38, $J_{5,6a}$ 4.34, $J_{4,5}$ 10.53Hz, *H*-5), 4.09 (1H, dd, $J_{5,6a}$ 4.34, J_{gem} 11.10Hz, *H*-6(a)), 4.14 (1H, dd, $J_{5,6b}$ 3.38, J_{gem} 11.10Hz, *H*-6(b)) 5.02 (1H, t, $J_{3,4}$ 9.17, $J_{4,5}$ 10.61Hz, *H*-4), 5.03 (1H, t, $J_{1,2}$ 8.20, $J_{2,3}$ 9.17Hz, *H*-2), 5.19 (1H, t, *J* 9.17Hz, *H*-3), 5.64 (1H, d, $J_{1,2}$ 8.20Hz, *H*-1(β)), 7.33 (2H, d, *J* 8.20Hz, *p*-$SO_2C_6H_4CH_3$), 7.76 (2H, d, *J* 8.20Hz, *p*-$SO_2C_6H_4CH_3$). δ_C(75MHz; $CDCl_3$) 20.7, 20.9 (4x OCOCH_3), 21.8 (*p*-$SO_2C_6H_4CH_3$), 66.9, 68.1, 70.2, 72.3, 72.7 (*C*-2,3,4,5,6), 91.6 (*C*-1), 128.25, 129.9 (*C*-2,3,5,6 of Ar), 132.5, 145.2 (*C*-1,4 of Ar), 168.8, 169.2, 169.3, 170.1 (4x O*C*OCH$_3$). MS (EI), M^+ (-AcOH) 442.09 (+/- 1.6ppm), MALDI-TOF, M+Na 525.10 (+/- 5.5ppm). When the reaction was repeated using double the quantity of reagents, a crude yield of 24% was still obtained.

6.19.2 Preparation of 1,2,3,4-Tetra-*O*-acetyl-6-*S*-acetyl-6-thio-*β*-D-glucopyranose[47] [87].

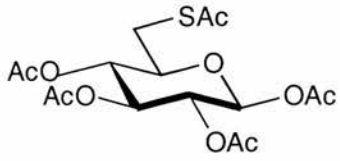

1,2,3,4-Tetra-*O*-acetyl-6-tosyl-*α*/*β*-D-glucopyranose [86] (100mg, 1.99 x10^{-4} mol) in dry acetone (6ml) was stirred for 48 hours with 4 equivalents of potassium thioacetate (91mg, 7.96 x10^{-4} mol). TLC analysis (ethyl acetate : hexane, 1:3) showed the reaction to be incomplete after this time period. Consequently more potassium thioacetate (91mg, 7.96 x10^{-4} mol) was added. However the reaction was only driven to completion after refluxing for 2 hours and 30 minutes. The resulting brown mixture was initially filtered, to remove the salt by-product, before being flushed through a charcoal bed to obtain a clear yellow solution. This was diluted into dichloromethane (100ml) which was then washed with 10% sodium carbonate (100ml) and water (100ml). Drying ($MgSO_4$) and concentrating gave a yellow oil. Crystallisation from diethyl ether and separately from methanol, was unsuccessful. Purification was eventually possible by column chromatography (ethyl acetate : distilled hexane, 1:3), giving the desired compound in quantitative yield. When repeated on a 5g scale, crystallisation from diethyl ether was possible after the same chromatographic process and a second filtration through charcoal. From two crops, this gave a white crystalline material, 2.14g, 53% [lit.[47] 76%], mp 125°C [lit.[47] mp 127-8°C (from ethanol), lit.[48] mp 130-1°C (from ethanol)], $[\alpha]_D^{25}$ -17.1° (c, 3.4 in chloroform) [lit.[47] $[\alpha]_D^{25}$ -14.7° (c, 3.4 in chloroform), lit.[48] $[\alpha]_D^{24}$ -19.0° (c, 1 in chloroform)], [R_f = 0.16 (charred pink), ethyl acetate : hexane, 1:3. Solvent front: 57mm]. δ_H(300MHz; $CDCl_3$) 2.00, 2.02, 2.08, 2.105 (12H, 4x s, 4x OCOC*H*$_3$), 2.33 (3H, s, SCOC*H*$_3$), 3.13 (1H, dd, $J_{5,6a}$ 6.04, J_{gem} 14.55Hz, *H*-6(a)), 3.22 (1H, dd, $J_{5,6b}$ 3.30, J_{gem} 14.56Hz, *H*-6(b)), 3.795 (1H, ddd, $J_{5,6b}$ 3.30, $J_{5,6a}$ 6.05, $J_{4,5}$ 9.35Hz, *H*-5), 5.015 (1H, t, *J* 9.06, *J* 9.89Hz, *H*-3/*H*-4), 5.09 (1H, dd, $J_{1,2}$ 8.24, $J_{2,3}$ 9.34Hz, *H*-2), 5.21 (1H, t, *J* 9.34Hz, *H*-3/*H*-4), 5.665 (1H, d, $J_{1,2}$ 8.24Hz, *H*-1(β)). δ_C(75MHz; $CDCl_3$) 20.6, 20.7, 20.8 (4x OCO*C*H$_3$), 29.8 (*C*-6), 30.4 (SCO*C*H$_3$), 69.9, 70.4, 72.9, 73.9 (*C*-2,3,4,5), 91.8 (*C*-1), 169.2, 169.5, 169.9, 170.3 (4x O*C*OCH$_3$), 194.85 (S*C*OCH$_3$). MALDI-TOF, M+Na 429.08 (+/-3.3ppm).

6.19.3 Preparation of 1,2,3,4-Tetra-*O*-acetyl-6-thio-*β*-D-glucopyranose [88].

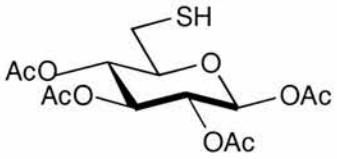

(a) Using the same protocol as outlined in section 6.2.4(b), 1,2,3,4-tetra-*O*-acetyl-6-*S*-acetyl-6-thio-*β*-D-glucopyranose [87] (600mg, 1.48mmol) in dry tetrahydrofuran (15ml) was stirred, under nitrogen, with 2 equivalents of benzylamine (324μl, 2.95 mmol). TLC analysis (ethyl acetate : hexane, 1:3) suggested the reaction was incomplete after 1 hour. Consequently more benzylamine (162μl, 1.48mmol) was introduced. Due to the slow progress of the reaction, 2 further equivalents of benzylamine (324μl, 2.95 mmol) were added after a reaction time of 6 hours. Since TLC observations suggested initial disulphide production, after 7 hours, the reaction was halted. Work-up [section 6.13.7] and column chromatography (ethyl acetate : distilled hexane, 1:2) gave a clear oil, 202mg, 38%. ^{1}H and ^{13}C nmr provided diagnostic data to suggest that the de-*S*-acetylation was unsuccessful: δ_H(300MHz; $CDCl_3$) 2.33 (3H, s, SCOCH_3). δ_C(75MHz; $CDCl_3$) 30.5 (SCOCH$_3$).

(b) This procedure was based on work by Brands and co-workers,[49] in which 1,2,3,4-tetra-*O*-acetyl-6-*S*-acetyl-6-thio-*β*-D-glucopyranose [87] (100mg, 2.46 x10^{-4}mol) in dry acetonitrile (15ml), was combined with 1 equivalent of silver triflate (63.2mg, 2.46 x10^{-4}mol). The system was stirred under nitrogen and minimal light conditions for 2 hours. TLC analysis (ethyl acetate : hexane, 1:3) showed no shift in R_f value during this time period. Following the addition of 2 equivalents of benzylamine (54μl, 4.92 x10^{-4}mol), there was still no change by TLC. Changing the solvent system did not separate the reaction mixture from the starting material, so more benzylamine (54μl, 4.92 x10^{-4}mol) was introduced.

Upon standing overnight, at room temperature, a large amount of white crystalline material formed. Filtration and washing with ice-cold acetonitrile resulted in the majority of the solid passing back into the filtrate. The solid that remained was insoluble in alcohol, dichloromethane, acetonitrile and dimethylsulphoxide. It was suspected that the solid may have been the thio-silver sugar, so this was combined with the filtrate, diluted into dichloromethane and washed with 1M HCl (200ml).

Upon drying ($MgSO_4$) and concentrating the organic layer, a yellow oil was produced which was difficult to characterise.

The process was repeated using just 1 equivalent of benzylamine (27μl, 2.46 $x10^{-4}$ mol) and a white precipitate was again achieved, this time after just 7 hours. Filtration was again unsuccessful. Column chromatography (ethyl acetate) gave a clear, pale yellow oil, 43mg, 48%. This was diluted in methanol (20ml) and stirred with DOWEX/50WX8-200 ion exchange resin (2.0g). Filtering and concentrating gave an oil. The resulting NMR was difficult to interpret and MALDI-TOF did not give the desired M+Na peak at 387 or 494, corresponding to the free thiol or the silver salt, respectively. The solvent was changed from acetonitrile to tetrahydrofuran but this modification was just as fruitless in providing the title compound.

6.20 Synthesis of *S*-Nitroso-3-thio-1,2-propanediol (SNO-GLY) [90] & *S*-Nitroso-3-thio-1,2-di-*O*-acetyl propane, (SNA-GLY) [93].

6.20.1 Preparation of *S*-Nitroso-3-thio-1,2-propanediol, (SNO-GLY) [90].

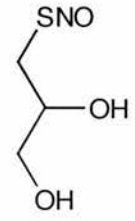

3-Thio-1,2-propane-diol (34.7μl, 4.12 $x10^{-4}$mol) dissolved in HPLC grade ethanol (10ml) was nitrosated by the gaseous method described in section 6.2.5. This resulted in the production of a clear red solution (41.2mM) which proved to be very stable. λ_{max}(EtOH:H_2O, 1:1)/nm 334.5 & 546.0 (ε/dm^3 mol^{-1} cm^{-1} 1183.3 & 33.3 respectively).

6.20.2 Preparation of 1,2-Di-*O*-acetyl-*S*-acetyl-3-thio propane [91].

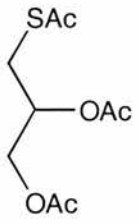

(a) An excess of acetic anhydride (7.5ml, 7.95mmol) was mixed with pyridine (25ml), before 3-thio-1,2-propane-diol (1.93ml, 23.1mmol) was introduced to the reaction vessel. The resulting lime coloured solution was stirred for 12 hours, after which time, TLC analysis (ethyl acetate : hexane, 1:1) showed the reaction to be complete. Following dilution into dichloromethane (100ml), the organic phase was washed with ice-cold 1M HCl (2x 100ml), ice-cold 10% sodium carbonate (2x 100ml) and finally with water (100ml). Drying ($MgSO_4$) and concentrating gave a yellow solution. Unreacted acetic anhydride was removed by co-evaporation with toluene (100ml), to give the desired compound, in pure form, 5.225g, 96.5%. [R_f = 0.51 (charred pink), ethyl acetate : hexane, 1:1. Solvent front: 57mm]. δ_H(300MHz; $CDCl_3$) 2.03, 2.035 (6H, 2x s, 2x OCOCH_3), 2.31 (3H, s, SCOCH_3), 3.025 (1H, dd, $J_{2,3a}$ 6.87, J_{gem} 14.29Hz, *H*-3(a)), 3.22 (1H, dd, $J_{2,3b}$ 5.77, J_{gem} 14.28Hz, *H*-3(b)), 4.08 (1H, dd, $J_{1a,2}$ 5.77, J_{gem} 11.81Hz, *H*-1(a)), 4.22 (1H, dd, $J_{1b,2}$ 3.85, J_{gem} 11.82Hz, *H*-1(b)), 5.06-5.13 (1H, m, *H*-2). δ_C(75MHz; $CDCl_3$) 20.7, 20.8 (2x OCO*C*H_3), 29.3 (*C*-1), 30.4 (SCO*C*H_3), 63.65, 70.0 (*C*-2,3), 170.2, 170.7 (2x O*C*OCH$_3$), 194.5 (S*C*OCH$_3$). MALDI-TOF, M+Na 257.05 (+/-6.6ppm).

(b) The title compound was also synthesised by the slow addition of 3-thio-1,2-propane-diol (1.93ml, 23.1mmol) to 1.13 equivalents of acetic anhydride (7.5ml, 79.5mmol) pre-mixed with a catalytic amount of iodine (7mg, 2.76 x10^{-5} mol). The addition of the starting material initially generated a lot of heat. Though it was envisaged that this may catalyse the reaction further, TLC analysis (ethyl acetate : hexane, 1:1) suggested the reaction to be slower that that involving pyridine [section 6.20.2(a)]. Consequently after 12 hours, more iodine (3mg, 1.18 x10^{-5} mol) was added. A third portion of iodine and heating was still insufficient to drive the reaction to completion. Work-up involved dilution into dichloromethane (100ml) and successive washes with 10% sodium carbonate (2x 100ml) and water (100ml). Drying ($MgSO_4$) and concentrating gave a clear pale yellow oil, 4.71g, 87%. Column

chromatography (ethyl acetate : distilled hexane, 1:5) was necessary to obtain a clean product, 3.26g, 60%.

The longer reaction time, lower yield and the need to purify make this a less attractive synthetic route, for this particular compound, when compared with the procedure described previously [section 6.20.2(a)].

6.20.3 Preparation of 1,2-Di-*O*-acetyl-3-thio propane [92].

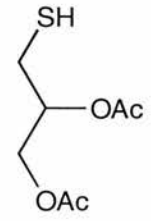

Under nitrogen, 1,2-di-*O*-acetyl-*S*-acetyl-3-thio-propane [91] (1.0g, 4.27mmol) in dry tetrahydrofuran (25ml) was stirred with 1 equivalent of benzylamine (468µl, 4.27mmol). The reaction was continually monitored by TLC analysis (ethyl acetate : hexane, 1:3) over 45 minutes. Due to a lack of reactivity shown even after further TLC analysis (ethyl acetate : hexane, 1:5), a second equivalent of benzylamine (468µl, 4.27mmol) was introduced. The starting material was clearly still present, thus the reaction was abandoned. A repeat of the procedure, using dry acetonitrile was attempted, but a lack of reactivity, as reported earlier [section 6.19.3], was again experienced.

6.21 References

1 P.W. Riddles, *Analytical Biochem.*, 1979, **94**, 75.

2 L.C. Green, D.A. Wagner, J. Glogowski, P.L. Skipper, J.S. Wishnok and S.R. Tannenbaum, *Analytical Biochem.*, 1982, **126**, 131.

3 J.A. Cook, S.Y. Kim, D. Teague, M.C. Krishna, R. Pacelli, J.B. Mitchell, Y. Vodovotz, R.W. Nims, D. Christodoulou, A.M. Miles, M.B. Grisham and D.A. Wink, *Analytical Biochem.*, 1996, **238**, 150.

4 K.P.R. Kartha and H.J. Jennings, *J. Carbohydr. Chem.*, 1990, **9**, 777.

5 E. Fischer, *Ber.*, 1911, **44**, 1898.

6 D.H. Brauns, *J. Am. Chem. Soc.*, 1925, **47**, 1280.

7 W.A. Bonner and J.E. Kahn, *J. Am. Chem. Soc.*, 1951, **73**, 2241.

8 M. Cerny, J. Vrkoc and J. Stanek, *Collect. Czech. Chem. Commun.*, 1959, **24**, 64.

9 J. Stanek, M. Sindlerova and M. Cerny, *Collect. Czech. Chem. Commun.*, 1965, **30**, 297.

10 T.W. Hart, *Tetrahedron Lett.*, 1985, **26**, 2013.

11 J. Loscalzo, *J. Clin. Invest.*, 1985, **76**, 703.

12 L.J. Ignarro, H. Lippton, J.C. Edwards, W.H. Baricos, A.L. Hyman, P.J. Kadowitz and C.A. Gruetter, *J. Pharmacol. Exp. Ther.*, 1981, **218**, 739.

13 D. Horton, Methods in Carbohydrate chemistry, Academic Press, New York and London, 1972, **6**, 282.

14 D. Horton, and M.L. Wolfrom, *J. Org. Chem.*, 1962, **27**, 1794.

15 W. Meyer zu Reckendorf and W. A. Bonner, *J. Org. Chem.*, 1961, **26**, 4596.

16 M.A. Probert, J. Zhang and D.R. Bundle, *Carbohydr. Res.*, 1996, **296**, 149.

17 J.J. Fox and I. Goodman, *J. Am. Chem. Soc.*, 1951, **73**, 3256.

18 Z. Tarasielska and R.W. Jeanloz, *J. Am. Chem. Soc.*, 1958, **80**, 6325.

19 N. Rakotomanomana, J-M. Lacombre and A.A. Pavia, *Carbohydr. Res.*, 1990, **197**, 318.

20 K.P.R. Kartha and R.A. Field, *Tetrahedon*, 1997, **53**, 11753.

21 G.J.F. Chittenden, *Carbohydr. Res.*, 1972, **25**, 35.

22 E. Fischer and E.F. Armstrong, *Ber.*, 1902, **35**, 833.

23 M. Cerny, J. Stanek, J. Pacak, *Monatsh. Chem.*, 1963, **94**, 290.

24 M.J. Kiefel, R.J. Thomson, M. Radovnovic and M. von Itzstein, J. Carbohydr. Chem., 1999, **18**, 937.

25 C.S. Hudson and J.M. Johnson, *J. Am. Chem. Soc.* 1915, **37**, 2751.

26 J.K. Dale, *J. Am. Chem. Soc.* 1915, **37**, 2746.

27 L.C. Kreider and W.L. Evans, *J. Am. Chem. Soc.*, 1936, **58**, 797.

28 M. Gehrke and F.X. Aichner, *Ber.*, 1927, **60**, 918.

29 C.V. Holland, D. Horton and M.J. Miller, *J. Org. Chem.*, 1967, **32**, 3077.

30 E. Fischer and H. Fischer, *Ber.*, 1910, **43**, 2521.

31 C.S. Hudson and A. Kunz, *J. Am. Chem. Soc.*, 1925, **47**, 2052.

32 B. Albrecht, U. Putz and G. Schwarzmann, *Carbohydr. Res.*, 1995, **276**, 289.

33 D.H. Brauns, *J. Am. Chem. Soc.*, 1929, **51**, 1820.

34 E. Fischer and E.F. Armstrong, *Ber.*, 1902, **35**, 3153.

35 V. Laine and J. Defaye, *J. Chem. Soc. Perkin Trans. 2*, 1995, **7**, 1479.

36 W.A. Bonner, C.D. Hurd and S.M. Cantor, *J Am. Chem. Soc.*, 1947, **69**, 1816.

37 K.P.R. Kartha and R.A. Field, *J. Carbohydr. Chem.*, 1998, **17**, 693.

38 K.P.R. Kartha and R.A. Field, *Tetrahedron Lett.*, 1997, **38**, 8233.

39 K.P.R. Kartha and R.A. Field, *Carbohydr. Lett.*, 1998, **3**, 179.

40 I.A. Wolff, *J. Am. Chem. Soc.*, 1945, **67**, 1623.

41 J. Defaye, A. Gadelle and C. Pedersen, *Carbohydr. Res.*, 1991, **217**, 51.

42 H.G. Fletcher, *Methods in Carbohydr. Chem.*, academic Press, New York and London, 1963, **2**, 234.

43 H.G. Fletcher and C.S. Hudson, *J. Am. Chem. Soc.*, 1947, **69**, 1145.

44 R.K. Ness, H.G. Fletcher and C.S. Hudson, *J. Am. Chem. Soc.*, 1950, **72**, 2200.

45 E. Hardegger and R.M. Montavan, *Helvetica Chemica Acta*, 1946, **29**, 1199.

46 J. Compton, *J. Am. Chem. Soc.*, 1938, **60**, 395.

47 R.L. Whistler and P.A. Seib, *Carbohydr. Res.*, 1966, **2**, 93.

48 M. Akagi, S. Tejima, M. Haga, *Chem. Pharm. Bull. (Tokyo).*, 1962, **10**, 562.

49 K.M.J. Brands, *Tetrahedron. Lett.*, 1998, **39**, 1677.

Appendices

Appendix A

The crystal data and structure refinement for pre-SNAG [4]

Identification code	rpab1
Empirical formula	$C_{14}H_{20}O_9S$
Formula weight	364.36
Temperature	293(2) K
Wavelength	0.71073 Å
Crystal system	Monocyclic
Space group	$p2_1$
Unit cell dimensions	a = 8.0071(11) Å alpha = 90°
	b = 12.027(2) Å beta = 102.816(2)°
	c = 9.5110(13) Å gamma = 90°
Volume, z	893.1(2) $Å^3$, 2
Density (calculated)	1.355 Mg/m^3
Absorption coefficient	0.223 mm^{-1}
F(000)	384
Crystal size	.15 x .1 x .05 mm
θ range for data collection	2.61 to 23.40°
Limiting indices	$-8 \leq h \leq 7, -13 \leq k \leq 13, -9 \leq l \leq 10$
Reflections collected	4470
Independent reflections	2512 (R_{int} = 0.0928)
Absorption correction	Sadabs
Max. and min. transmission	1.00000 and 0.791514
Refinement method	Full-matrix least-squares on F^2
Data / restraints / parameters	2488 / 2 / 231
Goodness-of-fit on F^2	0.915
Final R indices [$I > 2\sigma(I)$]	R1 = 0.0566, wR2 = 0.1497
R indices (all data)	R1 = 0.0710, wR2 = 0.1855

Absolute structure parameter	-0.09(14)
Extinction coefficient	0.000(8)
Largest diff. peak and hole	0.260 and -0.289 eÅ^{-3}

Appendix B

Using a Swinbourne plot to calculate the half-life ($t_{1/2}$) of each test compound.
Example: based on SNAG [5]

A Swinbourne plot for SNAG [5]

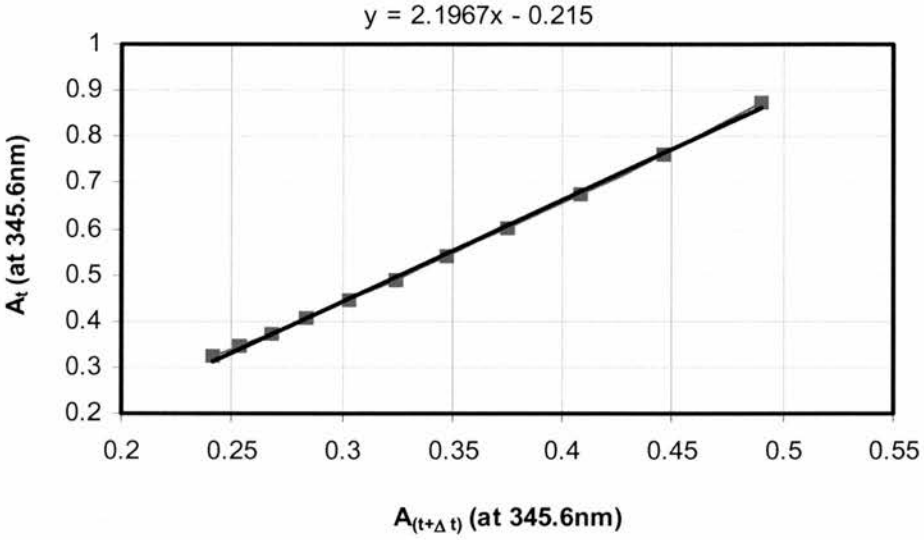

This plot of A_t versus $A_{(t+\Delta t)}$ using data that is also presented in figure 63, gives virtually a straight line which is in accordance with first order kinetics. The gradient of the slope (k) is calculated as 2.1967.

The mathematics:

Using first order kinetics,

$$\ln = \frac{(A_t - A_\infty)}{(A_0 - A_\infty)} = -kt$$

$$(A_t - A_\infty) = (A_0 - A_\infty)\exp[-kt] \qquad \text{-(a)}$$

At time $t+\Delta t$, absorbance = A_t'

So, when $t' = t+\Delta t$,

$$(A_t' - A_\infty) = (A_0 - A_\infty)\exp[-k(t+\Delta t)] \qquad \text{-(b)}$$

Divide (a) by (b) to give,

$$\frac{(A_t-A_\infty)}{(A_t'-A_\infty)} = \frac{\exp[-kt]}{\exp[-k(t+\Delta t)]}$$

$$A_t-A_\infty = A_t' \frac{\exp[-kt]}{\exp[-k(t+\Delta t)]} - A_\infty \frac{\exp[-kt]}{\exp[-k(t+\Delta t)]}$$

$$= A_t' \exp k\Delta t - A_\infty \exp k\Delta t$$

$$A_t = A_\infty (1-\exp k\Delta t) + A_t' \exp k\Delta t$$

So, if we plot A_t against A_t', then the slope of the straight line = exp $k\Delta t$

ln slope = $k\Delta t$

therefore,

$\frac{\text{ln slope}}{\Delta t} = k$ then we can calculate the half-life, since, $t_{1/2} = \frac{\ln 2}{k}$

Thus in the case of SNAG [5],

Slope of line = 2.1967 & Δt = 5 hours.

Therefore, ln slope = 0.787, and k = 0.787/5

= 0.157 h^{-1}

$t_{1/2}$ = ln2/k

= 4.4 hours

Appendix C

The apparatus and principle behind the potentiometric titration method to measure Log P.

The apparatus.

Potentiometric titrations of compounds were performed with the GlpKa apparatus (Sirius Analytical Instruments Ltd, Forrest Row, East Sussex, UK) equipped with an Ag/AgCl double-junction pH electrode, a temperature probe, an overhead stirrer, a precision dispenser and a six-way valve for distribution reagents and titrants (0.5 M HCl, 0.5 M KOH and 0.15 M KCl). The weighed sample (3 - 4 mg) was

added manually, whereas the n-octanol and all the other reagents were supplied automatically. The pK_a and log P values were estimated from difference Bjerrum plots and refined by a linear least squares procedure.

The principle.

Briefly, the pH-metric technique is based on two successive titrations. First, the solute in water is titrated against standard acid or base to obtain ionization constants. Then the titration is repeated in the presence of a water-immiscible organic solvent and a new ionization constant is determined. In the presence of the dual-solvent mixture, the pK_a value shifts in response to the partitioning of some of the substance into the organic phase, giving an apparent constant called p_oK_a. The shift in pK_a is used in the calculation of log P, since the two are related.

Brief method.

To obtain lipophilicity data at least four separate titrations of ca. 0.5 mM for each compound, containing various volumes of octan-1-ol (from 1 ml of organic solvent/20 ml of H_2O to 13 ml of organic solvent/7 ml of H_2O), were performed in the pH range 3.5 to 12.2. The titrations were carried out under $N_{2(g)}$ at room temperature. Final data were obtained by the Multiset approach.

Appendix D

The method used for determining Log P by shake flask in conjunction with Ellman's reagent.

The methodology used

Ellman's test for UV absorbance

Ellmans reagent (see section 2.1)

1.966mM solution: 39mg into 50ml of PBS (DTNB solution)
[PBS = phosphate buffer, DTNB = 5,5'-dithiobis(2-nitrobenzoic acid)]

Thiol concentration

Require 1 x 10^{-4}M
So, For SNOG [79]
25mg / 196.22 in 50ml PBS (= 2.548 x 10^{-3}M)

Then,
take 177µl of the thiol solution.

For UV (at 412nm),

PBS 3.873ml
DTNB 450µl
Thiol 177µl After shaking with octanol (Require 25.548 fold dilution to get 1 x 10^{-4}M)

Then take 3ml of this solution for UV analysis.

For blank: (for contribution due to Ellman's reagent),

PBS (4.05ml)
DTNB (450µl)

Again take 3ml for UV analysis.

For Mother Liquor: (=Max. absorbance),

PBS 3.873ml
DTNB 450µl
Thiol 177µl (from mother liquor eg. not shaken with octanol)

Again take 3ml for UV analysis.

Appendix E

The theory behind X-ray photoelectron spectroscopy (XPS)

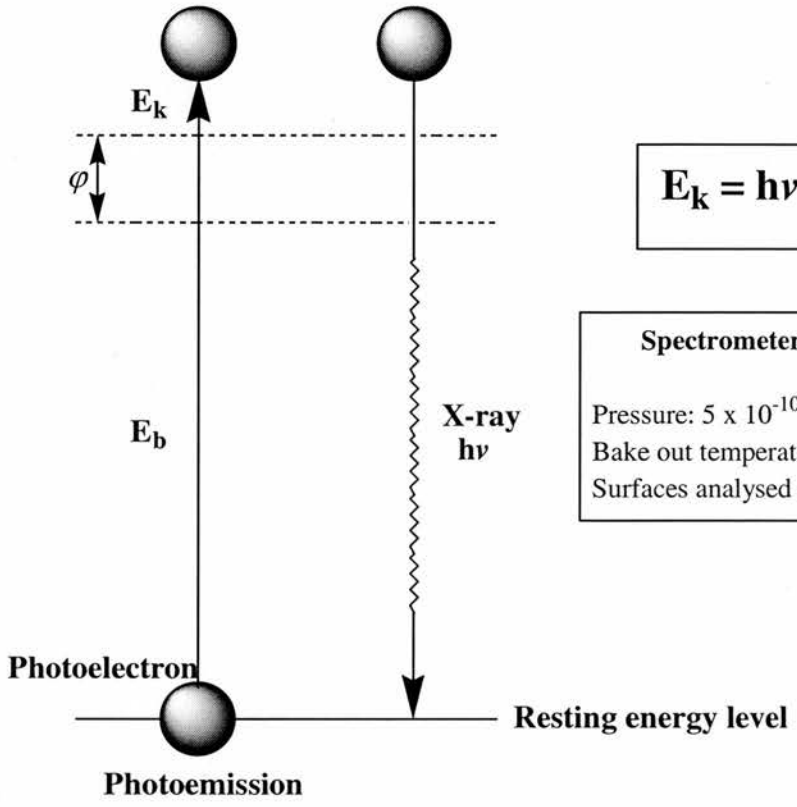

$$E_k = h\nu - E_b - \varphi$$

Spectrometer specification

Pressure: 5 x 10^{-10} Torr
Bake out temperature: 160 deg. Celcius
Surfaces analysed down to 100nm

E_k = kinetic energy of photoelectron

h = Planck's constant

ν = frequency of exciting radiation

E_b = binding energy of the valence electron

φ = work function of spectrometer

An atom absorbs a photon of energy $h\nu$; next a core or valence electron with binding energy E_b is ejected with kinetic energy E_k. Using the equation shown above, the binding energy of an ejected valence electron can be calculated and therefore the atom from which it was emitted can also be deduced. So powerful is this technique that the chemical environment in which the atom exists, including its oxidation state, can ultimately be proposed.